火星と宇宙生物学

- 1.宮本正太郎と月・火星（ホイッグ史観と複雑系の科学の発展）
- 2.火星の起源、歴史と生命存在可能性（40分＋5分議論）

- 3.宇宙生物学の未来（40分＋5分議論）

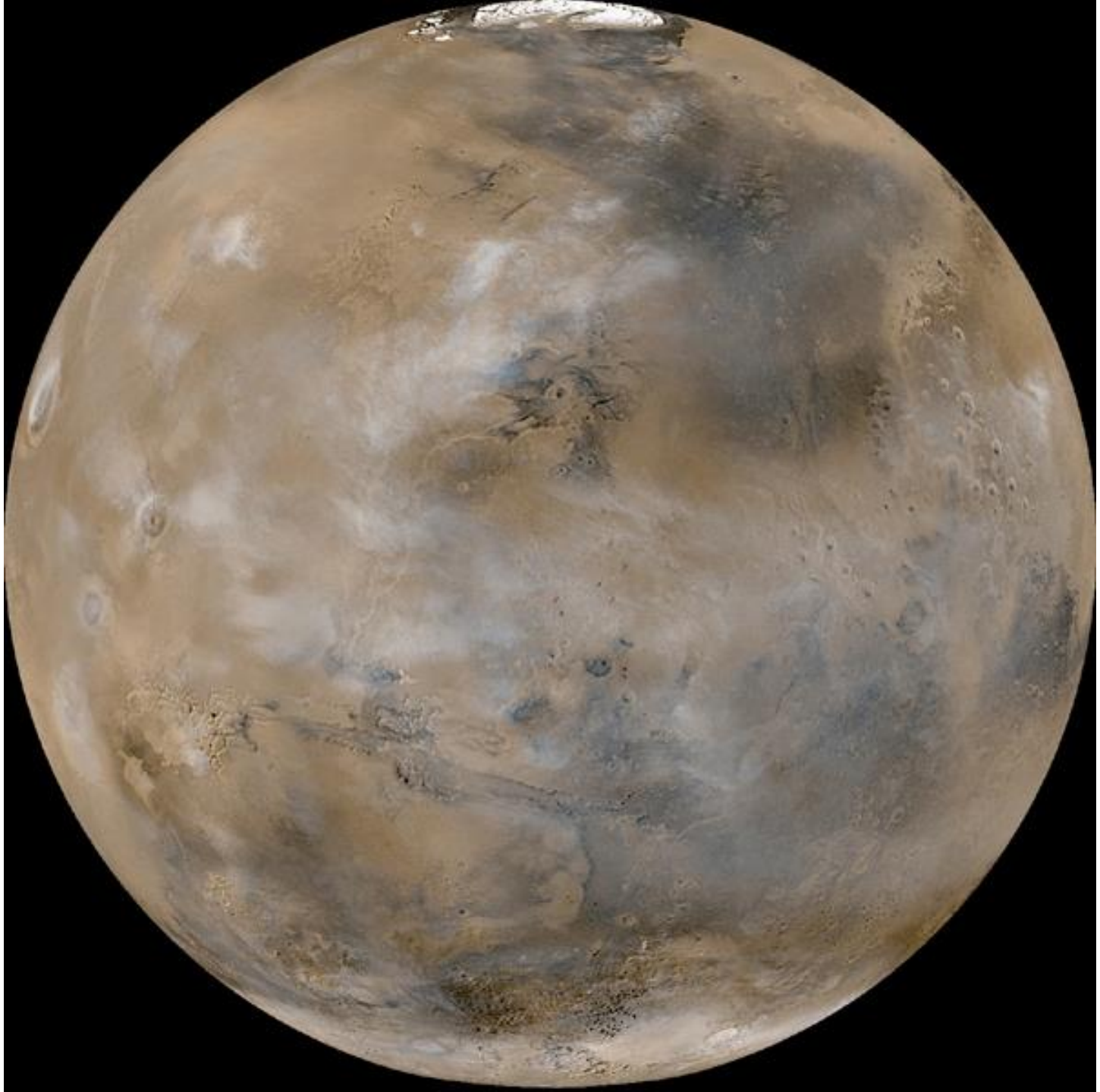

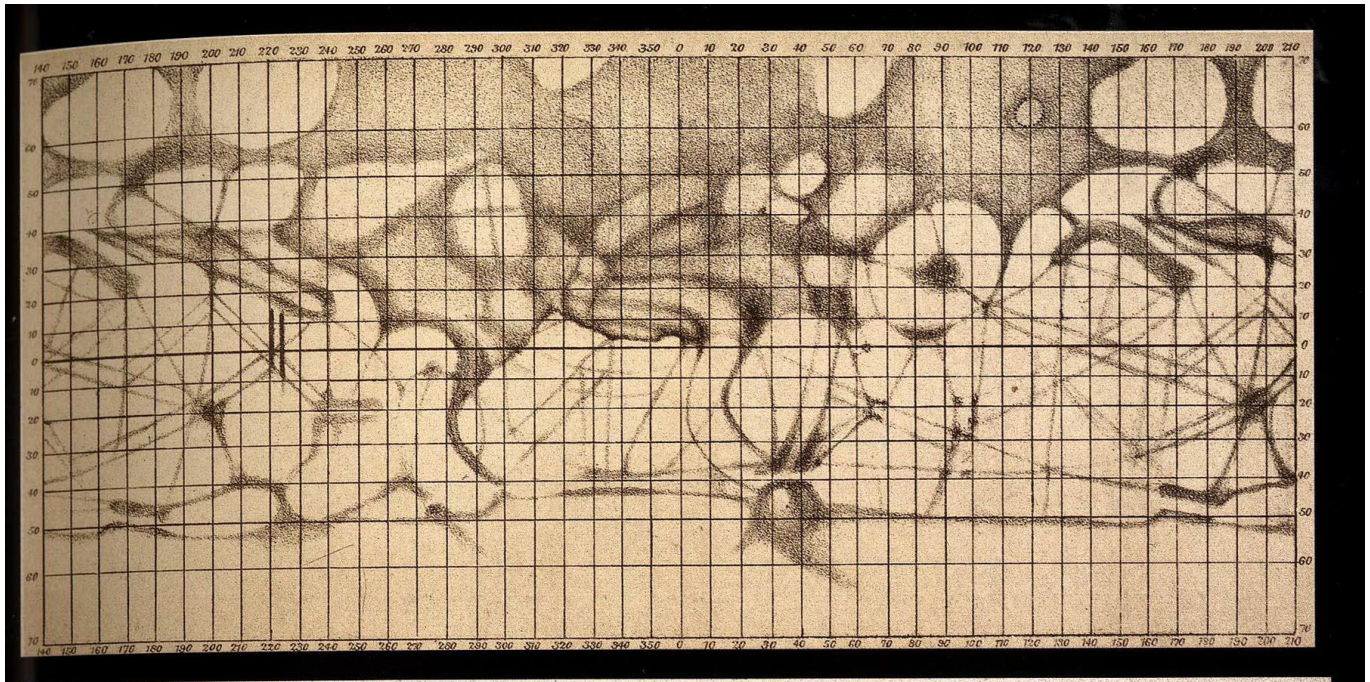

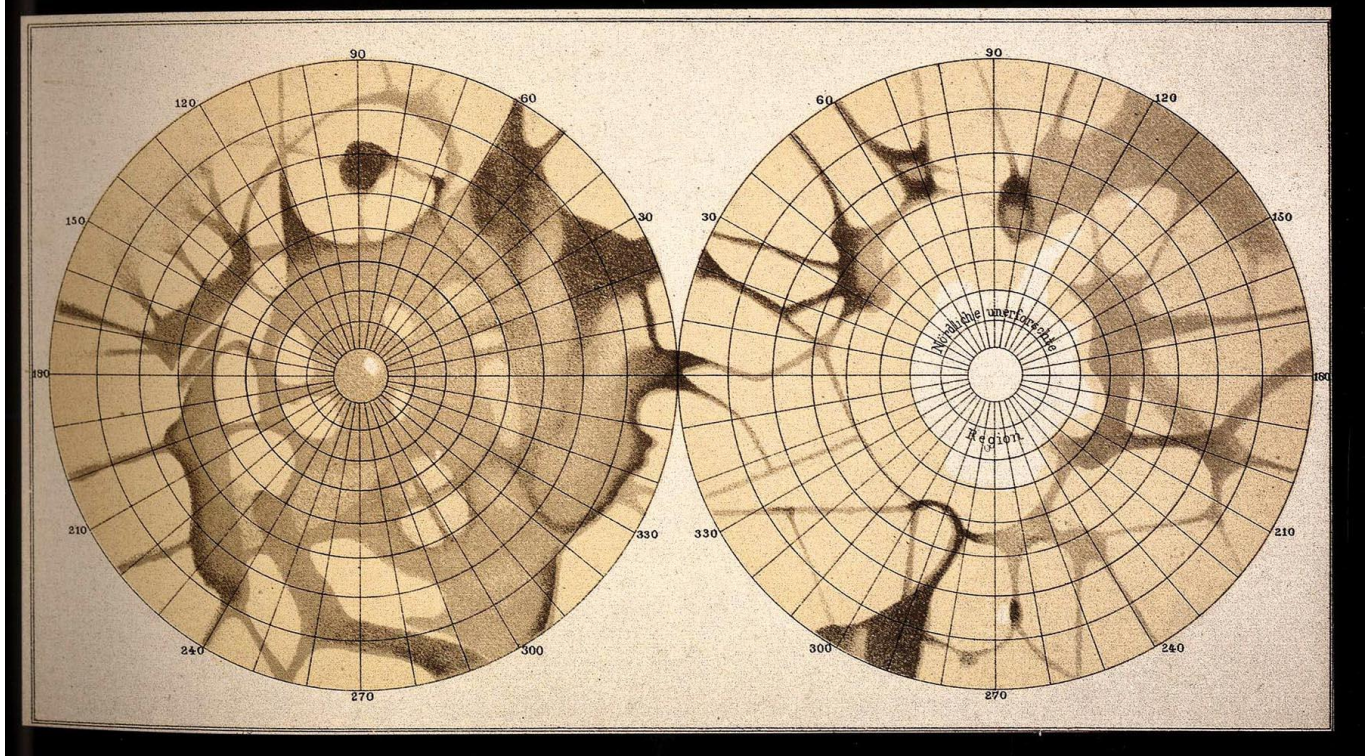
Nördliche unerforschte
Region

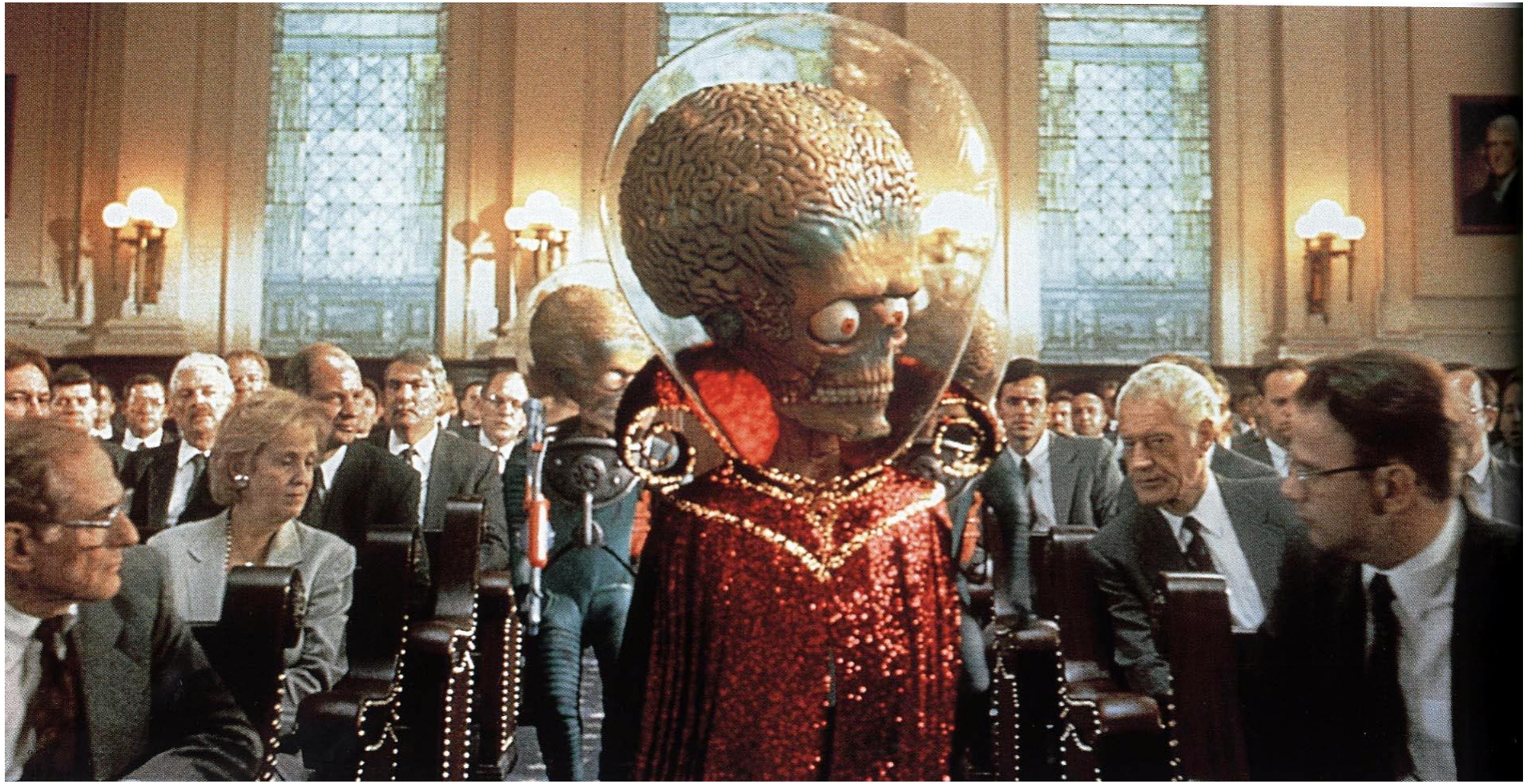

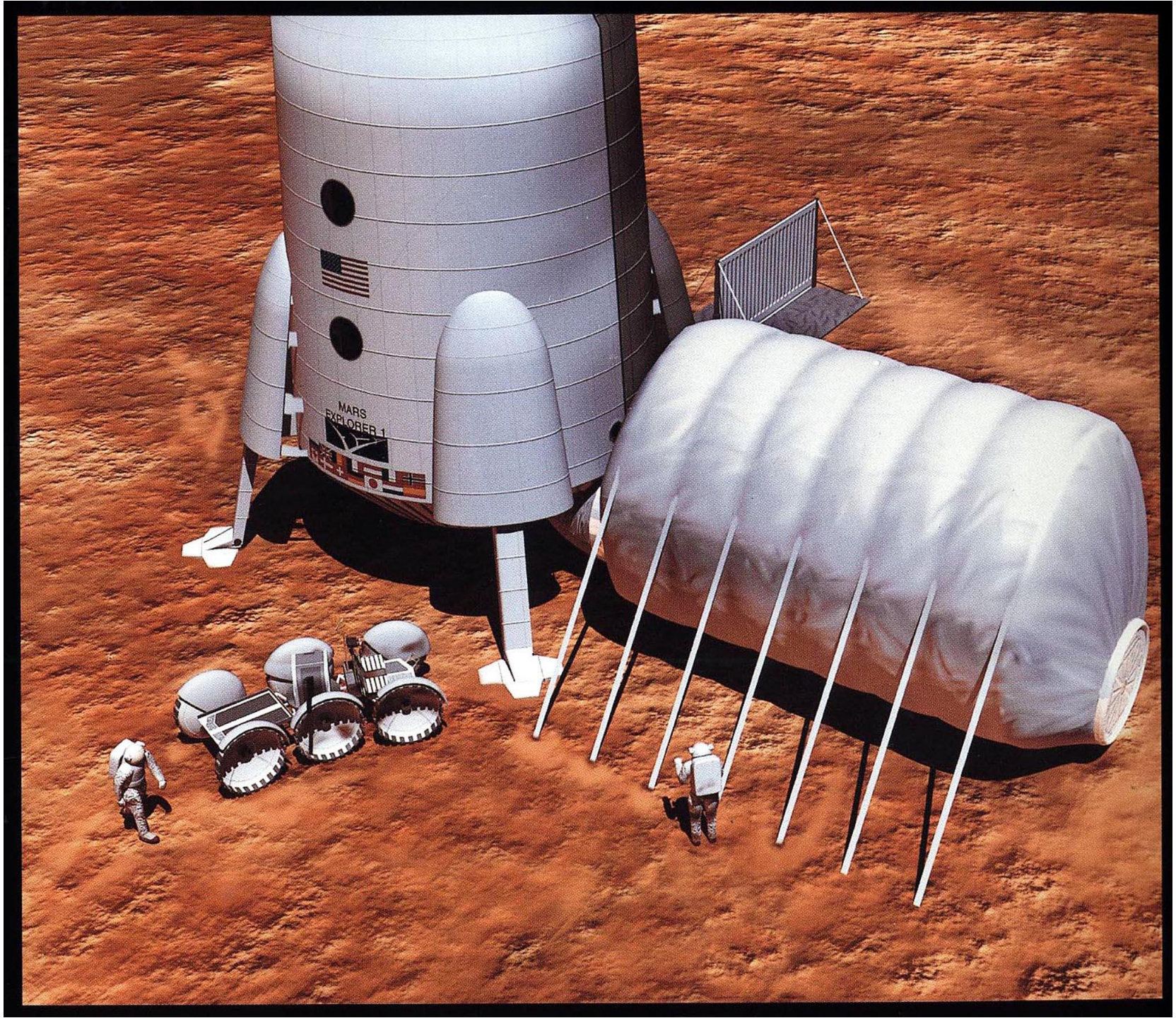
MARS
EXPLORER 1

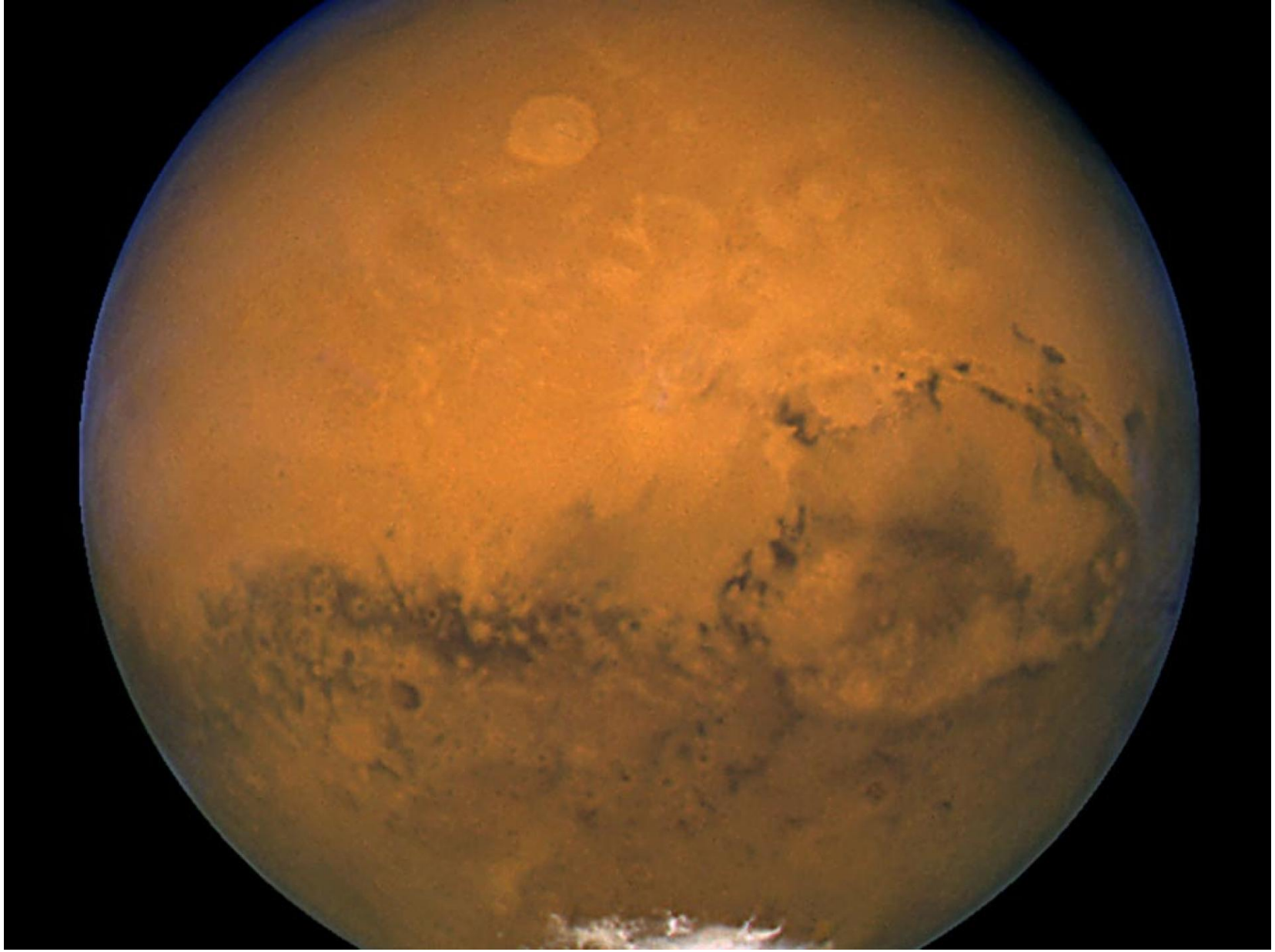

MARS NEARING EARTH

In 2003, the Hubble Space Telescope snapped this photo of the red planet 11 hours before its closest approach to Earth in 60,000 years. How close? It was a mere 34,648,840 miles (55,760,220 kilometers) away. The next closest approach will be in 2287.

PHOTOGRAPH COURTESY NASA

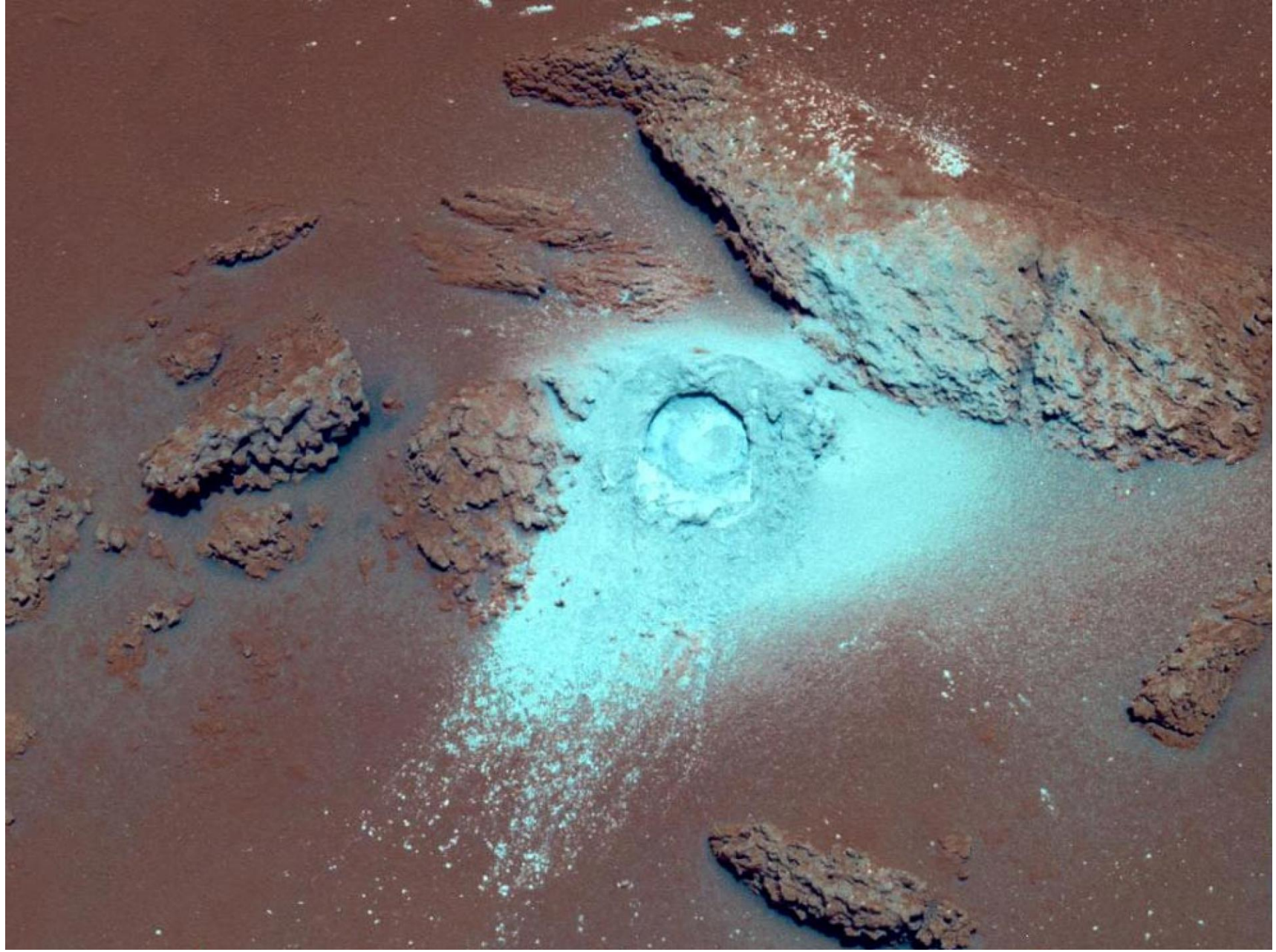

SULFUR-RICH ROCKS ON MARS

Sulfur-rich rocks in the Columbia Hills on Mars stand out in bright blue in this false-color image from the Spirit rover. Spirit used its rock abrasion tool, or RAT, to grind a hole in the rock. The rock's high sulfur content and softness are probably evidence of past alteration by water.

PHOTOGRAPH COURTESY NASA/JPL/CORNELL

MARS'S LOW RIDGE

The rover Spirit made this picture of the surface of Mars over 118 Martian days, or sols. (A sol lasts 24 hours, 39 minutes, and 35 seconds.) It was taken from a small hill known as Low Ridge—Spirit's wintering grounds.

PHOTOGRAPH COURTESY NASA/JPL/CORNELL

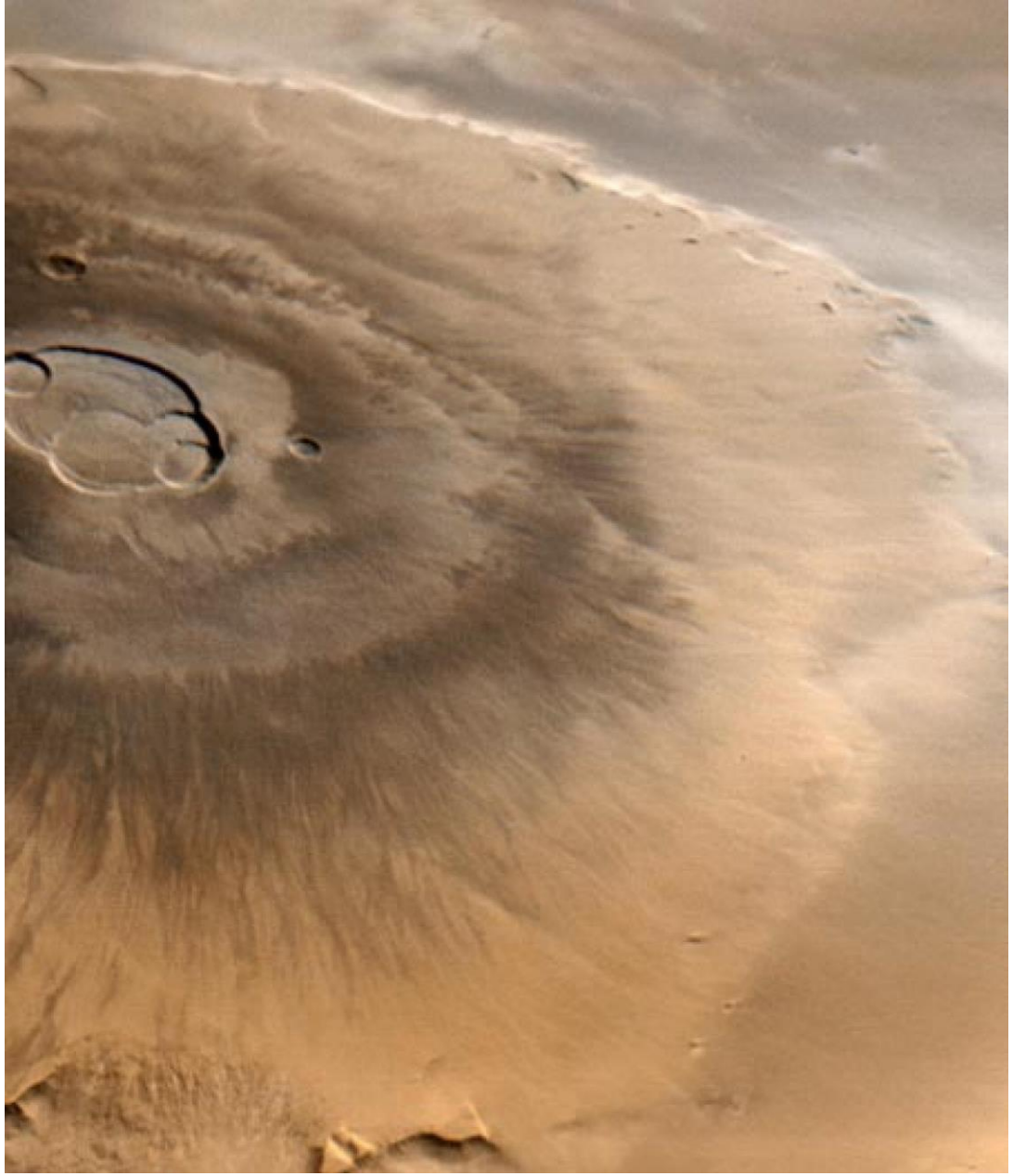

OLYMPUS MONS ON MARS

Looming larger than any volcanic mountain in the solar system, Olympus Mons on Mars is taller than three Mount Everests and is about as wide as the entire Hawaiian Islands chain. There's no dramatic summit, though—it's nearly as flat as a pancake.

PHOTOGRAPH COURTESY NASA/JPL/MALIN SPACE SCIENCE SYSTEMS

NEW COLOR
This piece of rock, dubbed Tintina, was crushed under one of Curiosity's wheels to reveal a surprisingly white interior. The minerals of the rock contain water, further suggesting the planet was once watery.
PHOTOGRAPH BY NASA/JPL-CALTECH/MSSS

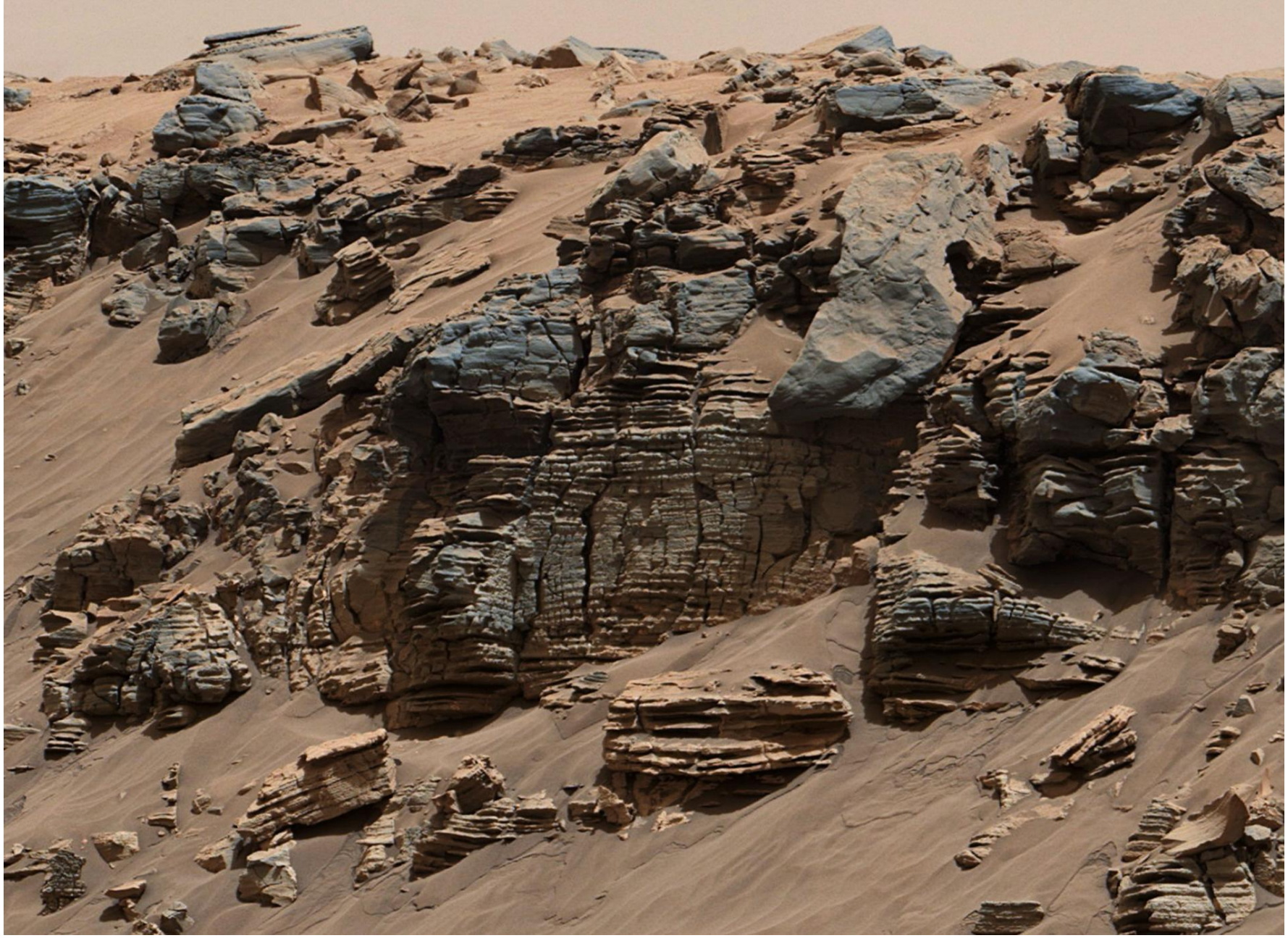

MARTIAN LAKE

Scientists believe that the even layers of this Martian rock were first deposited near the edge of an ancient lake, close to where water flowed into the basin. These formations are one of the many features that signal the planet's watery past.

PHOTOGRAPH BY NASA/JPL-CALTECH/MSSS

WALKING THROUGH TIME

Scientists believe that the layers of rock on the lower flanks of Mount Sharp will help them untangle Mars' geologic history. Scientists will examine the mountain layer by layer, as if leafing through the pages of a book.

PHOTOGRAPH BY NASA/JPL-CALTECH/MSSS

SUNSET ON MARS
The rover caught this stunning view of the sun setting over the rim of Gale crater on April 15, 2015. Unlike our red-hued sunsets, Martian views are tinted blue thanks to fine particles that allow more blue light into the atmosphere.
PHOTOGRAPH BY NASA/JPL-CALTECH/MSSS/TEXAS A&M UNIV

This image from Gale crater in 2018 prompted speculation that some shapes were worm-like fossils, but they were geological formations probably formed under water. (Wikipedia)

Panorama of Gusev crater, where *Spirit* rover examined volcanic basalts

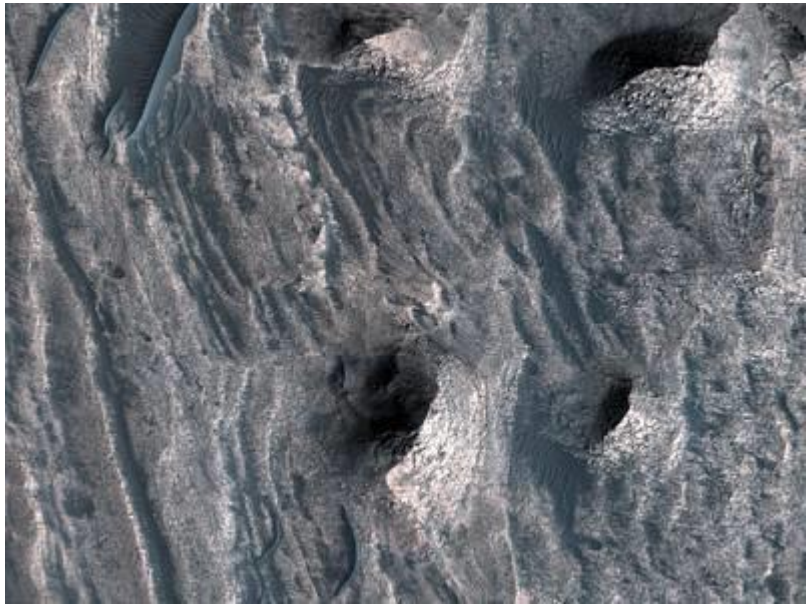
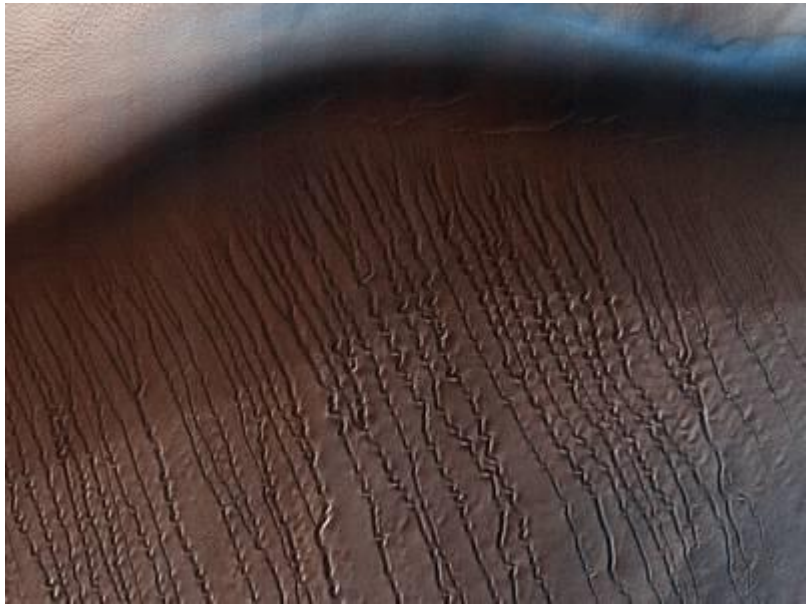

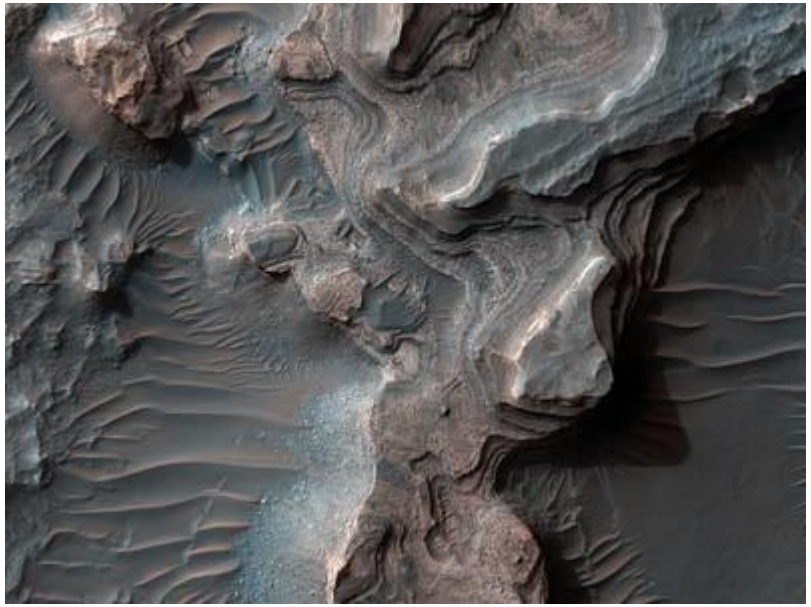

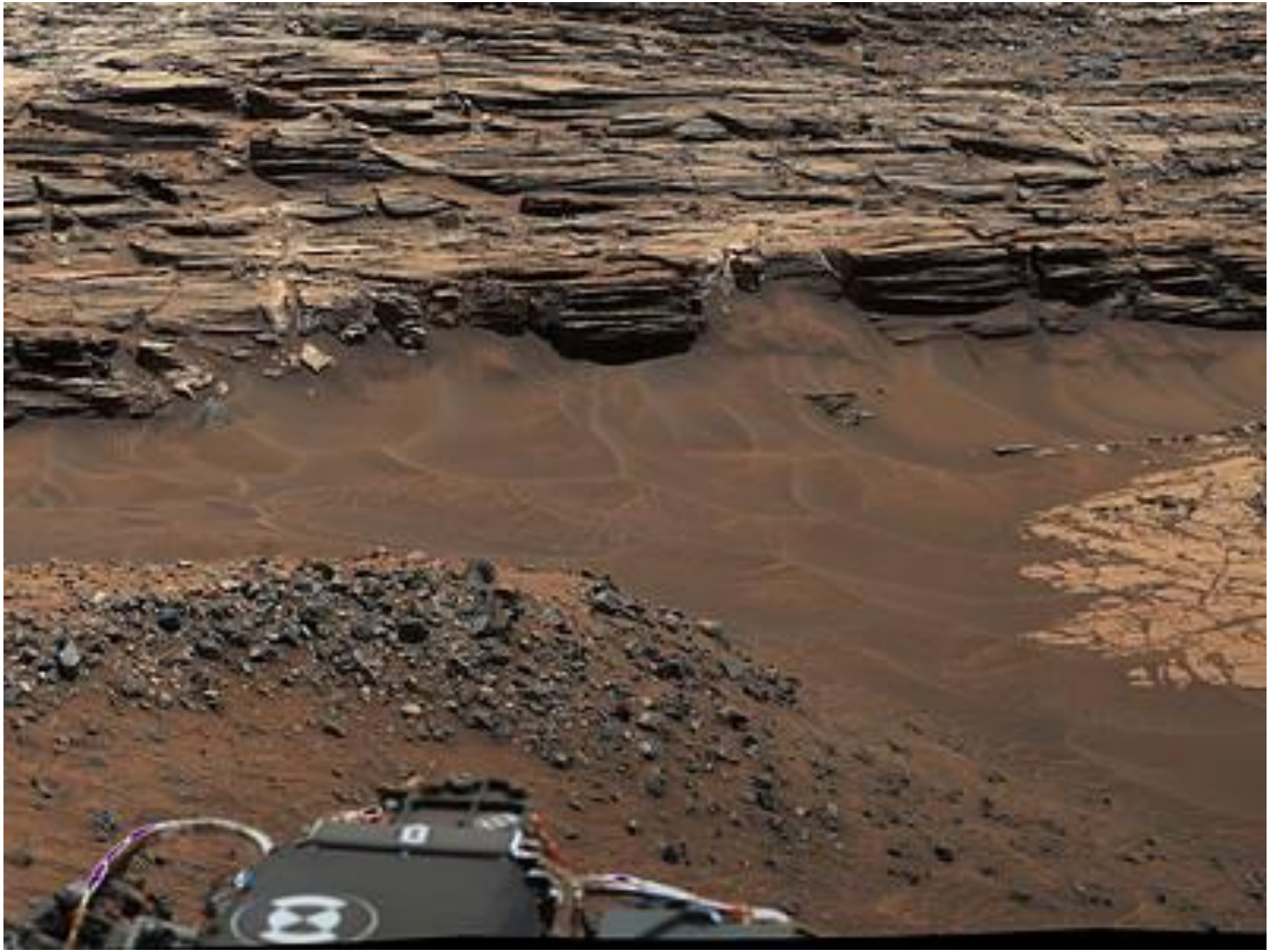

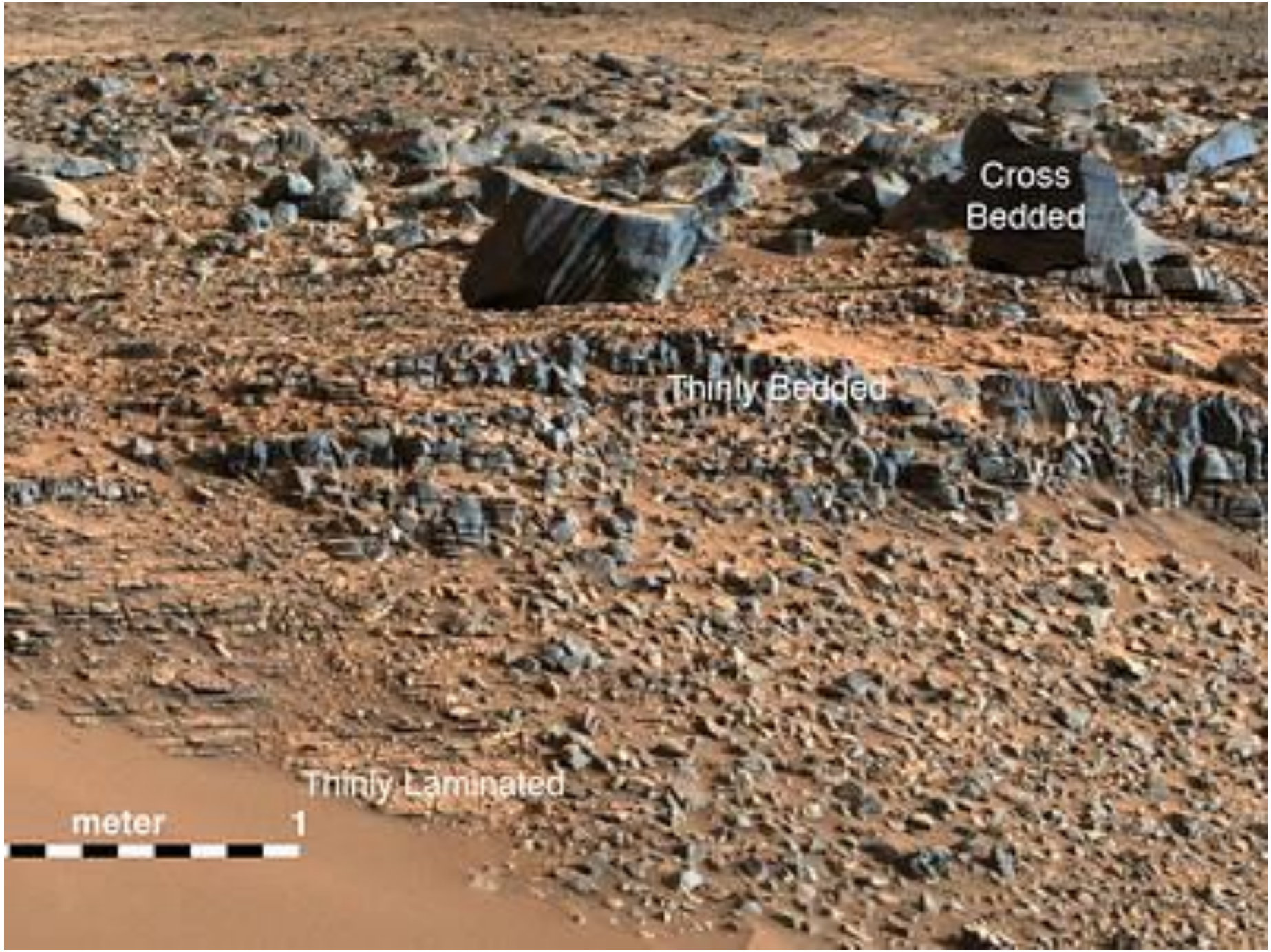
Cross
Bedded
Thinly Bedded
Thinly Laminated
meter
1

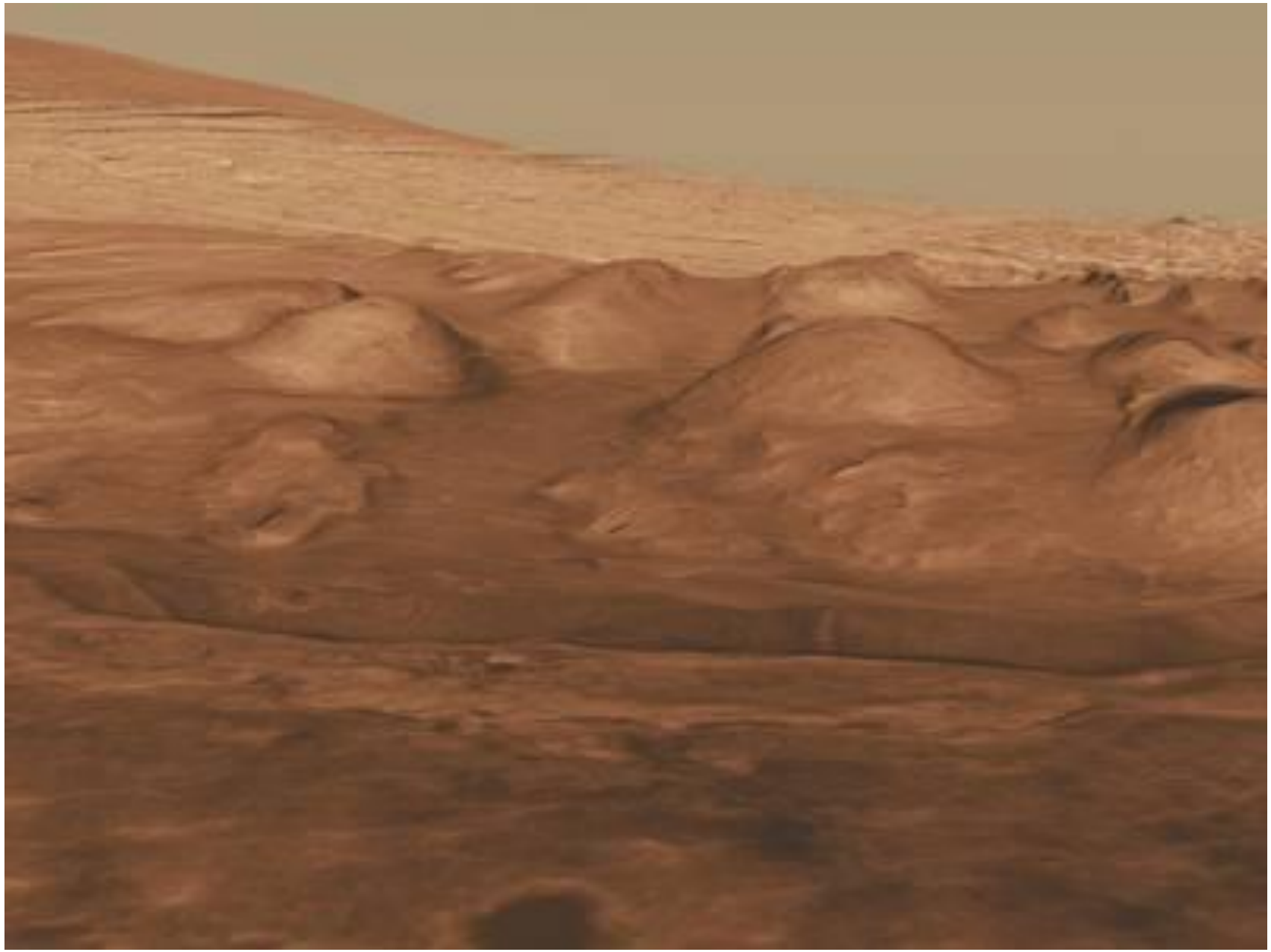

火星の研究が地質学の対象になった

- １　観測で分かったこと→火星の起源と歴史のモデルを立てること（作業仮説１）が必要；そのモデルを提案した（丸山ほか、アリゾナ大学G）
- ２　その前に、複雑系の科学の方法論と科学哲学の紹介（特に日本人はこの問題に無関心）→それをベースに宮本正太郎の貢献を評価しよう

複雑系科学の行方；串刺し科学と反証可能性

- 目次
- １近代科学の発展
- ２疑似科学と串刺し科学
- ３複雑系科学の研究の手法
- ４反証可能性（falsifiability, Carl Popper）
- ５結論

科学と技術の発展が加速度的に人類の理解を進めてきた

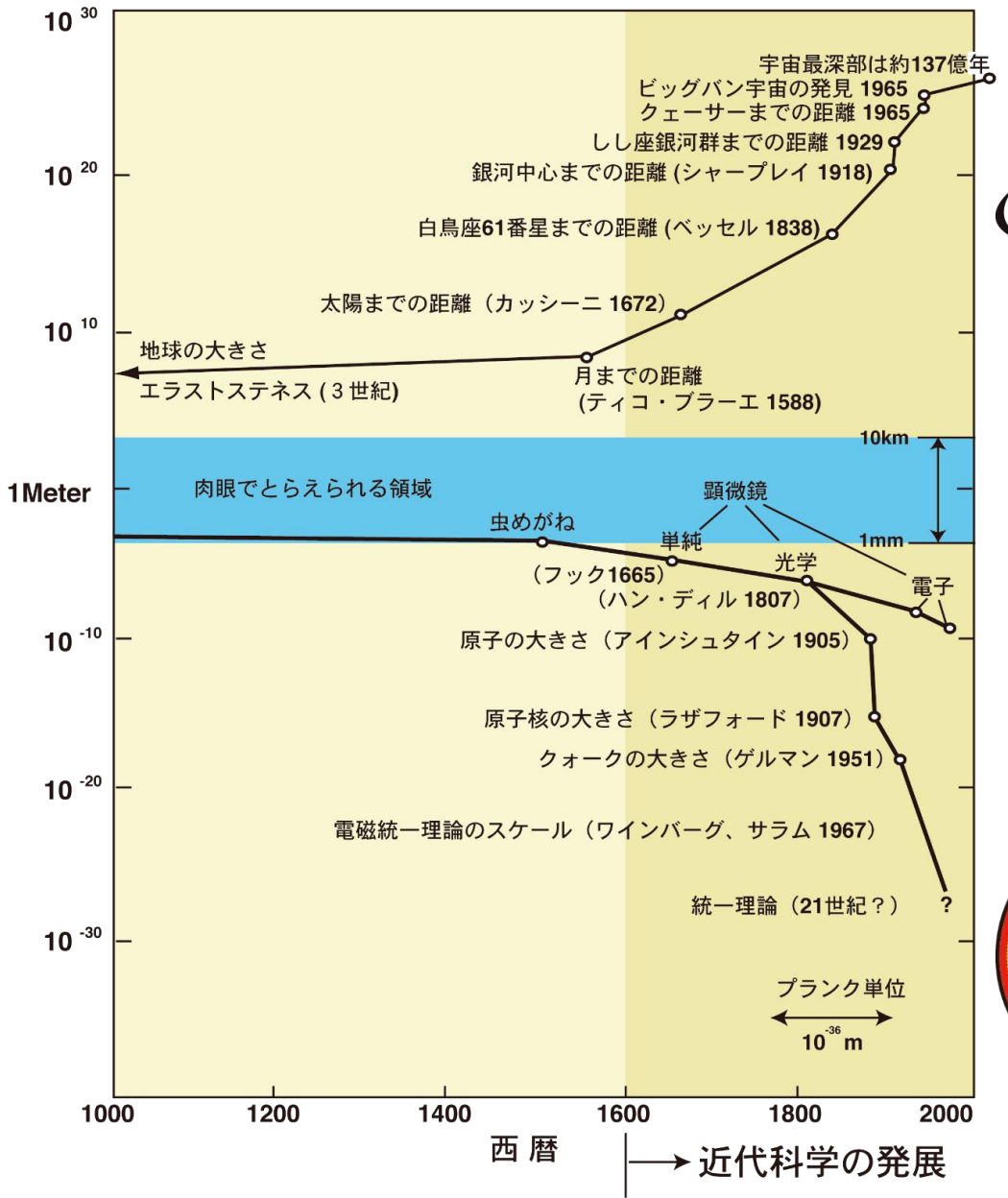

宇宙のはて

●実験・観測できる空間の飛躍的な広がり
→ 革命的な理解の飛躍を導いた。
- ゲノム科学
- 海洋地質
- 地球深部の観察
- 宇宙深部観測
- 素粒子物理学

●今世紀は超学際研究が更に加速する時代

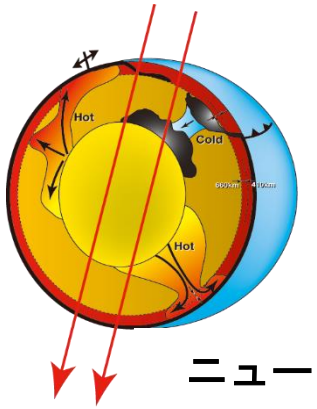

ニュートリノ

その裏面に出てくる問題

↓

疑似科学の横行

疑似科学とは何か？

科学的に正しいものであるかのように説明している提案

あるいは

反証可能性のないモデル

疑似科学の具体的な例

1. P/T境界の新説：洪水玄武岩起源CO_2によって地球が温暖化。
   その結果、90%を超える大型生物が絶滅した （古生物学）
   地質記録によれば温暖化などしていない
2. 生命の起源に関する新説：毎日数万トンの有機物が地球に降り注ぎ、地球生命へと進化した（アストロバイオロジー）
   有機物は宇宙から地球にほとんど降り注いでいない
3. エンスタタイトコンドライトは水を含んでいる（隕石学）
   エンスタタイトコンドライトは水を含んでいない
4. IPCCによる過去の気温曲線（気候学）
   中世の温暖期を完全に無視した気温曲線を採用

その他、枚挙にいとまがない

疑似科学の手法：串刺し科学

- 自分のモデルを説明するために都合のよい観測事実だけを採用する
- 自分のモデルの反証となるデータは一切引用しない

- たとえばP/T境界の新説（Wignall, 2007）の場合
  なぜ古生代ー中生代境界で大量絶滅が起きたのか？

疑似科学の手法：串刺し科学

P/T境界の理解（共通認識）：火山活動によるCO2の増加と酸素の現象がこの時代にあった　→では大量絶滅の原因は？

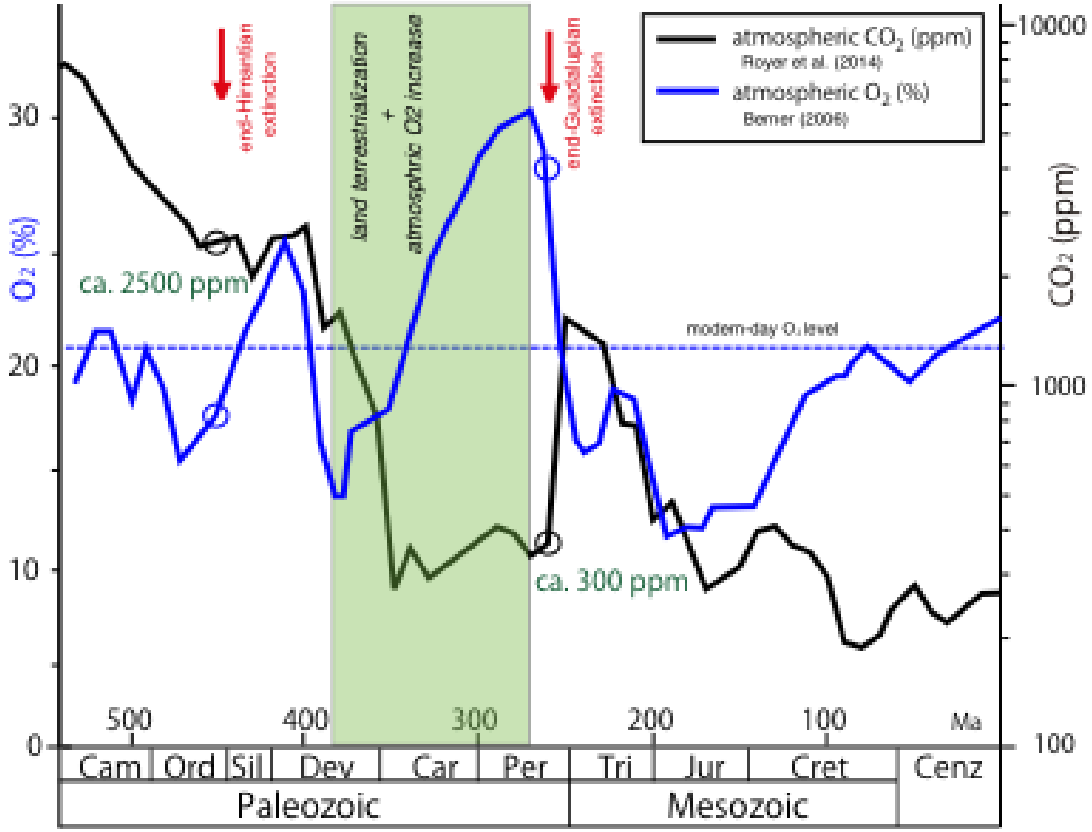

Isozaki & Servais, (2018)

疑似科学の手法：串刺し科学

1）Wignall(2007)による提案：
「洪水玄武岩によるCO2の増加が温暖化を引き起こし
その結果大量絶滅」

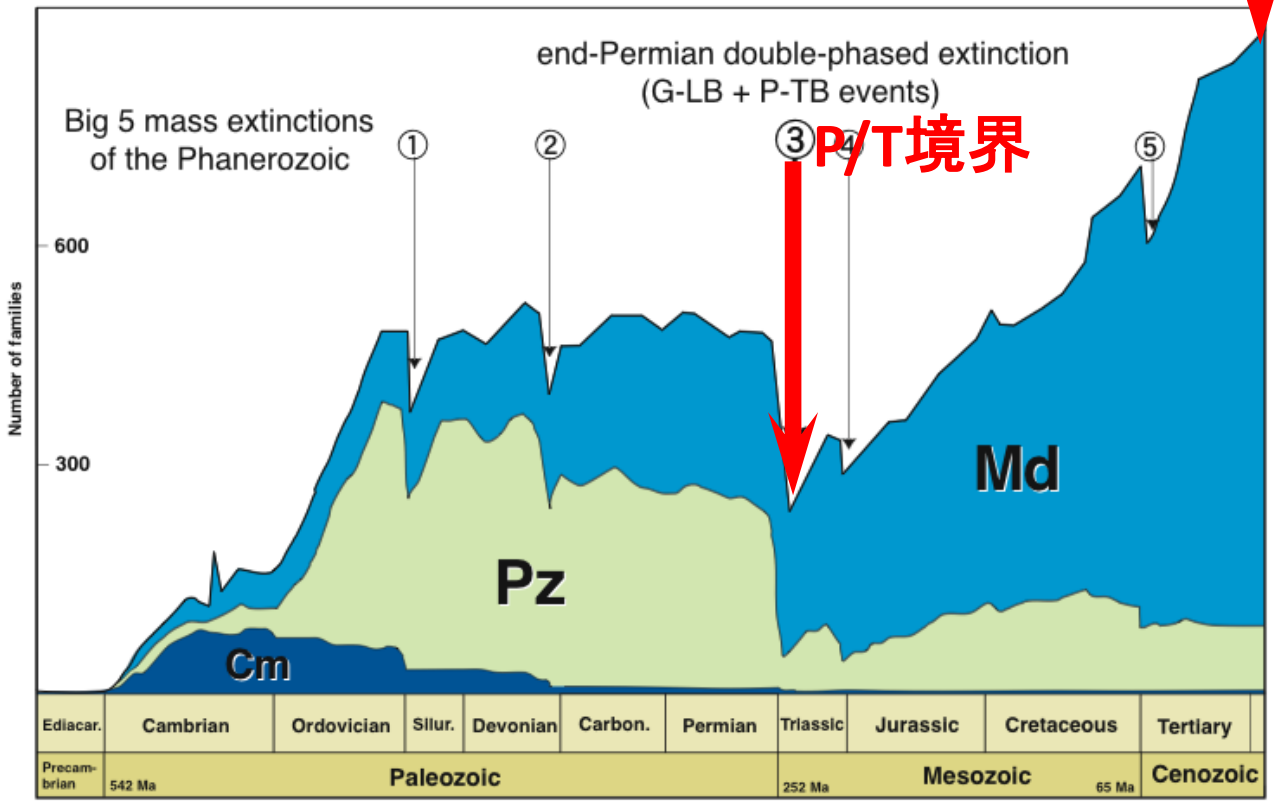

現代の大量絶滅

人為起源CO_2による地球温暖化が21世紀末に人類を含む大量絶滅を引き起こすと説明した

疑似科学の手法：串刺し科学

２）Wignallが無視した事実：

P/T境界は寒冷な時代

◇氷河の存在

◇海水準最低時代

◇ Sr同位体比

→　疑似科学の手法

P/T境界の大量絶滅は人為起源CO2による地球温暖化が21世紀末に人類を含む大量絶滅を引き起こすとする「現在の社会情勢」を巧みに利用し、科研費獲得を目指す。

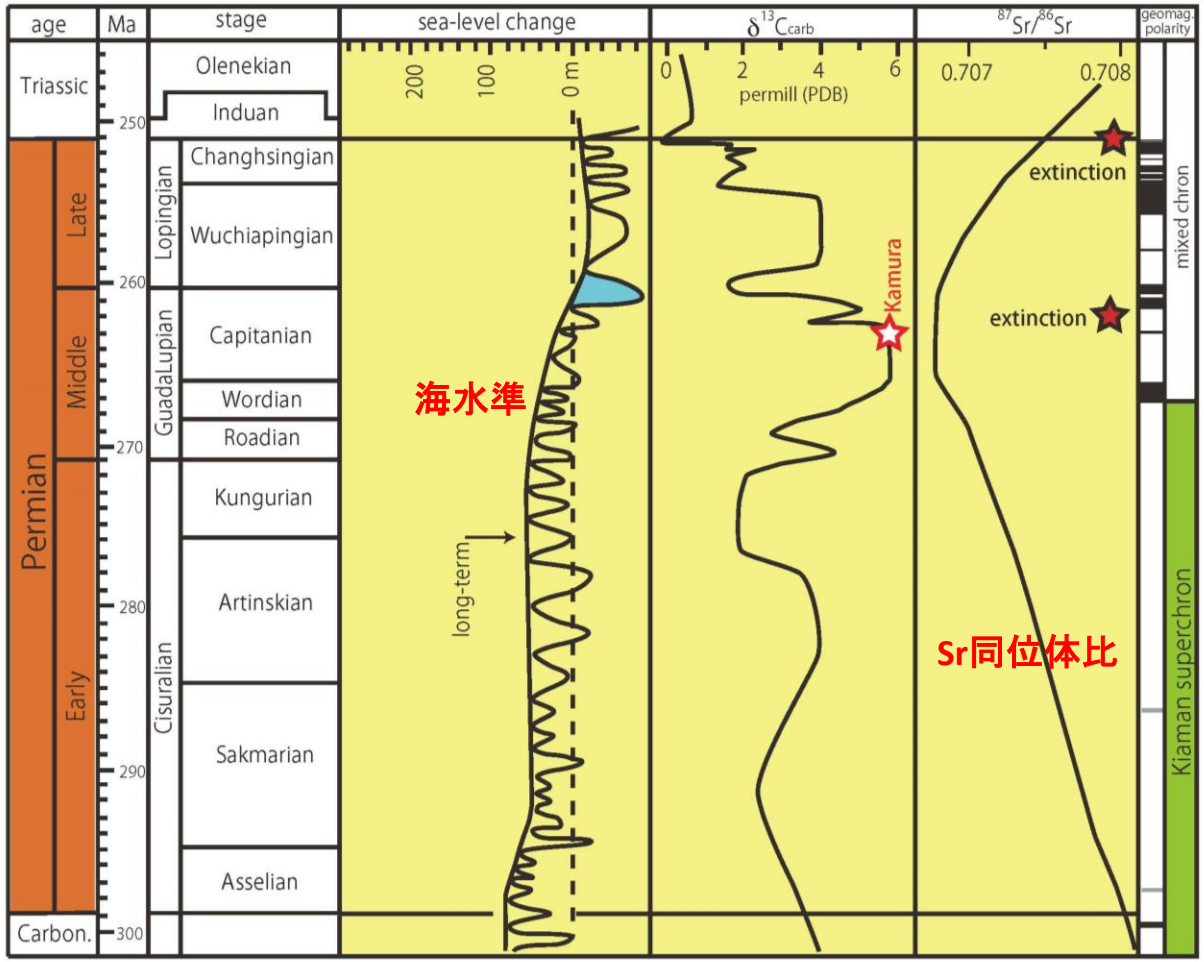

Isozaki & Servais, (2018)

社会が科学に重大な影響を与える時代

1. 近年の業績至上主義の結果、新しいモデルや斬新なアイデアを発表するために疑似科学や串刺し科学が横行
2. 科学者の思想の低下
   大学や研究所の教授職についたあとは、研究活動などしない
3. 組織に埋没する
   組織の本来の目的を忘れ、自己の権利に執着し、自己主義的にふるまう→内部崩壊の始まり

●研究者は真実に対して誠実であるか？

→　幻想にすぎない

複雑系科学研究の進め方

複雑系科学の発展の法則

●天文、惑星、地球科学、生物学、化学、物理学の全分野

1）記載の時代
2）分類の時代
3）成因論や仮説を提案する時代

●複雑系科学の方法論
数学
熱力学
電磁気学
統計学
ニュートン力学

→方法論は物理学者が創った

	天文学	惑星科学	地球科学	生物学	物理学
1. 図鑑の時代 どこにどんな物体があるかの記載の時代		①第I期図鑑の時代 （コペルニクス 1473-1543） （ブラーエ 1546-1601） ②第I期分類の時代 （ガリレオ, 1564-1642） ③第I期体系化の時代 （ケプラー 1571-1630）	①図鑑の時代	①第I期図鑑の時代 ②第I期分類の時代 （リンネ, 1707-78） ③第I期総合化の時代 （ダーウイン, 1809-82）	（デカルト, 1596-1650） （ニュートン, 1647-1727） 物理学の充実
2. 分類の時代 系統樹を作り 血縁関係を調べる		①第II期図鑑の時代	②分類の時代 （1970-1980） プレートテクトニクス ③総合化・体系化の時代 （より深部へ, より昔へ）	①第II期図鑑の時代 （分子生物学）	黄金時代 （20世紀）
3. 総合化・体系化の時代 最もおいしい時代		②第II期分類・系統樹の時代 ③第II期統合化・体系化の時代		②第II期分類・系統樹の時代 ③第II期統合化・体系化の時代	21世紀

専門細分化の時代

地球学の体系化(社会科学との融合)

複雑系科学の研究の方法と理論の構築

1. 記載→分類→成因論（理論）
2. 作業仮説を立てて、実証/検証する。
3. 現実的には実証は不能だが反証は可能（科学哲学）
4. 反証可能性（Falsifiability, Karl R. Popper, 1902-1994）によって、科学は発展する。

反証可能性とは
（Falsifiability, Karl Popper）

●100羽の黒いカラス；（1）経験則（実験式）の限界、（2）反証の重要
●理論的背景を持つ新たな手法が導入されると作業仮説が「法則」に昇格する
例：遺伝子科学において、突然変異のメカニズムが解明される

総合化の時代のプロセス
1）モデル（作業仮説）が提案される。
2）モデルの検証が始まる。たった一つの反証によってモデルが否定される。
3）反証を包含する新たなモデルが提案されて、モデルは少しずつ真実に近づく

研究を前進させるには、
新たな研究手法の提案と技術の開発が鍵

５結論

1. 現在は超学際研究の時代である。
2. 複雑系科学の研究では疑似科学や串刺し科学が横行している。
3. 反証可能性の重要性を改めて理解しよう
4. 反証可能性によって、複雑系科学のモデルは真実に近づく

（ホイッグ史観と複雑系の科学の発展）

- １天動説と地動説
- ●はじめに：我々後世の科学者は「天動説の提案者は悪玉で、地動説の提案者が善玉だ」と評価しがちである。この評価は間違っている。論争の時代に遡って、当時の観察事実に基づいた議論と評価が最も大事な視点で評価しなくてはならない＝ホイッグ史観。
- ●コペルニクス（地動説の提案者）は教会から批判されず、なぜガリレオ（Galileo）が激しく糾弾されたのか？当時の惑星の軌道を説明する上では天動説も地動説のどちらでも数学的に説明できた。Galileoは高解像力の望遠鏡を創って観測して、惑星が周期的に大きくなったり小さくなったりするが太陽はそうならないことを説明できるのは地動説だといって論争に決着

1.宮本正太郎と月・火星

- 月の表層のクレータは火山起源か隕石衝突か？
- 望遠鏡の観察（クレータが巨大すぎるが決定的証拠ではない）
- アポロ計画で、決着（＋衝突実験、月の地質、年代他）
- 隕石衝突（サイズとプロセス）→惑星形成論が加速
- 我々はホイッグ史観に囚われていないか？
- ローウエルの火星運河と火星人説は疑似科学か？

火星

火星の起源と進化に関する新事実（火星の観測：地球物理学、地質学、隕石学）から火星の起源と進化のモデル＝検証可能な作業仮説を提案する

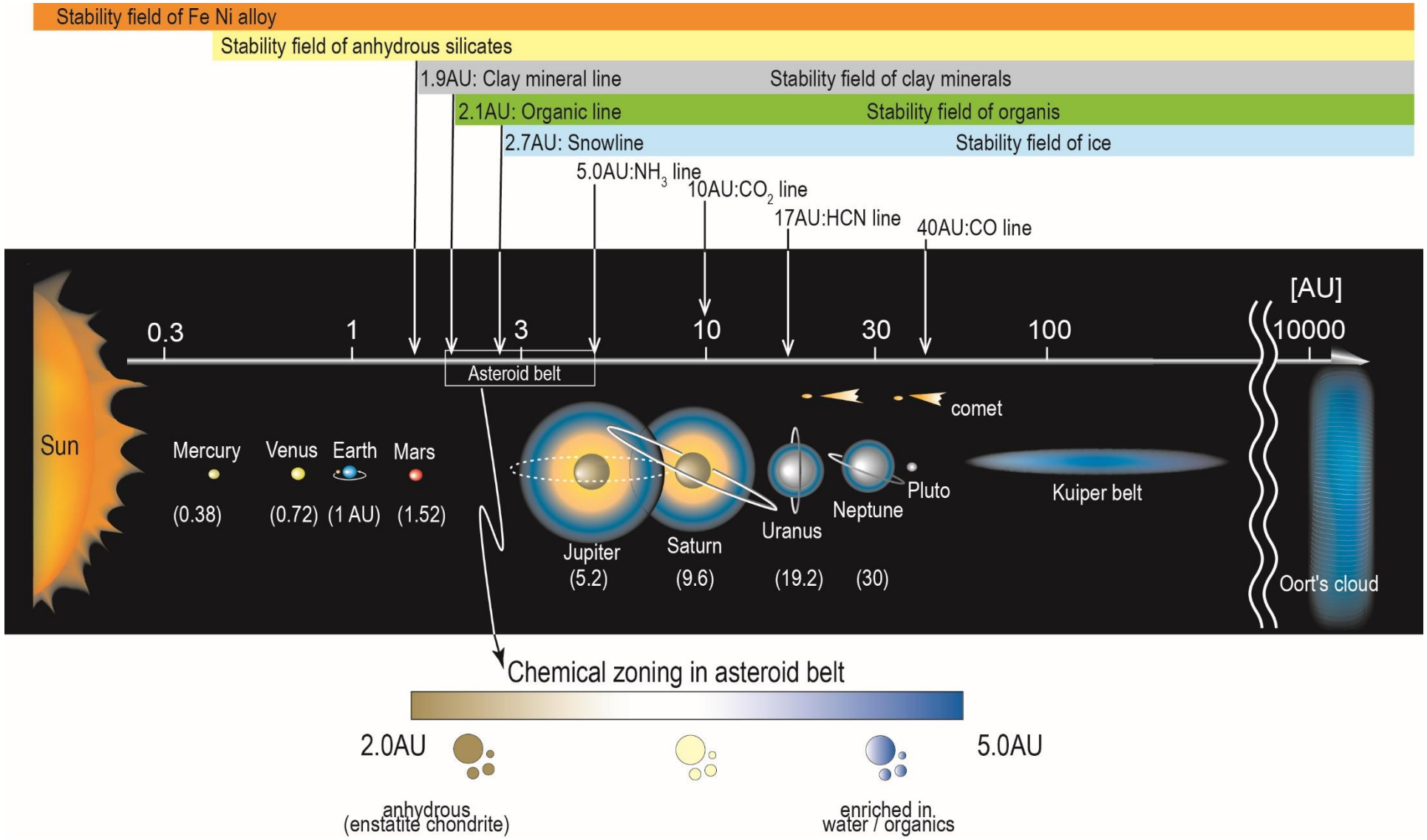

Maruyama & Ebisuzaki, (2016)

火山活動、海洋の安定性

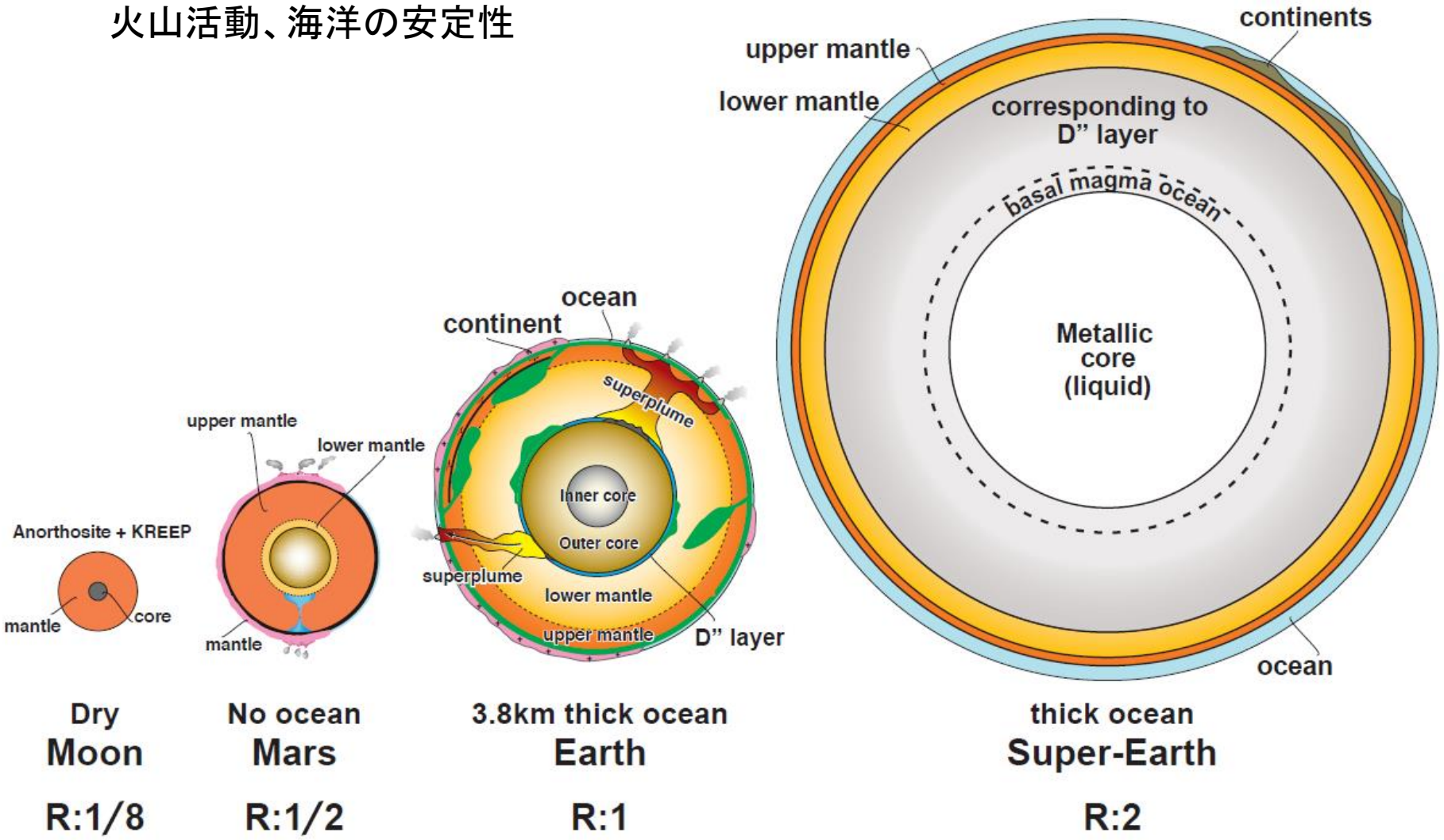

Maruyama et al., 2013

Appropriate size

Venus < size < 2RE?

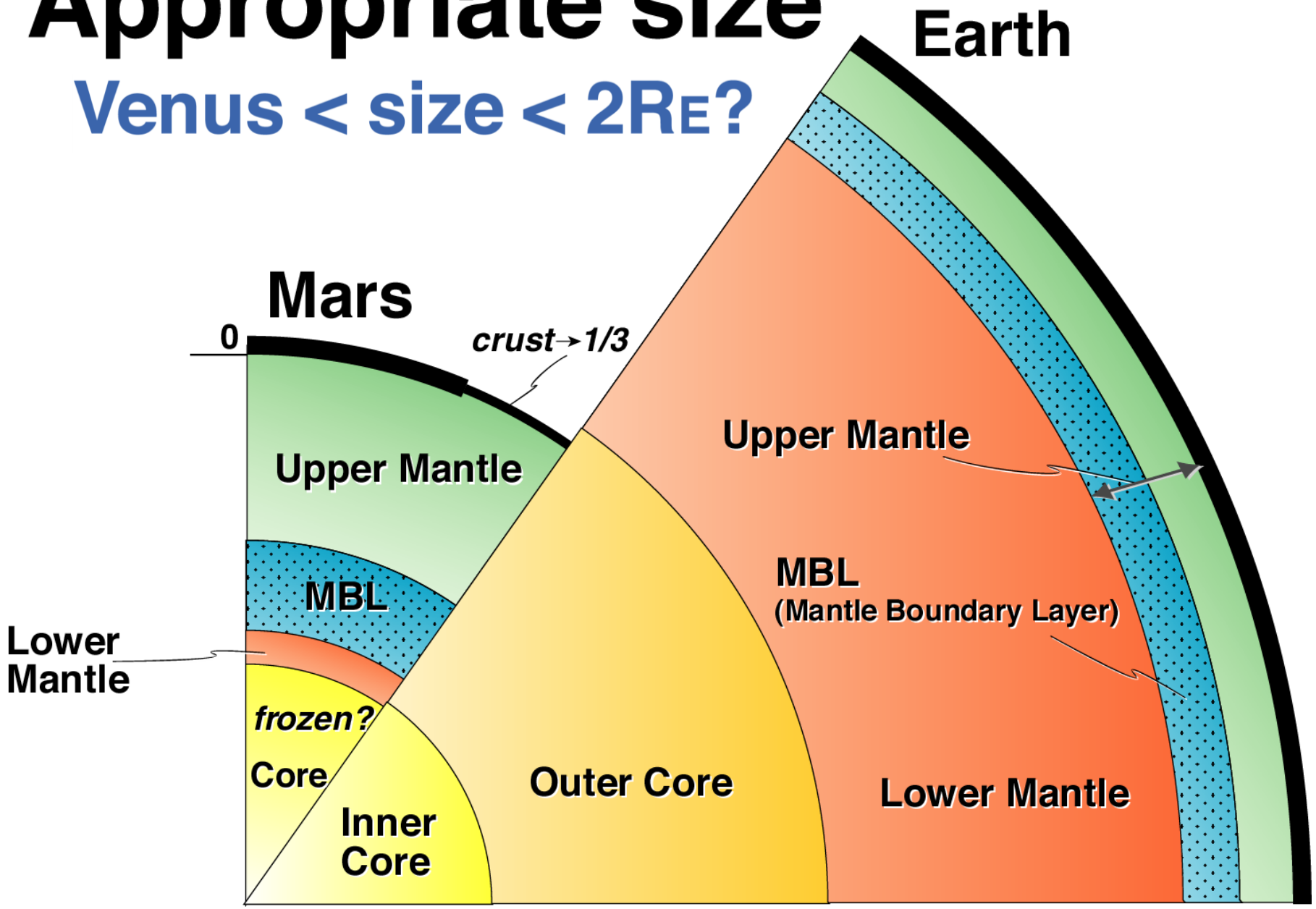

Mars Topography, MARS GLOBAL SURVEYOR, NASA

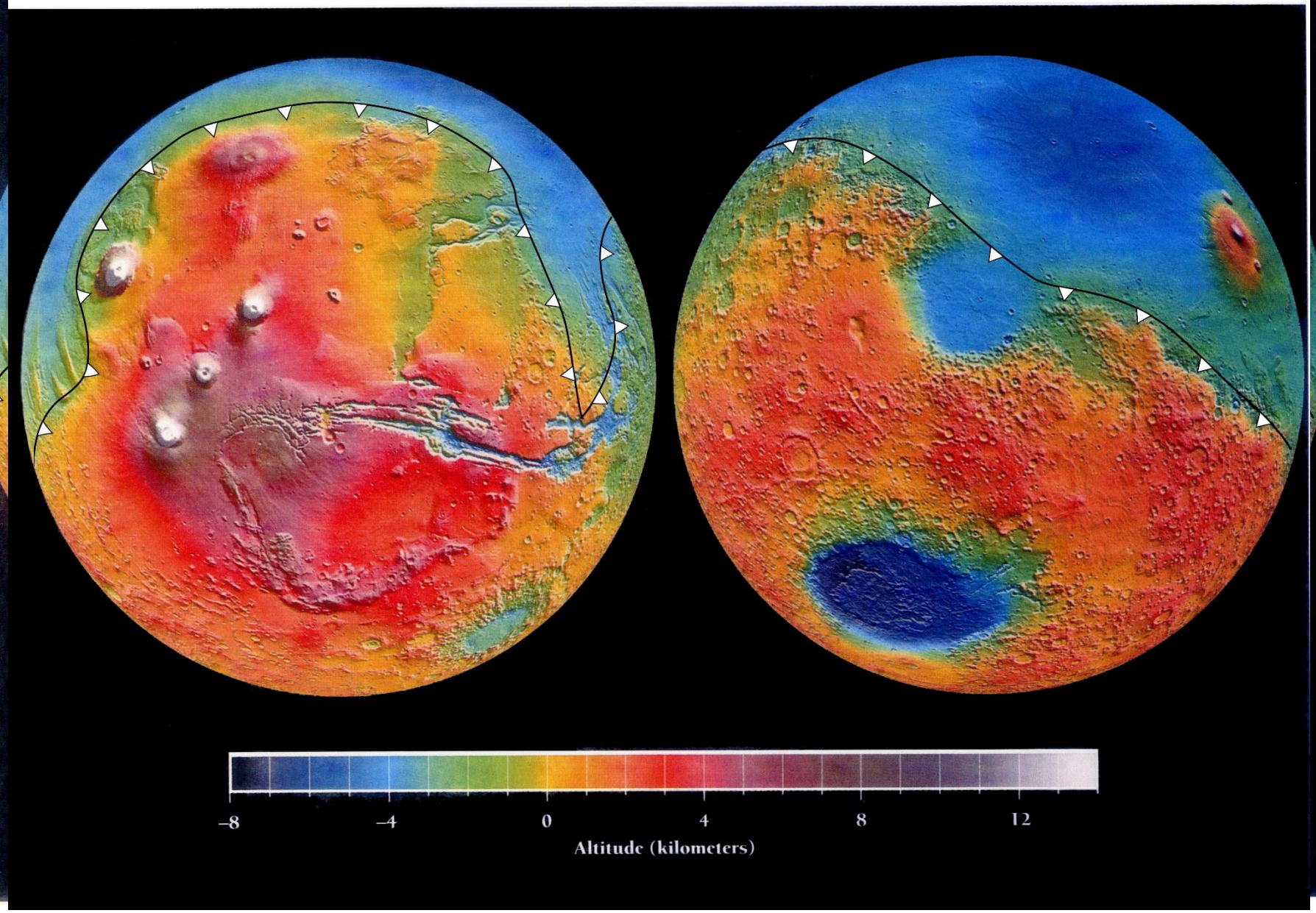

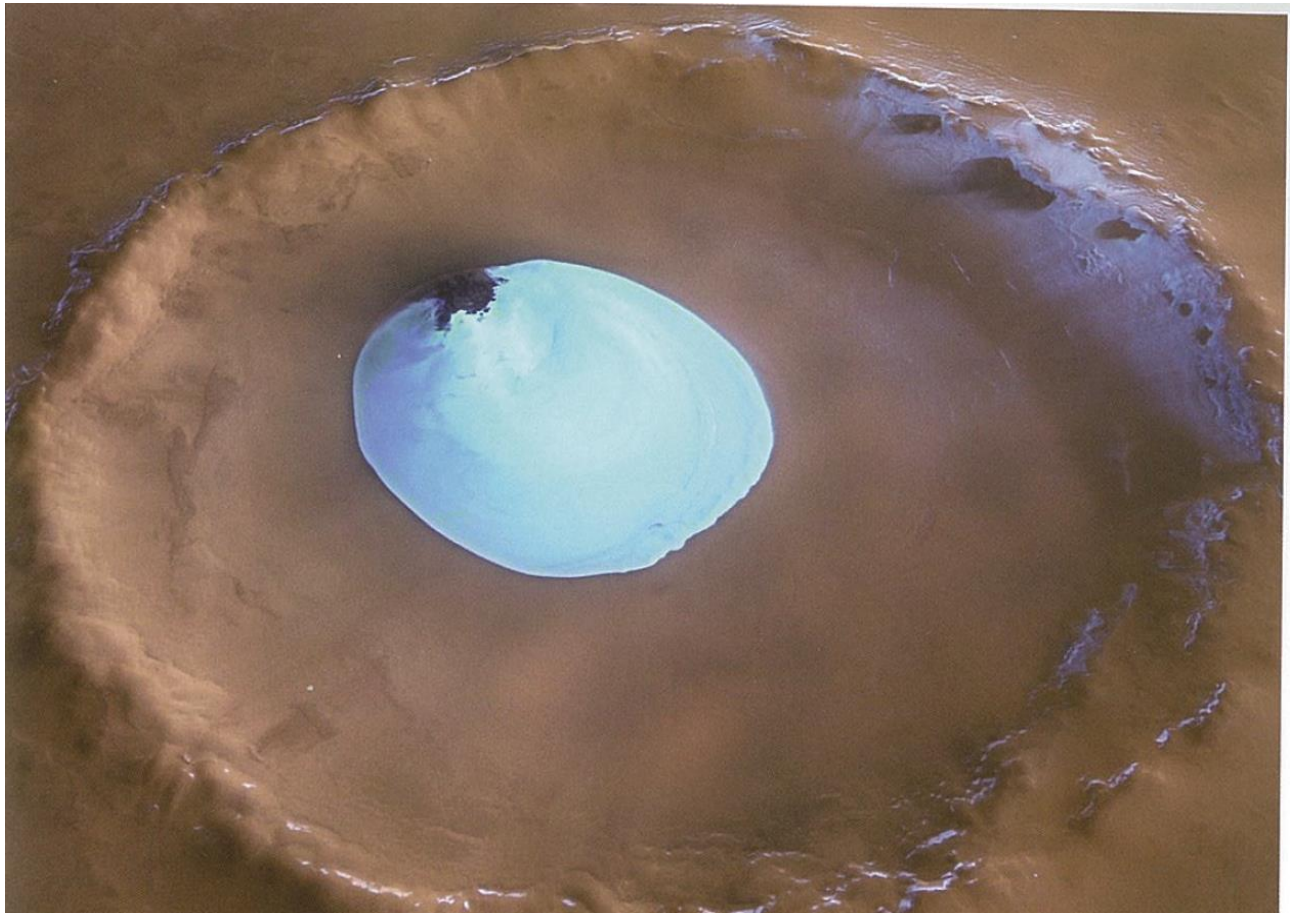

Sparrow (2012) The Universe, Quercus Editions Ltd.

火星表層を覆った海水の総量

- １ 現在の火星表層の水（極冠＋クレータ内部の氷河＋つらら）
- ２ 厚い堆積岩層（＞9km、マリネリス峡谷の崖）
- ３ オリンポス火山（卓状火山の崖、9km→9kmの厚さの巨大氷床の存在）
- ４ 北部低地の厚い堆積物中の間隙水を絞り出すと600m程度の海
- ５ 論争（地中海の海洋質量程度 vs 9kmの厚さの海洋が火星表層の1/3-2/3を覆った（40億年前）→多くは後にマントルへ吸収された→太陽風で水素が宇宙に選択的に散逸

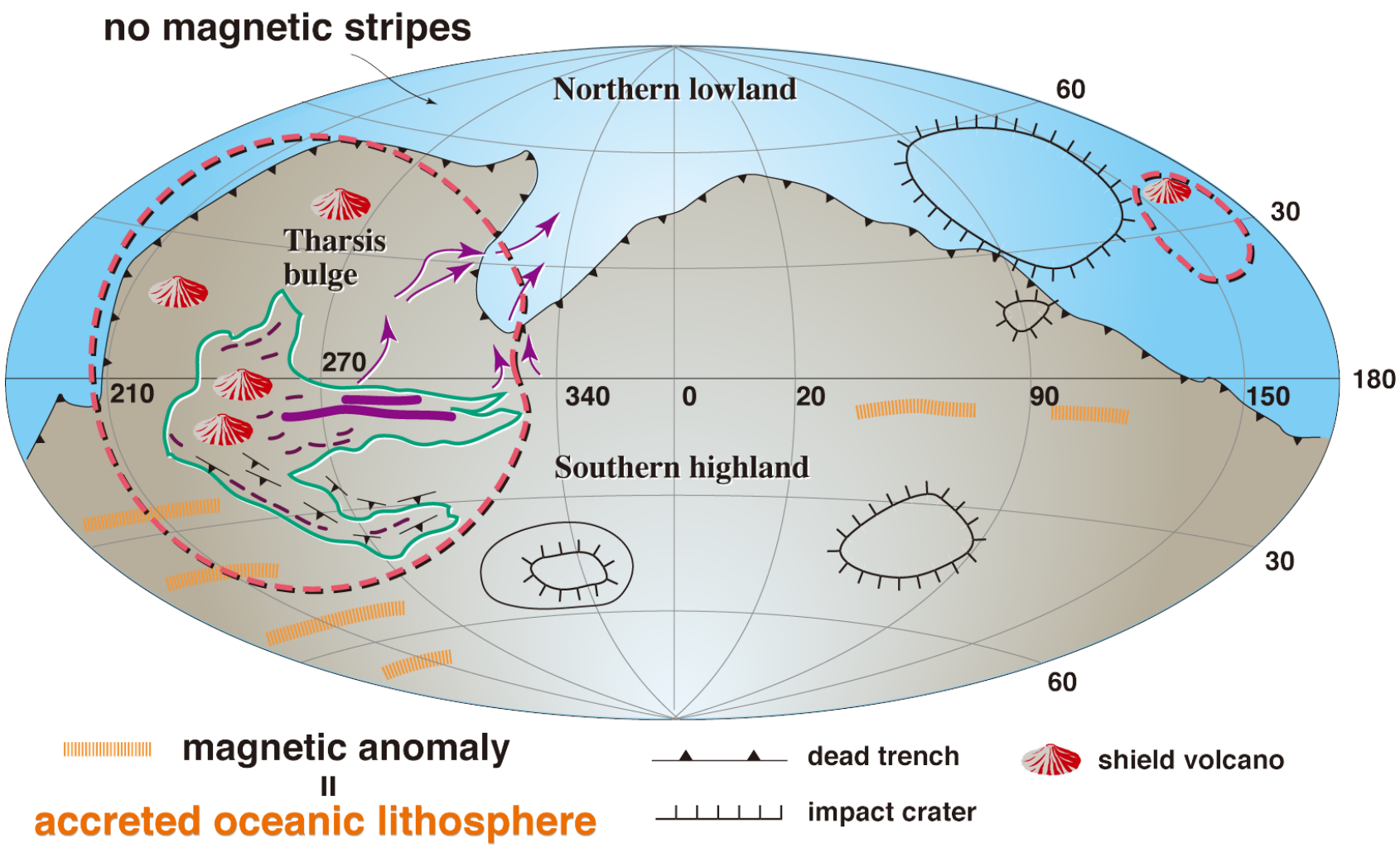
no magnetic stripes
Northern lowland
Tharsis bulge
Southern highland
60
30
180
150
90
20
0
340
270
210
30
60
magnetic anomaly
II
accreted oceanic lithosphere
dead trench
impact crater
shield volcano

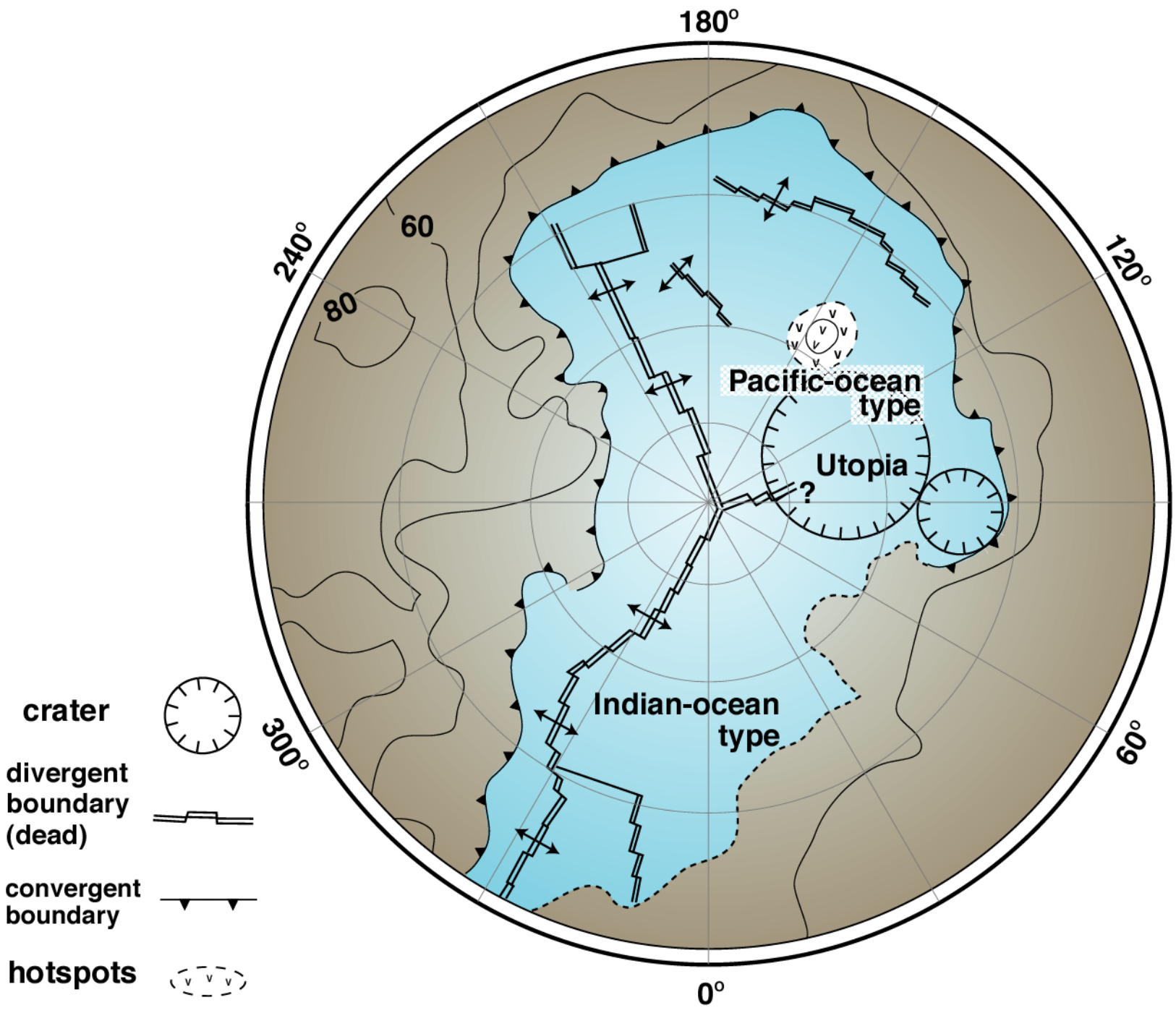
180°
120°
60°
0°
300°
240°
60
80
Pacific-ocean type
Utopia
?
Indian-ocean type
crater
divergent boundary (dead)
convergent boundary
hotspots

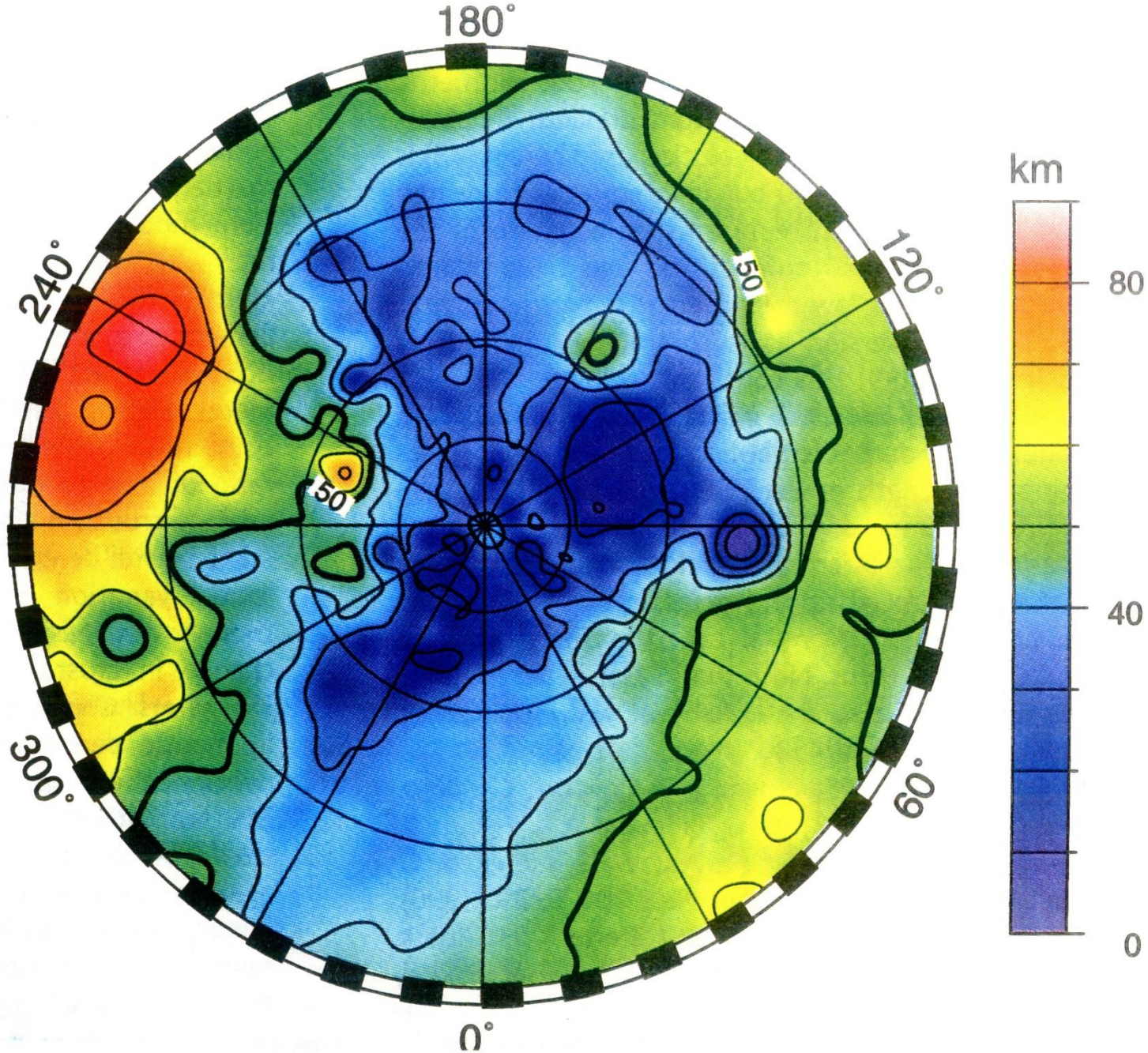
180°
240°
120°
300°
60°
0°
50
150
km
80
40
0

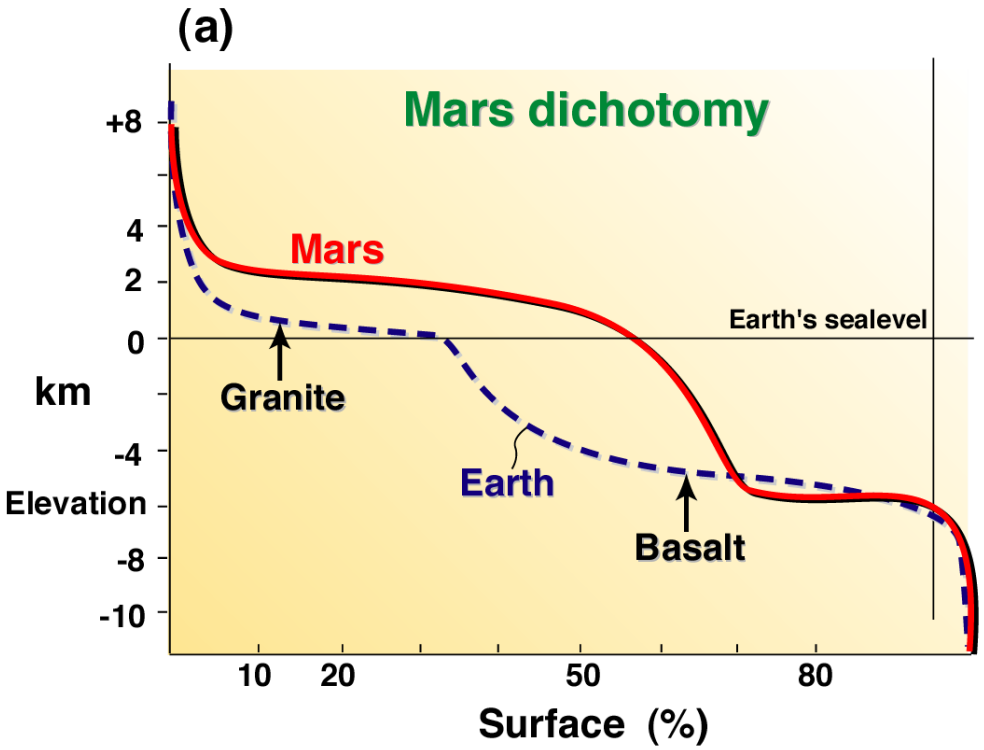
(a)
Mars dichotomy
+8
4
2
0
-4
-8
-10
km
Elevation
Mars
Earth
Granite
Basalt
Earth's sealevel
10
20
50
80
Surface (%)

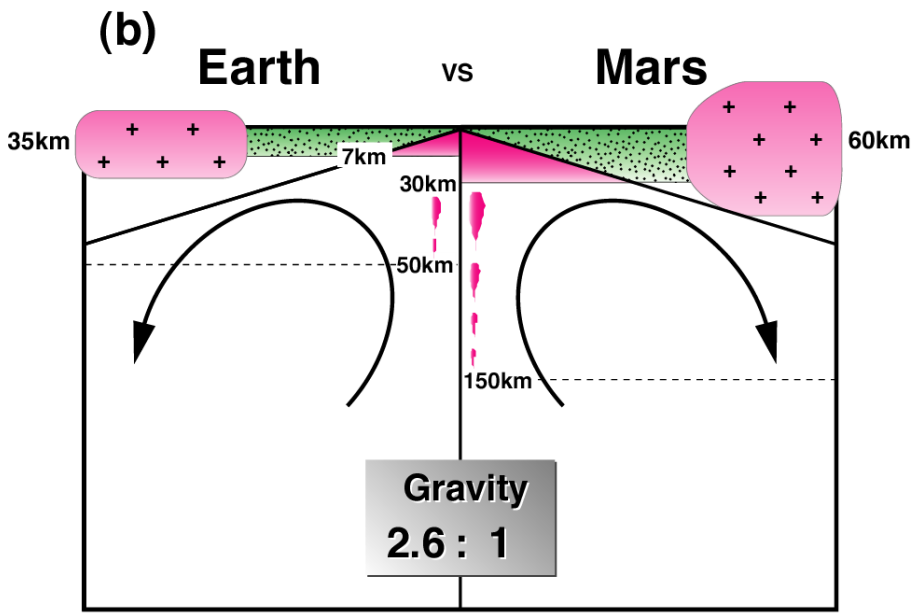
(b)
Earth
vs
Mars
35km
7km
30km
50km
60km
150km
Gravity
2.6 : 1

POST-SURFACE CRATERS

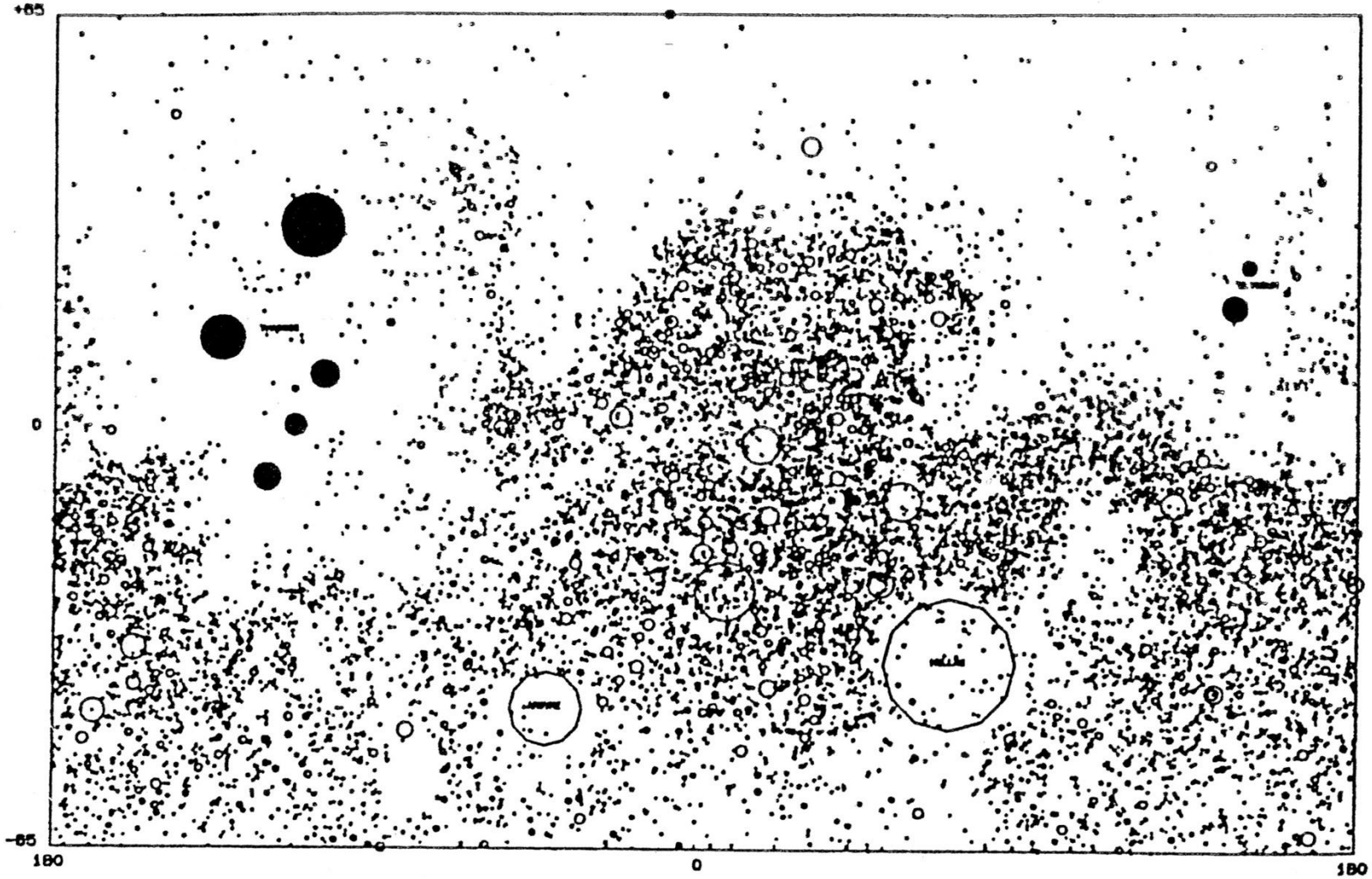

オフィオライト、南部高地南部の残留磁気異常地域

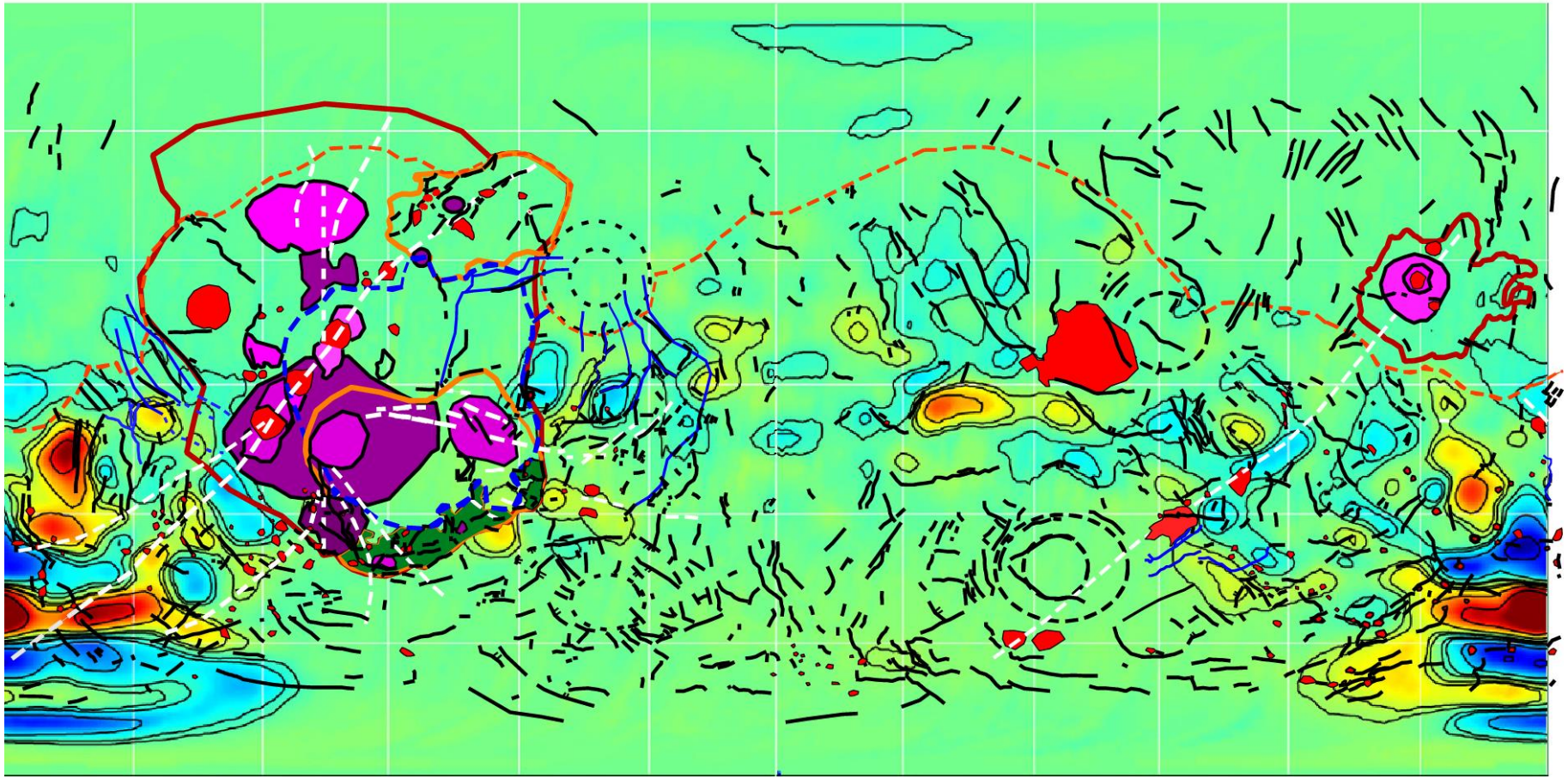

Sparrow (2012) The Universe, Quercus Editions Ltd.

Diagnostic features: Sratigraphy such as candidate olistostrome

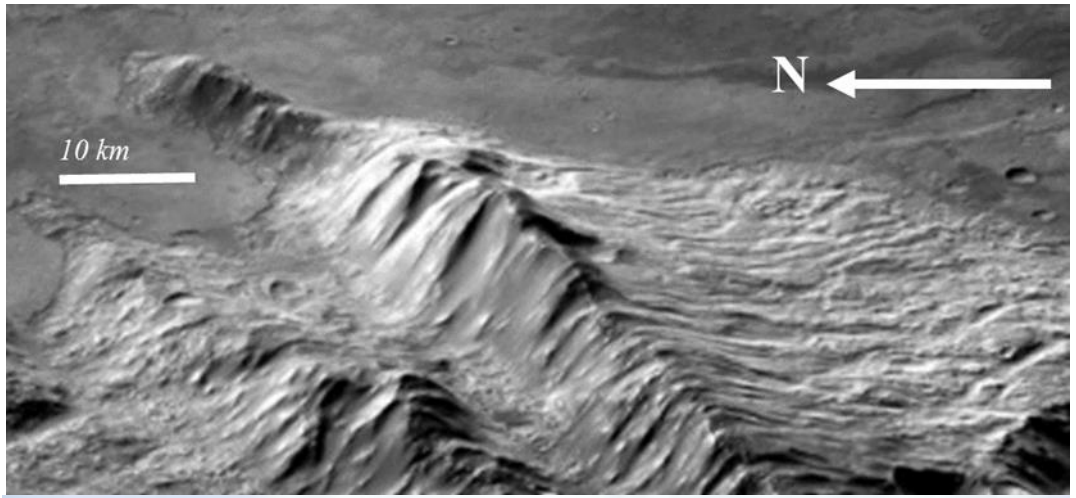

Courtesy of the members of
Maruyama Lab, Tokyo Tech, Japan

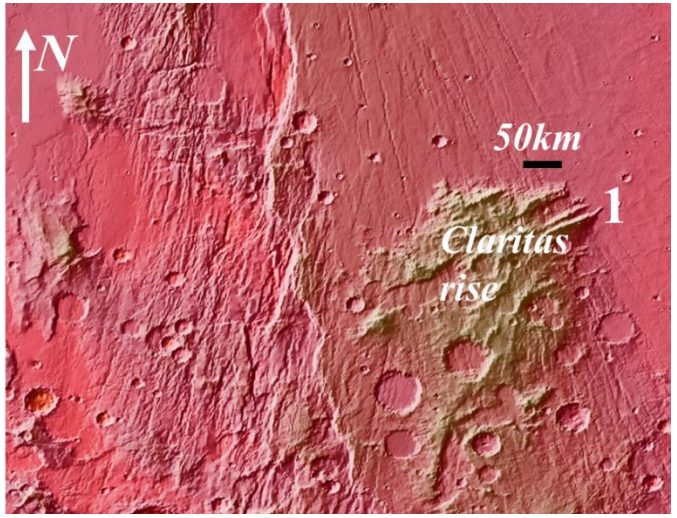

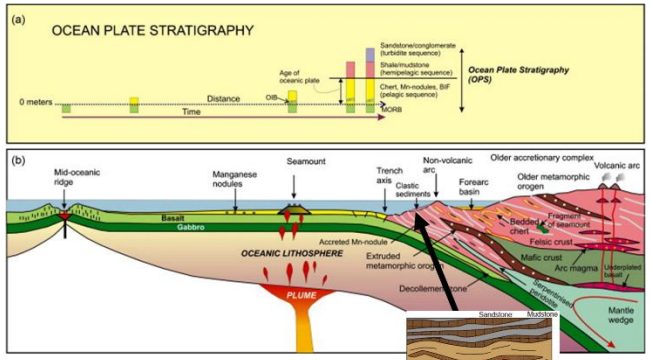

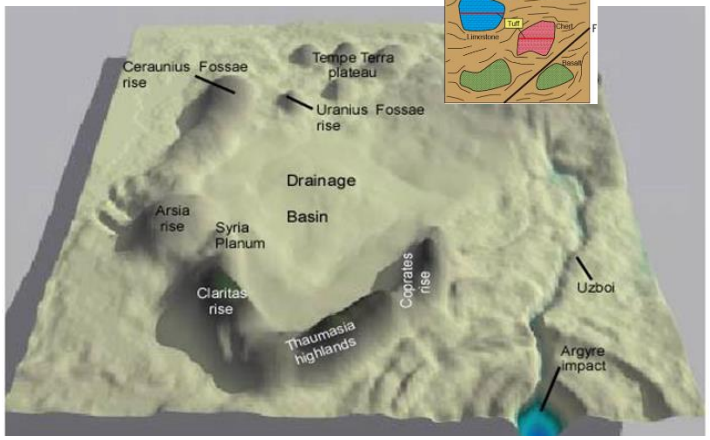

Diagnostic features: Candidate accretionary complex

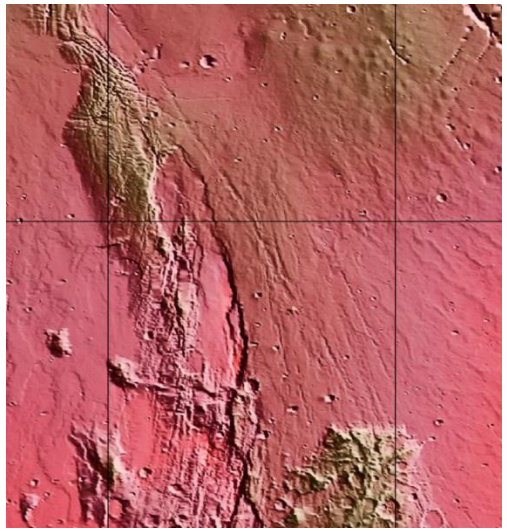

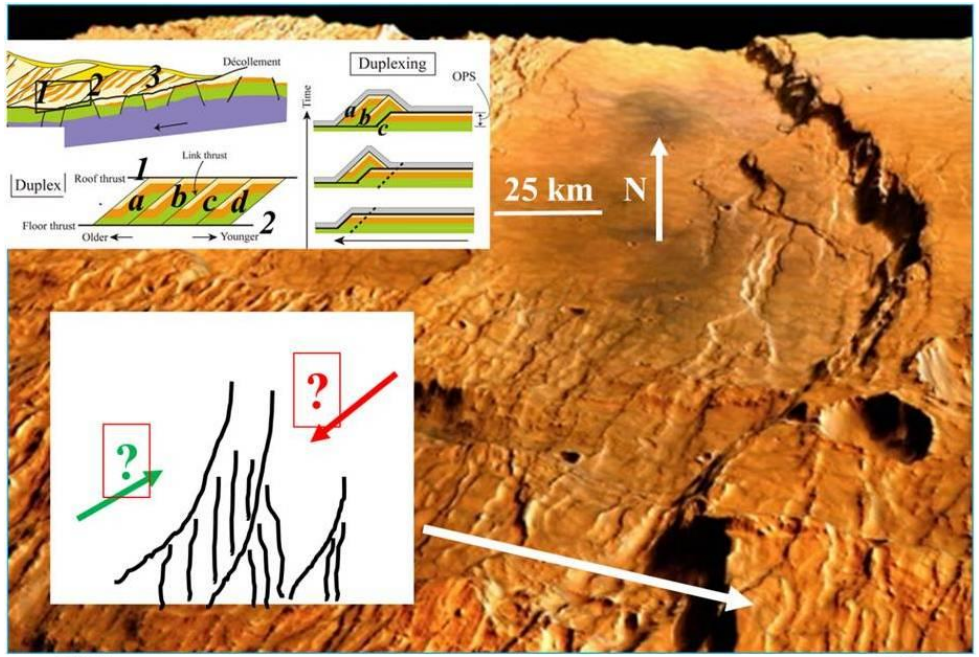

HRSC data courtesy of ESA and DLR

Shigenori Maruyama

Bonita Cover, near San Francisco

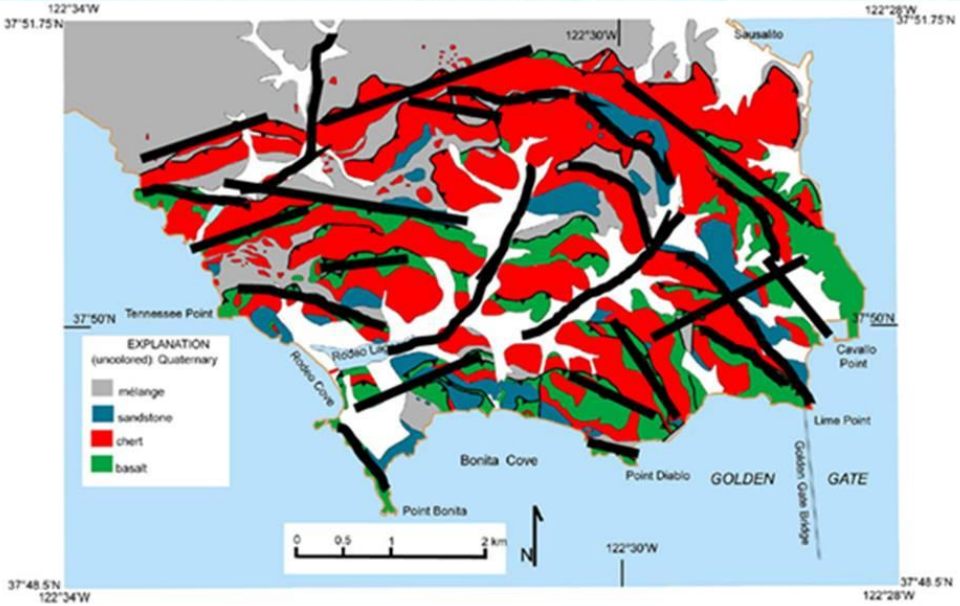

Modified from Wahrhaftig, 1984

付加体の存在と花崗岩の普遍的存在＝プレート運動の存在（＋海洋の存在）

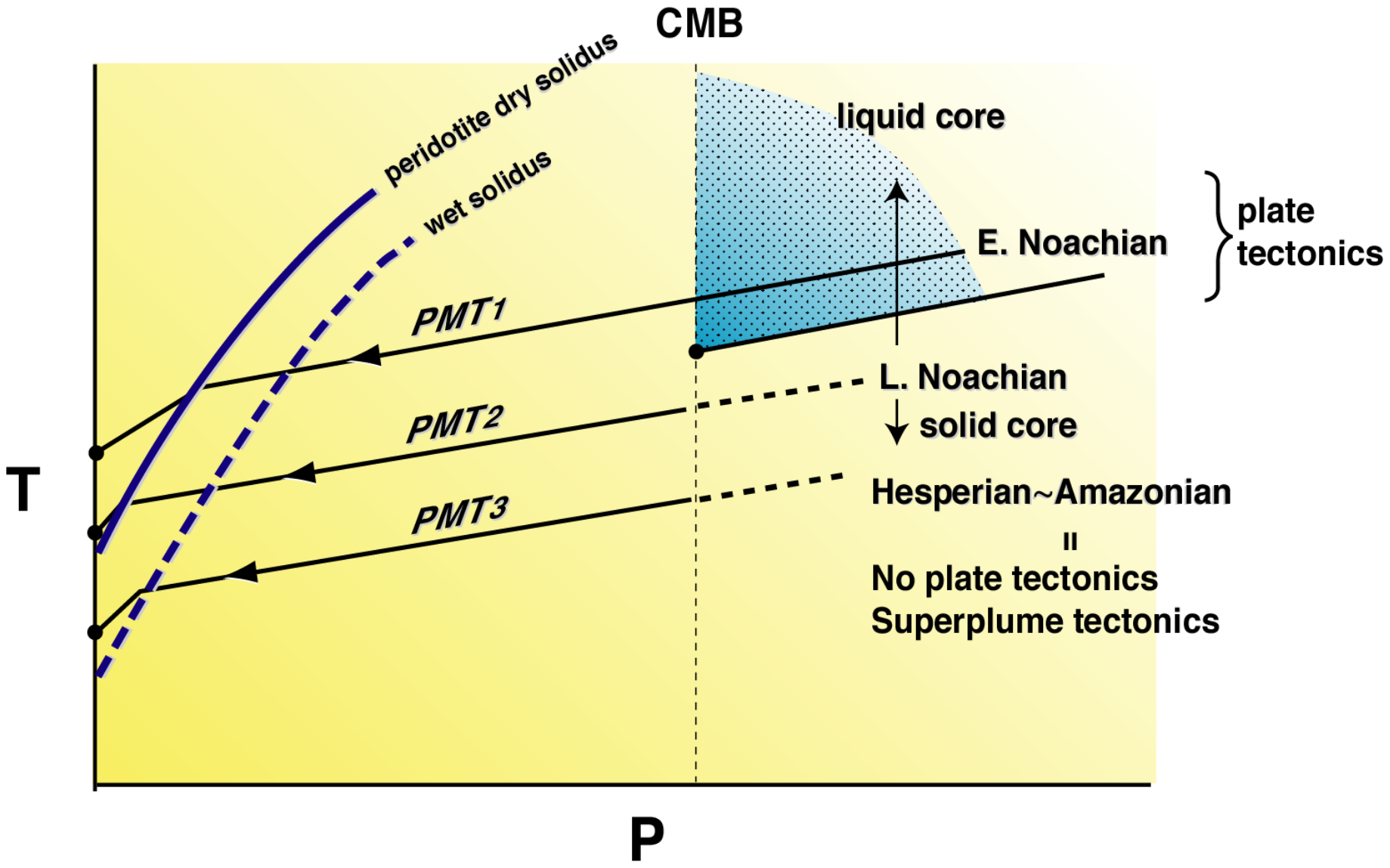
CMB
peridotite dry solidus
wet solidus
liquid core
E. Noachian
plate tectonics
PMT1
PMT2
PMT3
L. Noachian
solid core
Hesperian~Amazonian
=
No plate tectonics
Superplume tectonics
T
P

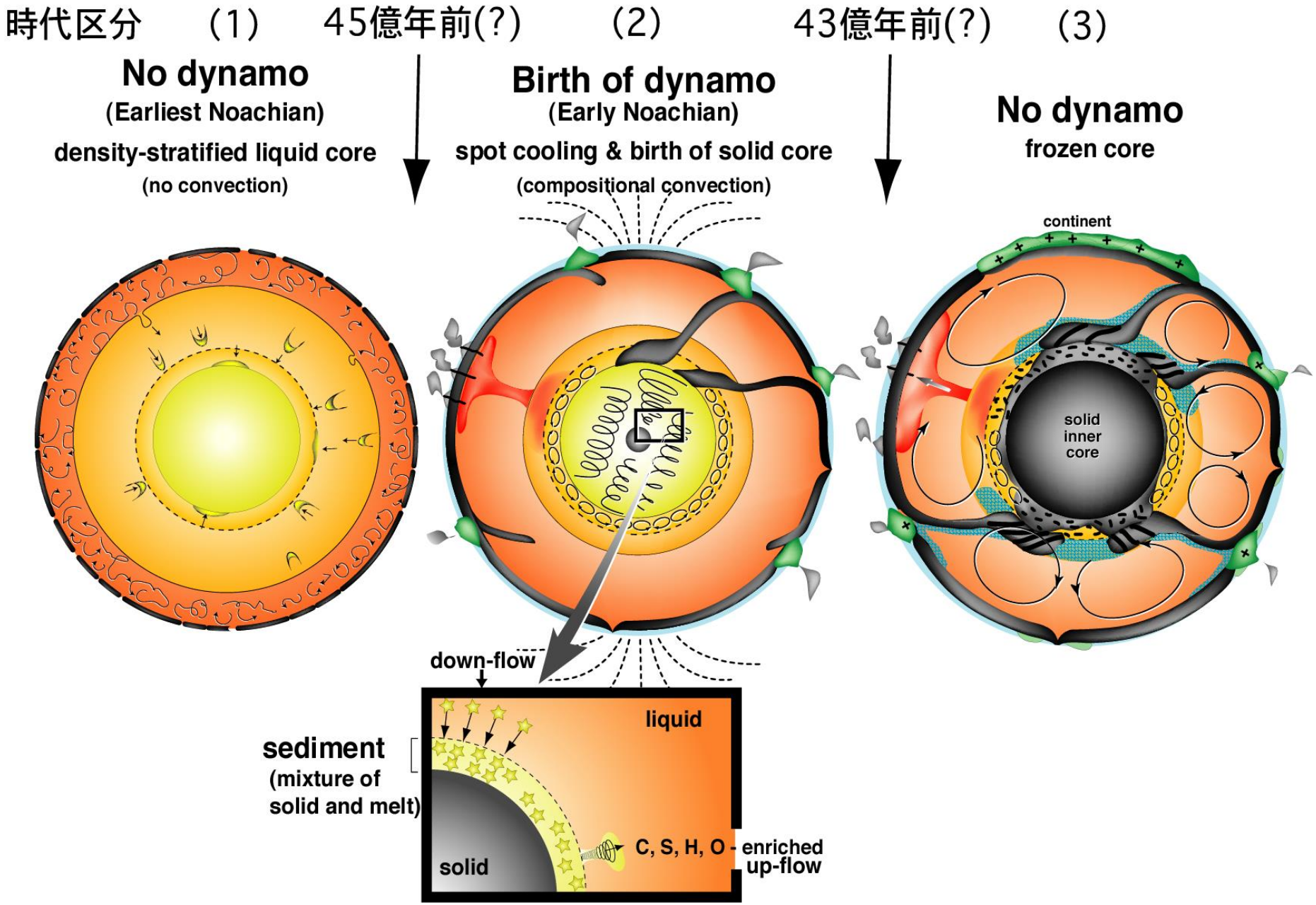
時代区分
(1)
45億年前(?)
(2)
43億年前(?)
(3)
No dynamo
(Earliest Noachian)
density-stratified liquid core
(no convection)
Birth of dynamo
(Early Noachian)
spot cooling & birth of solid core
(compositional convection)
No dynamo
frozen core
continent
solid
inner
core
down-flow
liquid
sediment
(mixture of
solid and melt)
solid
C, S, H, O - enriched
up-flow

核の温度の歴史が分かる
マントルの温度の歴史が
分かる

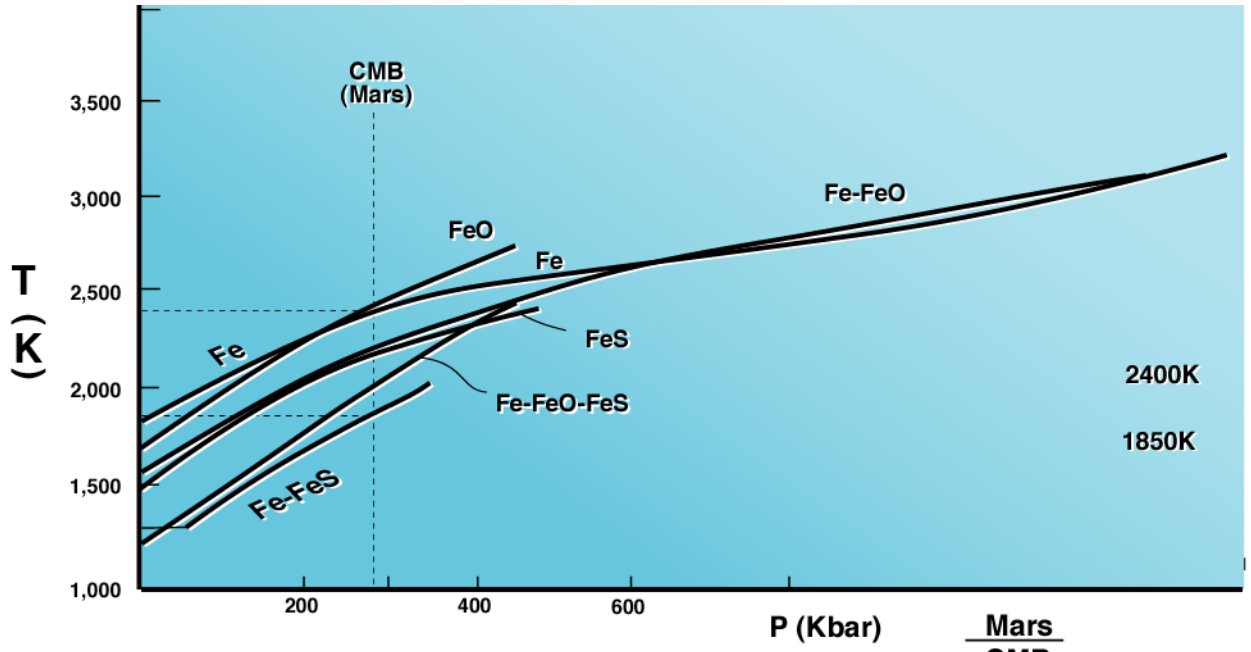

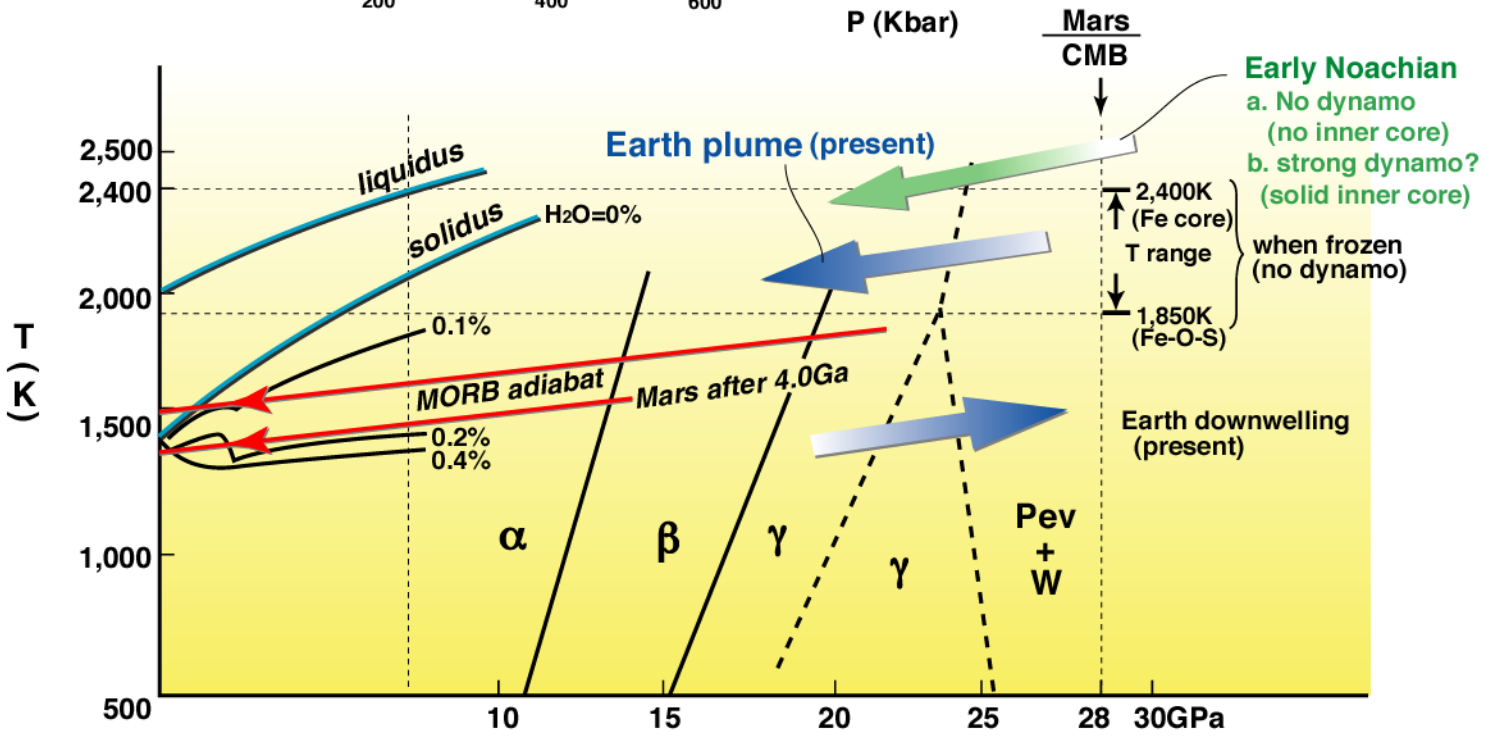

火星の大陸地殻は花崗岩;堆積岩の平均化学組成

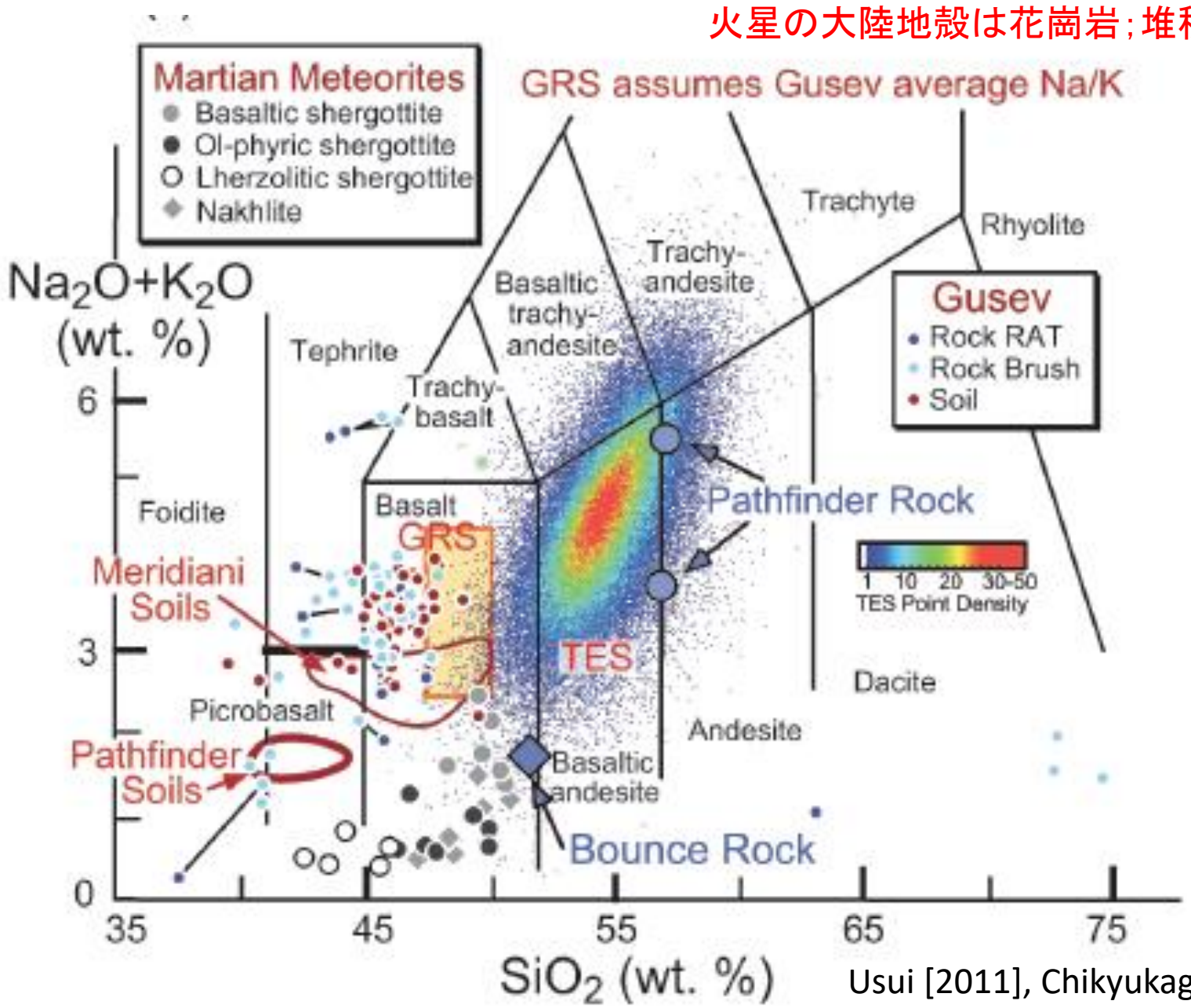

Usui [2011], Chikyukagaku v45. 159-173

火山岩の起源マントルの温度と化学組成がわかる

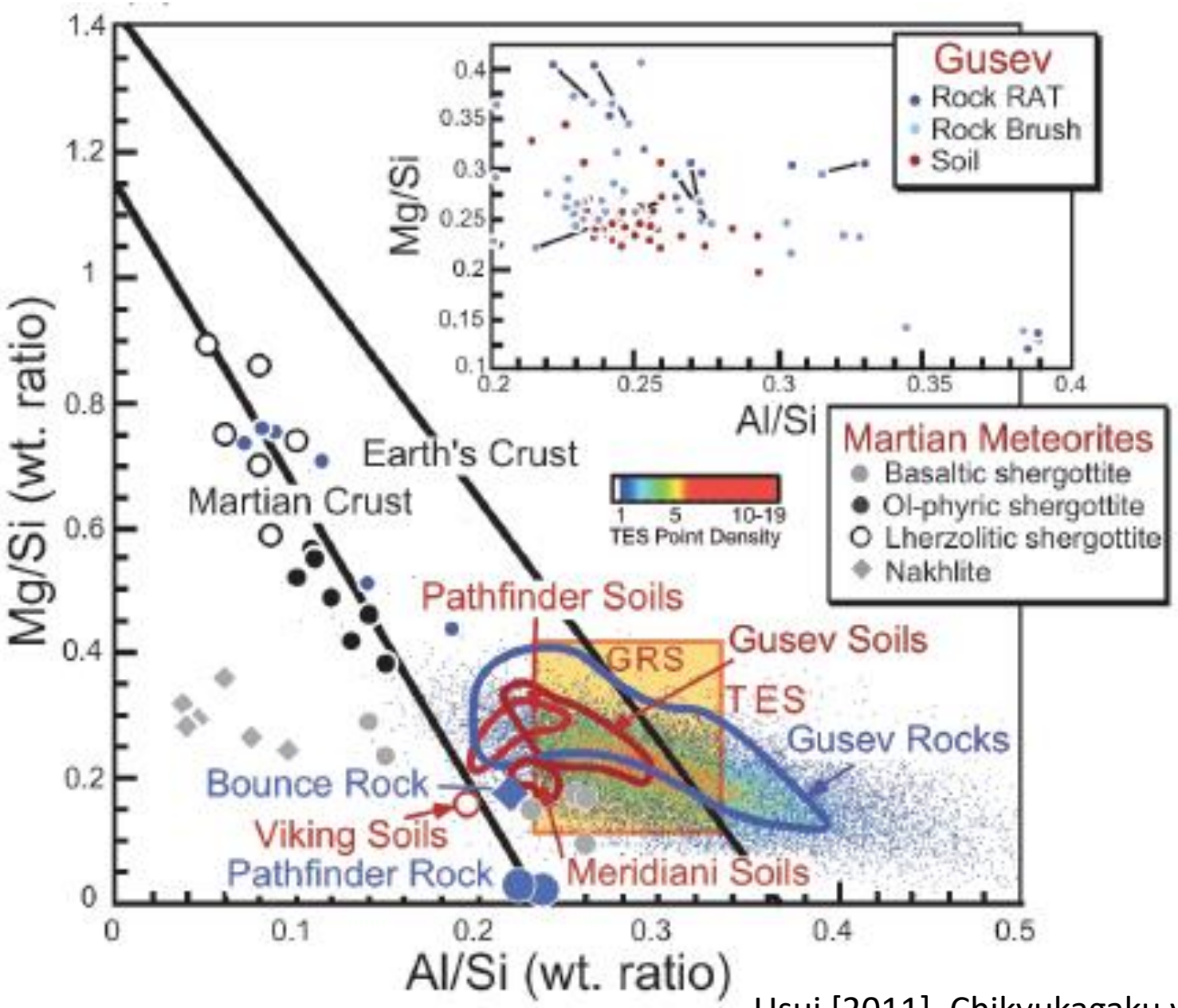

Usui [2011], Chikyukagaku v45. 159-173

マリネリス峡谷の崖＝9kmに達する堆積岩

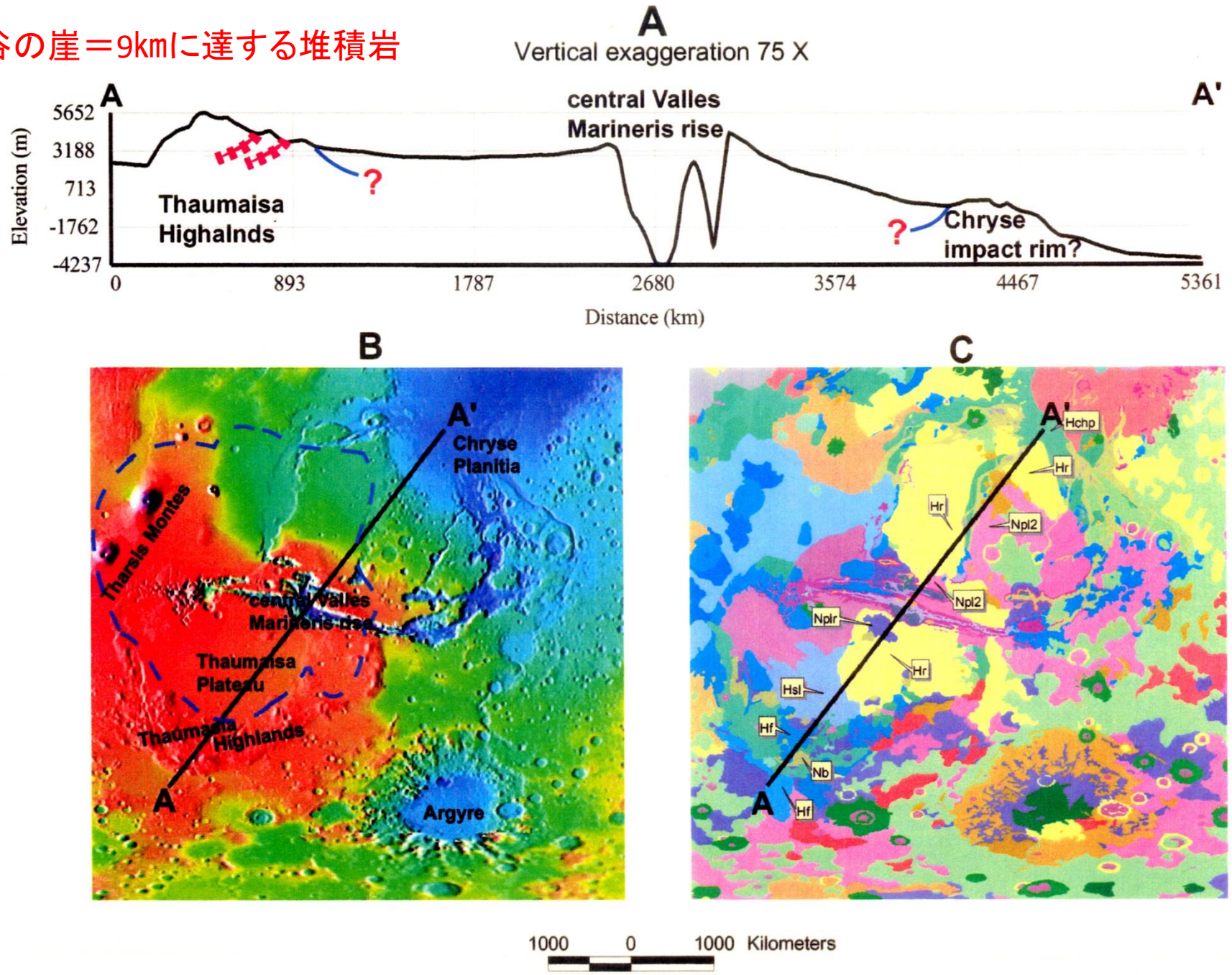

（３）火星探査計画

（１）表層地質のまとめが出発点

（概要、例えば最古の地質は何処にあるか？クレーター分布密度と表層地質から推定）

（２）問題点に基づいてターゲットの地域を絞り込む

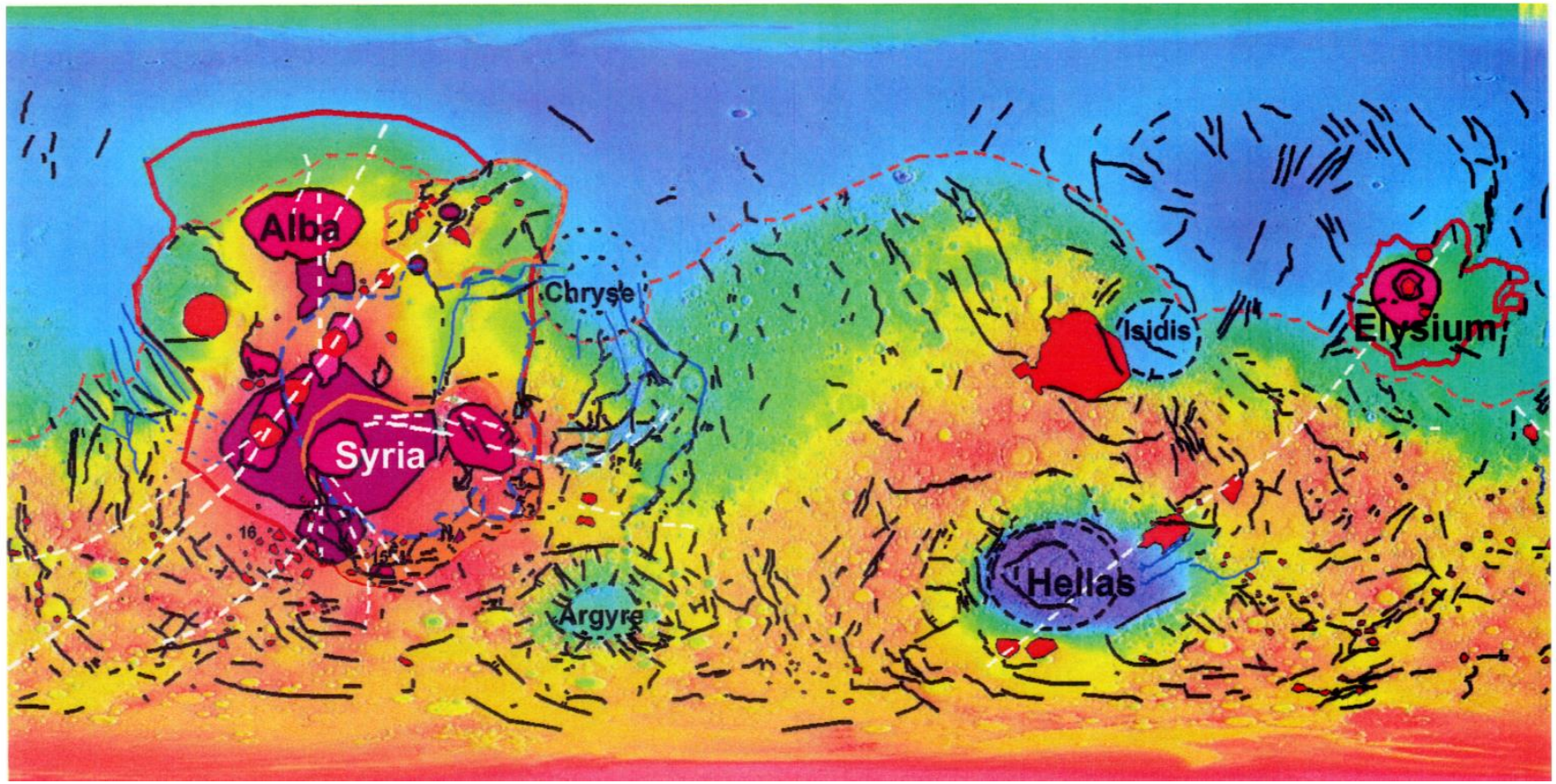

火星は最初期の6億年間が
プレート運動の活発な時代
スーパープルームがその時代に
生まれ、現在でも活動中？

火星史 柱状図

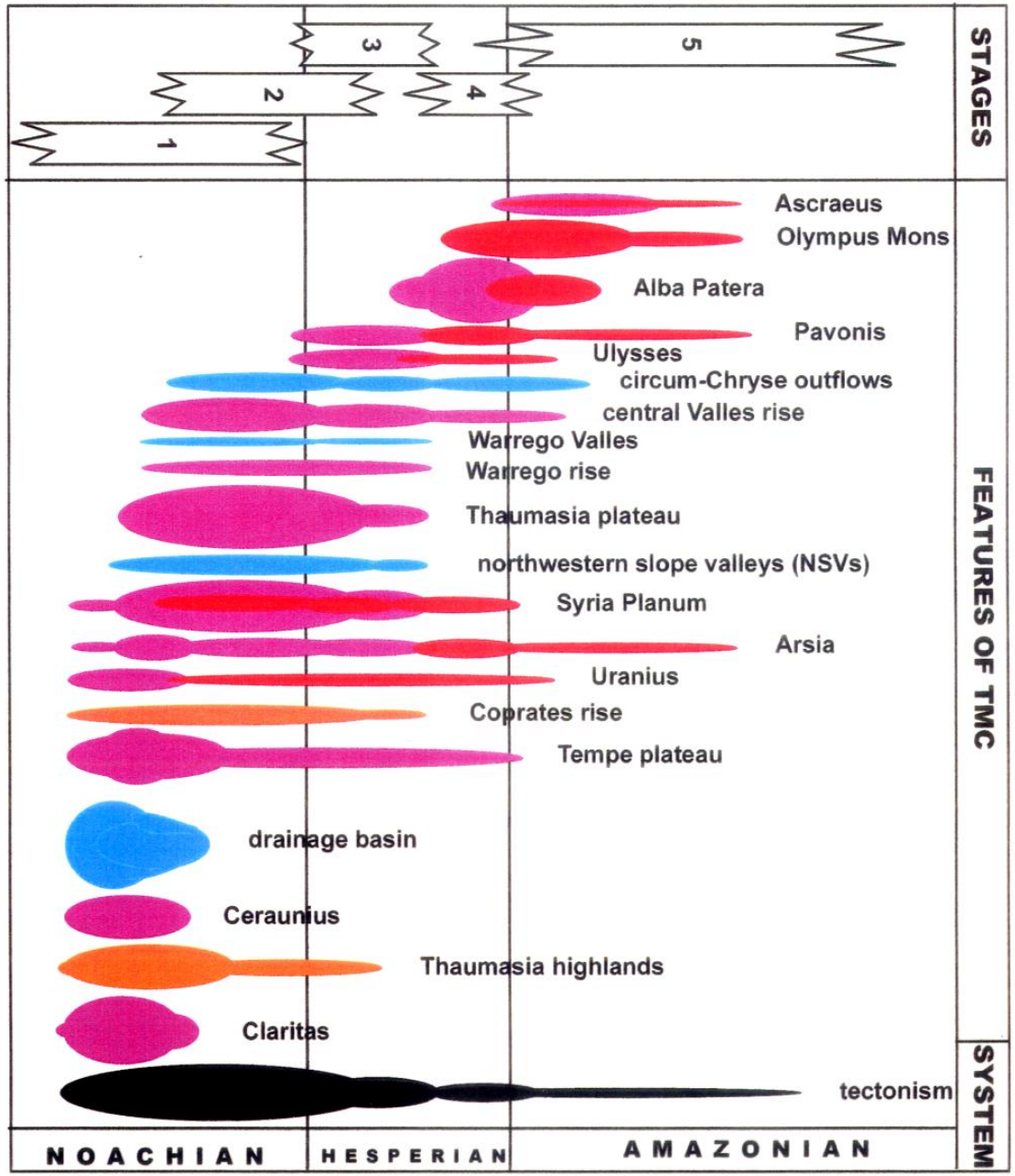

スーパープルームの存在

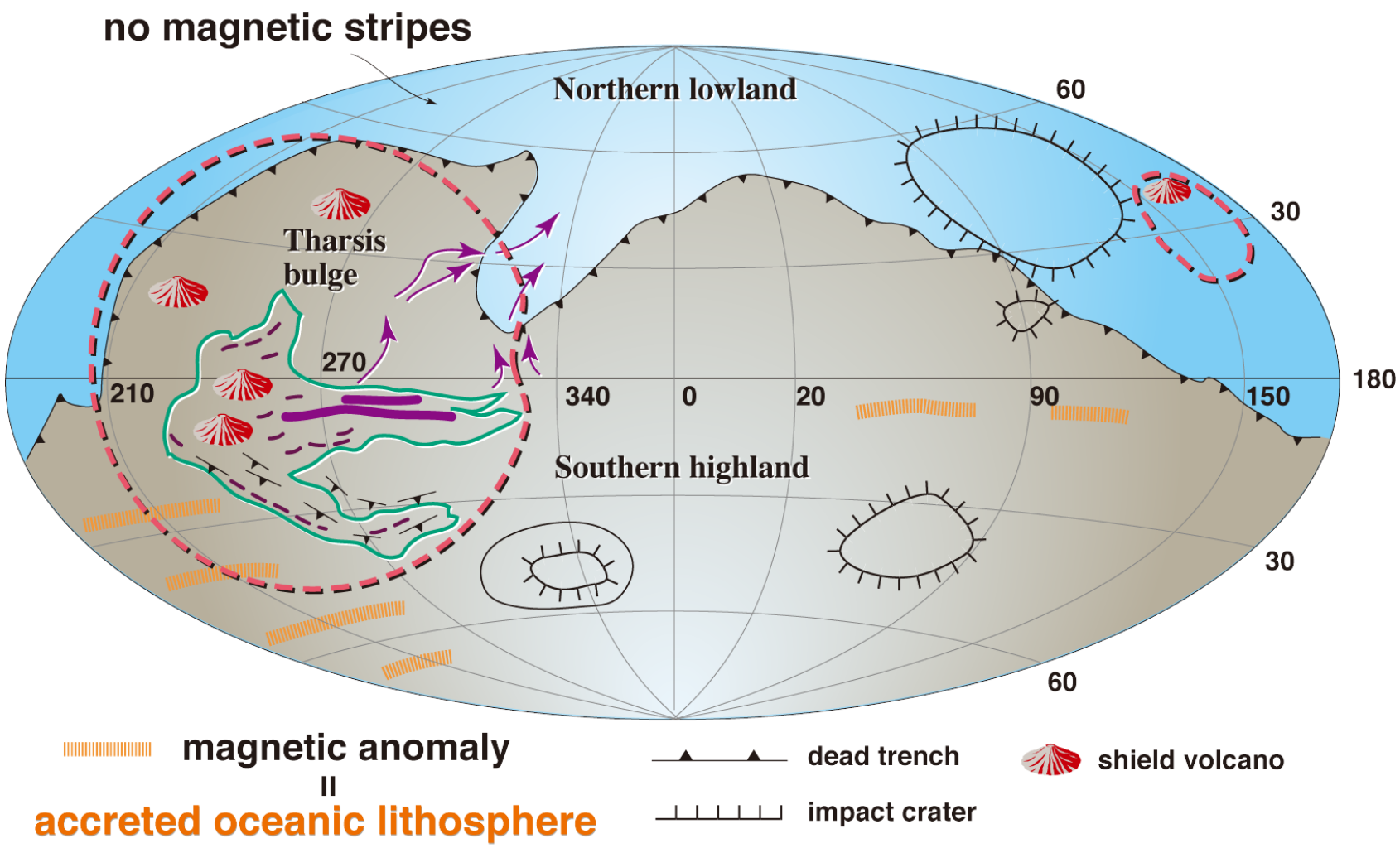

Plate tectonics stopped,
but Tharsis superplume has been active

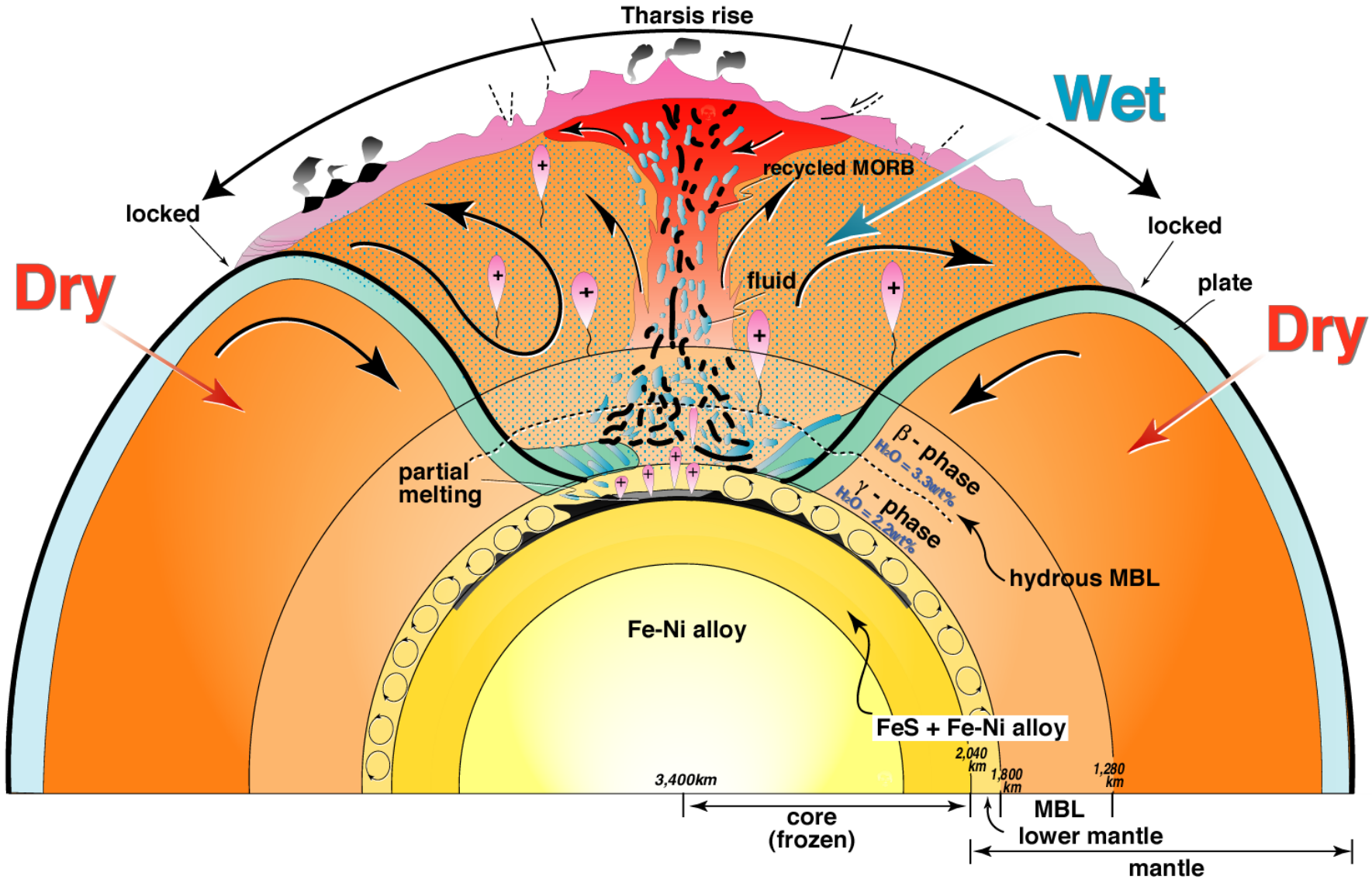

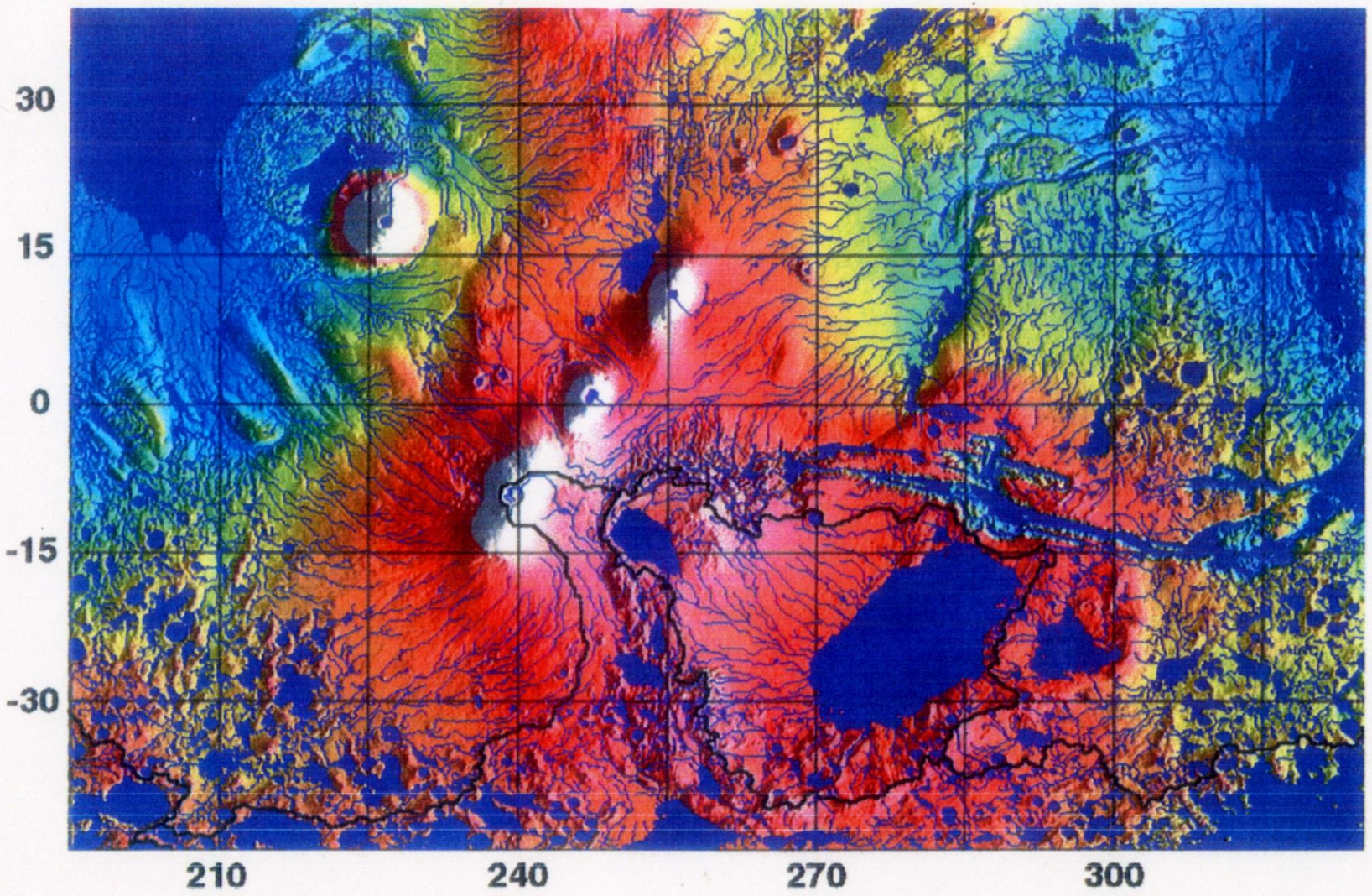
30
15
0
-15
-30
210
240
270
300

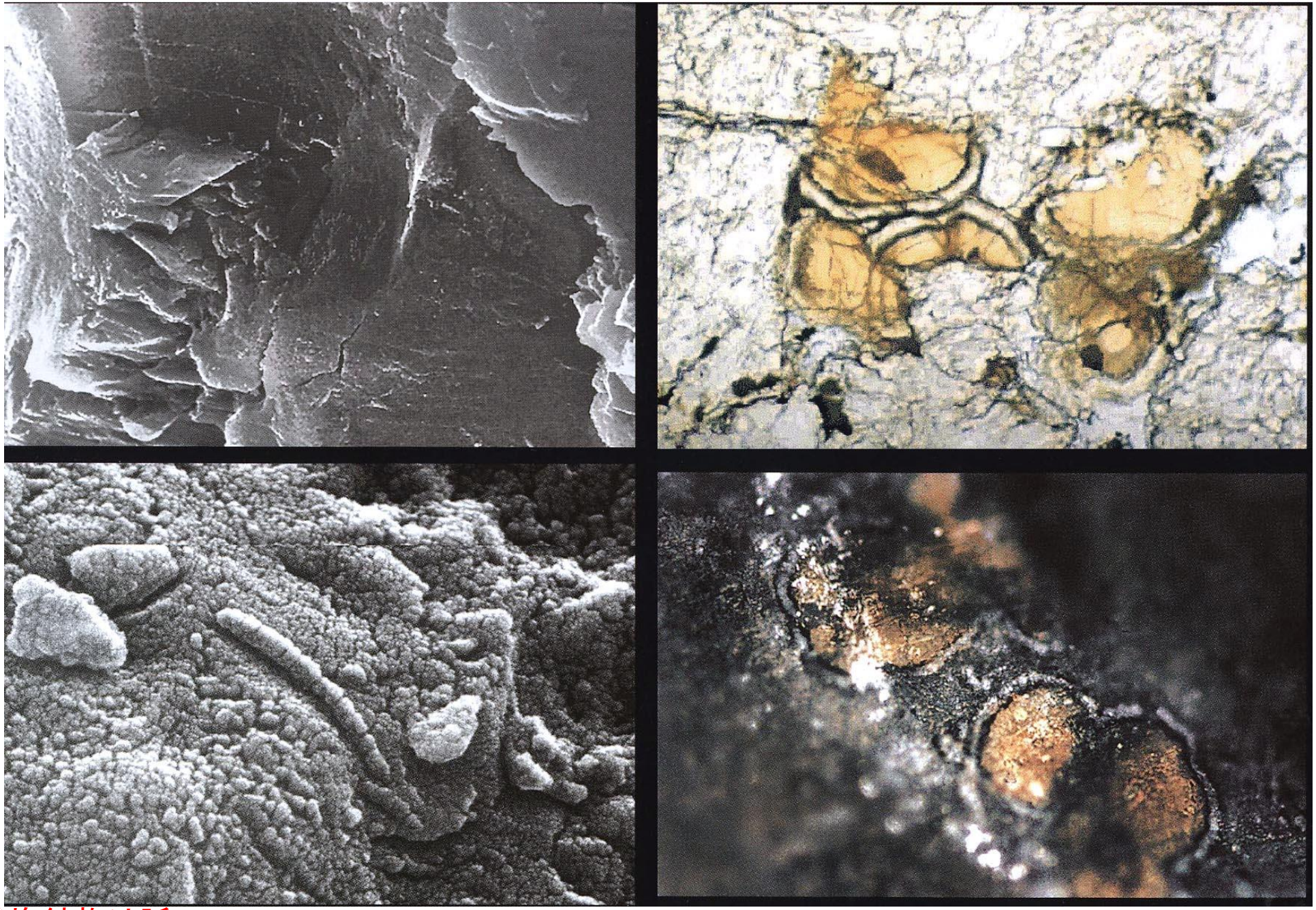

生物化石？
Q;小さすぎる
ホストの石＝
深成岩、炭酸塩鉱物は脈？

Table 2. Abundances of terrestrial C from *N*-methyl-*N*-(*tert*-butyldimethylsilyl) trifluoroacetamide (MTBSTFA) reaction products and dimethylformamide (DMF) compared with the measured abundances of chloromethane (CM), dichloromethane (DCM) and CO_2 detected during SAM evolved gas analysis (EGA) by the mass spectrometer.

Sample	Total detected MTBSTFA-derived C (μmol)*	Estimate of missing DMF C (μmol)†	Total CM + DCM C (μmol)	Estimated amount of MTBSTFA- and DMF-derived C for combustion (μmol)‡	Total CO_2 (μmol)	Estimated MTBSTFA + DMF C combustion in analysis relative to total CO_2§
JK blank	0.120 ± 0.024	0.030 ± 0.006	0.005 ± 0.001	≈ 0	≈ 0	≈ 0%
JK-1	0.051 ± 0.010	0.013 ± 0.003	0.066 ± 0.013	0.086 ± 0.043	7.0 ± 1.9	1.2 ± 0.7%
JK-2	0.044 ± 0.009	0.011 ± 0.002	0.061 ± 0.012	0.095 ± 0.041	8.1 ± 1.7	1.2 ± 0.5%
JK-3 (3× portion)	0.071 ± 0.014	0.018 ± 0.004	0.127 ± 0.025	0.061 ± 0.048	19.8 ± 4.8	0.3 ± 0.3%
JK-4	0.047 ± 0.009	0.012 ± 0.002	0.038 ± 0.008	0.091 ± 0.041	5.7 ± 1.3	1.6 ± 0.7%
CB blank	0.097 ± 0.019	0.025 ± 0.005	0.006 ± 0.001	≈ 0	≈ 0	≈ 0%
CB-1	0.068 ± 0.014	0.017 ± 0.003	0.025 ± 0.005	0.037 ± 0.041	2.0 ± 0.2	1.9 ± 2.1%
CB-2	0.041 ± 0.008	0.010 ± 0.002	0.022 ± 0.004	0.071 ± 0.034	2.5 ± 0.4	2.8 ± 1.4%
CB-3	0.032 ± 0.006	0.008 ± 0.002	0.021 ± 0.004	0.082 ± 0.032	3.1 ± 0.3	2.7 ± 1.1%
CB-5	0.018 ± 0.004	0.005 ± 0.001	0.011 ± 0.002	ND‖	3.1 ± 0.7	ND‖
RN blank	0.078 ± 0.016	0.020 ± 0.004	0.002 ± 0.001	≈ 0	≈ 0	≈ 0%
RN1-4 (average)	0.058 ± 0.012	0.015 ± 0.003	0.012 ± 0.002	0.025 ± 0.035	9.9 ± 1.2	0.3 ± 0.4%

*Total MTBSTFA C value in μmol determined from the sum of the EGA measured abundances of silylated products: *tert*-butyldimethylsilanol, 1,3-bis(1,1-dimethylethyl)-1,1,3,3-tetramethyldisiloxane, and *tert*-butyldimethylfluorosilane, plus the mole fraction of C from 2,2,2-trifluoro-*N*-methylacetamide in MTBSTFA relative to the sum of the silylated products. †DMF was not identified during pyrolysis by EGA or GCMS. However, the amount of DMF C was estimated from the total measured MTBSTFA C and the molar ratio of DMF/MTBSTFA carbon (0.25) that was originally loaded into the wet chemistry cups, to address a worst-case scenario. ‡Estimated amount of combusted MTBSTFA- and DMF-derived C equals the amount of C in the blank from these sources minus the amount of C from these sources that was observed and calculated for each solid sample run. §Percentage of the total MTBSTFA and DMF carbon in the preceding blank analysis, assumed to be representative of the MTBSTFA and DMF derived carbon available for combustion to CO_2, compared to total CO_2 measured in the sample runs. ‖ND: Values could not be determined because a comparable blank run was not carried out under the same experimental conditions that were used for CB-5.

Ming et al 2014

Fig. 4. SAM gas chromatogram of the major *m/z* values of the chlorinated hydrocarbons detected in JK and CB samples (cps, counts/s). (**A**) JK Sample 3 (JK-3; triple portion) compared with JK-2 (single portion) and the JK blank. (**B**) CB Sample 2 (CB-2, single portion) compared with the CB blank. (**C**) The mass spectra generated for the GC peaks detected in JK-3 are shown in red and compared with the mass spectra for chloromethane (CH_3Cl), dichloromethane (CH_2Cl_2), and trichloromethane ($CHCl_3$) in black from NIST/EPA/NIH Mass Spectral Database (*44*).

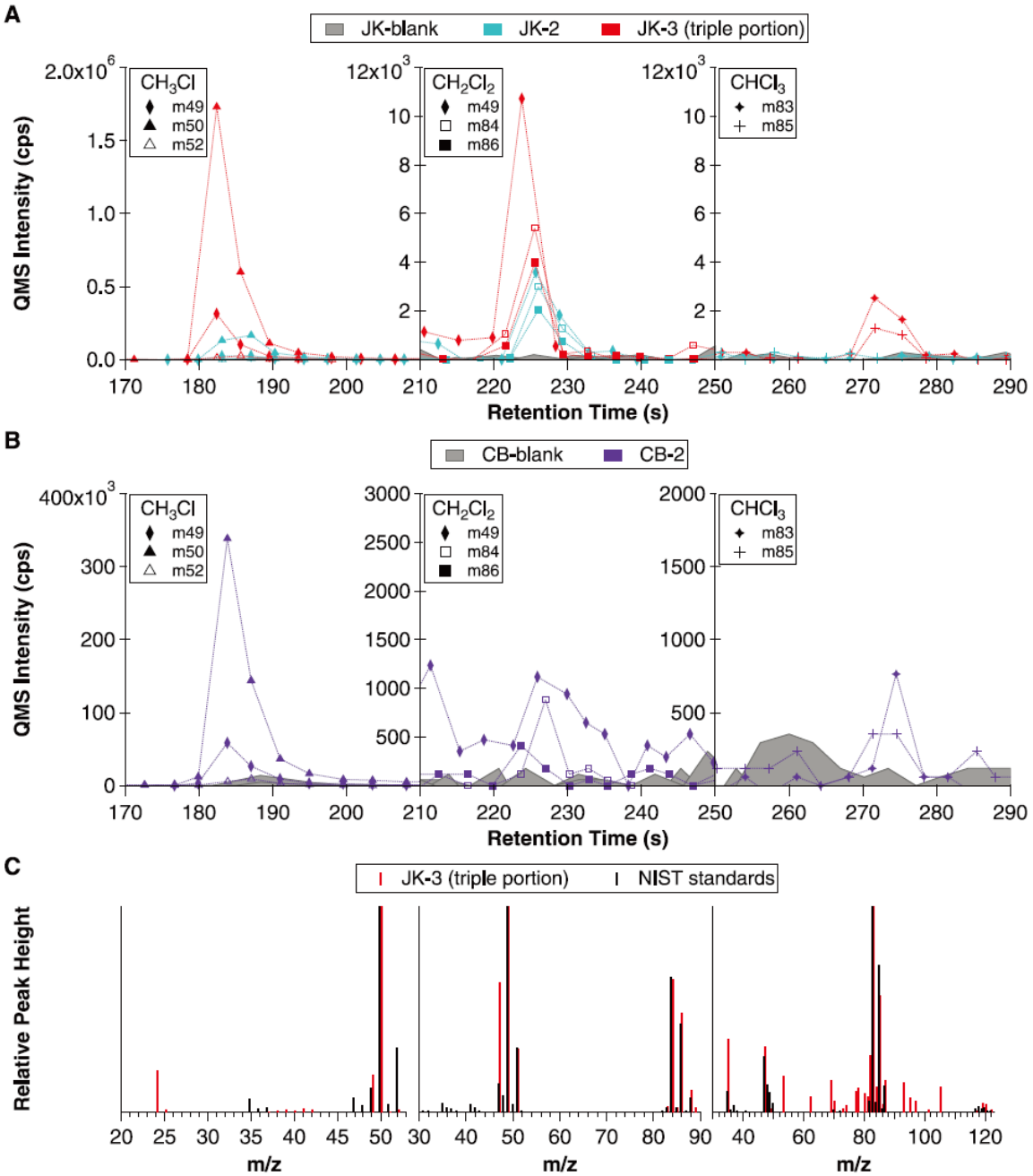

簡単な有機物が確認されたがまだ、アミノ酸さえ見つからない
Cf. 隕石にはアミノ酸まで報告されている
●硫黄と塩素に満ちている

Ming et al 2014

AGU PUBLICATIONS

JGR

Journal of Geophysical Research: Planets

RESEARCH ARTICLE
10.1002/2014JE004737

Organic molecules in the Sheepbed Mudstone, Gale Crater, Mars

Key Points:
- First in situ evidence of nonterrestrial organics in Martian surface sediments
- Chlorinated hydrocarbons identified in the Sheepbed mudstone by SAM
- Organics preserved in sample exposed to ionizing radiation and oxidative condition

C. Freissinet[1,2], D. P. Glavin[1], P. R. Mahaffy[1], K. E. Miller[3], J. L. Eigenbrode[1], R. E. Summons[3], A. E. Brunner[1,4], A. Buch[5], C. Szopa[6], P. D. Archer Jr.[7], H. B. Franz[1,8], S. K. Atreya[9], W. B. Brinckerhoff[1], M. Cabane[6], P. Coll[10], P. G. Conrad[1], D. J. Des Marais[11], J. P. Dworkin[1], A. G. Fairén[12,13], P. François[9], J. P. Grotzinger[14], S. Kashyap[1,8], I. L. ten Kate[15], L. A. Leshin[16], C. A. Malespin[1,17], M. G. Martin[1,18], F. J. Martin-Torres[19,20], A. C. McAdam[1], D. W. Ming[21], R. Navarro-González[22], A. A. Pavlov[1], B. D. Prats[1], S. W. Squyres[12], A. Steele[23], J. C. Stern[1], D. Y. Sumner[24], B. Sutter[7], M.-P. Zorzano[25], and the MSL Science Team

Abstract The Sample Analysis at Mars (SAM) instrument on board the Mars Science Laboratory Curiosity rover is designed to conduct inorganic and organic chemical analyses of the atmosphere and the surface regolith and rocks to help evaluate the past and present habitability potential of Mars at Gale Crater. Central to this task is the development of an inventory of any organic molecules present to elucidate processes associated with their origin, diagenesis, concentration, and long-term preservation. This will guide the future search for biosignatures. Here we report the definitive identification of chlorobenzene (150–300 parts per billion by weight (ppbw)) and C_2 to C_4 dichloroalkanes (up to 70 ppbw) with the SAM gas chromatograph mass spectrometer (GCMS) and detection of chlorobenzene in the direct evolved gas analysis (EGA) mode, in multiple portions of the fines from the Cumberland drill hole in the Sheepbed mudstone at Yellowknife Bay. When combined with GCMS and EGA data from multiple scooped and drilled samples, blank runs, and supporting laboratory analog studies, the elevated levels of chlorobenzene and the dichloroalkanes cannot be solely explained by instrument background sources known to be present in SAM. We conclude that these chlorinated hydrocarbons are the reaction products of Martian chlorine and organic carbon derived from Martian sources (e.g., igneous, hydrothermal, atmospheric, or biological) or exogenous sources such as meteorites, comets, or interplanetary dust particles.

火星史要約

History of Mars

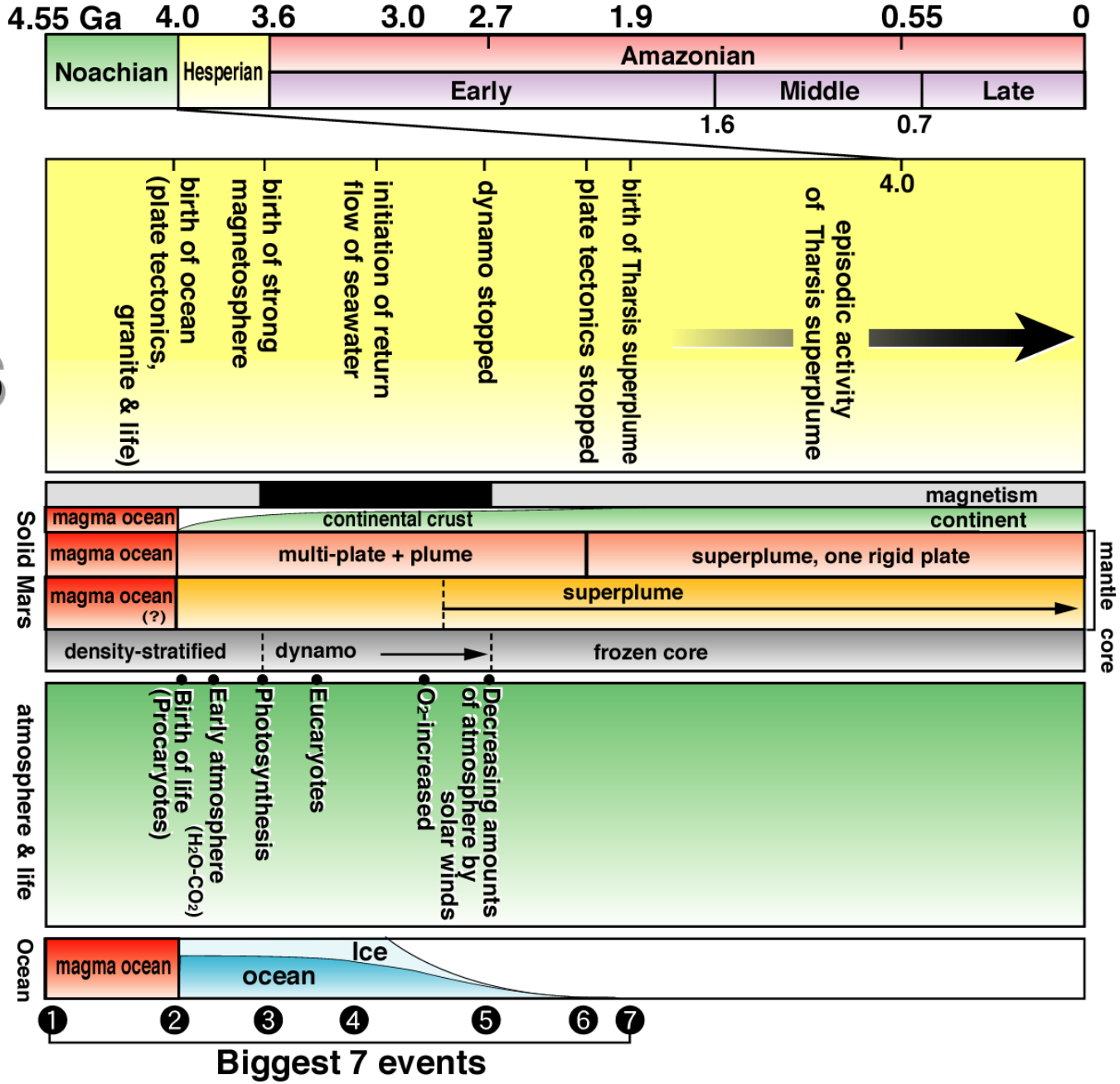

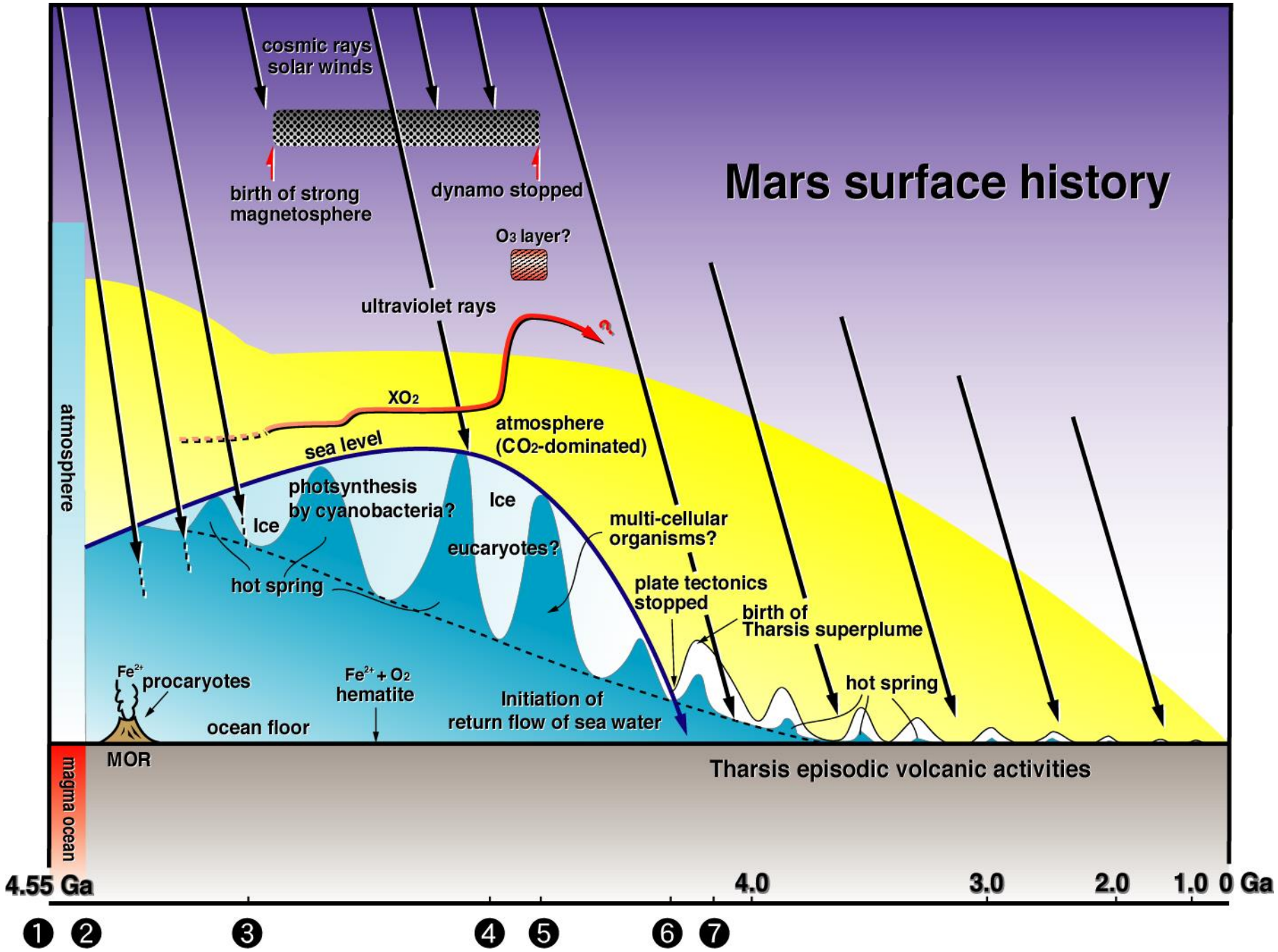
Mars surface history
cosmic rays
solar winds
birth of strong magnetosphere
dynamo stopped
O3 layer?
ultraviolet rays
XO2
atmosphere (CO2-dominated)
sea level
photsynthesis by cyanobacteria?
Ice
Ice
eucaryotes?
multi-cellular organisms?
hot spring
plate tectonics stopped
birth of Tharsis superplume
hot spring
Fe2+
procaryotes
Fe2+ + O2
hematite
Initiation of return flow of sea water
ocean floor
MOR
atmosphere
magma ocean
Tharsis episodic volcanic activities
4.55 Ga
4.0
3.0
2.0
1.0
0 Ga
1
2
3
4
5
6
7

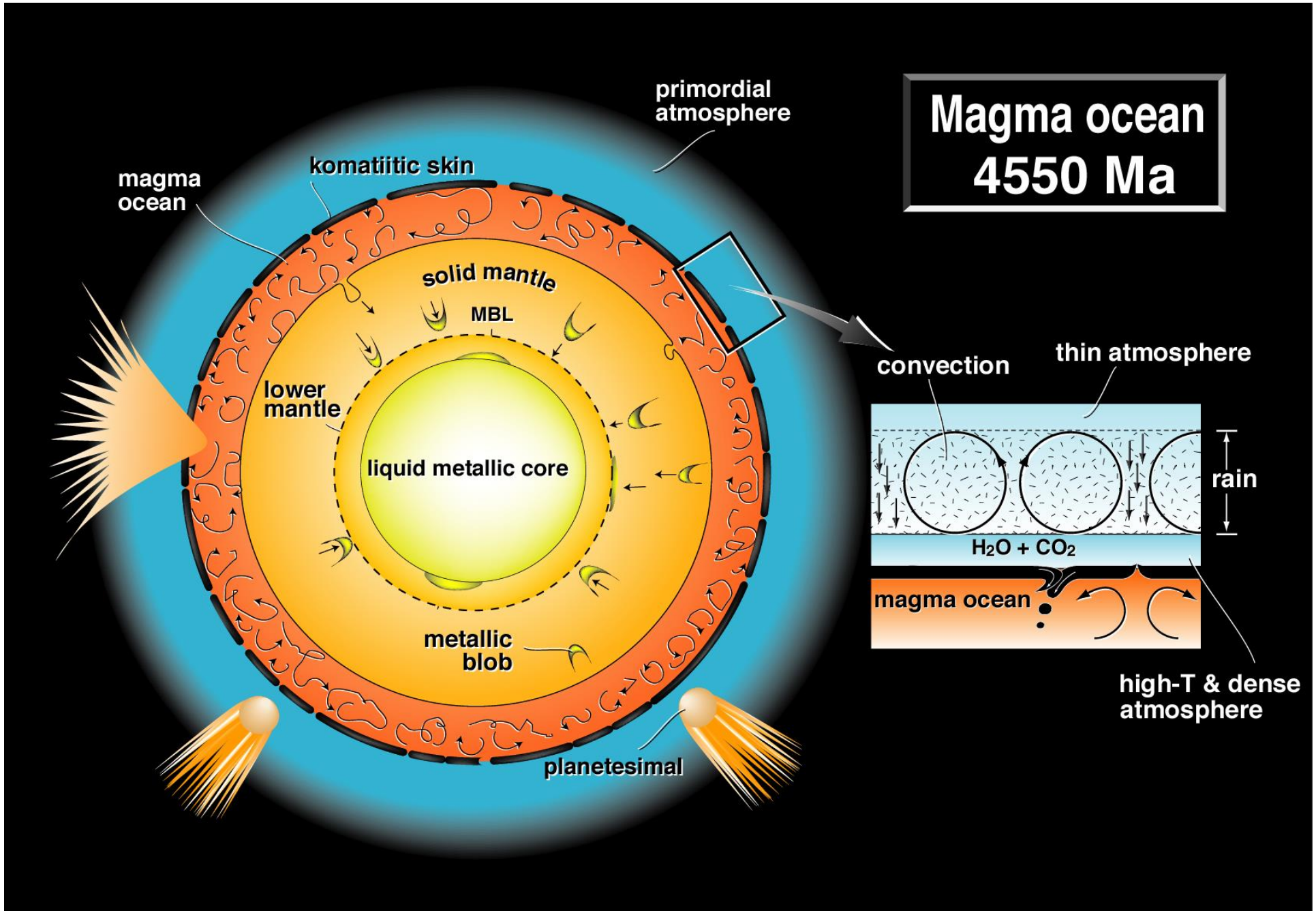
Magma ocean
4550 Ma
primordial atmosphere
komatiitic skin
magma ocean
solid mantle
MBL
lower mantle
liquid metallic core
metallic blob
planetesimal
convection
thin atmosphere
rain
$H_2O + CO_2$
magma ocean
high-T & dense atmosphere

Birth of Ocean

Initiation of plate tectonics
Birth of life
& continental crust

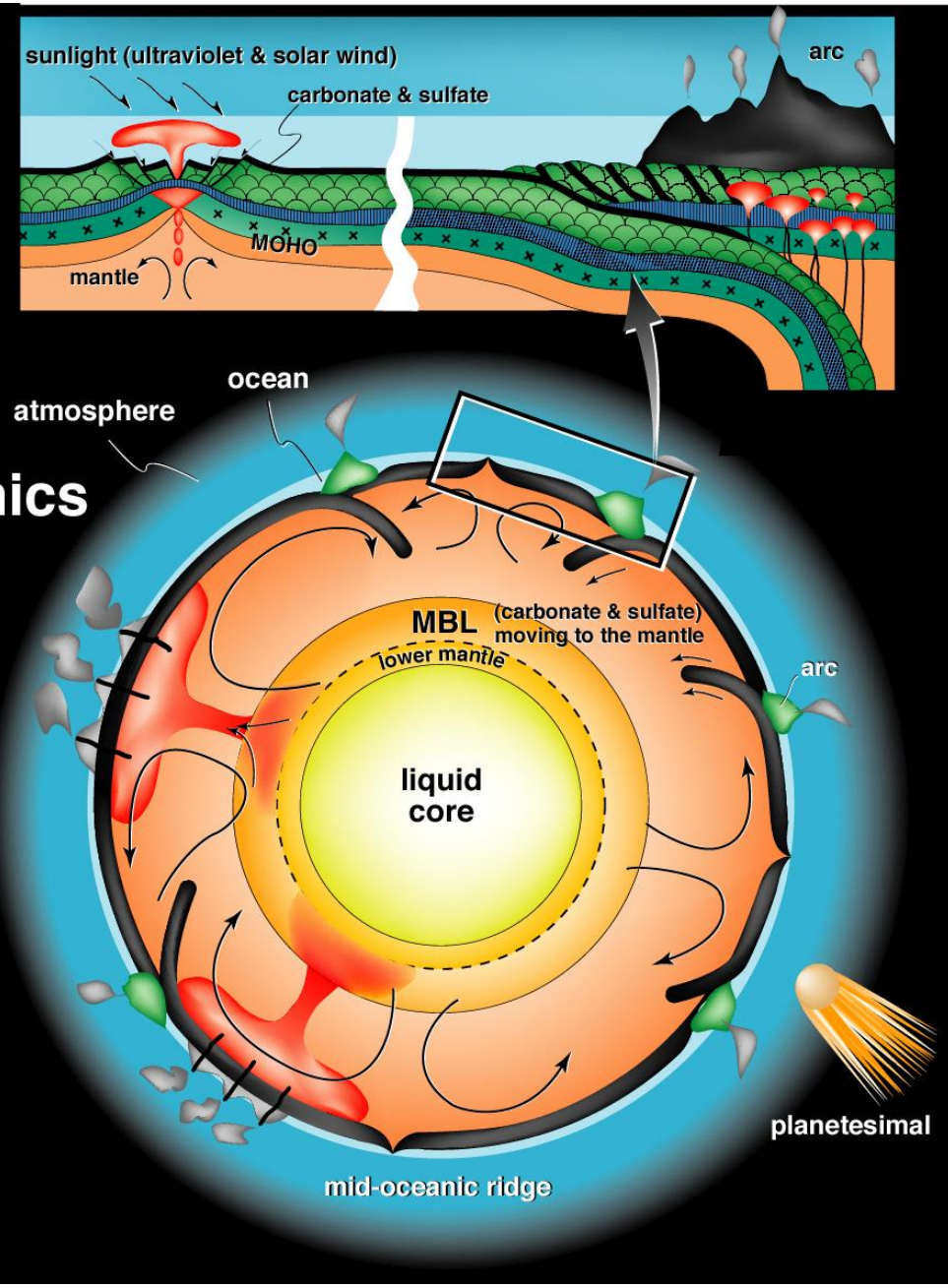

(2)の時代

強い残留磁気の正体
（オフィオライト？）

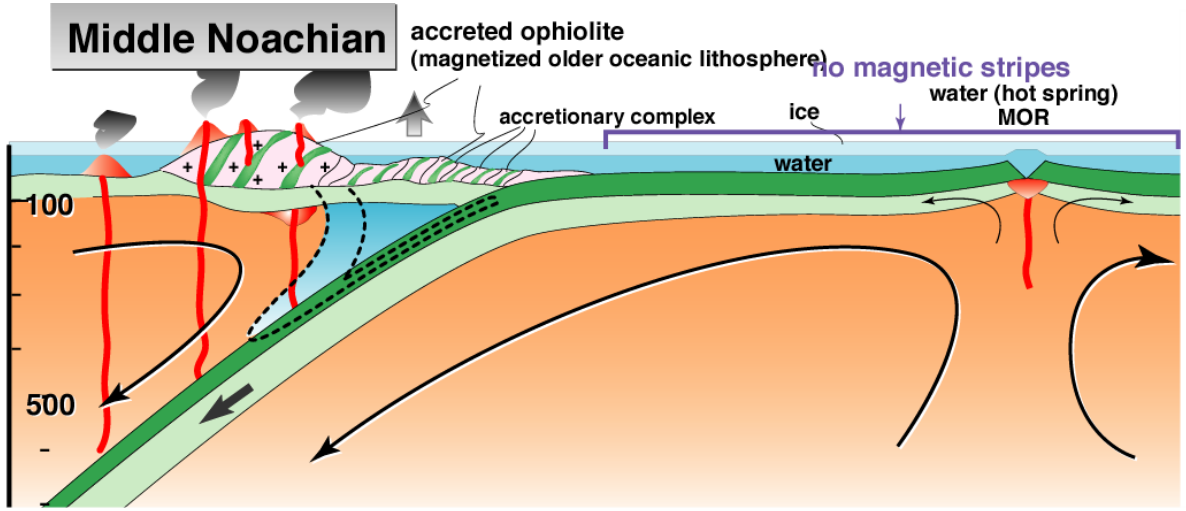

(3)の時代

磁場の消滅！
しかし
プレート運動は継続

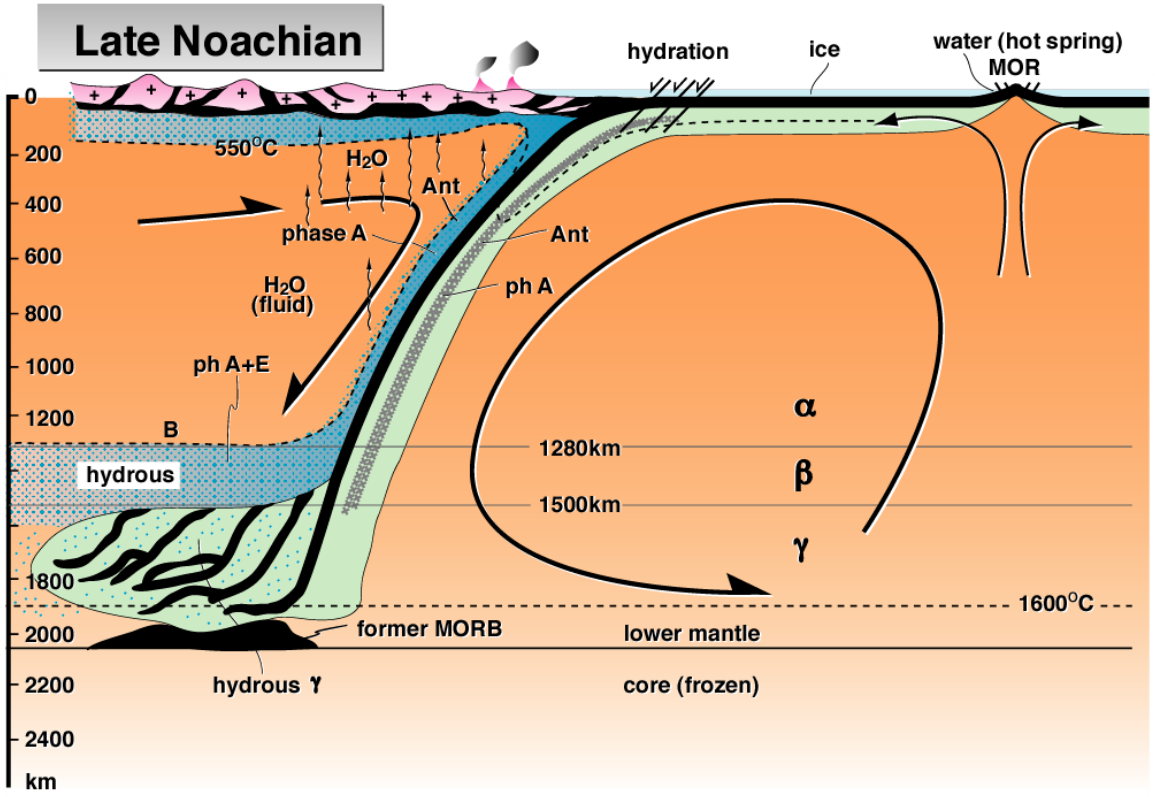

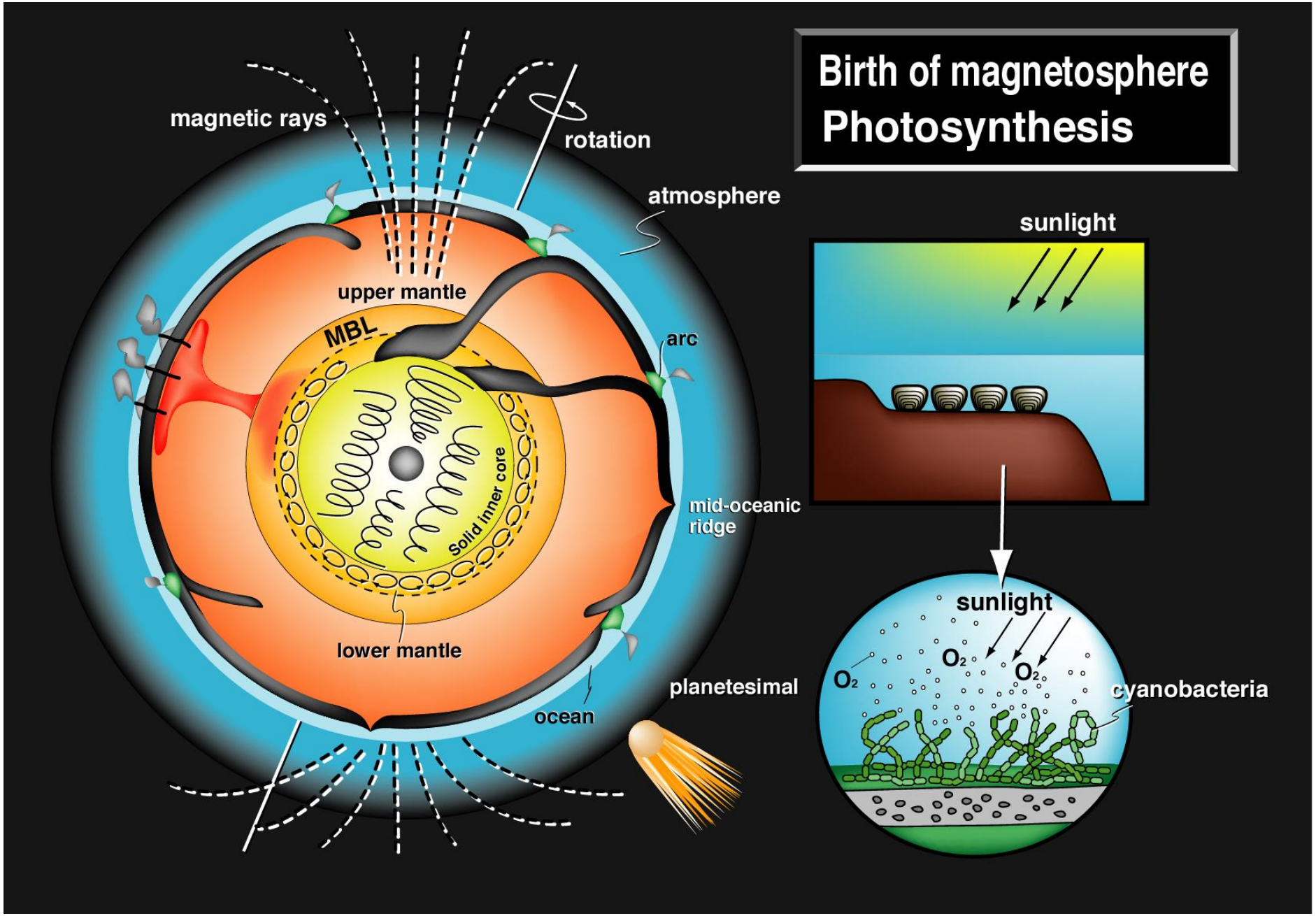
Birth of magnetosphere
Photosynthesis
magnetic rays
rotation
atmosphere
upper mantle
MBL
arc
Solid inner core
mid-oceanic ridge
lower mantle
ocean
planetesimal
sunlight
sunlight
O_2
O_2
O_2
cyanobacteria

Q : Where has water gone?

A : Deep mantle

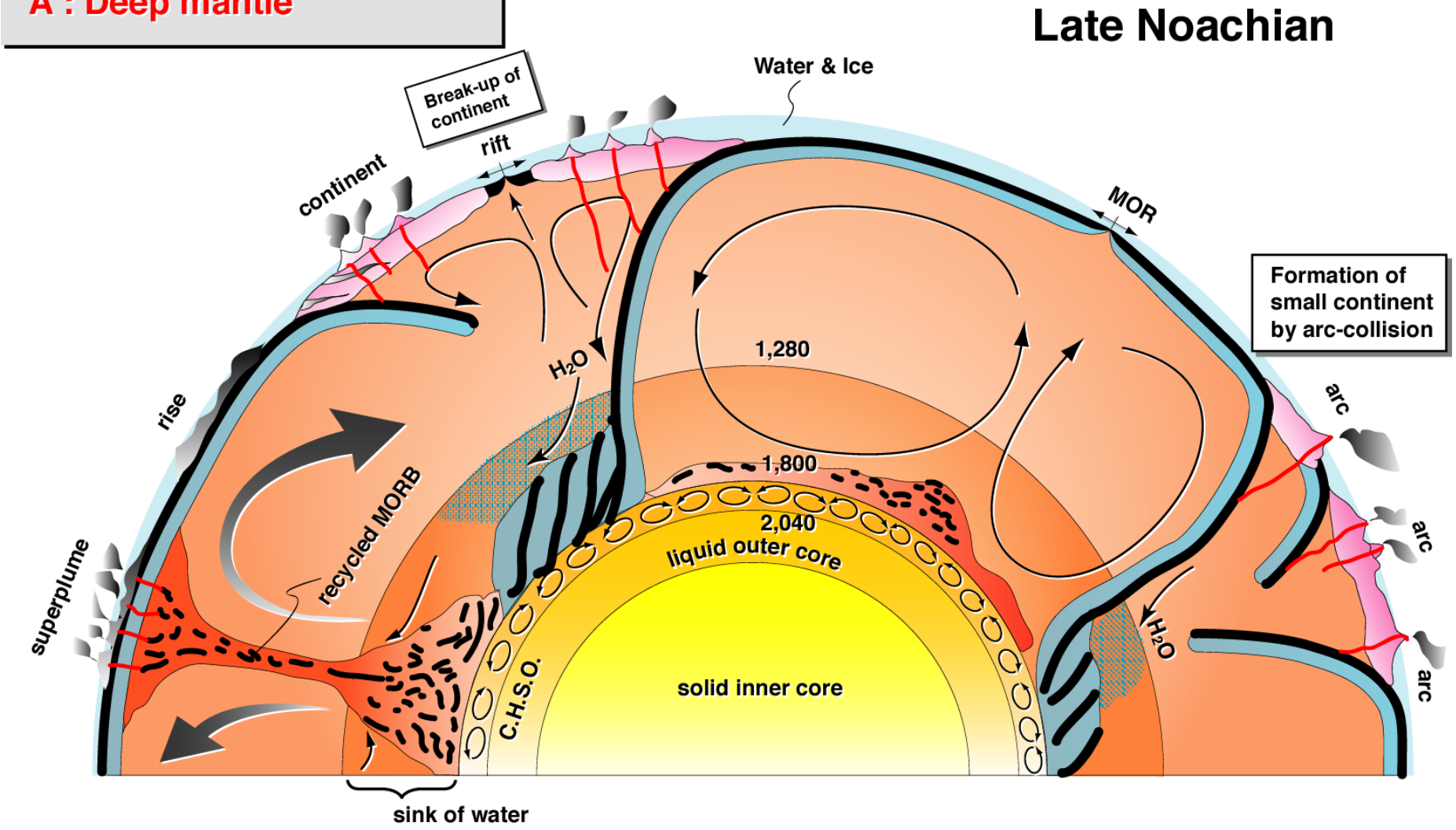

Formation mechanism of continents from arc-collision amalgamation

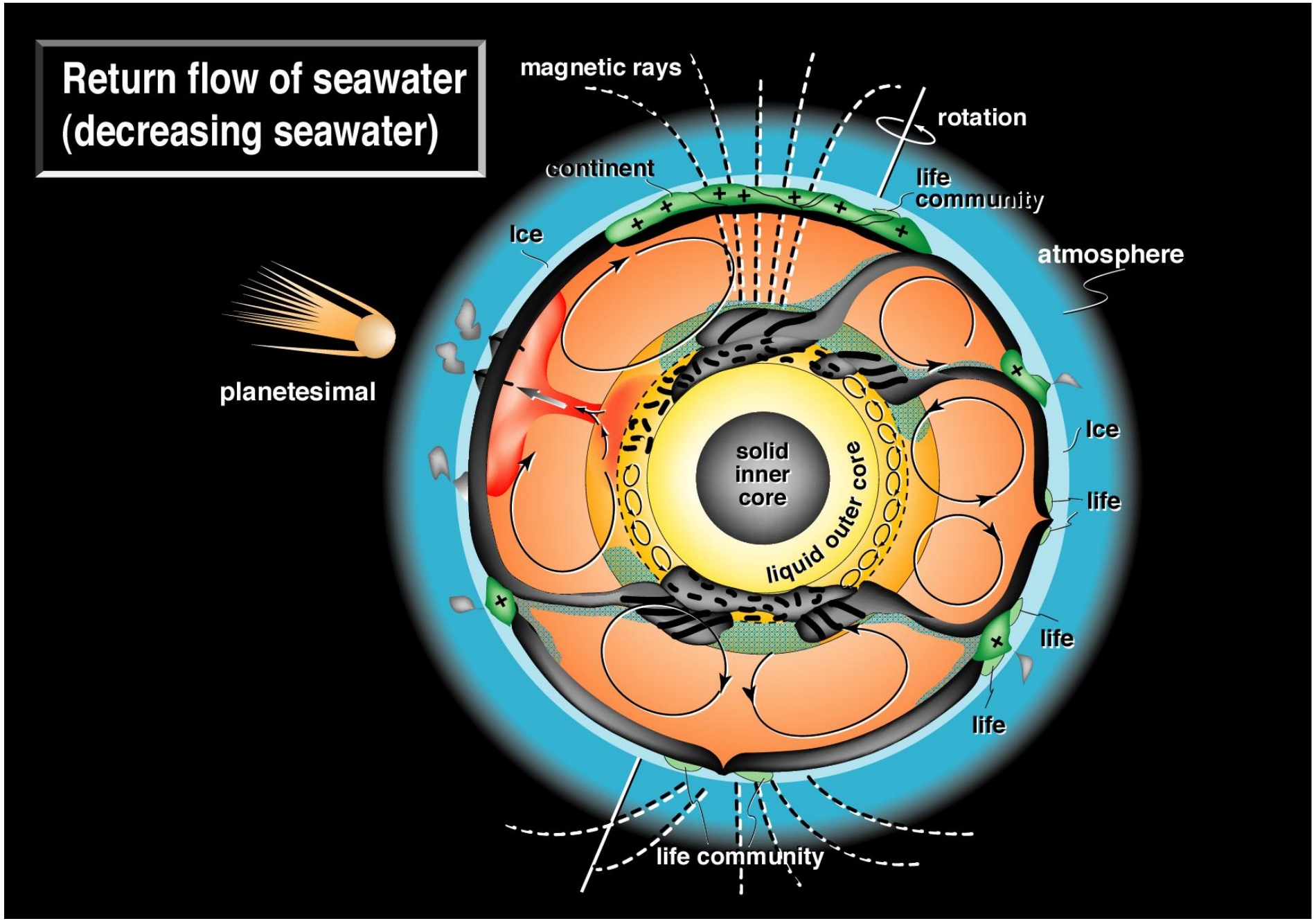
Return flow of seawater
(decreasing seawater)
magnetic rays
rotation
continent
life
community
Ice
atmosphere
planetesimal
solid
inner
core
liquid outer core
Ice
life
life
life
life community

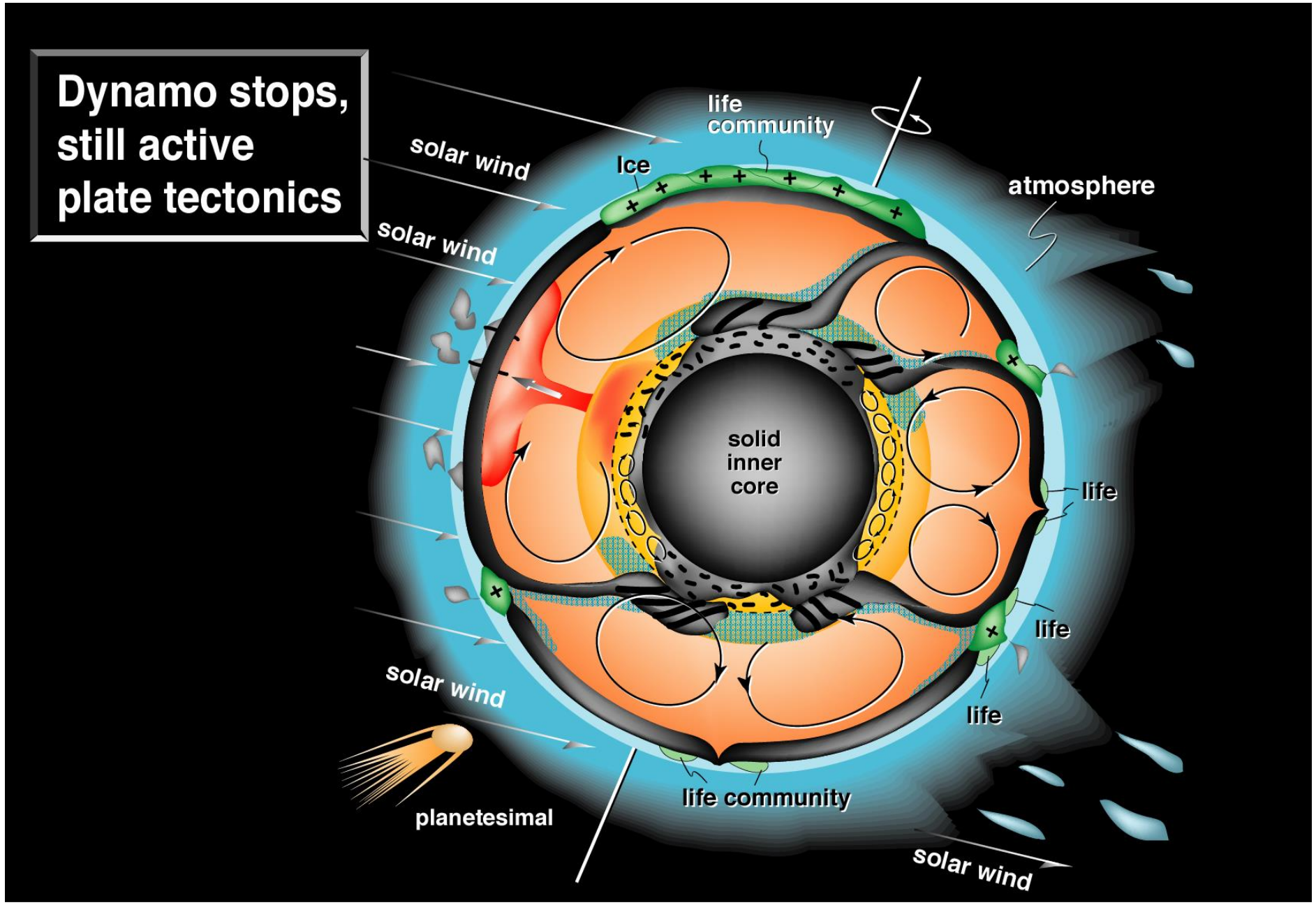
Dynamo stops,
still active
plate tectonics
solar wind
solar wind
solar wind
solar wind
life
community
Ice
atmosphere
solid
inner
core
life
life
life
life community
planetesimal

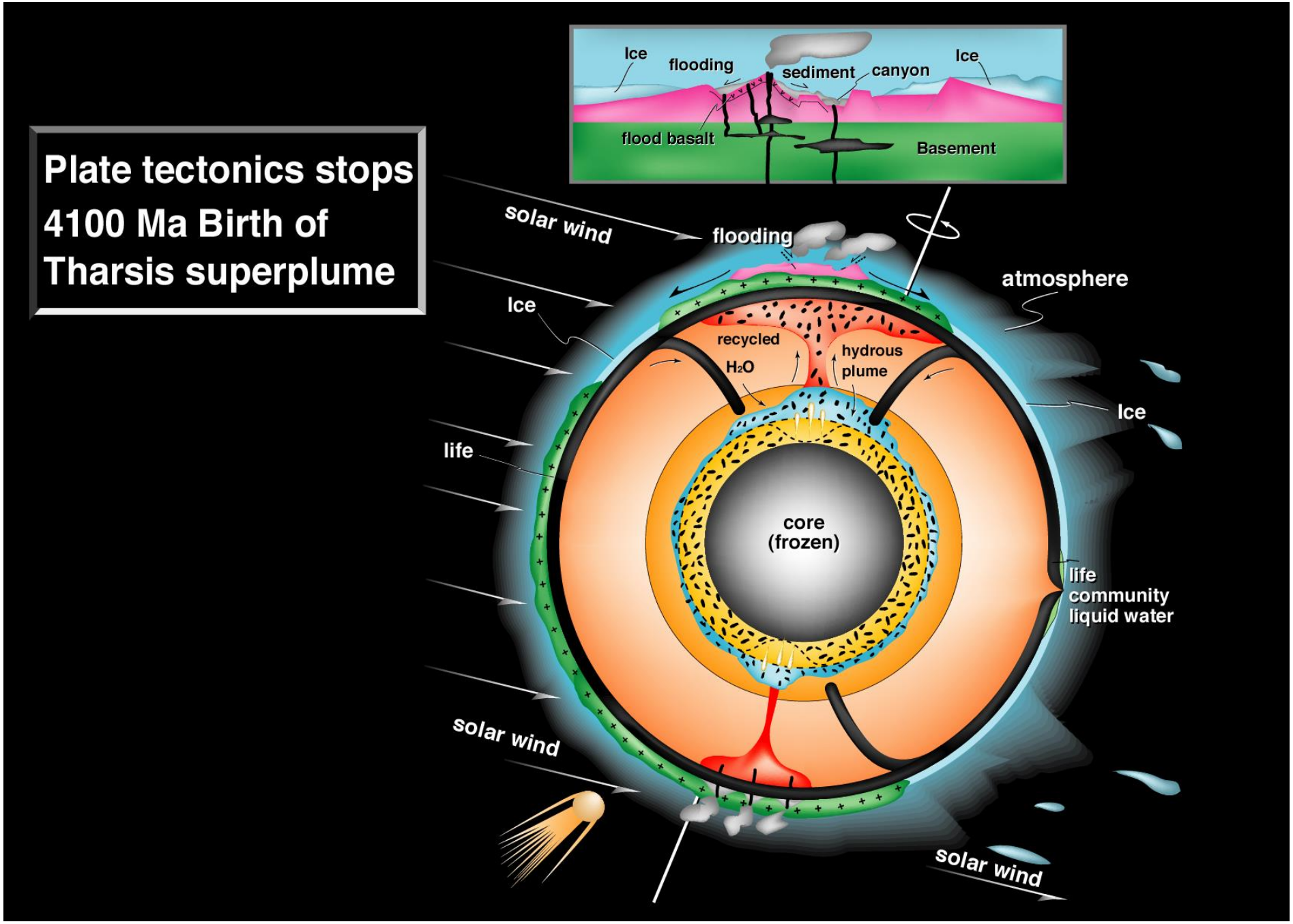
Plate tectonics stops
4100 Ma Birth of
Tharsis superplume
Ice
flooding
sediment
canyon
Ice
flood basalt
Basement
solar wind
flooding
atmosphere
Ice
recycled
H_2O
hydrous
plume
Ice
life
core
(frozen)
life
community
liquid water
solar wind
solar wind

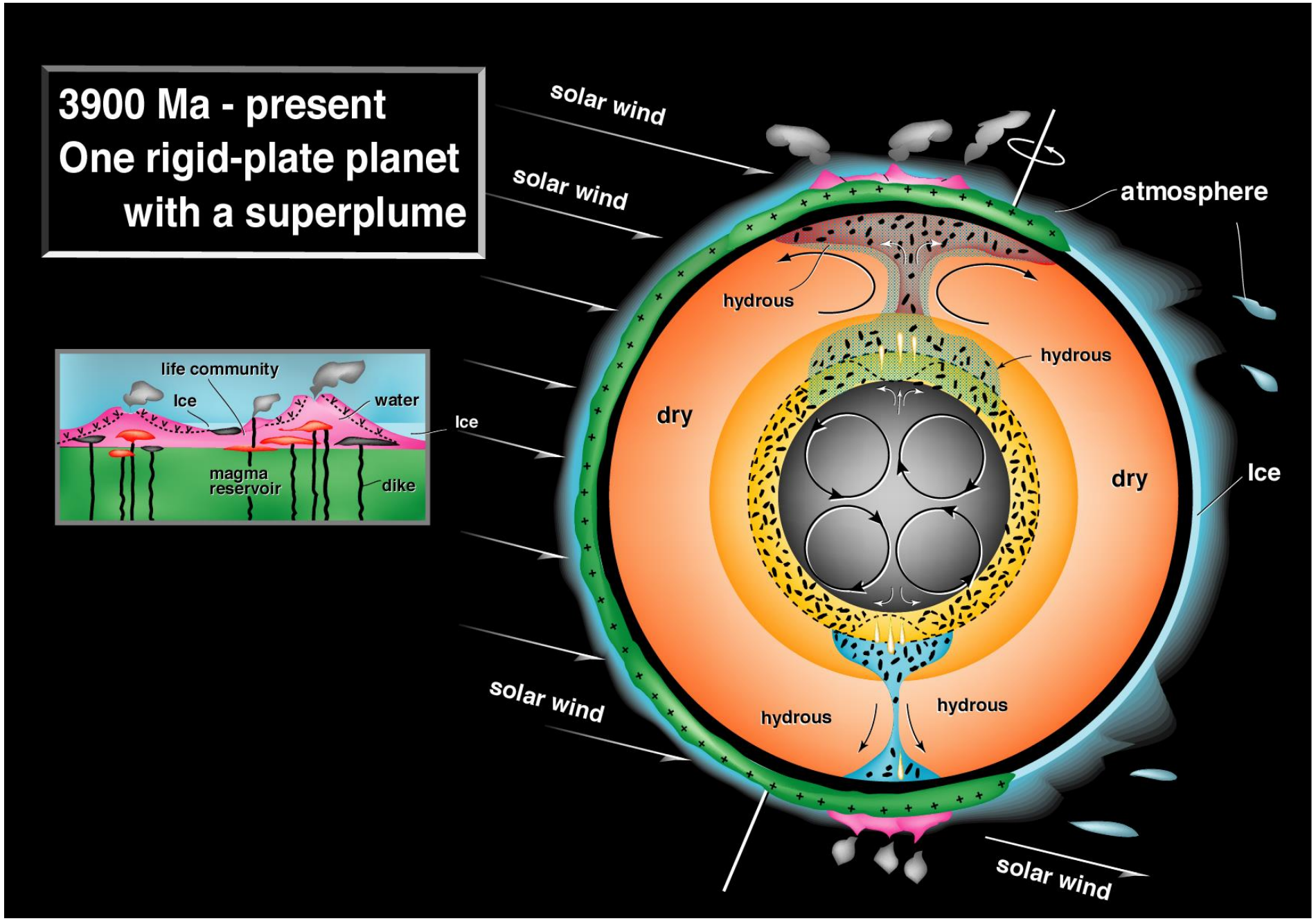
3900 Ma - present
One rigid-plate planet
with a superplume
solar wind
solar wind
atmosphere
hydrous
hydrous
dry
dry
Ice
Ice
solar wind
hydrous
hydrous
solar wind
life community
Ice
water
magma
reservoir
dike

火星史の作業仮説の改定

- １　火星の起源；太陽系惑星形成論の改定（次の講演）
- ２　大気・海洋の起源と進化（改定）
- ３　火星生命の議論（大幅改定）
- ４　火星の地質学の革新的な発展
- ５　超学際科学の必要性と危険性（カオスの時代）

Hypsographic Curves and Histogram on Earth and Mars

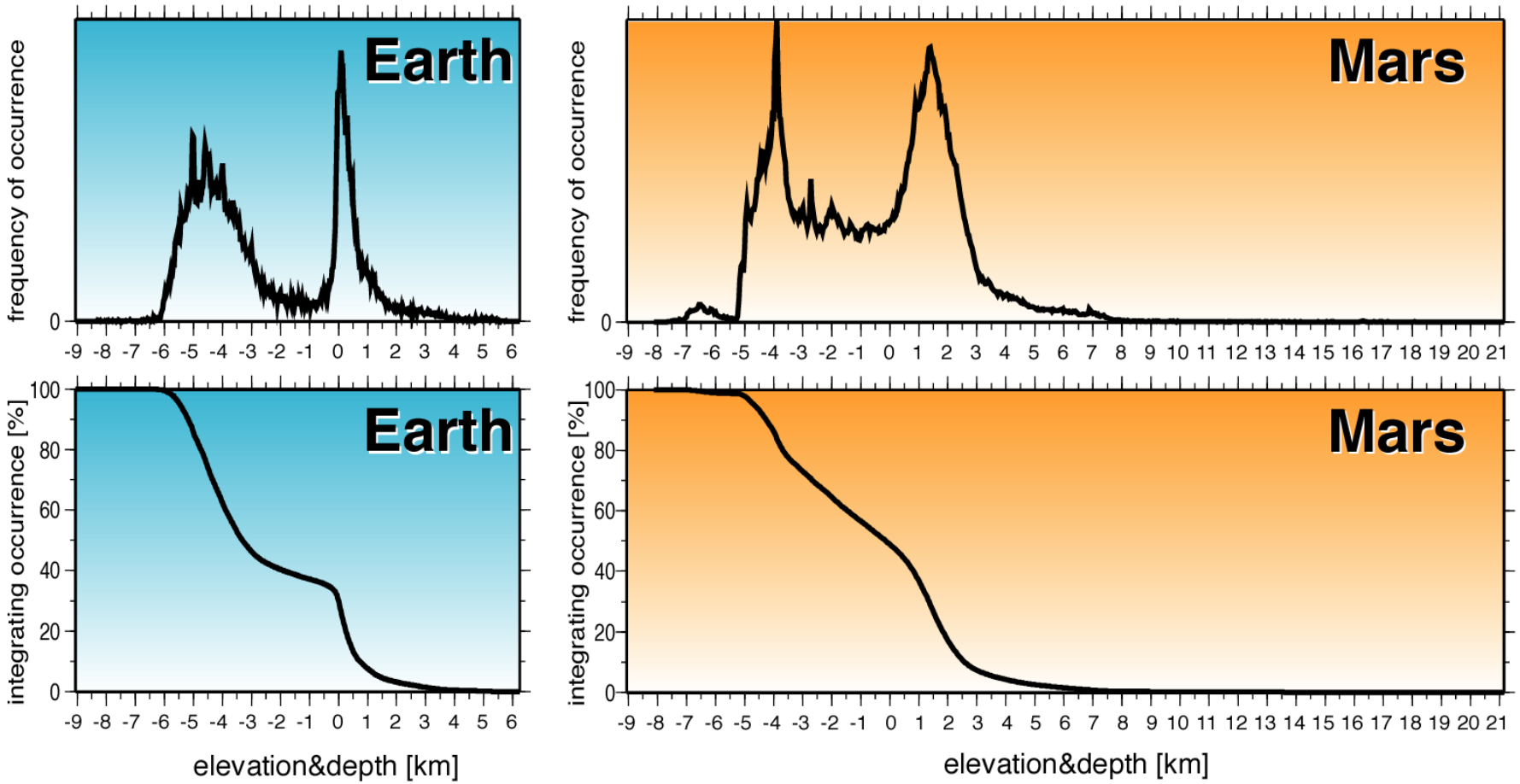

Kido (2002)

ロゼッタ探査
欧州宇宙機構、
２０１４－２０１５

Sparrow (2012) The Universe, Quercus Editions Ltd.

Capture of Dymos and Fobos

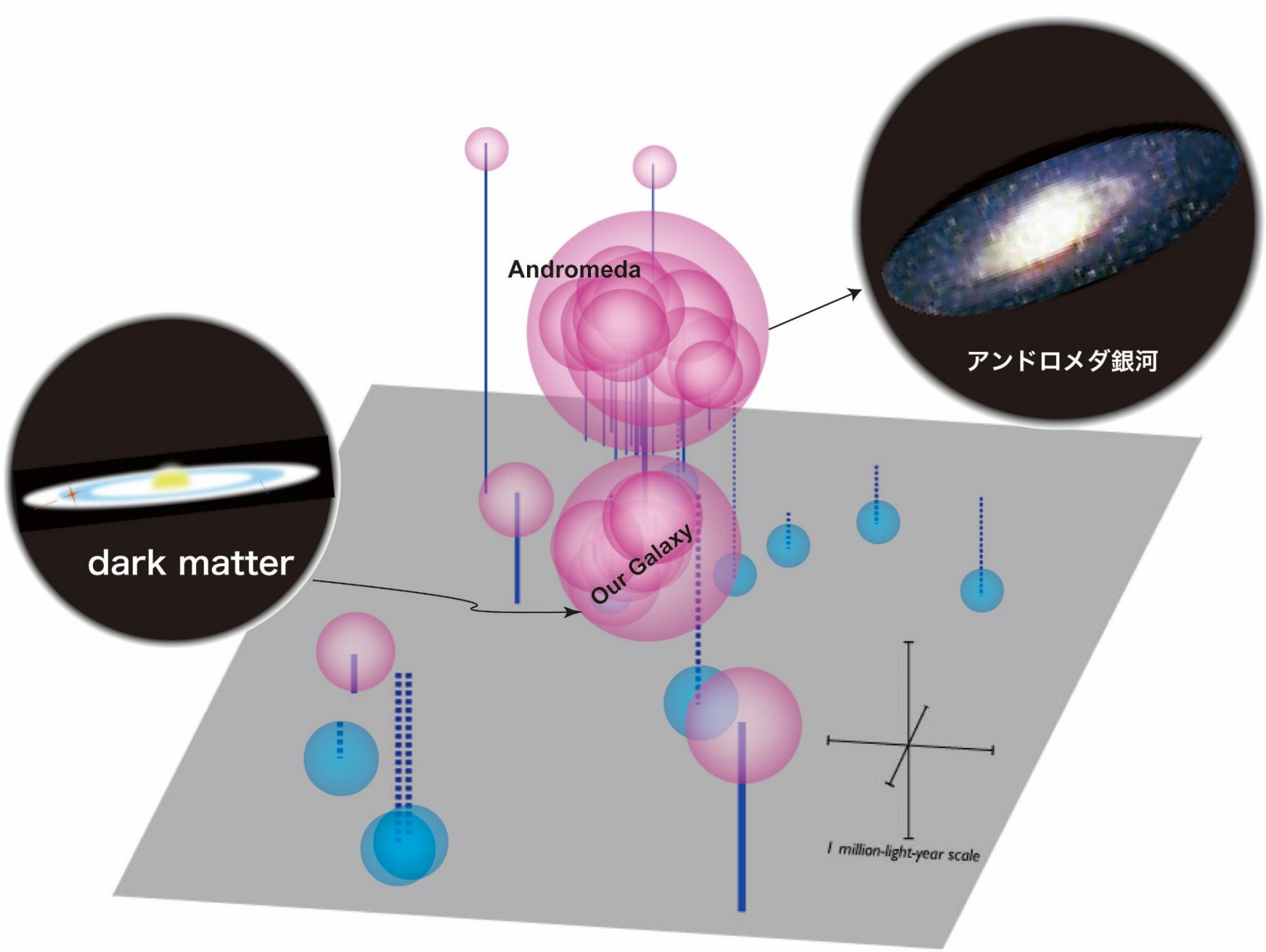
Andromeda
アンドロメダ銀河
dark matter
Our Galaxy
1 million-light-year scale

Reconstruction of Star Formation Rate (SFR)

Rocha-Pinto et al. (2000a,b)

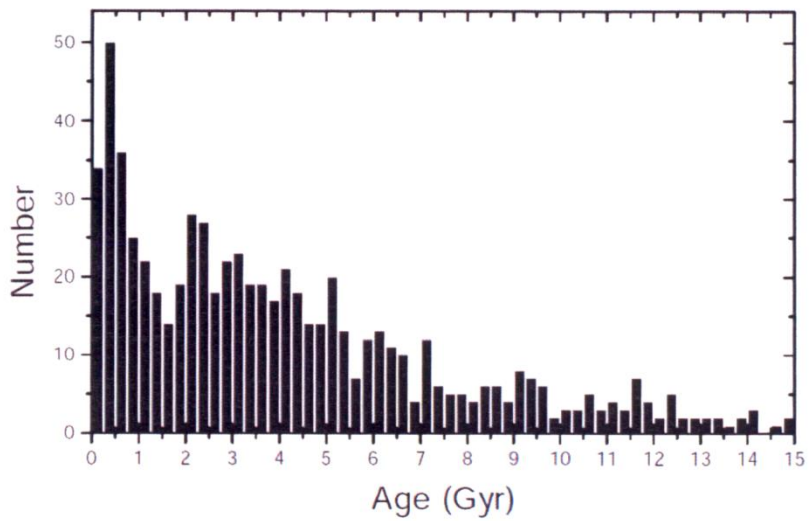

Original Data

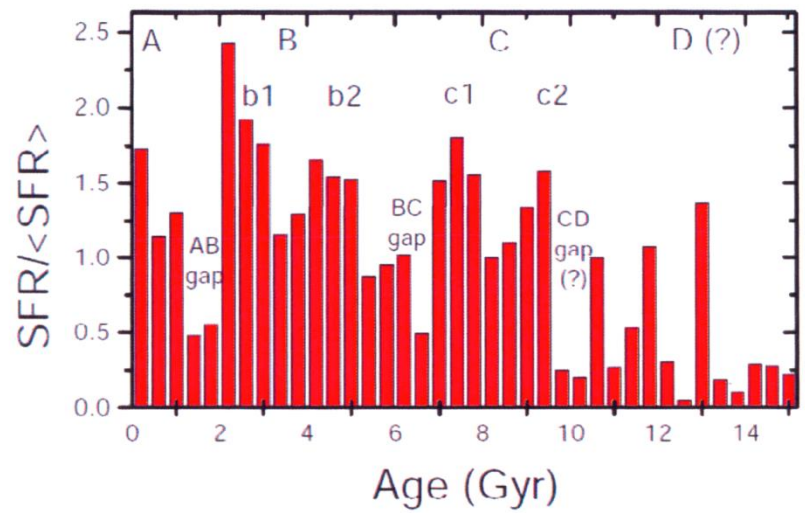

SFR after lots of "corrections"

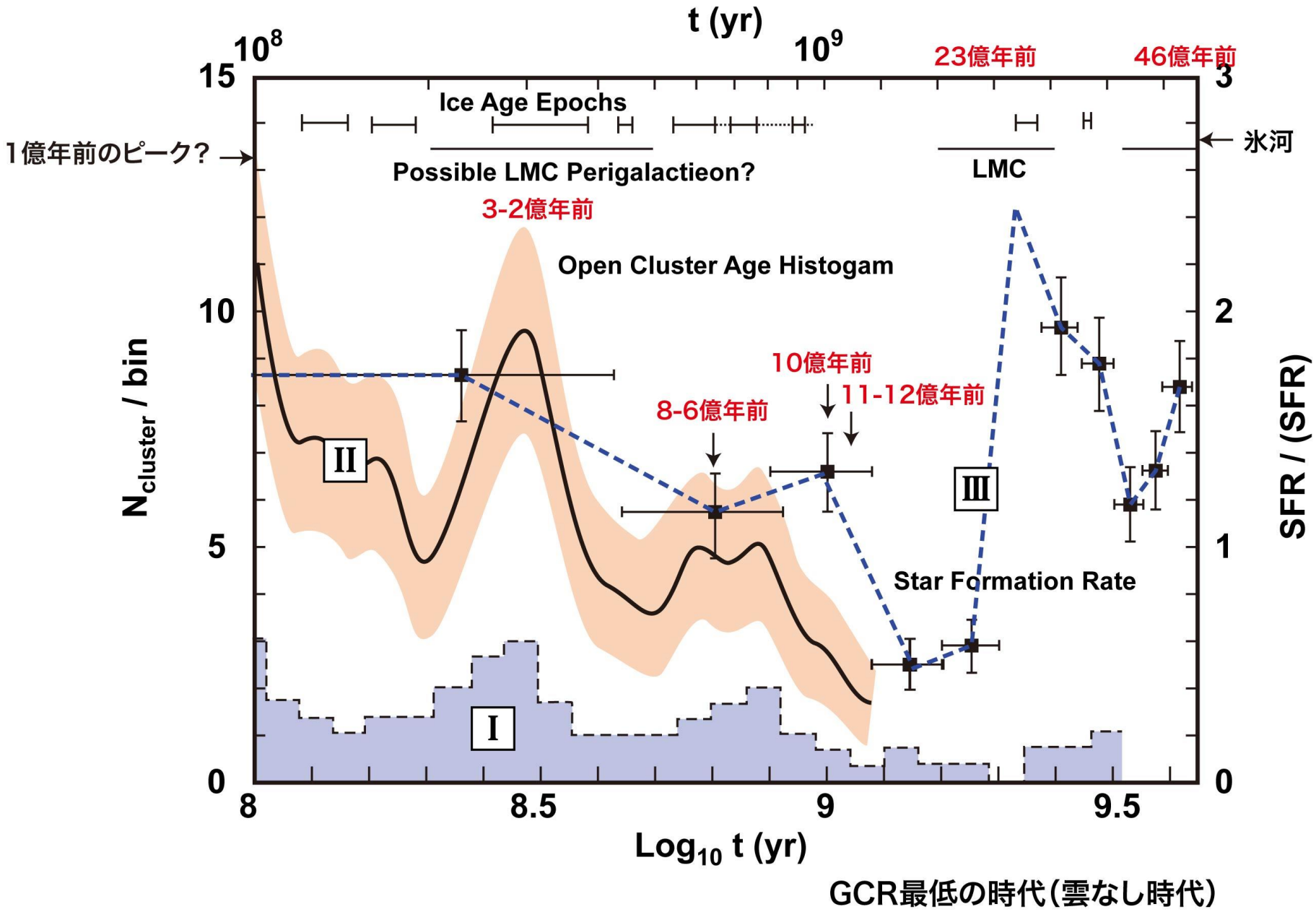
t (yr)
10^8
10^9
23億年前
46億年前
Ice Age Epochs
1億年前のピーク？
氷河
Possible LMC Perigalactieon?
LMC
3-2億年前
Open Cluster Age Histogam
10億年前
11-12億年前
8-6億年前
II
III
I
Star Formation Rate
$N_{cluster}$ / bin
SFR / (SFR)
15
10
5
0
3
2
1
0
8
8.5
9
9.5
Log_{10} t (yr)
GCR最低の時代（雲なし時代）

１回目の全球凍結

スターバースト（外力）に対する地球システムの応答

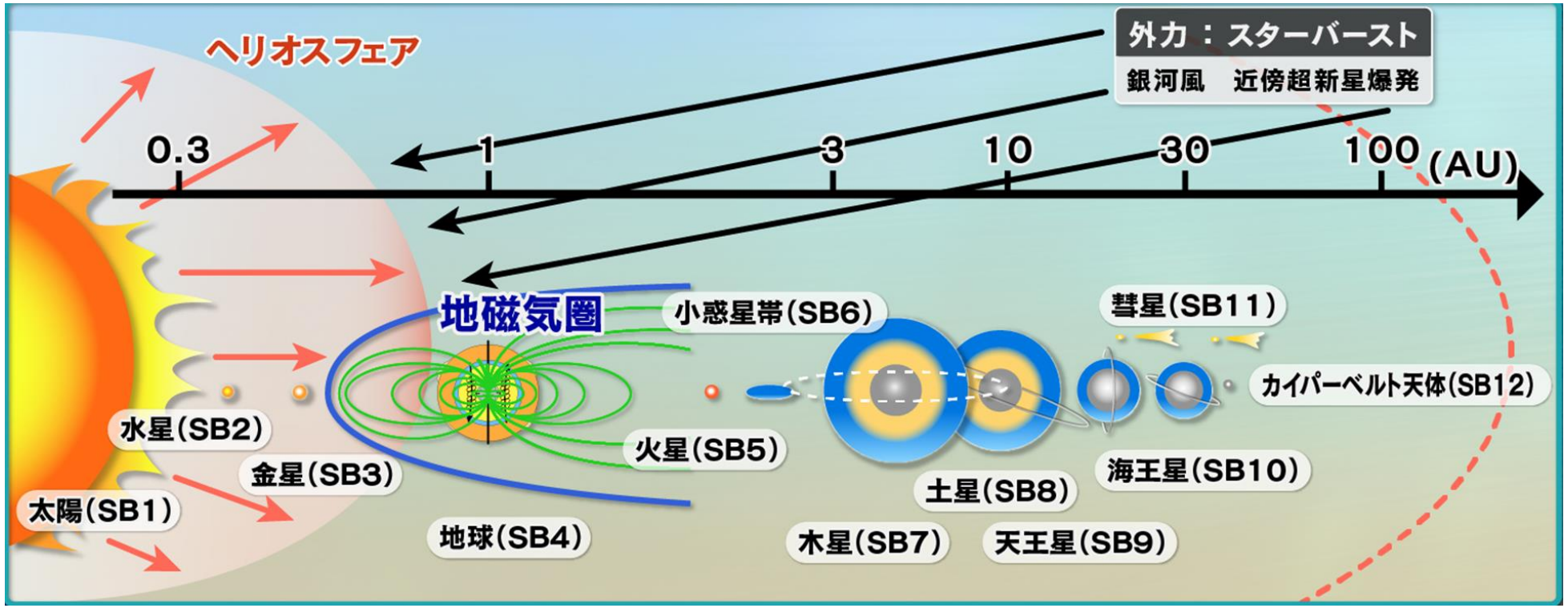

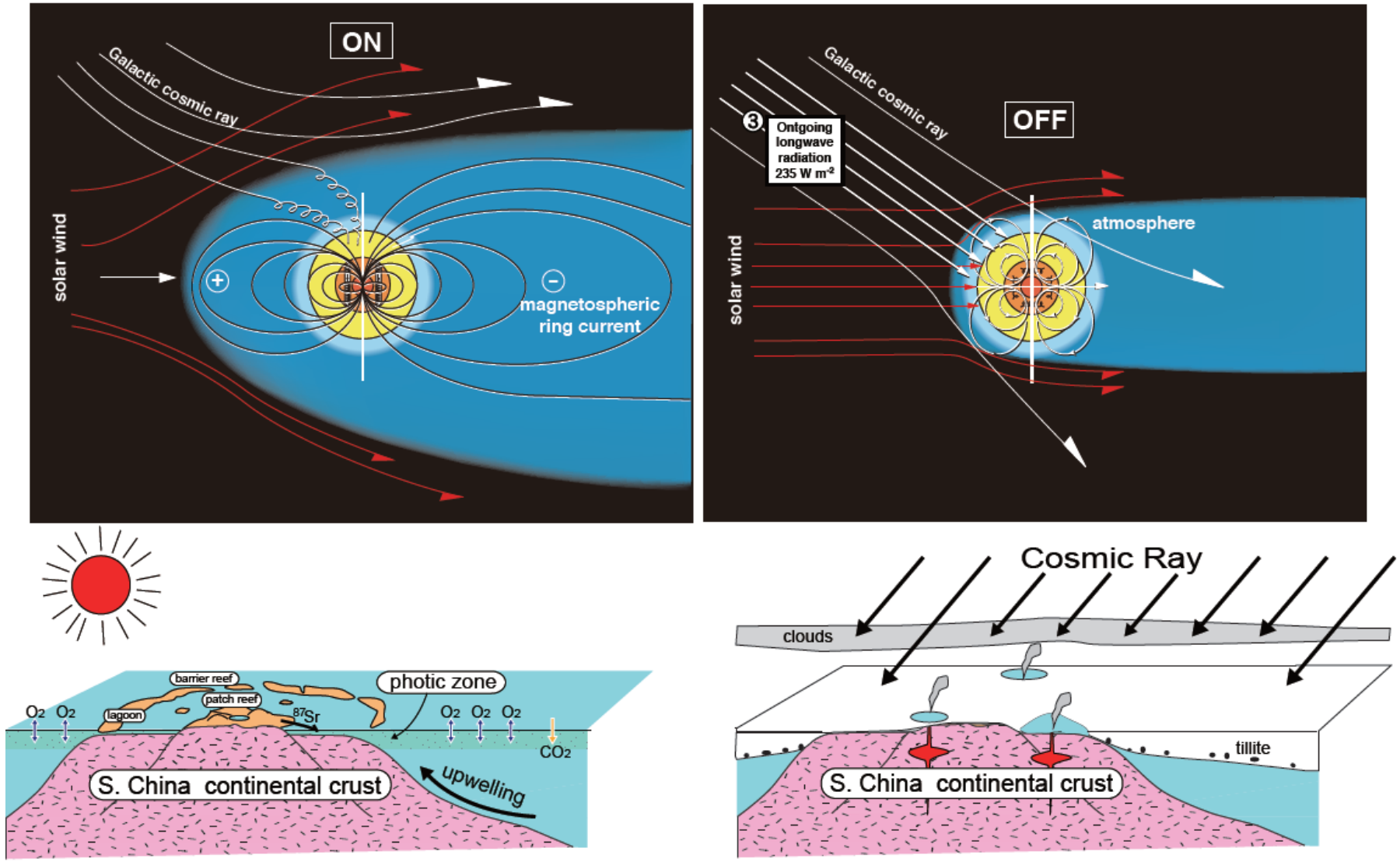

Maruyama et al., 2013

540Ma

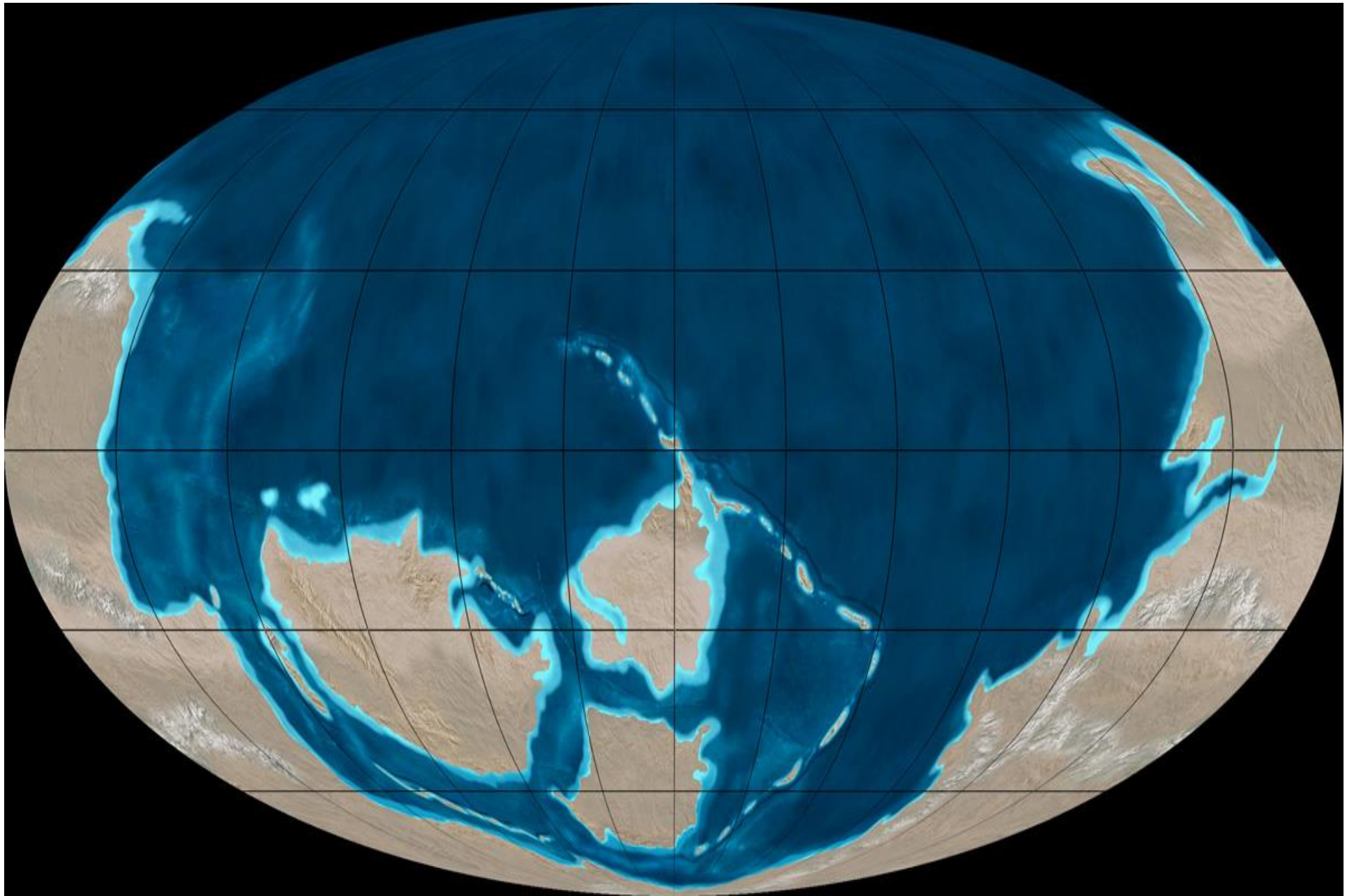

260Ma

ペルム紀末寒冷期

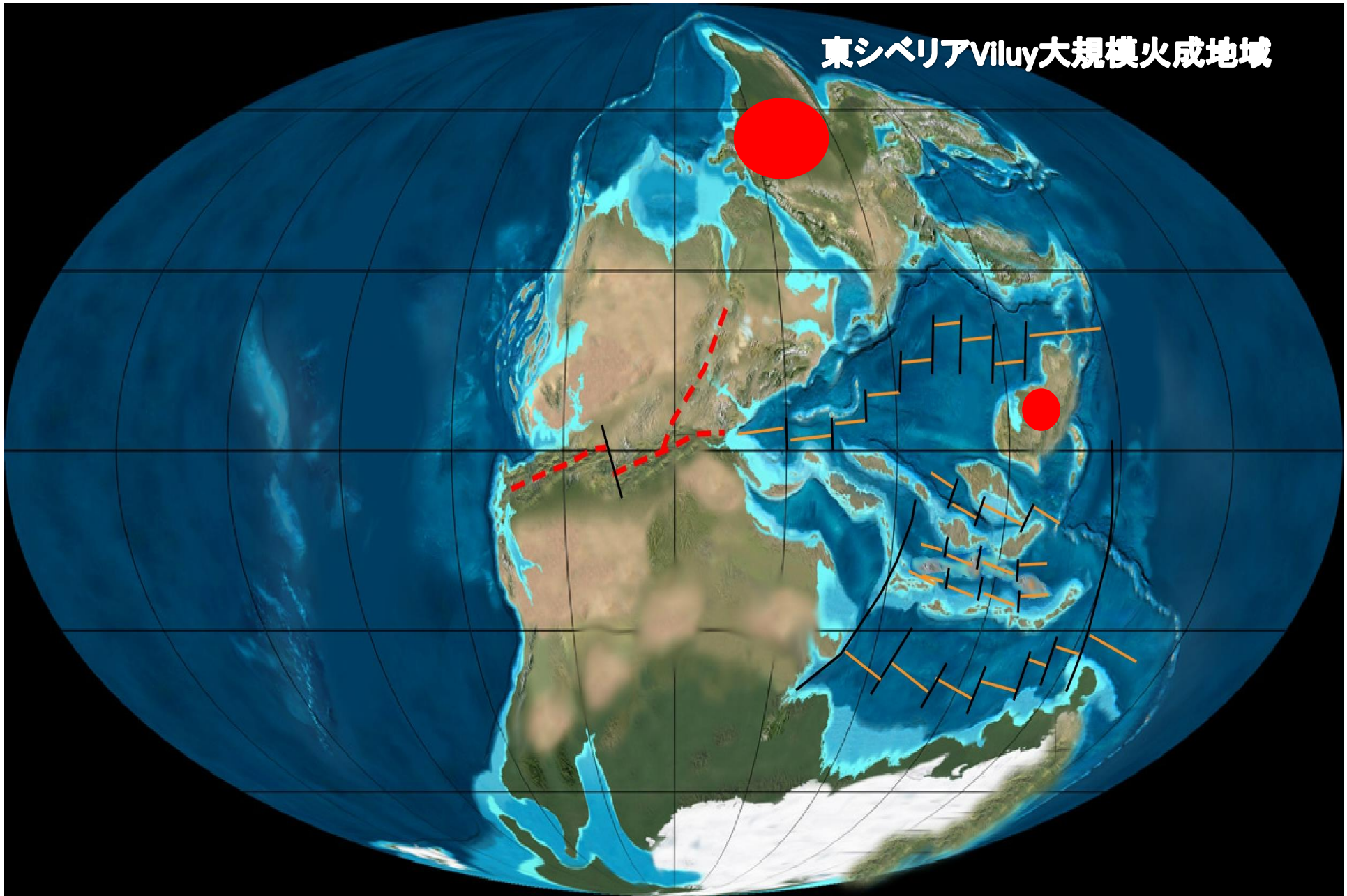

Chapter 1

Research History

2.火星の起源、歴史と生命存在可能性

3.宇宙生物学の未来

Chapter 2

General characteristics on Mars

Chapter 3 Geologic Mapping of Mars

Surface geology

How to demonstrate the presence of Accretionary complex

(1) Layer-parallel thrust
(2) Rock assemblages
(3) Ocean-plate stratigraphy

(1) How to determine OPS
(2) Hemipelagite indicates the arrival time of oceanic plate at trench.
(3) Thickness of chert (age difference) indicates how old is the oceanic plate
(4) Chemical composition of cap turbidite indicates the depositional environment, **continental margin or intra-oceanic.**

Bottom of OPS:MORB work by Saito shows the remnant **of subducted slabs**.

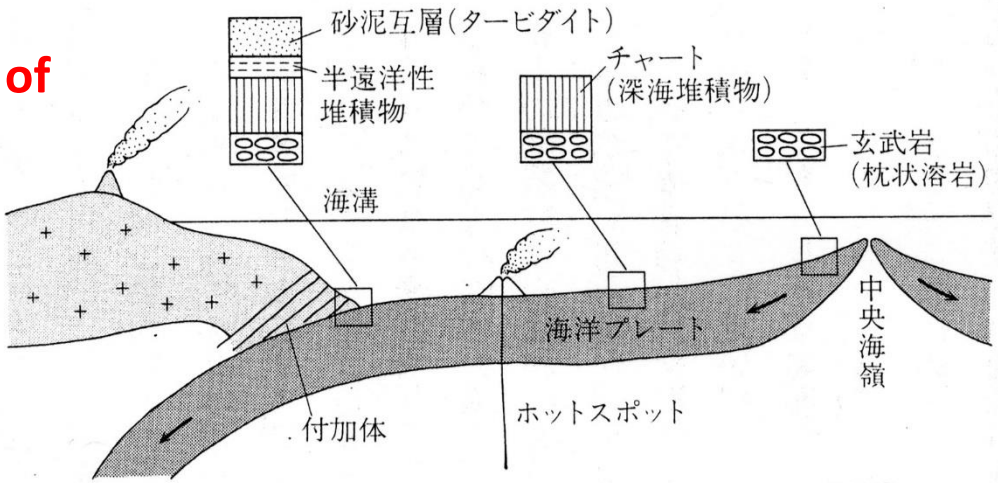

図8 海洋プレートの層序．海洋プレートの表層には，中央海嶺から離れるに従って地層の積み重なり(層序)が発達する．(磯崎たち，1990)

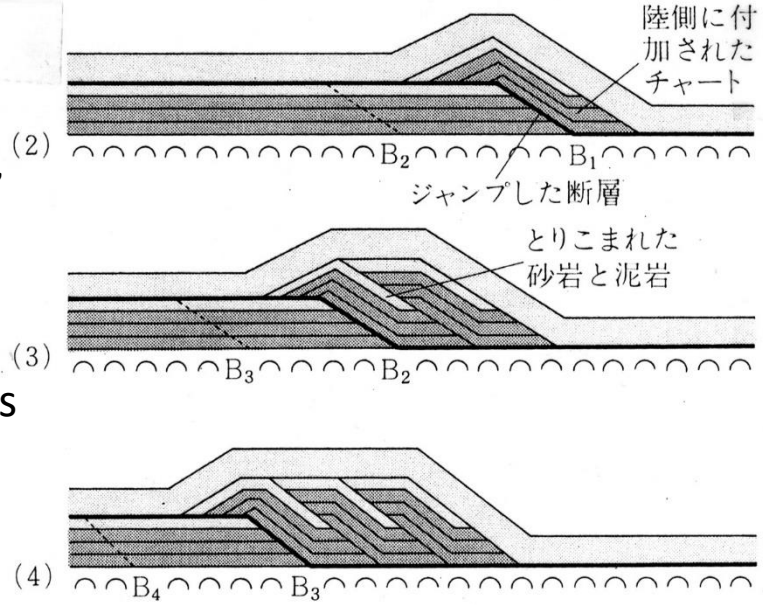

図7 デュープレックス構造のでき方(断面図)．海洋プレートが左から右下に沈み込むと，海洋プレート表層のチャート層が次々とたたみ込まれて，陸側に付加していく．

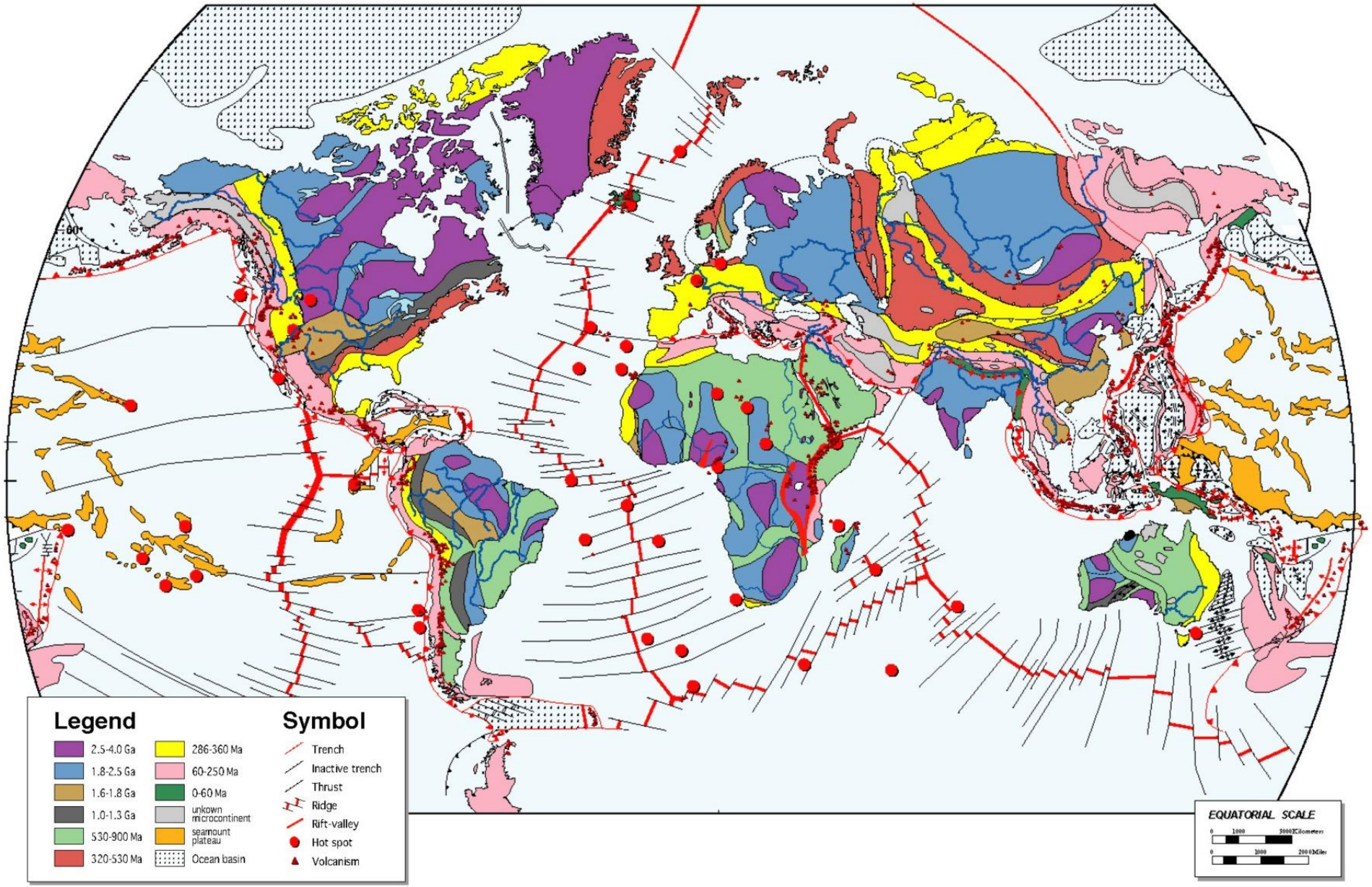
Legend
2.5-4.0 Ga
1.8-2.5 Ga
1.6-1.8 Ga
1.0-1.3 Ga
530-900 Ma
320-530 Ma
286-360 Ma
60-250 Ma
0-60 Ma
unkown microcontinent
seamount plateau
Ocean basin
Symbol
Trench
Inactive trench
Thrust
Ridge
Rift-valley
Hot spot
Volcanism
EQUATORIAL SCALE

Orogeny

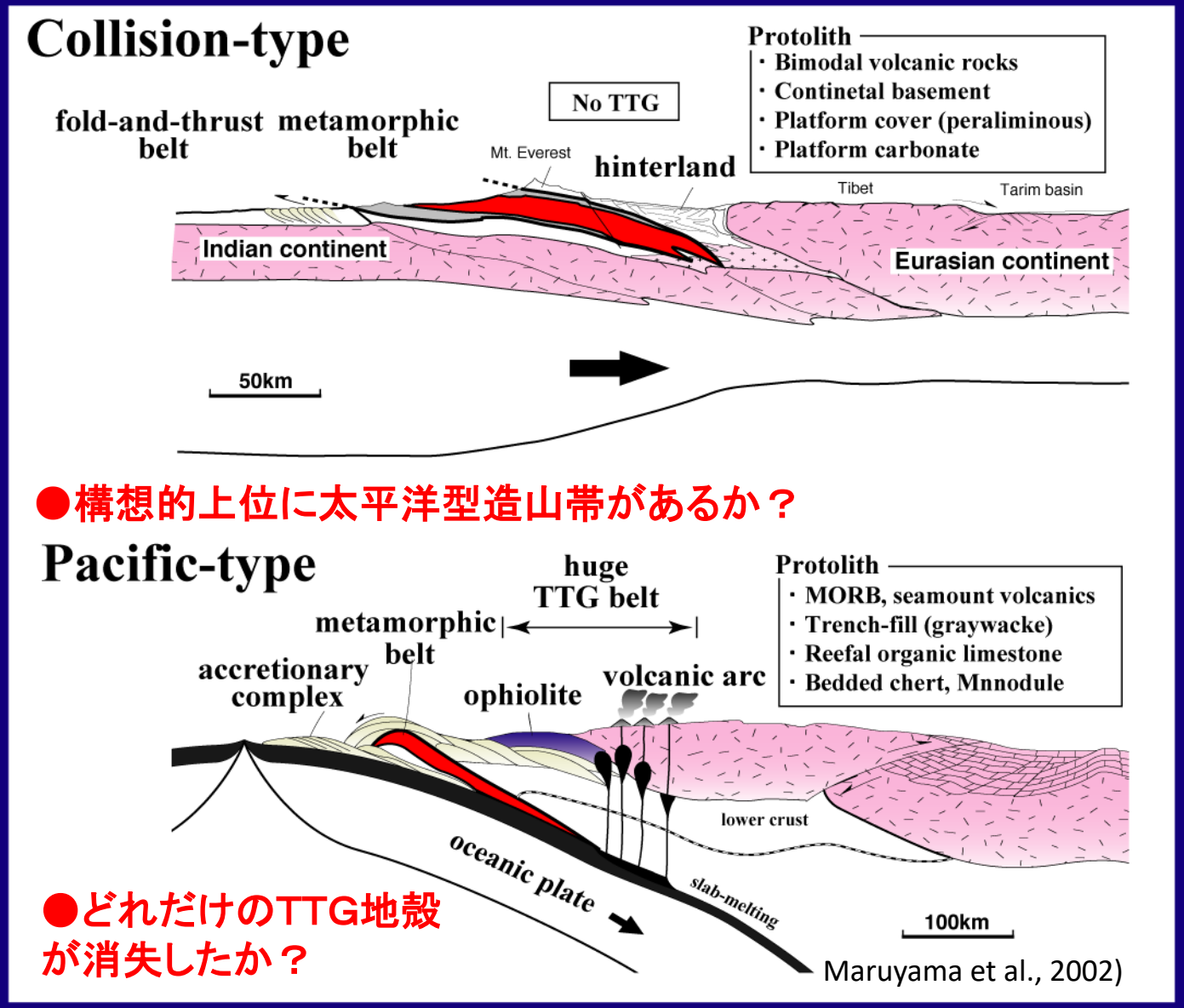
Collision-type
Protolith
・Bimodal volcanic rocks
・Continetal basement
・Platform cover (peraliminous)
・Platform carbonate
No TTG
fold-and-thrust belt
metamorphic belt
Mt. Everest
hinterland
Tibet
Tarim basin
Indian continent
Eurasian continent
50km
●構想的上位に太平洋型造山帯があるか？
Pacific-type
huge TTG belt
Protolith
・MORB, seamount volcanics
・Trench-fill (graywacke)
・Reefal organic limestone
・Bedded chert, Mnnodule
metamorphic belt
accretionary complex
ophiolite
volcanic arc
lower crust
oceanic plate
slab-melting
100km
●どれだけのTTG地殻が消失したか？
Maruyama et al., 2002)

Ophiolite and Alpine-peridotite

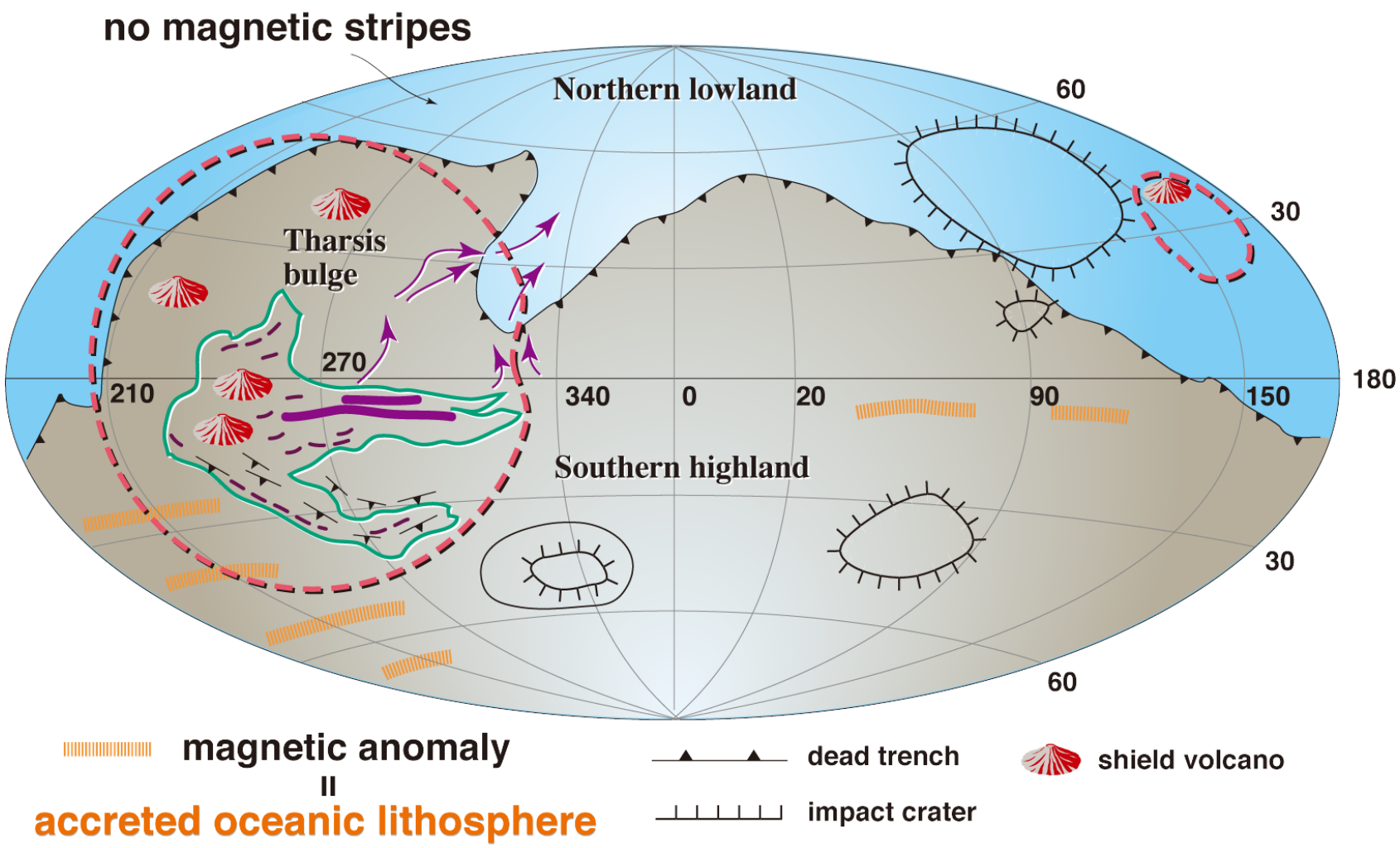
no magnetic stripes
Northern lowland
Tharsis bulge
Southern highland
60
30
180
150
90
20
0
340
270
210
30
60
magnetic anomaly
II
accreted oceanic lithosphere
dead trench
impact crater
shield volcano

Vertically-dipping duplex geologic units of olistostome-like accretionary complex

Concept of suture defined by ophiolite belt or Alpine-type peridotite

- If necesaary, Dewey gram is attached.

Chapter 4

Mantle and Core

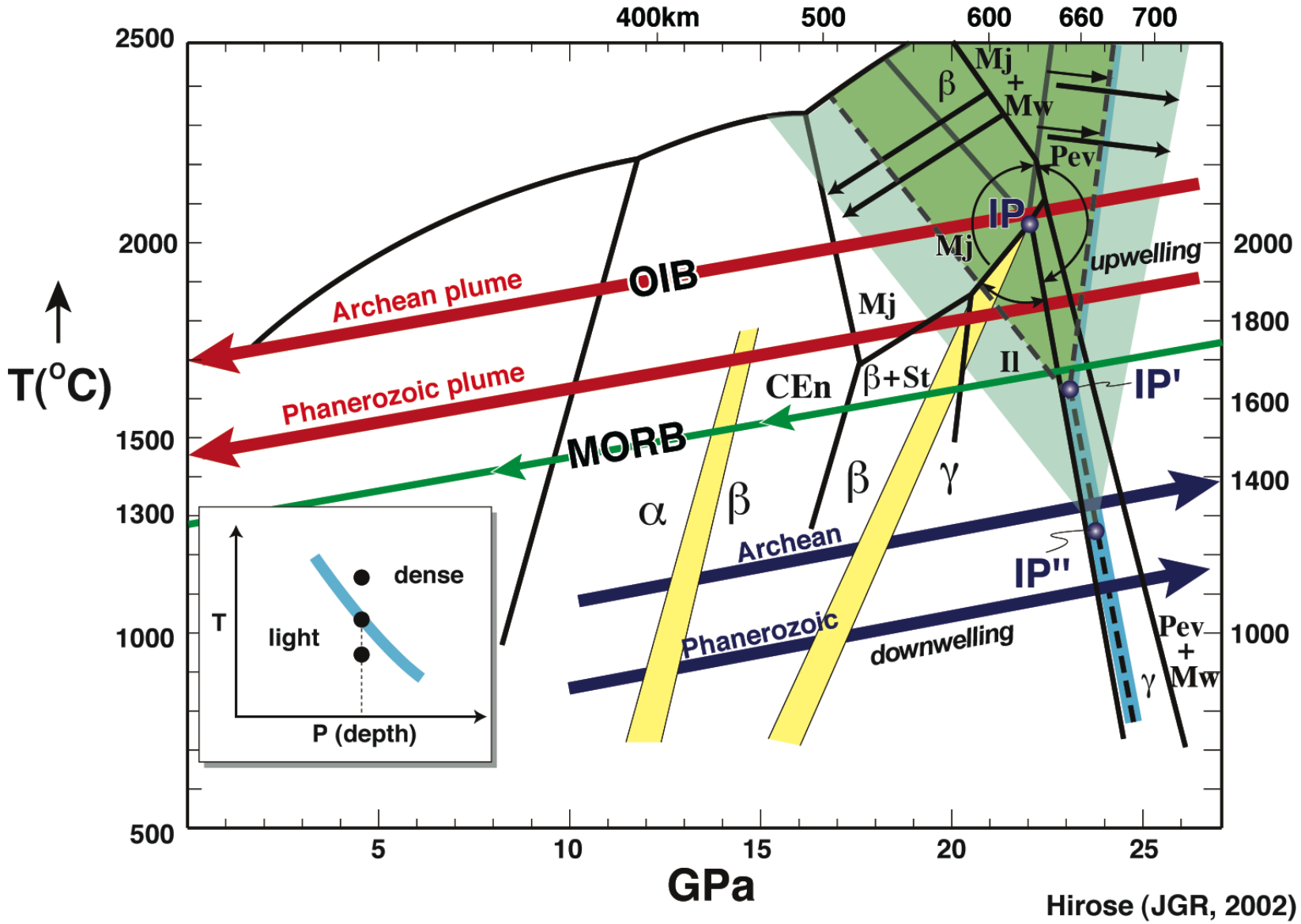

Hirose (JGR, 2002)

Earliest Noachian

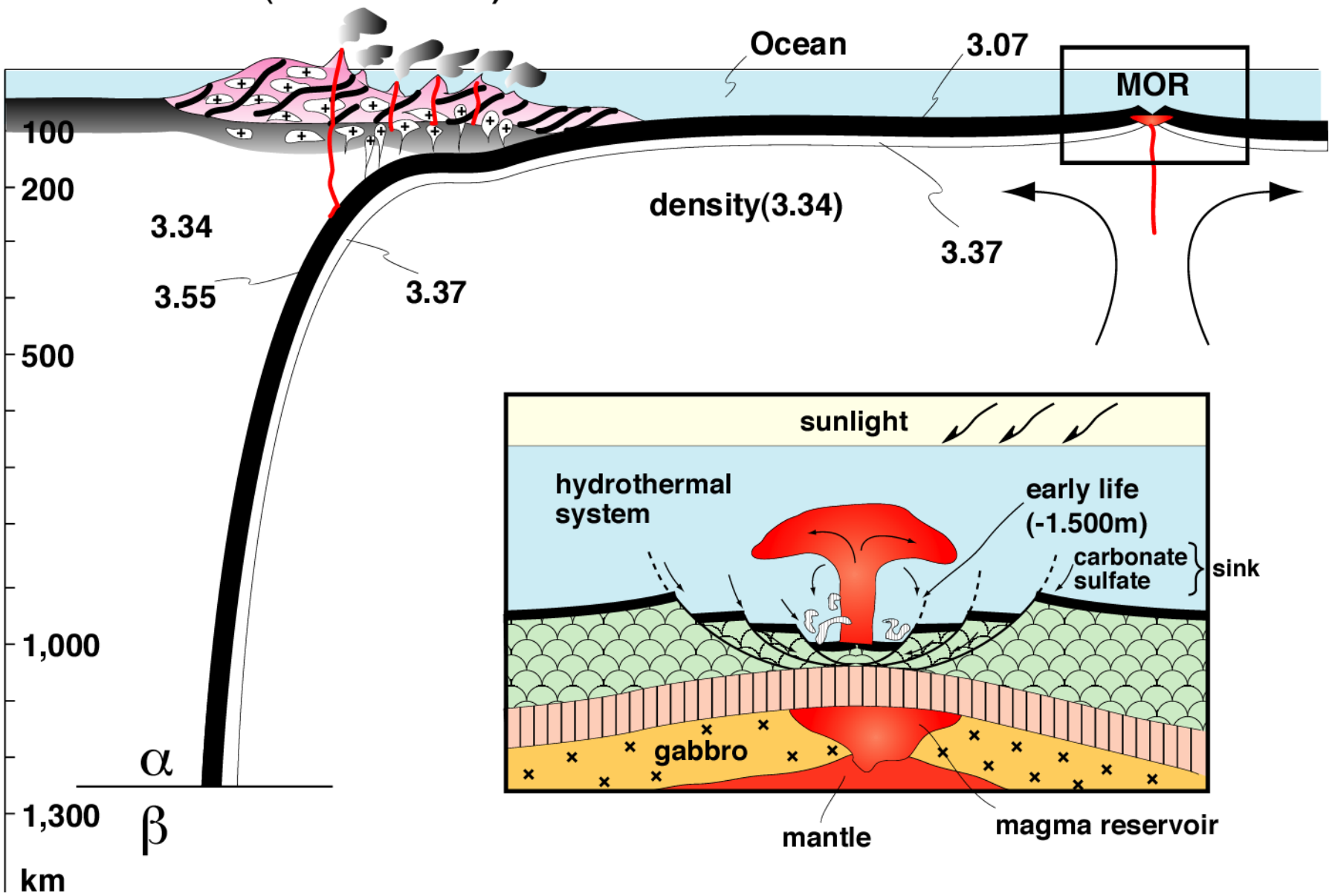

海水の逆流開始

↓

陸地面積の増大

↓

表層環境の多様性

↓

酸化大気

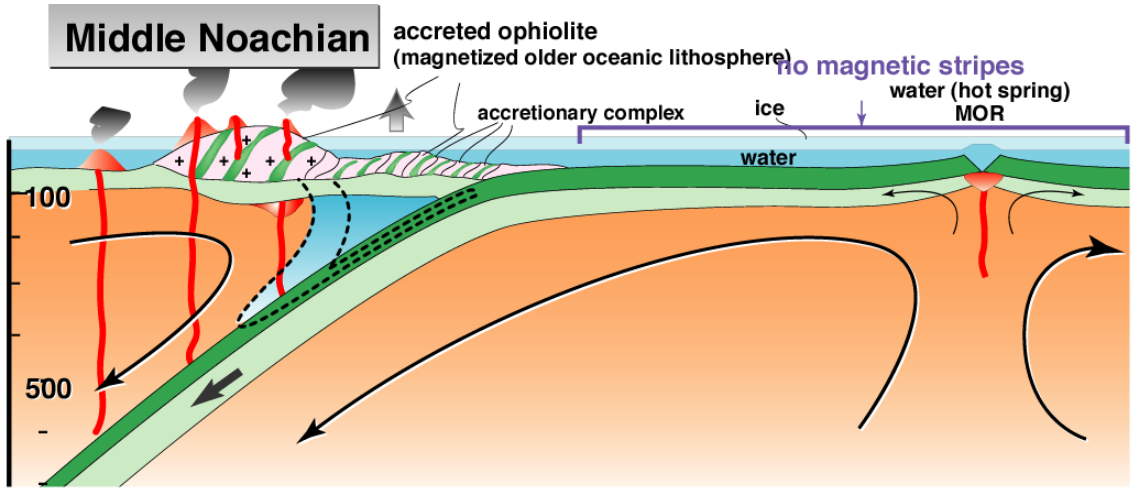

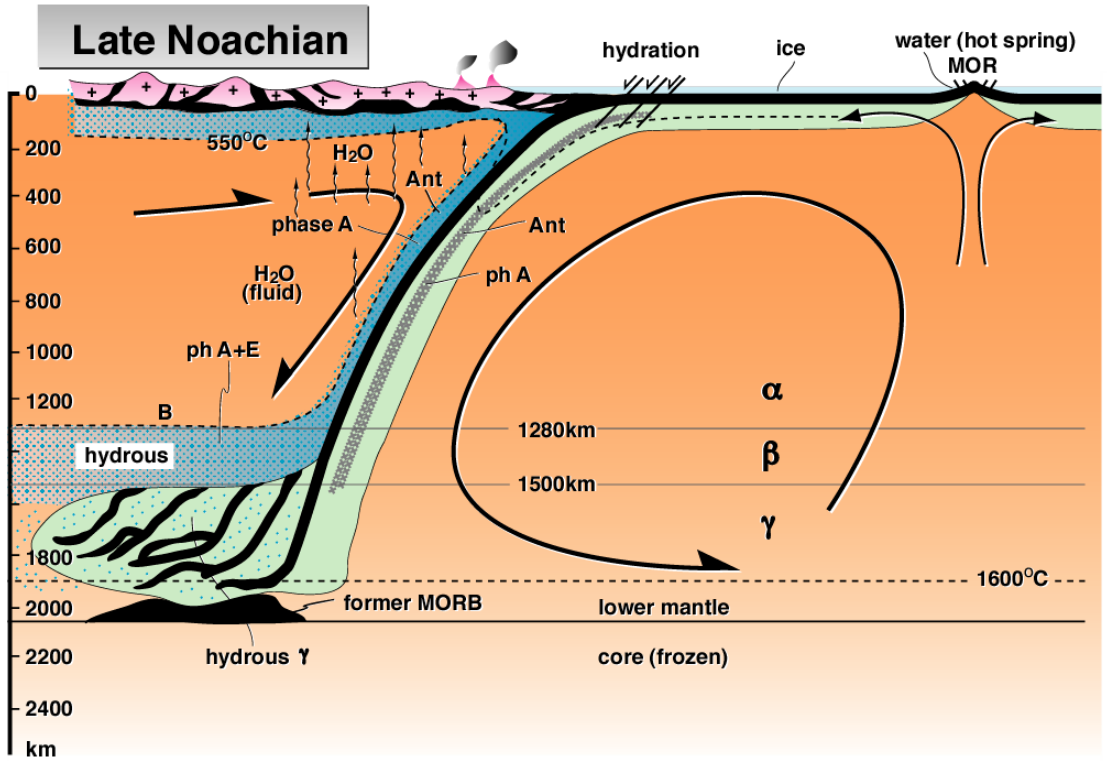

Subduction 200-520Ma

(1) Birth of a cold superplume at 300Ma in Asia
(2) Position of future supercontinent

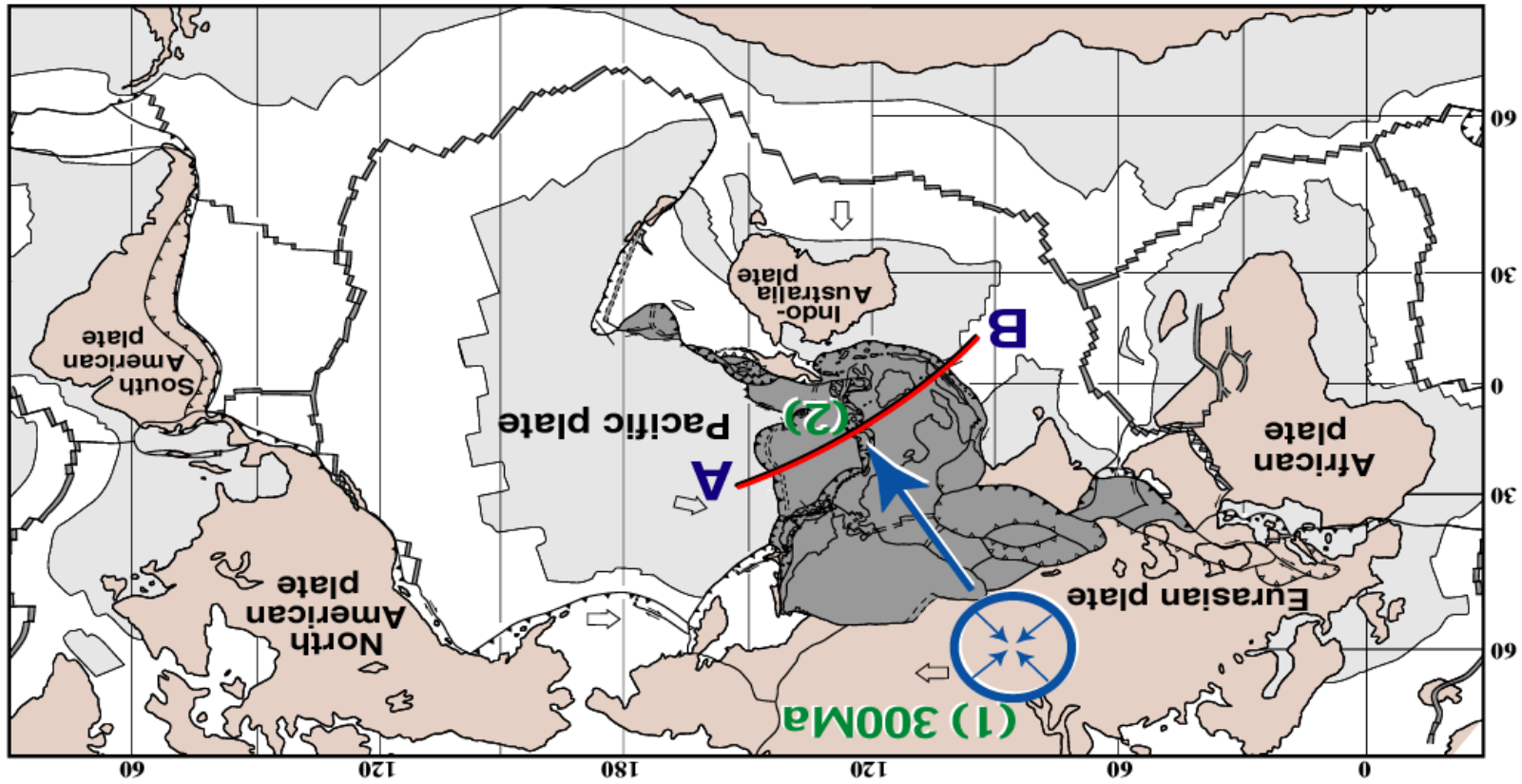

Mars vs Earth; If TTG is common on Mars, no difference in-between, what the difference in apparent Usui's Figure? Simply the difference of rock-types

AFM diagram is necessary

Petrogenesis of TTG magma

- 臼井論文→火星内部の温度と組成を推定する。火星の起源隕石は地球に近い（地殻・マントル・コアの比がほぼ同じ：enstatite chondriteに近いが100%同じではない、アルカリが多いだろう、表層は硫黄に満ちている）
- Blueberry minerals (List) and estimation for the host ponds to evaporate minerals enriched in S, salts (similar to the Archean ocean on the Earth)
- Petrogenesis of TTG (andesite) magma; point is the relative abundance of basaltic (gabbroic) part, cf. Moon and Earth

Augite earlier than plagioclase

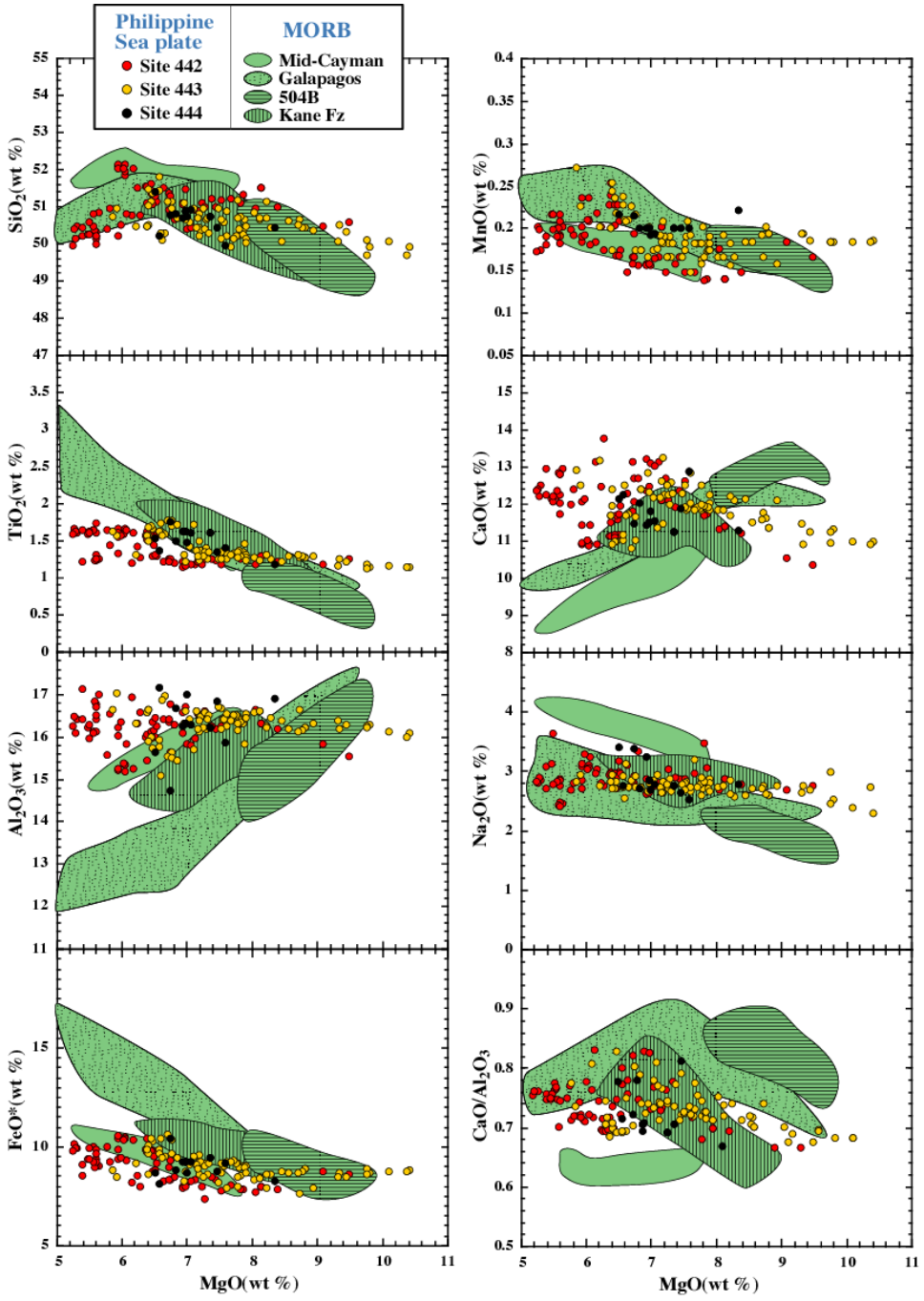

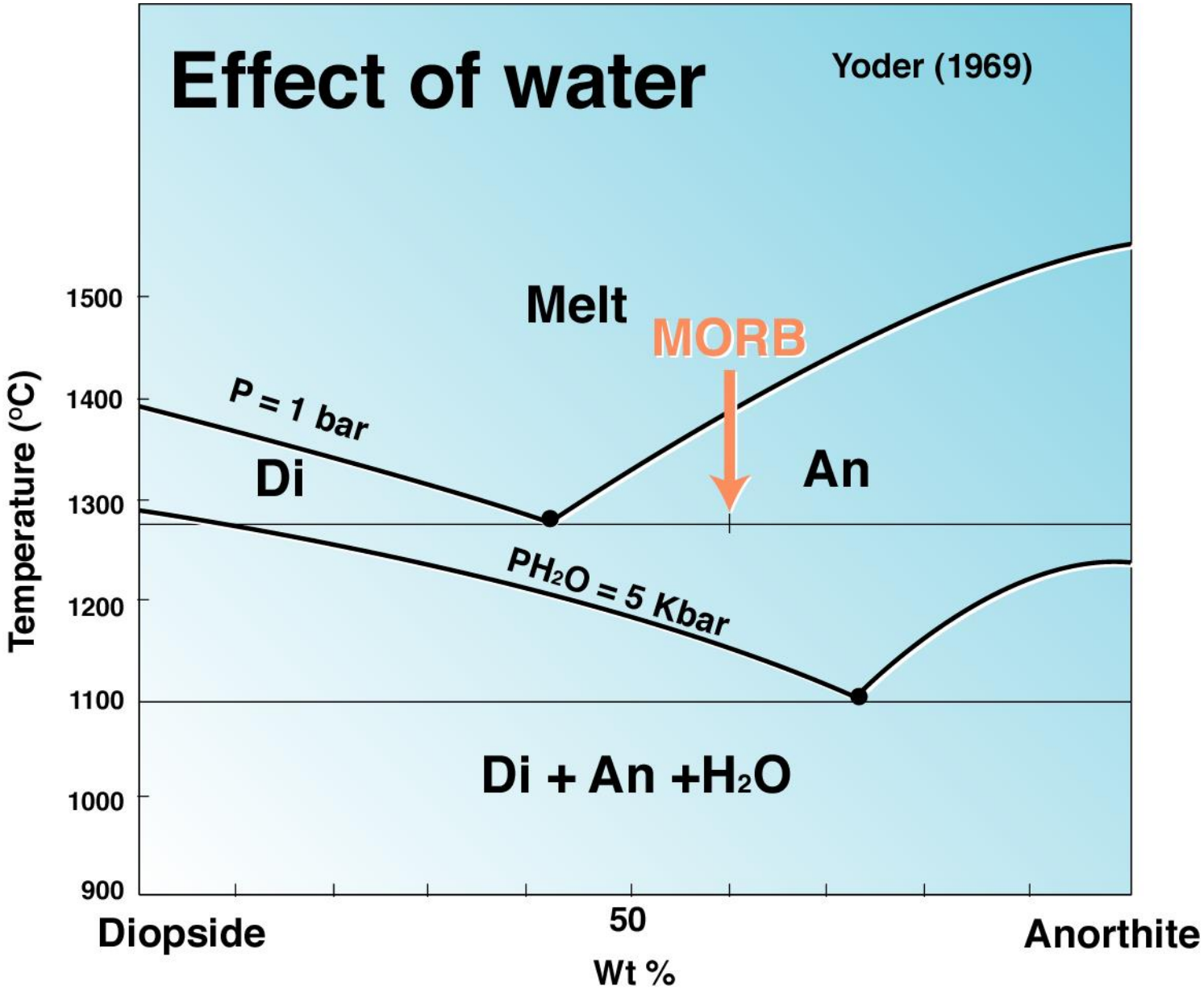
Effect of water
Yoder (1969)
Melt
MORB
P = 1 bar
Di
An
PH2O = 5 Kbar
Di + An +H2O
Temperature (°C)
1500
1400
1300
1200
1100
1000
900
Diopside
50
Anorthite
Wt %

Chapter 6

Tharsis Superplume

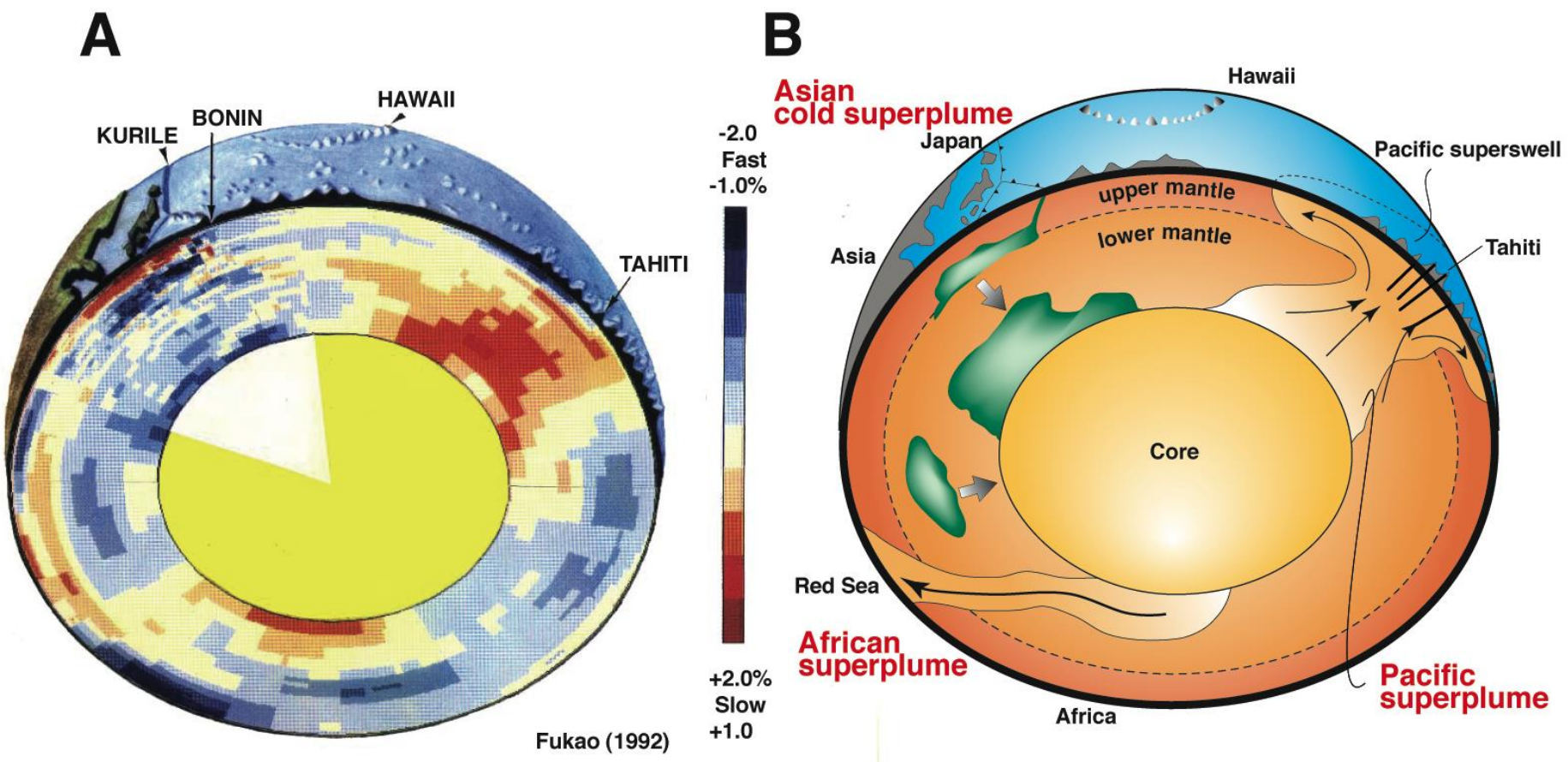
A
KURILE
BONIN
HAWAII
TAHITI
-2.0
Fast
-1.0%
+2.0%
Slow
+1.0
Fukao (1992)
B
Asian
cold superplume
Hawaii
Japan
Pacific superswell
upper mantle
lower mantle
Asia
Tahiti
Core
Red Sea
African
superplume
Africa
Pacific
superplume

Superplume: Concept and origin

- Difference from so-called plumes
- Shape of plume as a function of T
- Superplume and plume through time
- Example on Earth and Mars
- Origin: T and X, and role of SP through planetary evolution (+ heat source)

Observations

1. 200-300K lower-T at 410-660 km depth mantle than the surrounding mantle
2. 60K lower T at 80 km depth than MORB
3. High-water content

Mars Topography, MARS GLOBAL SURVEYOR, NASA

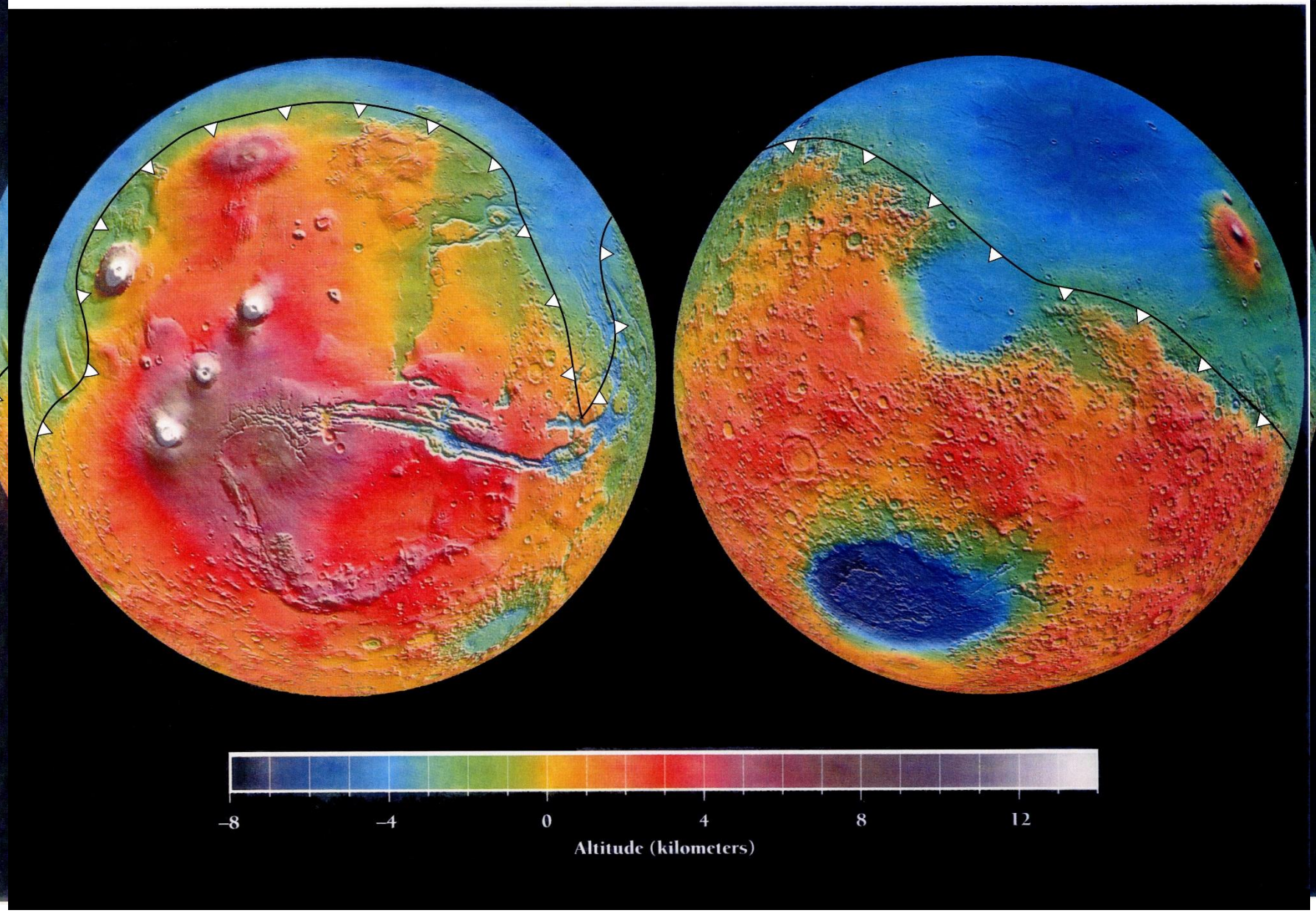

Chapter 6 History of Mars

Chapter 6-1 Early Mars; ABEL model for the inner rocky planets

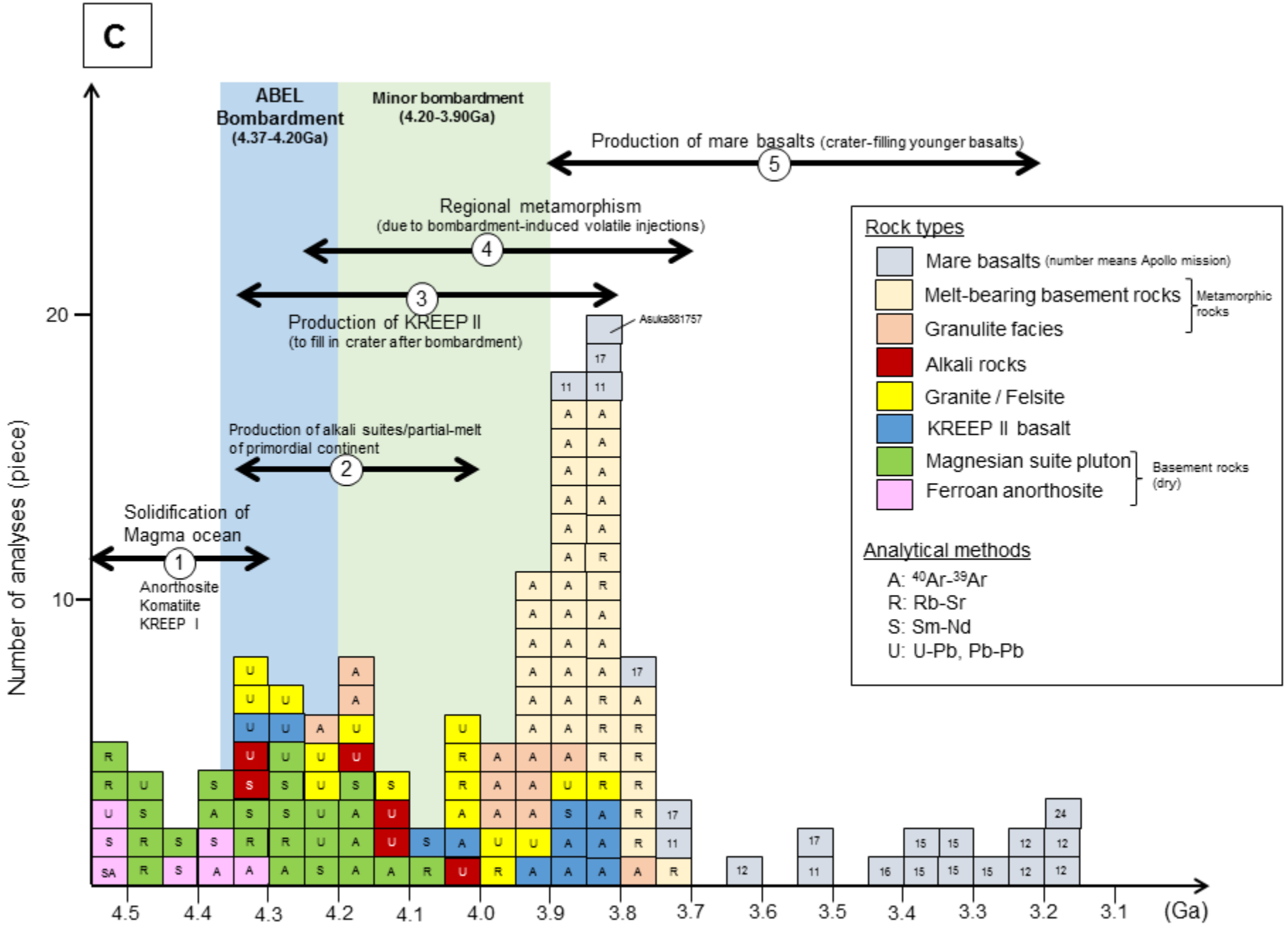
C
ABEL Bombardment (4.37-4.20Ga)
Minor bombardment (4.20-3.90Ga)
Production of mare basalts (crater-filling younger basalts)
5
Regional metamorphism
(due to bombardment-induced volatile injections)
4
3
Production of KREEP II
(to fill in crater after bombardment)
Asuka881757
Production of alkali suites/partial-melt of primordial continent
2
Solidification of Magma ocean
1
Anorthosite
Komatiite
KREEP I
Number of analyses (piece)
20
10
4.5
4.4
4.3
4.2
4.1
4.0
3.9
3.8
3.7
3.6
3.5
3.4
3.3
3.2
3.1
(Ga)
Rock types
Mare basalts (number means Apollo mission)
Melt-bearing basement rocks
Granulite facies
Metamorphic rocks
Alkali rocks
Granite / Felsite
KREEP II basalt
Magnesian suite pluton
Ferroan anorthosite
Basement rocks (dry)
Analytical methods
A: 40Ar-39Ar
R: Rb-Sr
S: Sm-Nd
U: U-Pb, Pb-Pb

アノーソサイト岩体の浮上

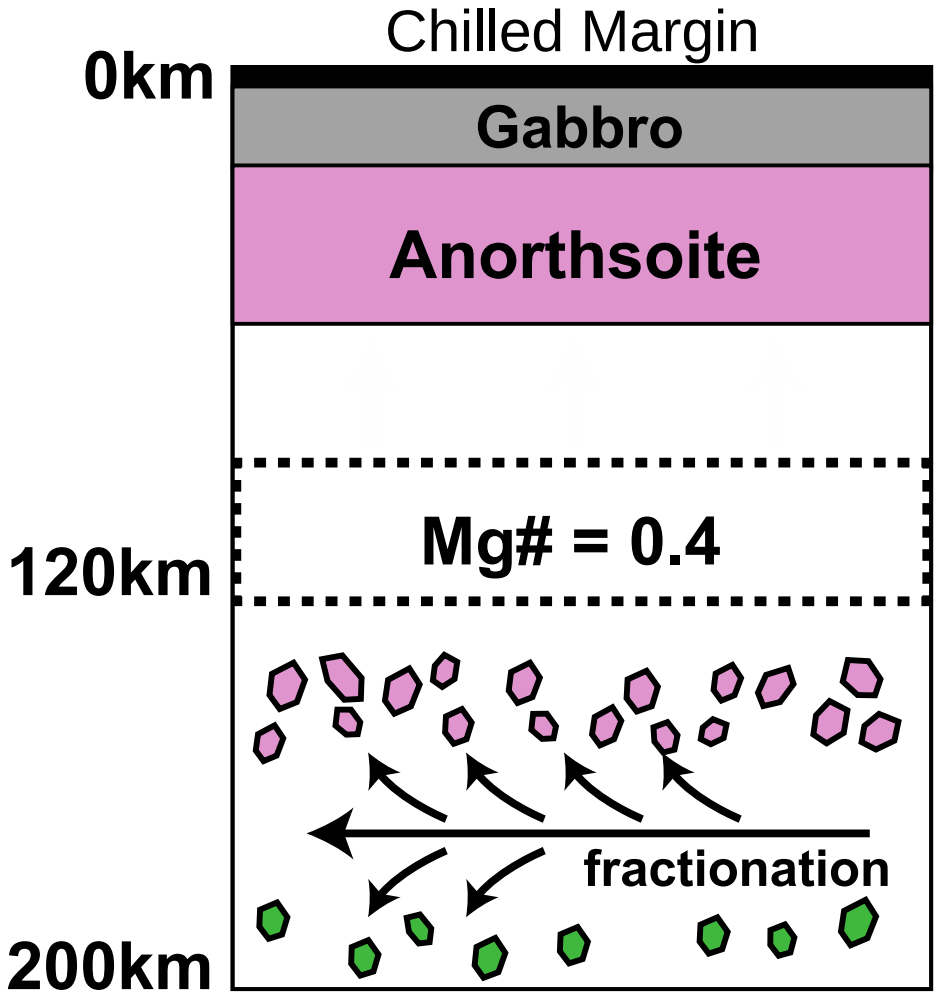

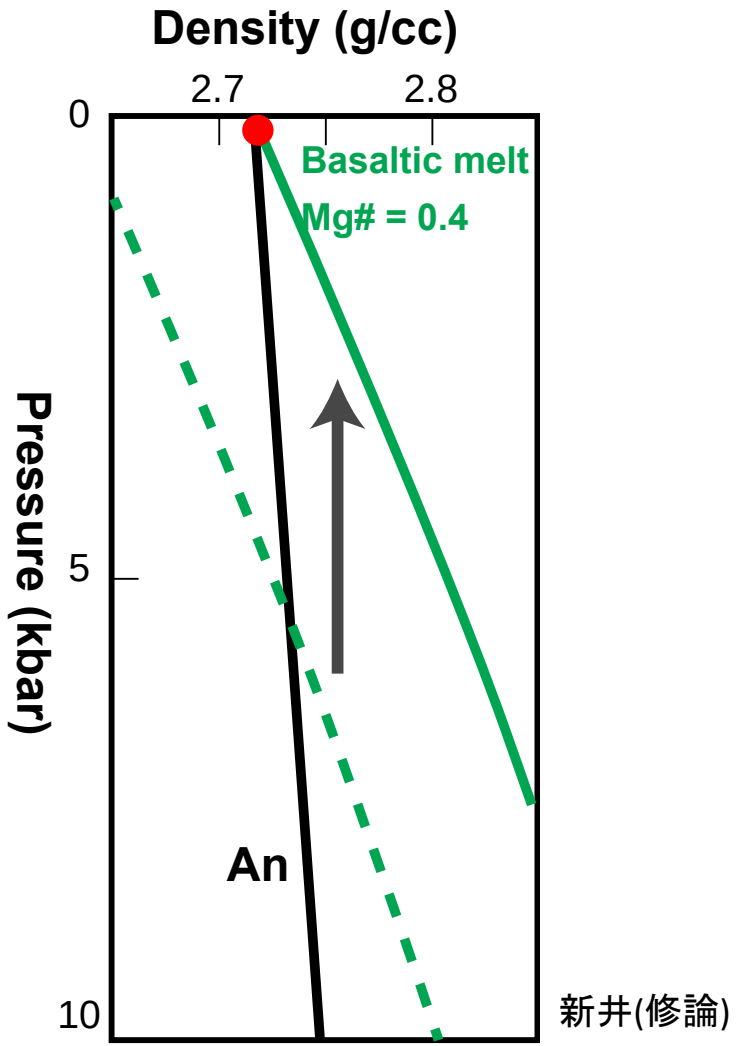

新井(修論)

メルトがFe-richになり、密度大きくなる。密度逆転層が上昇。
月の地質記録から検証する必要がある。

A

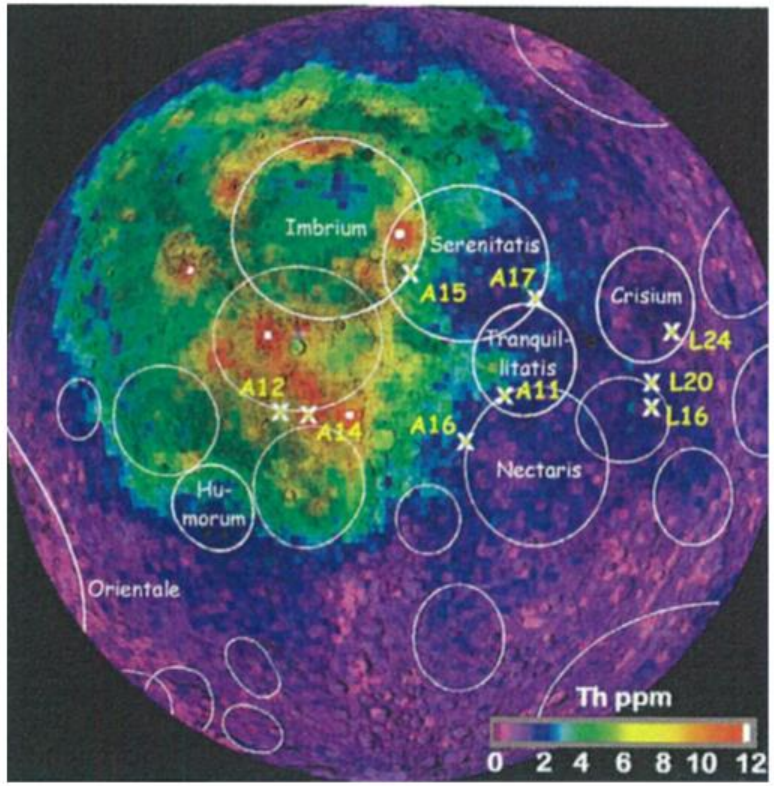

Jolliff et al (2006)

B

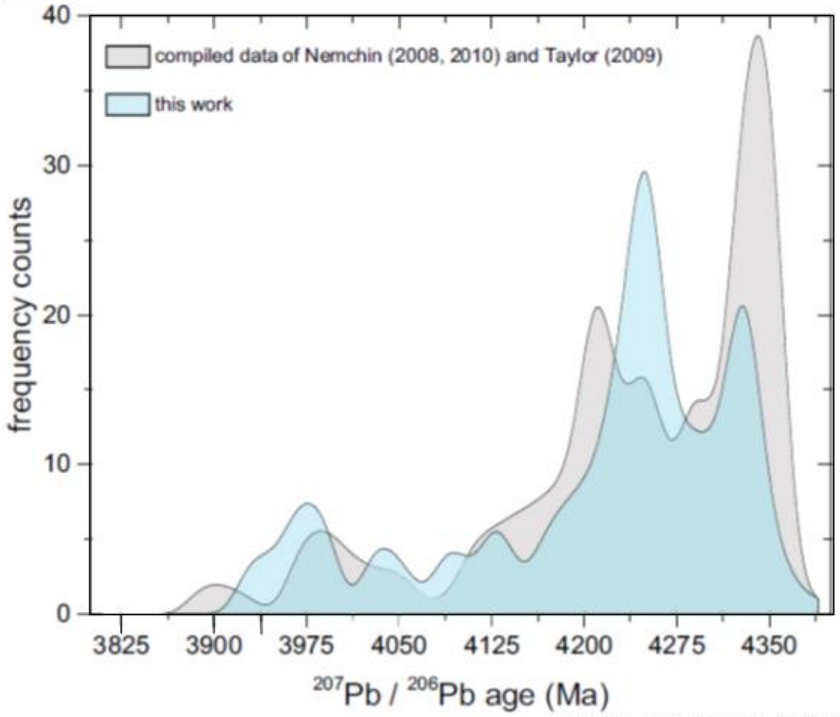

Hopkins and Mojzsis (2015)

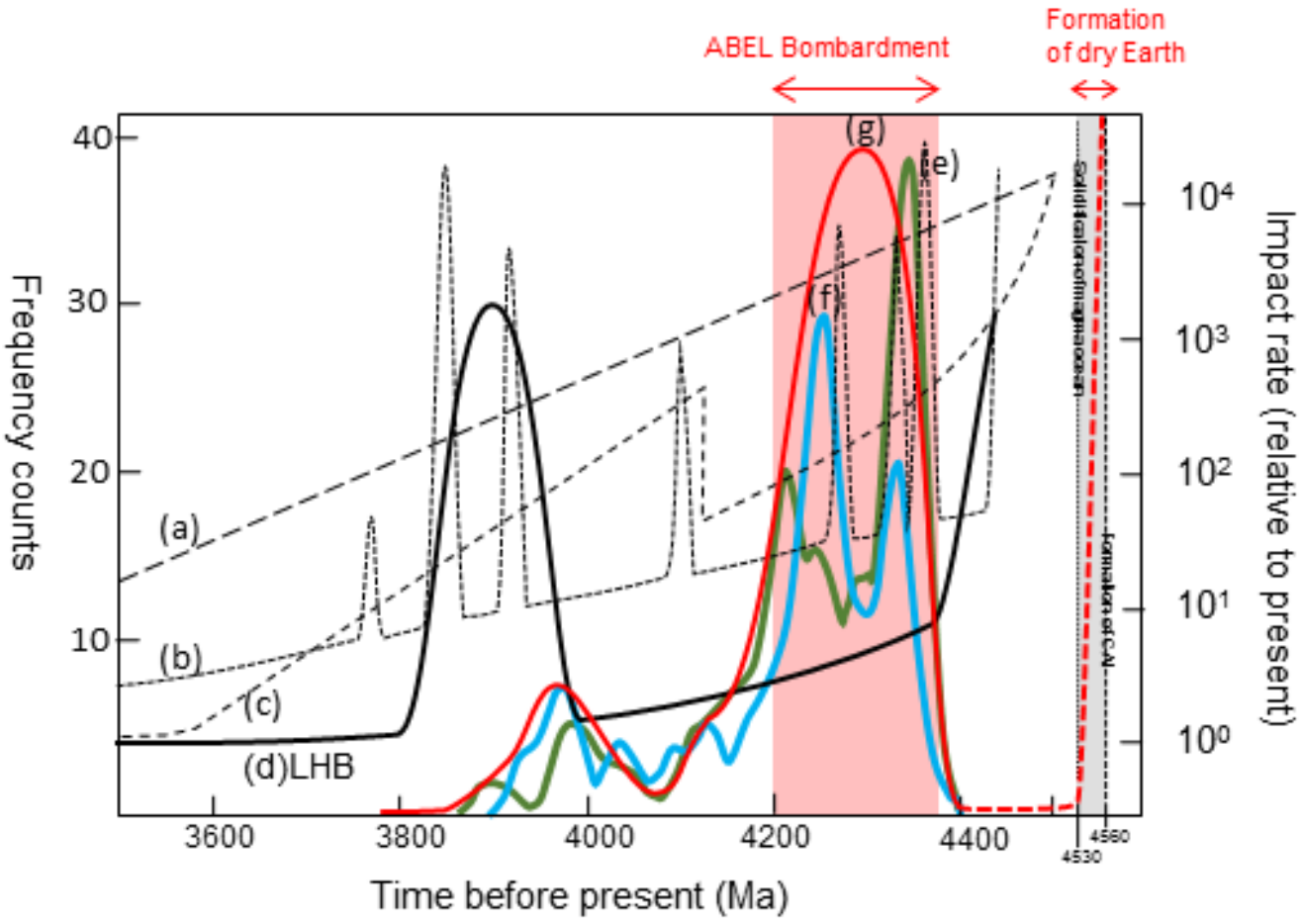

Modified after Hopkins and Mojzsis (2015)

From stagnant lid tectonics to plate tectonics

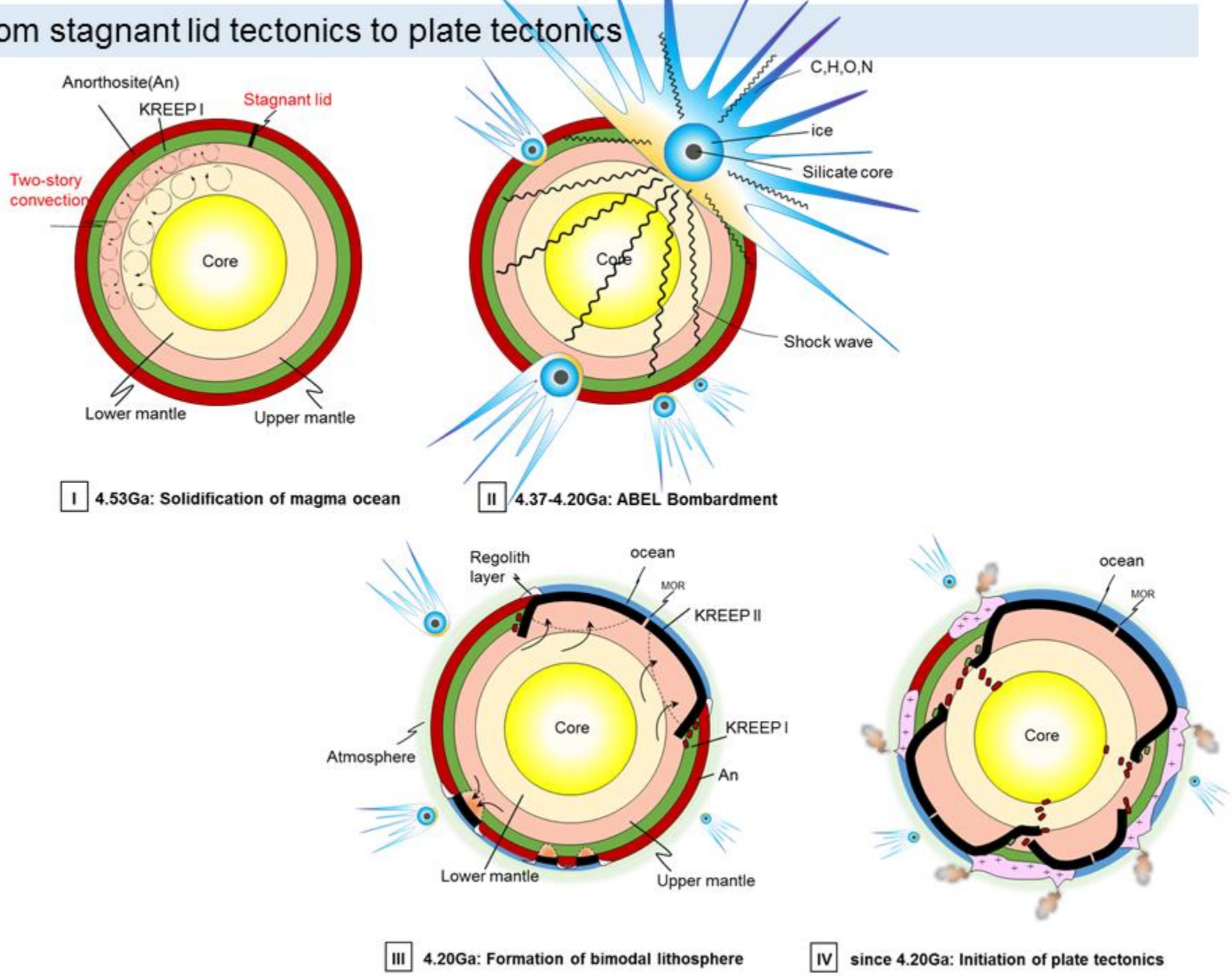

I 4.53Ga: Solidification of magma ocean

II 4.37-4.20Ga: ABEL Bombardment

III 4.20Ga: Formation of bimodal lithosphere

IV since 4.20Ga: Initiation of plate tectonics

Are there any facts remain on the Earth to support the ABEL Model? Yes!

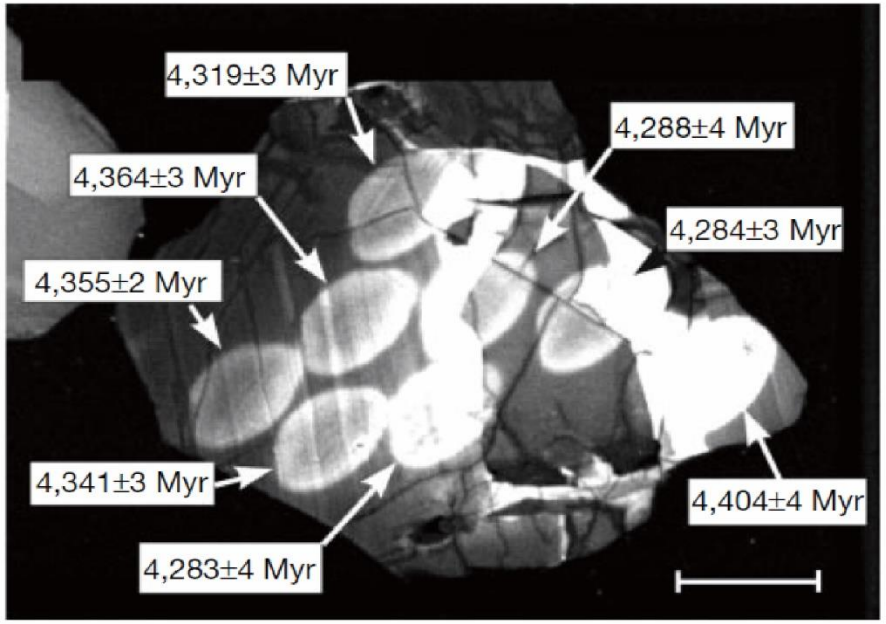

Wilde et al. (2001)

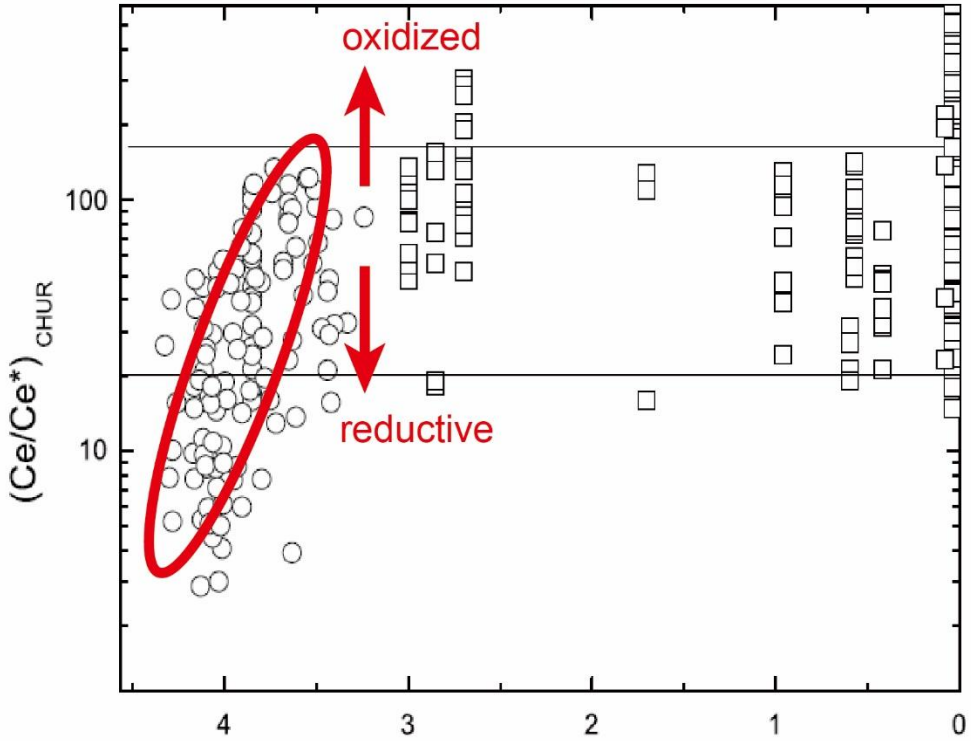

Modified after Yang et al. (2014)

mantle

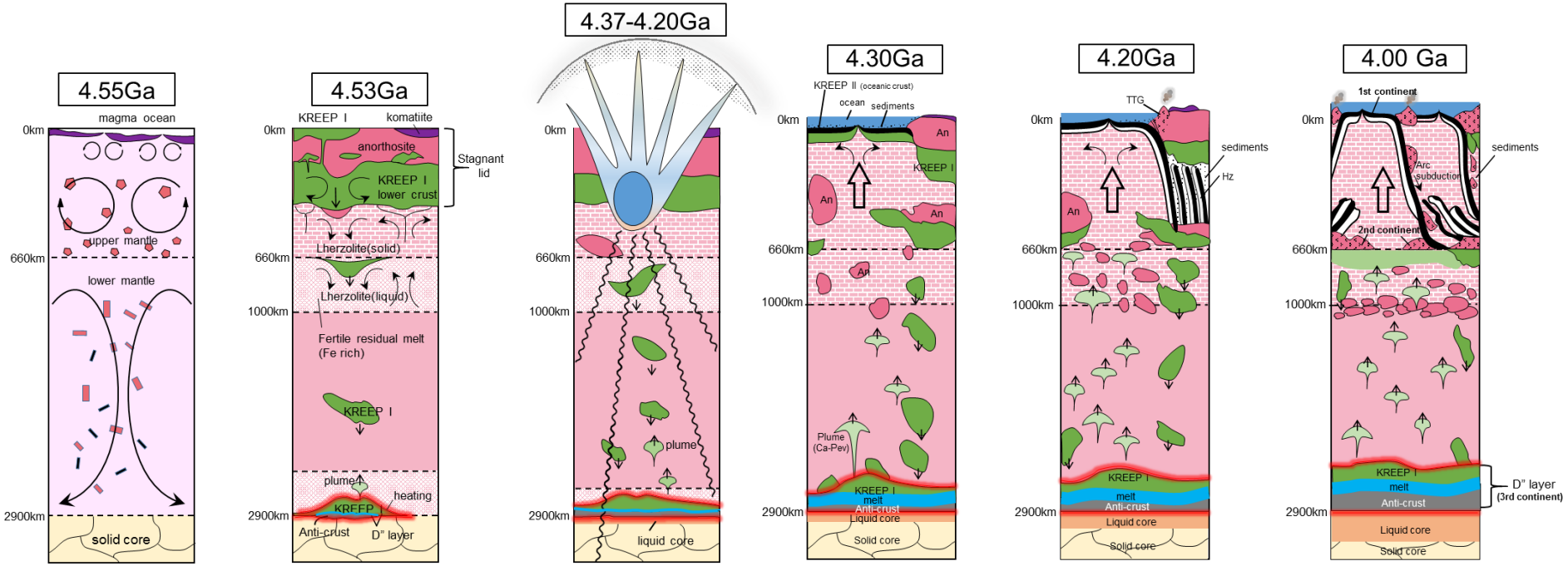
4.55Ga
magma ocean
0km
upper mantle
660km
lower mantle
2900km
solid core
4.53Ga
KREEP I
komatiite
0km
anorthosite
Stagnant lid
KREEP I lower crust
Lherzolite(solid)
660km
Lherzolite(liquid)
1000km
Fertile residual melt (Fe rich)
KREEP I
plume
heating
2900km
KREEP I
Anti-crust
D" layer
4.37-4.20Ga
0km
660km
1000km
plume
2900km
liquid core
4.30Ga
KREEP II (oceanic crust)
ocean
sediments
0km
An
KREEP I
660km
1000km
Plume (Ca-Pev)
KREEP I
melt
Anti-crust
Liquid core
2900km
Solid core
4.20Ga
TTG
0km
sediments
Hz
660km
1000km
KREEP I
melt
Anti-crust
Liquid core
2900km
Solid core
4.00 Ga
1st continent
0km
sediments
Arc subduction
2nd continent
660km
1000km
KREEP I
melt
Anti-crust
D" layer
(3rd continent)
Liquid core
2900km
Solid core

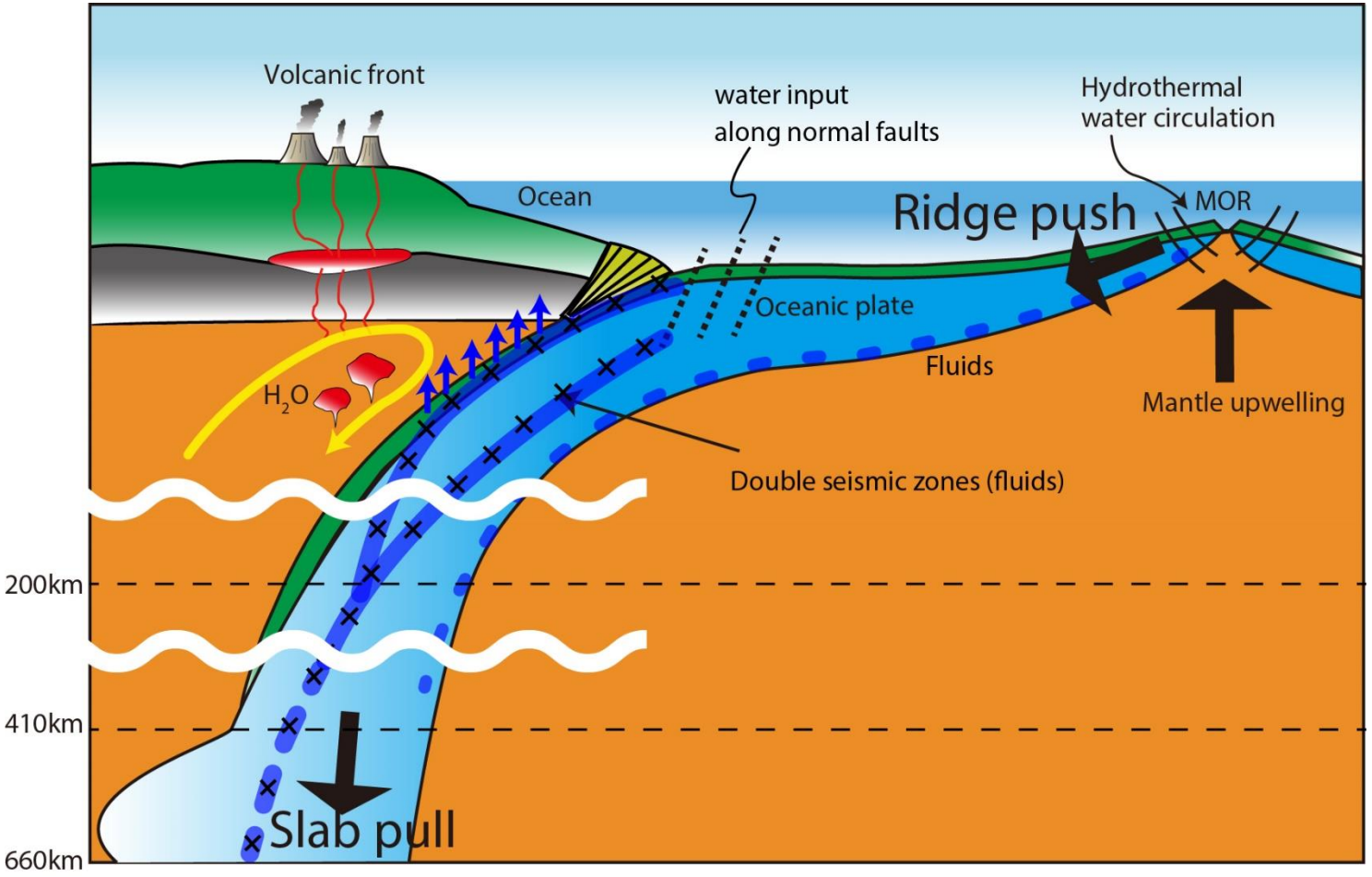
Volcanic front
water input
along normal faults
Hydrothermal
water circulation
Ocean
Ridge push
MOR
Oceanic plate
Fluids
H_2O
Mantle upwelling
Double seismic zones (fluids)
200km
410km
660km
Slab pull

水 の 効 果

(1) マントルの融点を下げる

例：２００km深度では

0.1 % H_2O 1,750 °C → 1,500 °C (-250 °C)

0.2 % H_2O 1,750 °C → 1,250 °C (-500 °C)

(2) 粘性を下げる

かんらん岩に **10^2-10^3 ppm H_2O** を加えると

10^{20} → 10^{18}(Pa・s) に下がる

(3) 水を加えると小さな力で岩石が割れやすくなる

Gravitational instability at trench inner wall

- Origin of huge-scale oliststrome

H2O=PT=TTG

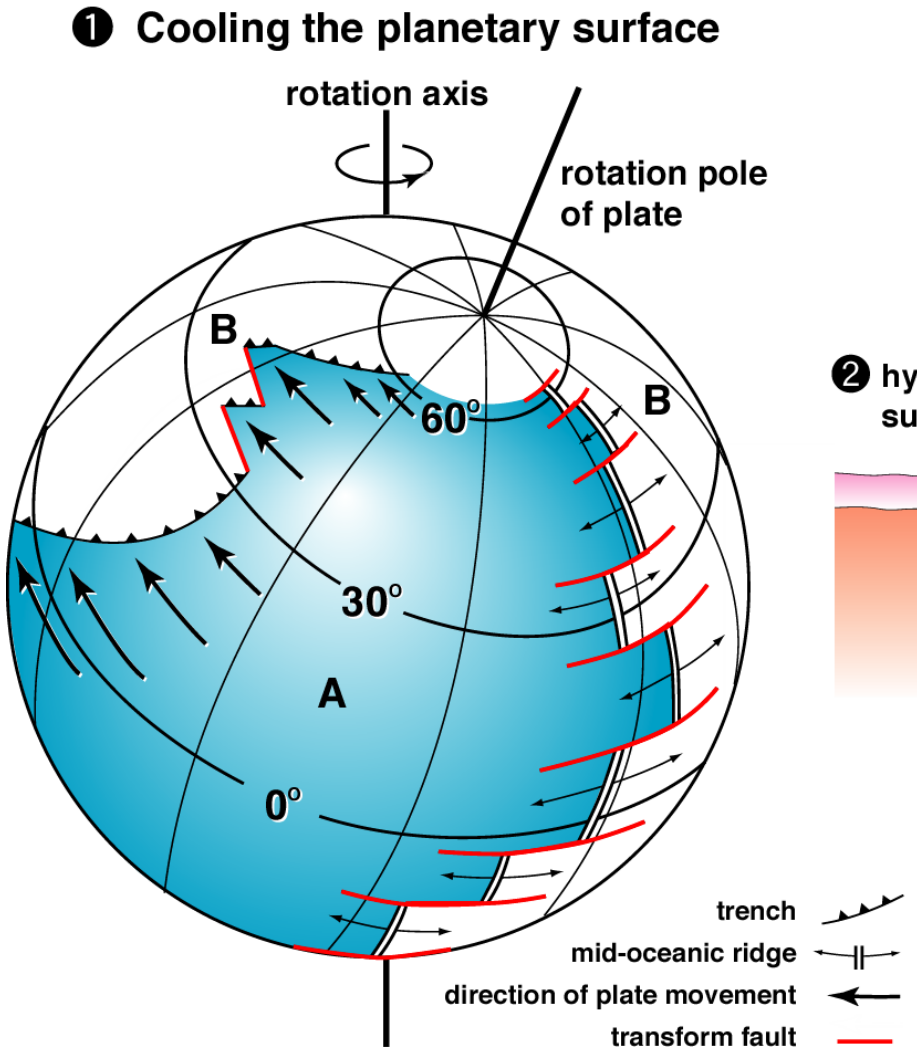
❶ Cooling the planetary surface
rotation axis
rotation pole of plate
B
B
60°
30°
A
0°
trench
mid-oceanic ridge
direction of plate movement
transform fault

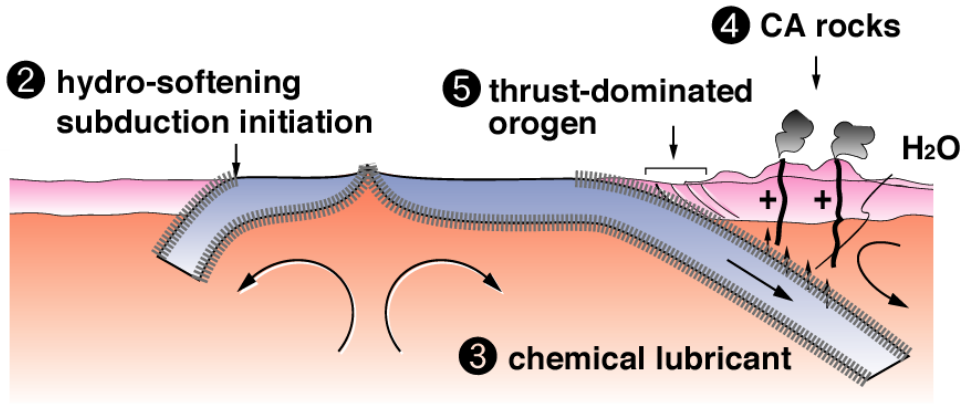
❷ hydro-softening subduction initiation
❺ thrust-dominated orogen
❹ CA rocks
H2O
❸ chemical lubricant

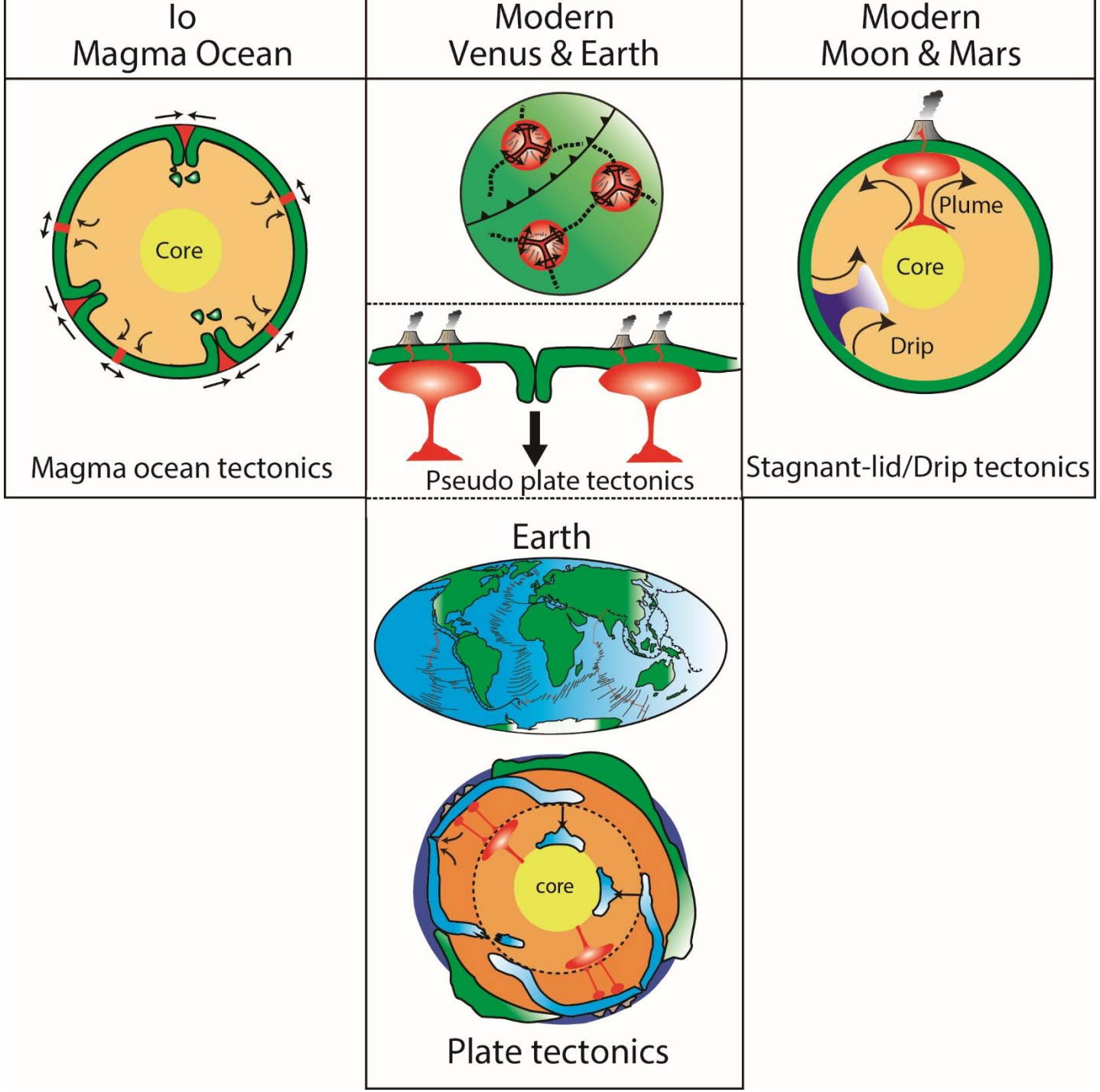
Io
Magma Ocean
Modern
Venus & Earth
Modern
Moon & Mars
Core
Magma ocean tectonics
Pseudo plate tectonics
Plume
Core
Drip
Stagnant-lid/Drip tectonics
Earth
core
Plate tectonics

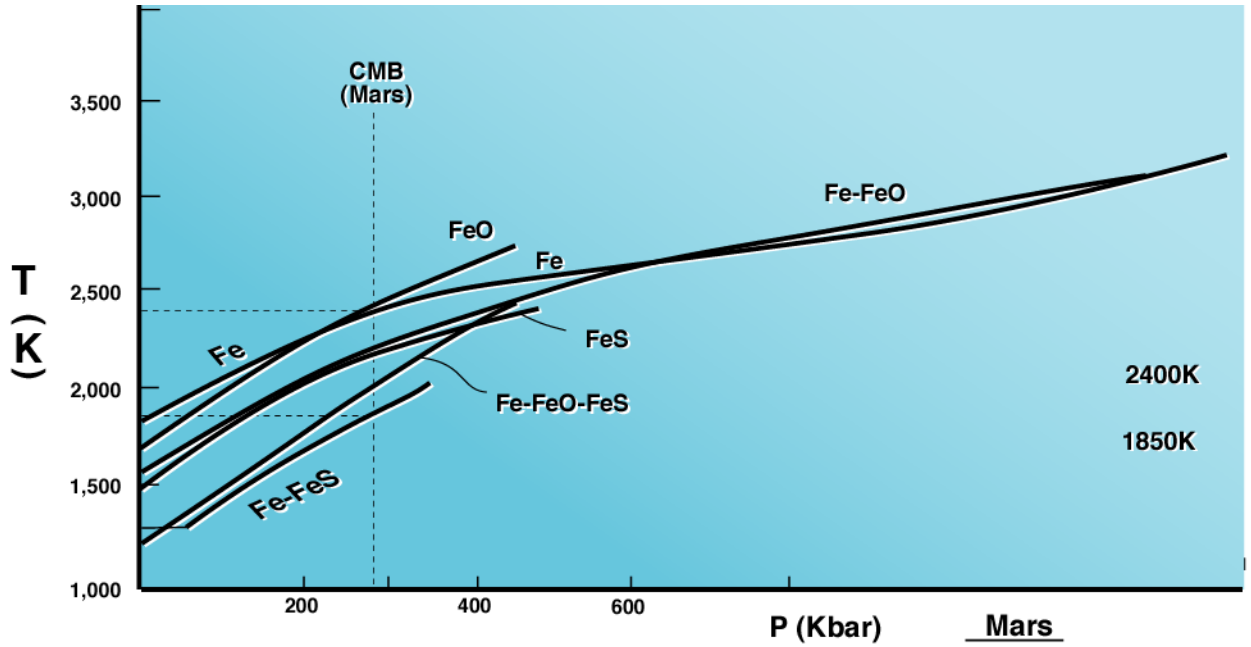
CMB
(Mars)
3,500
3,000
2,500
2,000
1,500
1,000
T
(K)
Fe-FeO
FeO
Fe
FeS
Fe
Fe-FeO-FeS
Fe-FeS
2400K
1850K
200
400
600
P (Kbar)

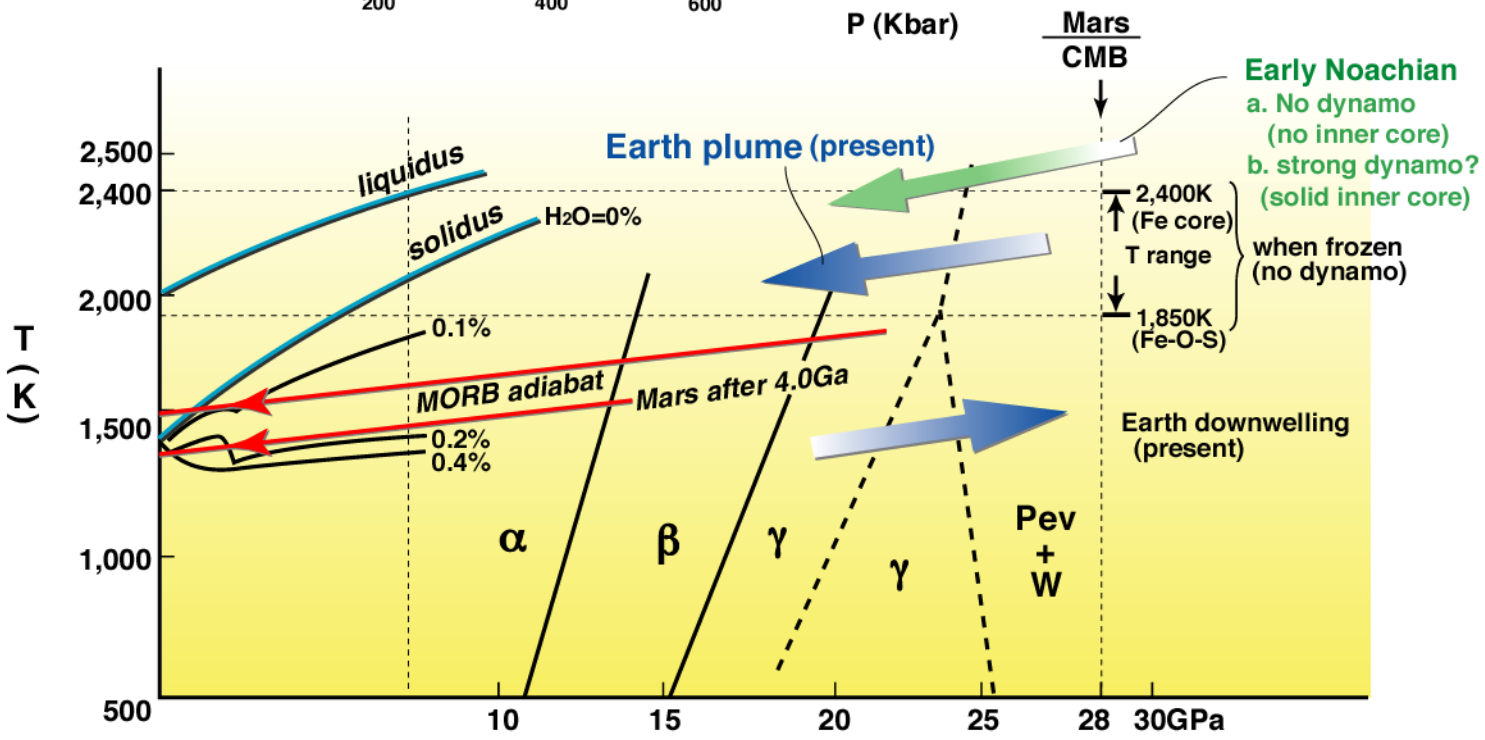
Mars
CMB
Early Noachian
a. No dynamo
(no inner core)
b. strong dynamo?
(solid inner core)
Earth plume (present)
2,500
2,400
2,000
1,500
1,000
500
T
(K)
liquidus
solidus
H2O=0%
0.1%
MORB adiabat
Mars after 4.0Ga
0.2%
0.4%
2,400K
(Fe core)
T range
1,850K
(Fe-O-S)
when frozen
(no dynamo)
Earth downwelling
(present)
α
β
γ
γ
Pev
+
W
10
15
20
25
28
30GPa

(1) 古環境の解読
(2) 化石からDNAを分離・増幅する (分子化石・タンパク質進化)

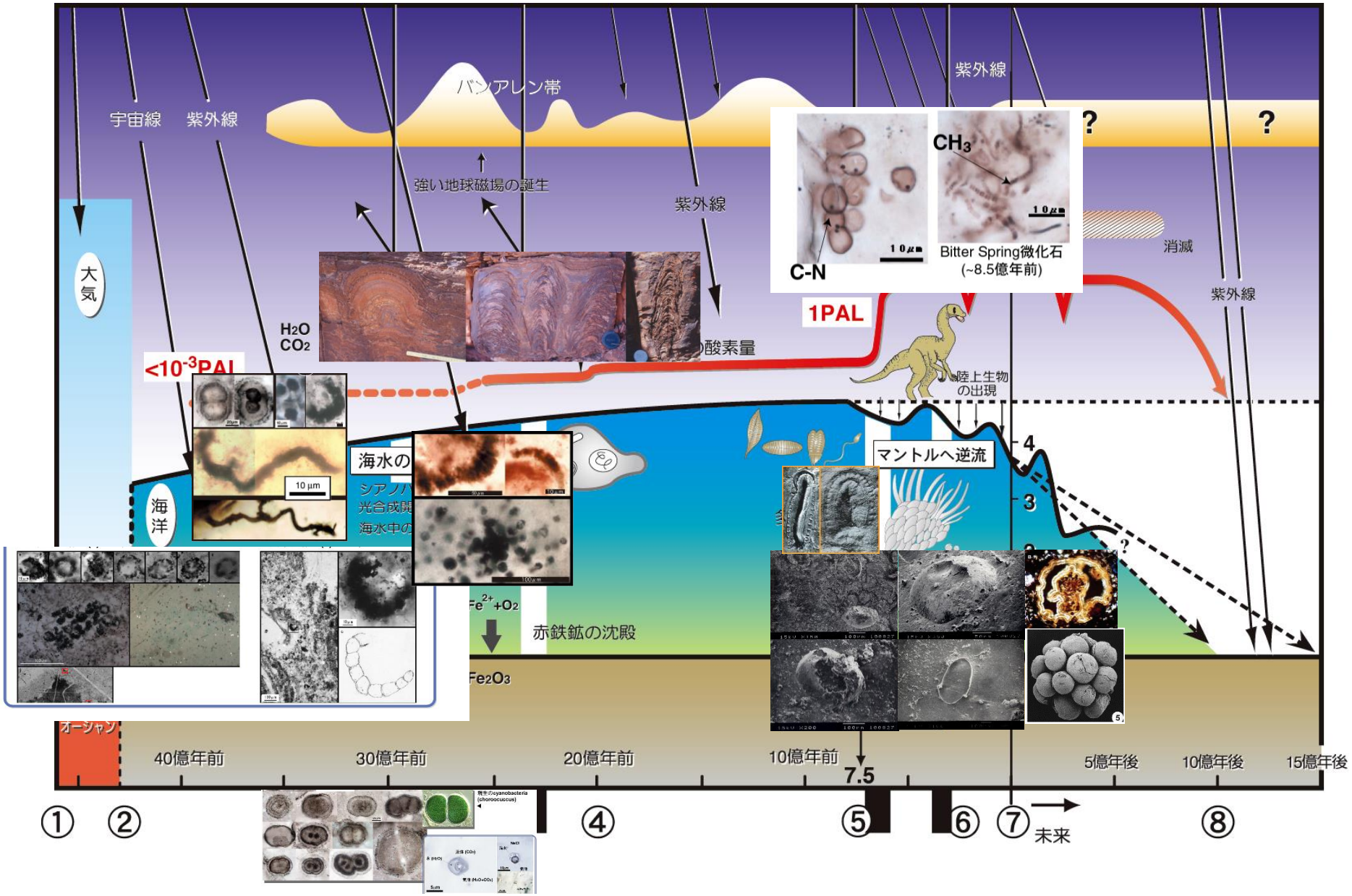

Chapter 8 Comparative planetology

Water vs Low-T

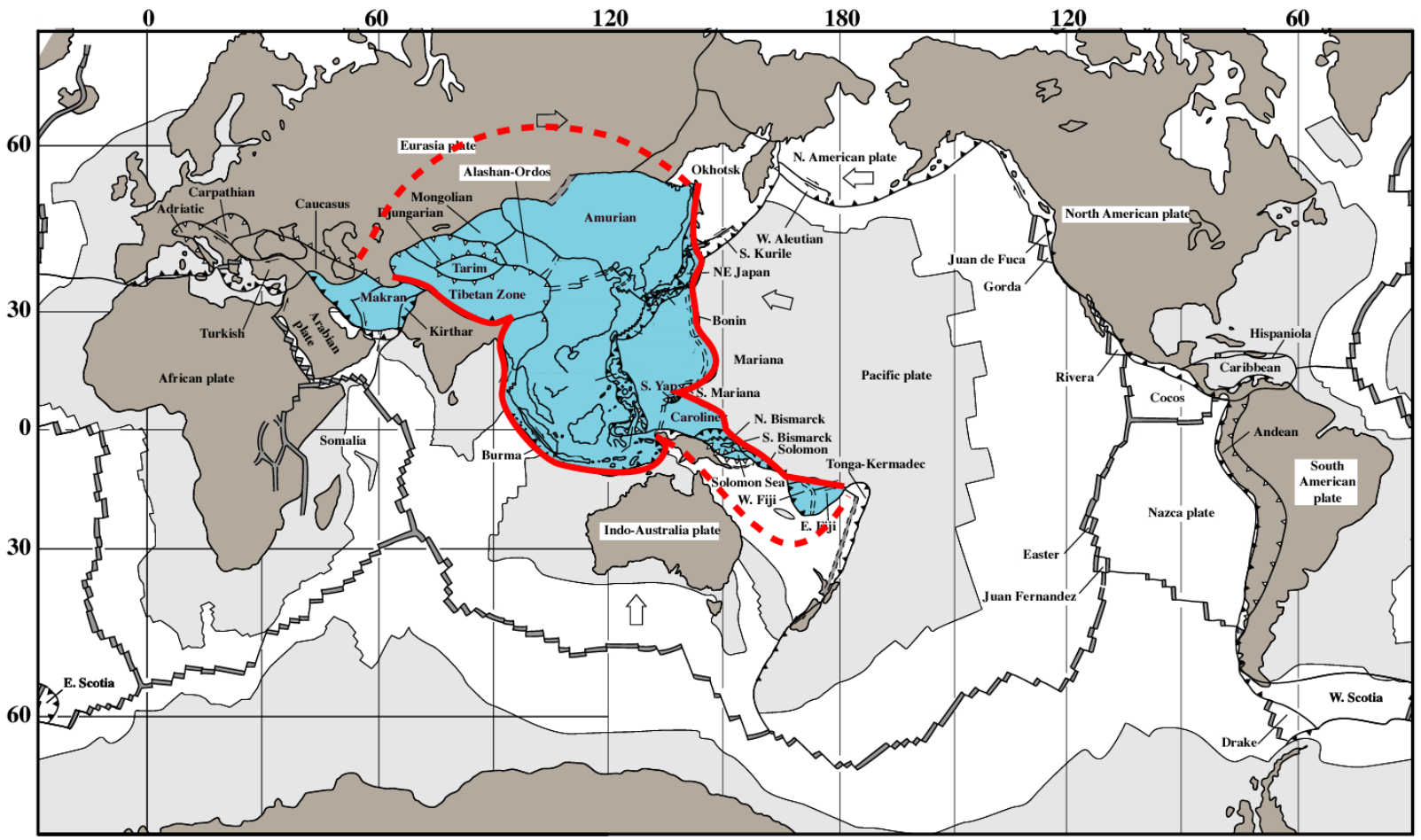

Chapter 6 System Movement?

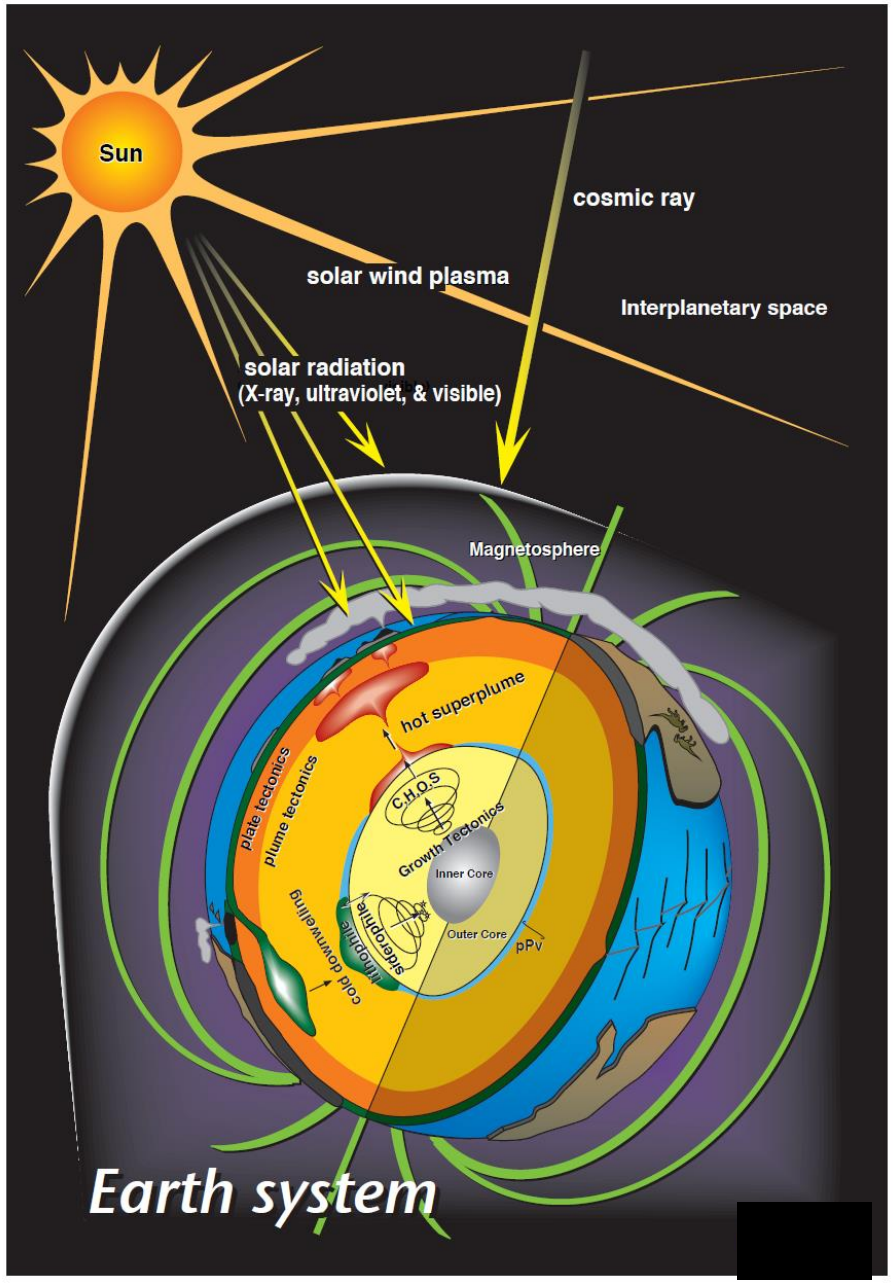

Maruyama et al., 2013

Recycling of slab

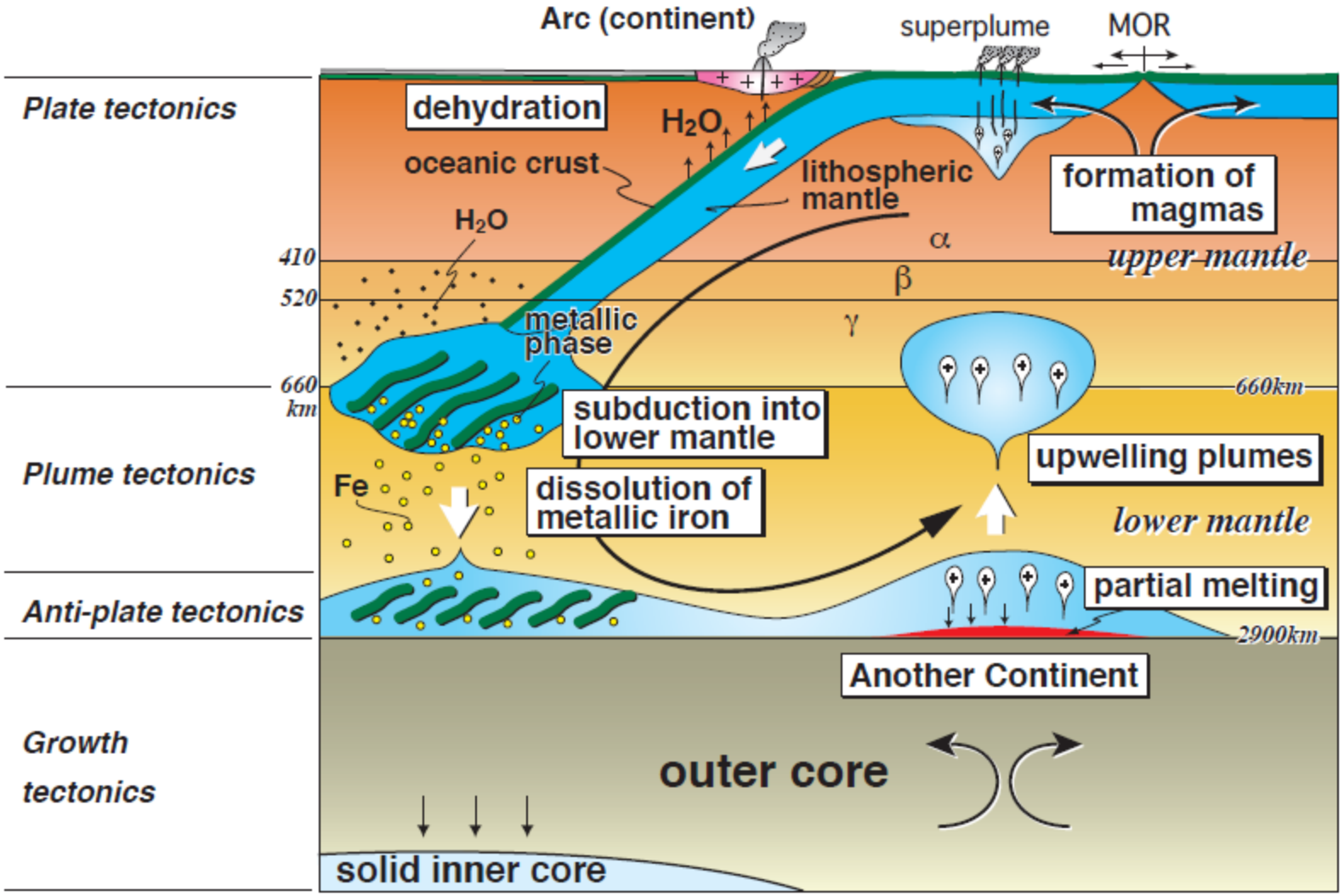

Maruyama et al., 2013

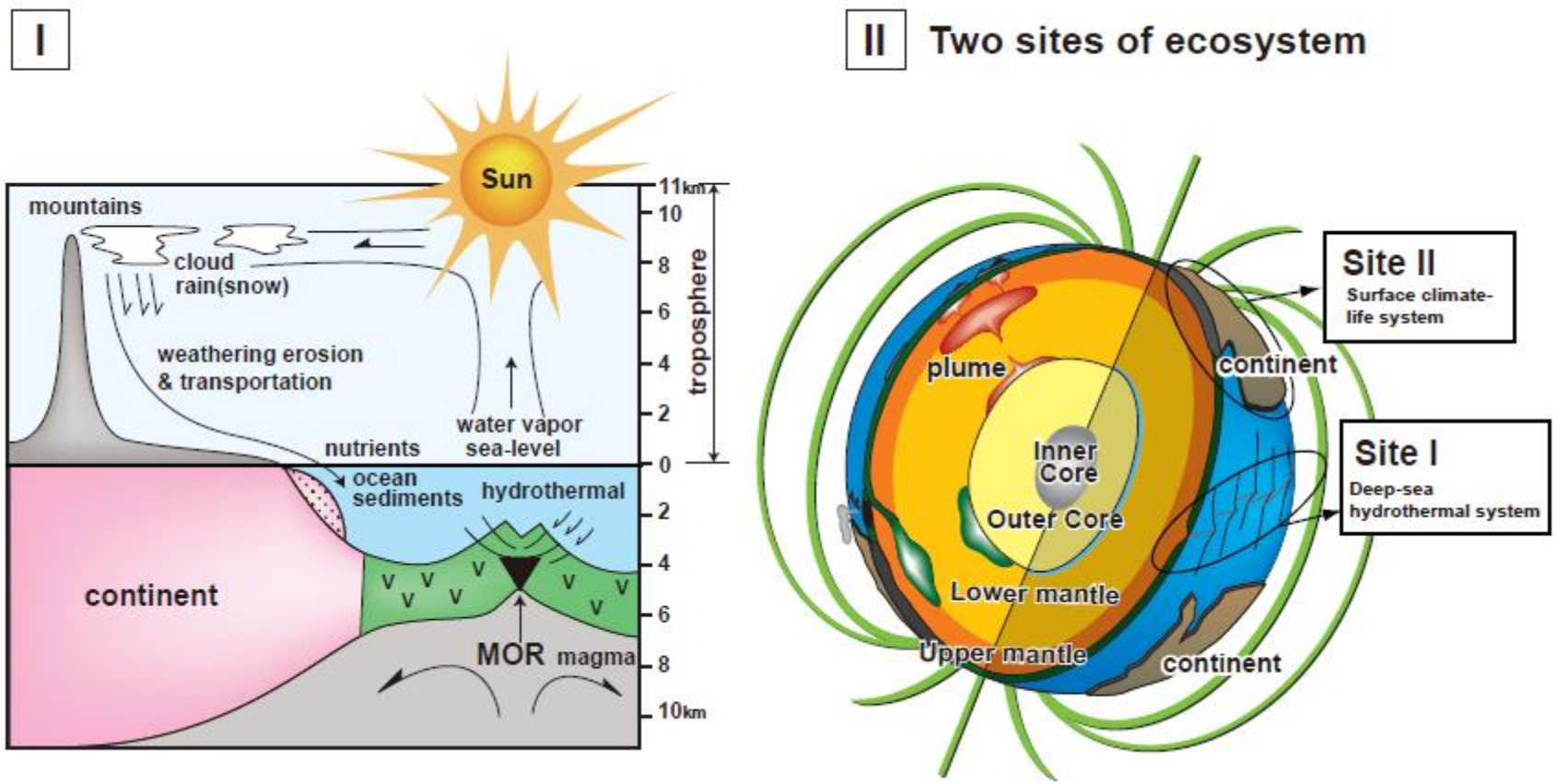

Maruyama et al., 2013

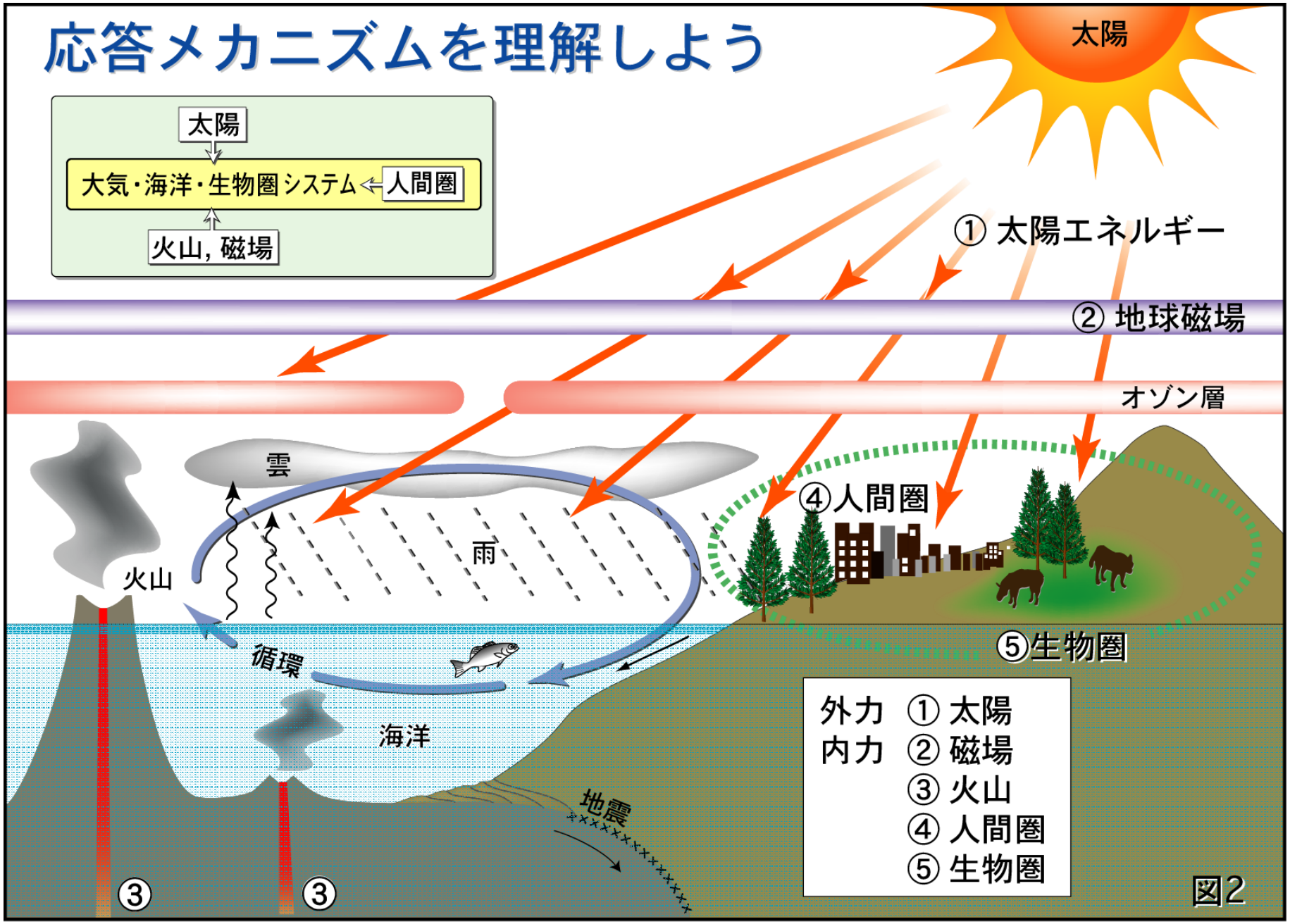
応答メカニズムを理解しよう
太陽
大気・海洋・生物圏システム
人間圏
火山，磁場
太陽
① 太陽エネルギー
② 地球磁場
オゾン層
雲
雨
火山
④人間圏
⑤生物圏
循環
海洋
地震
③
③
外力 ① 太陽
内力 ② 磁場
③ 火山
④ 人間圏
⑤ 生物圏
図2

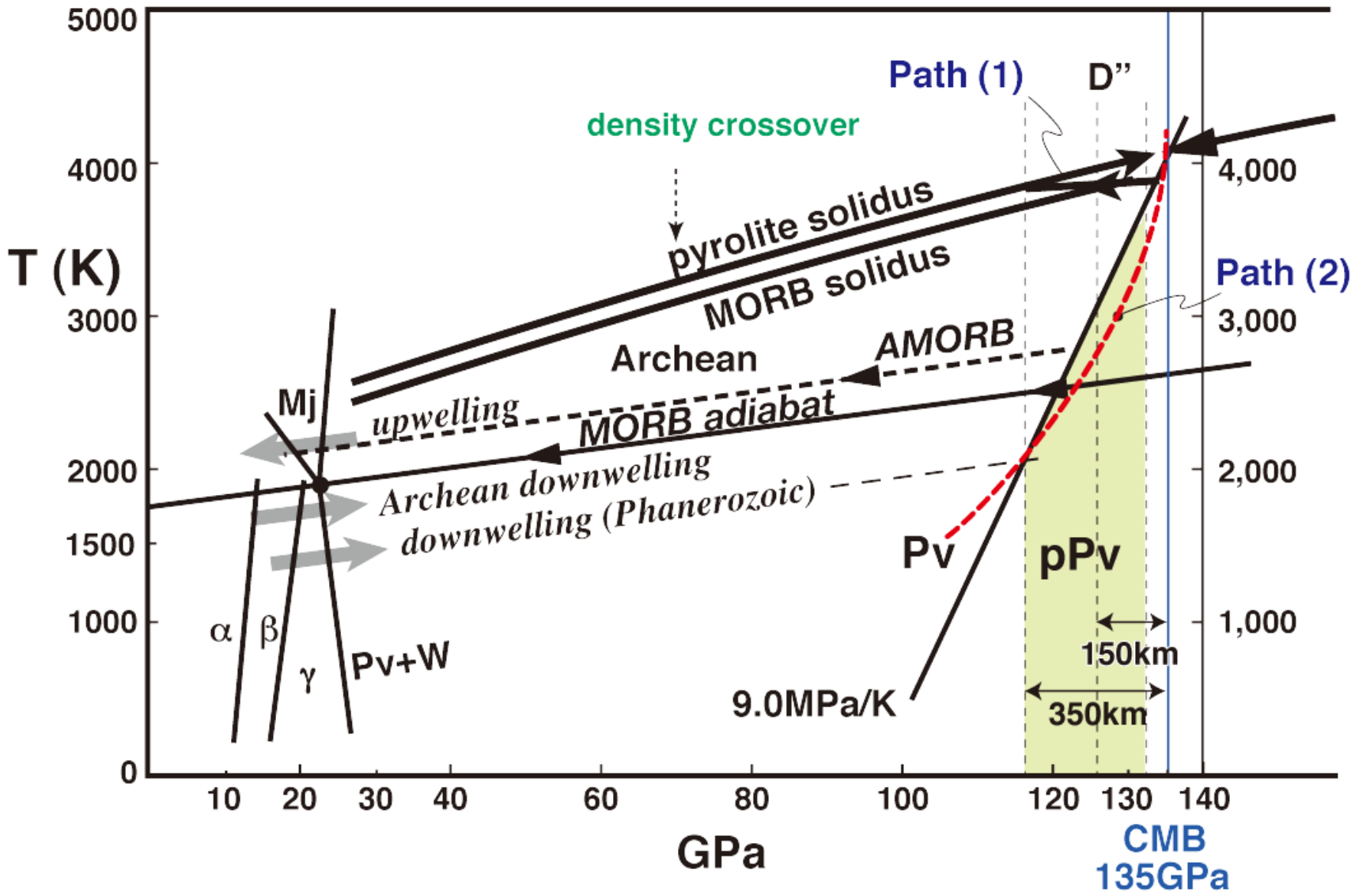
5000
4000
3000
2000
1500
1000
0
T (K)
10
20
30
40
60
80
100
120
130
140
GPa
4,000
3,000
2,000
1,000
Path (1)
D"
density crossover
pyrolite solidus
MORB solidus
Path (2)
Archean
AMORB
Mj
upwelling
MORB adiabat
Archean downwelling
downwelling (Phanerozoic)
Pv
pPv
α
β
γ
Pv+W
9.0MPa/K
150km
350km
CMB
135GPa

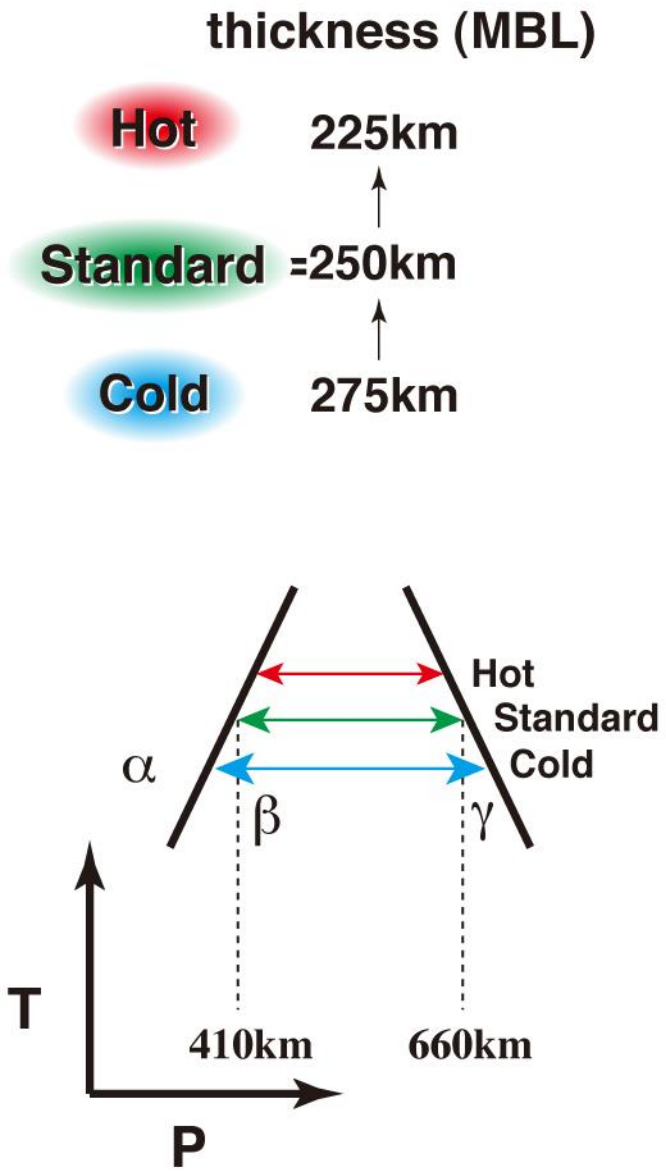
thickness (MBL)
Hot
225km
Standard
=250km
Cold
275km
Hot
Standard
Cold
α
β
γ
T
P
410km
660km

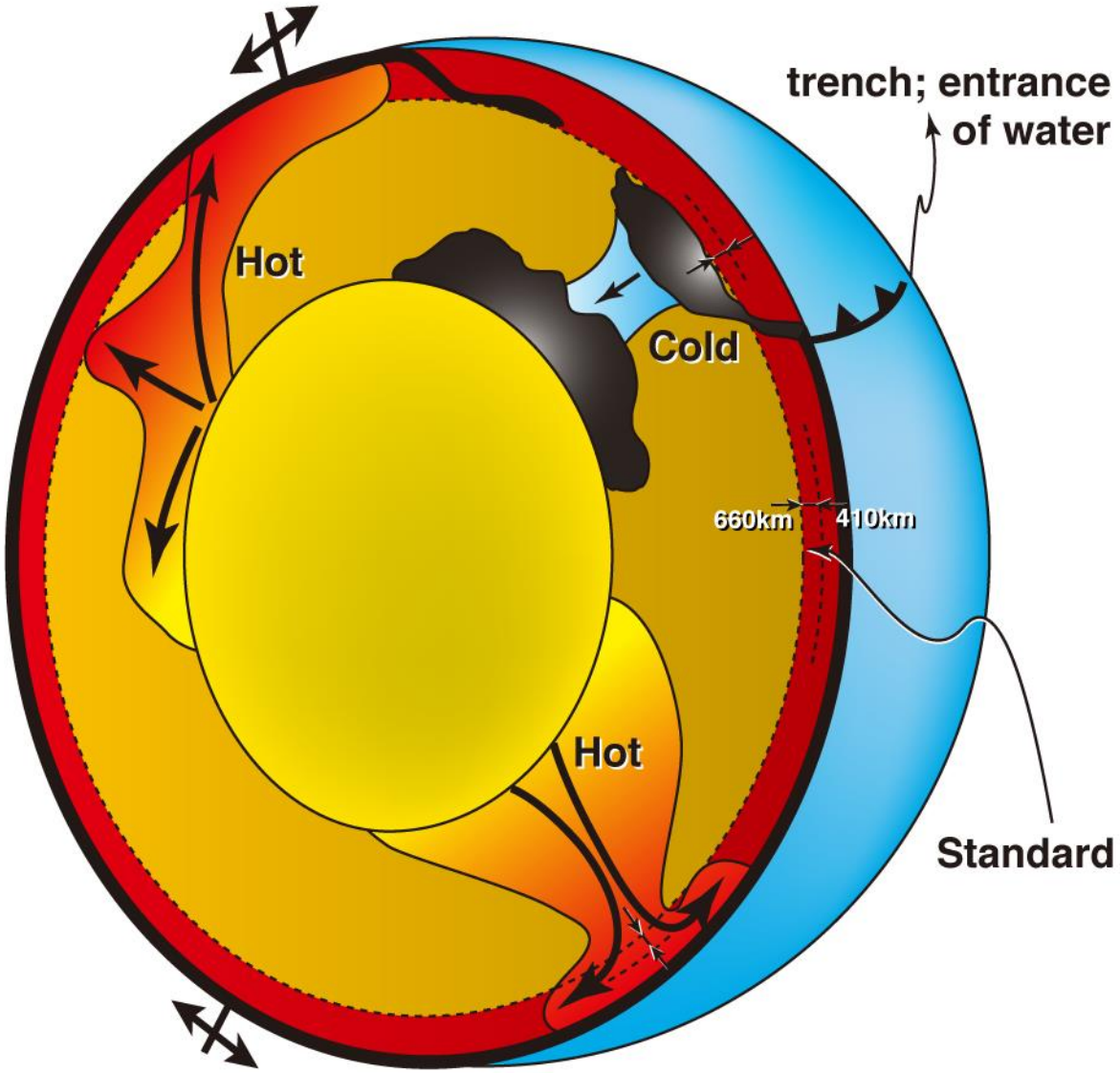
trench; entrance
of water
Hot
Cold
660km
410km
Hot
Standard

Transition zone thickness

(200-300K lower-T transition zone)

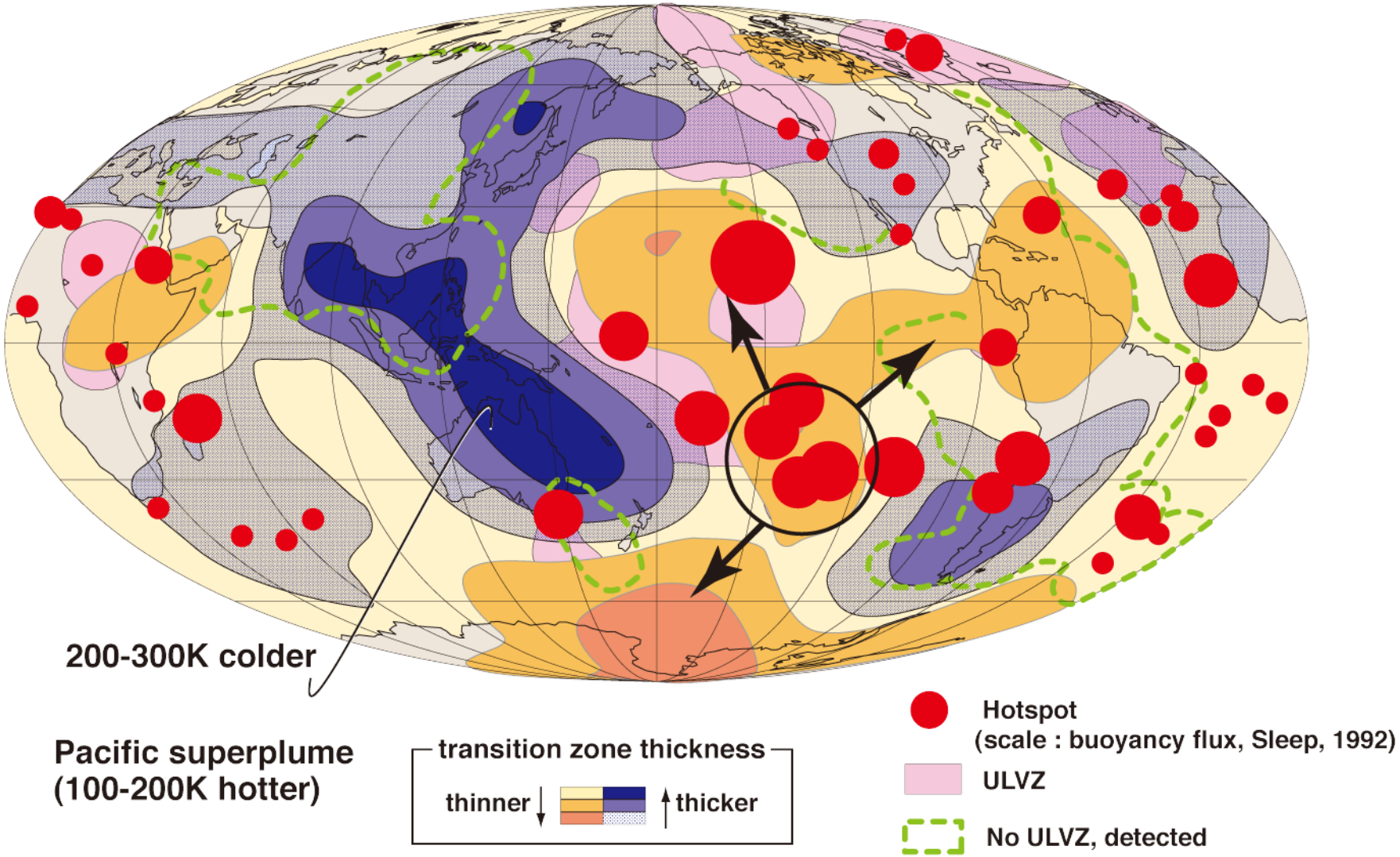

Thermal structure of the Earth

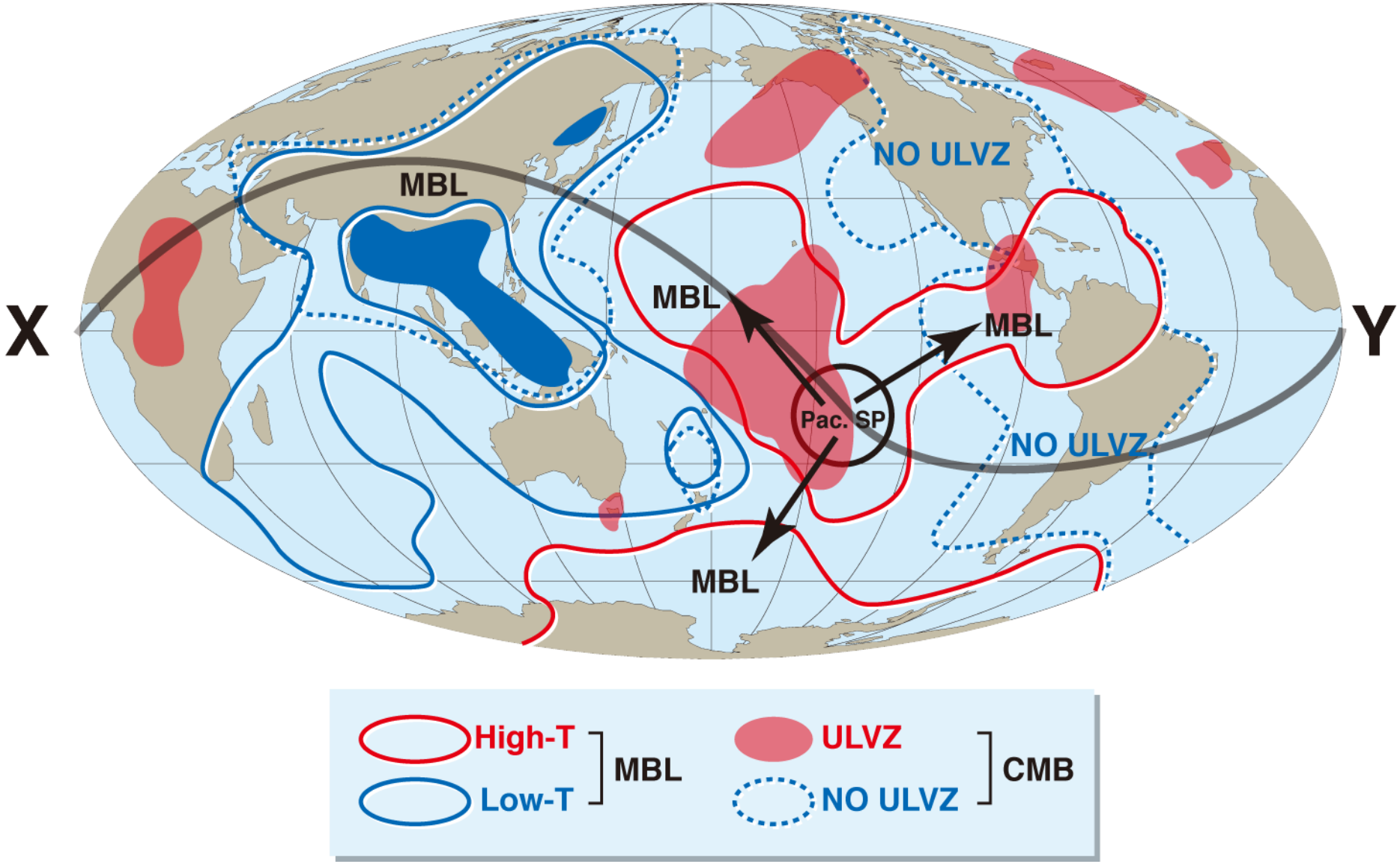

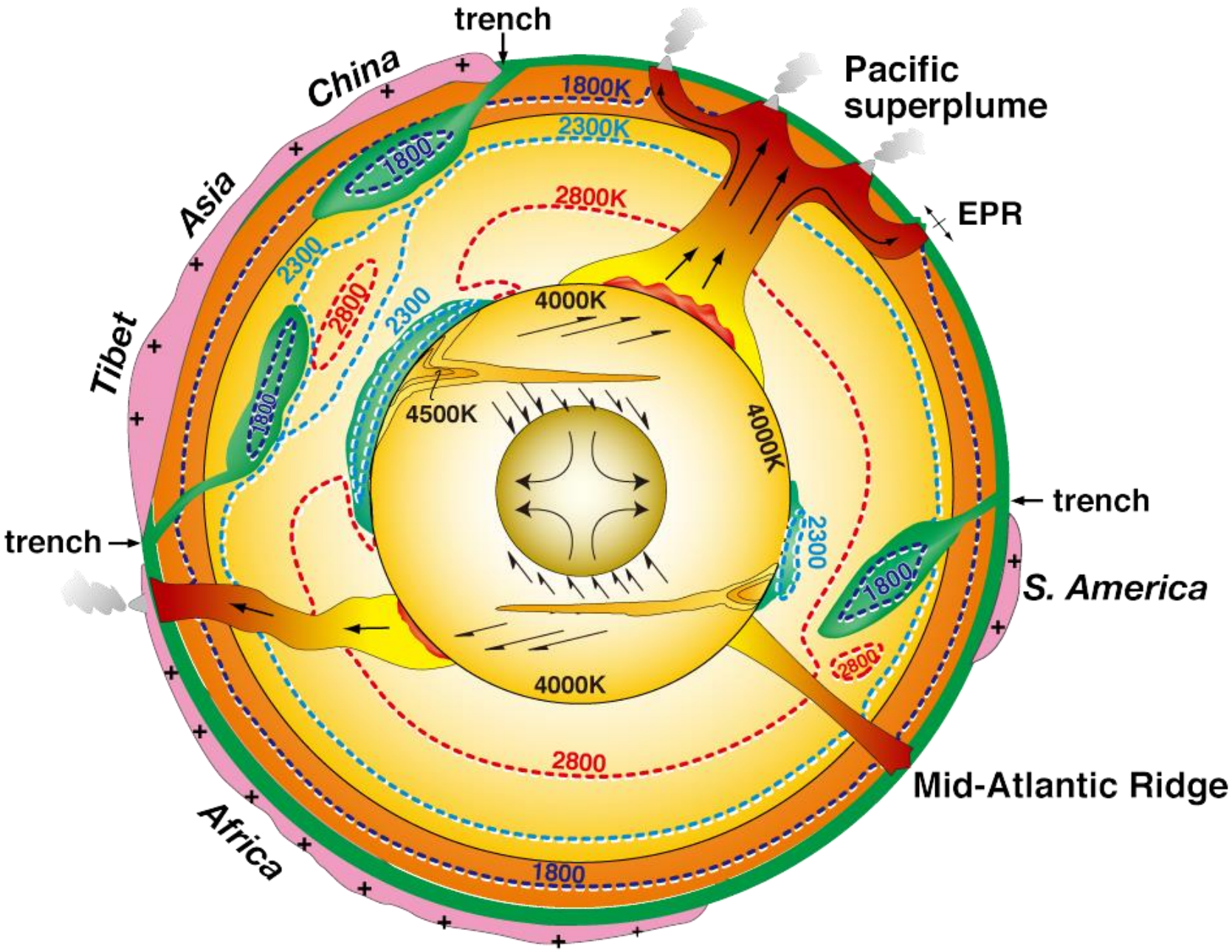
trench
China
Asia
Tibet
trench
1800K
2300K
2800K
Pacific
superplume
EPR
1800
2300
2800
2300
1800
4000K
4500K
4000K
2300
1800
2800
4000K
2800
1800
trench
S. America
Mid-Atlantic Ridge
Africa

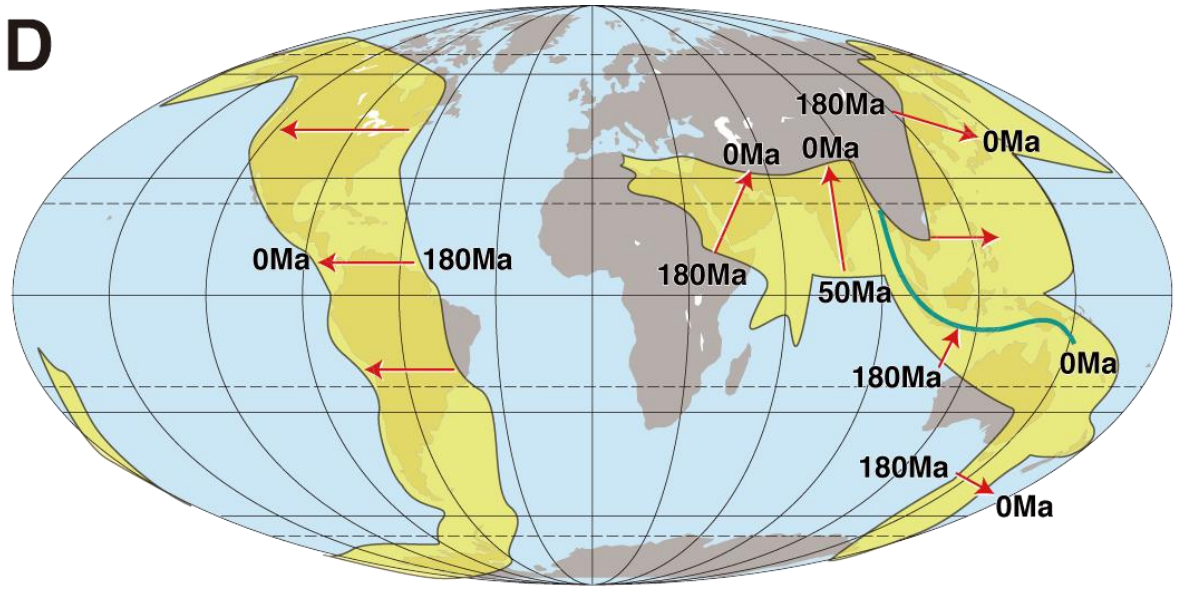
D
180Ma
0Ma
0Ma
0Ma
0Ma
180Ma
180Ma
50Ma
180Ma
0Ma
180Ma
0Ma

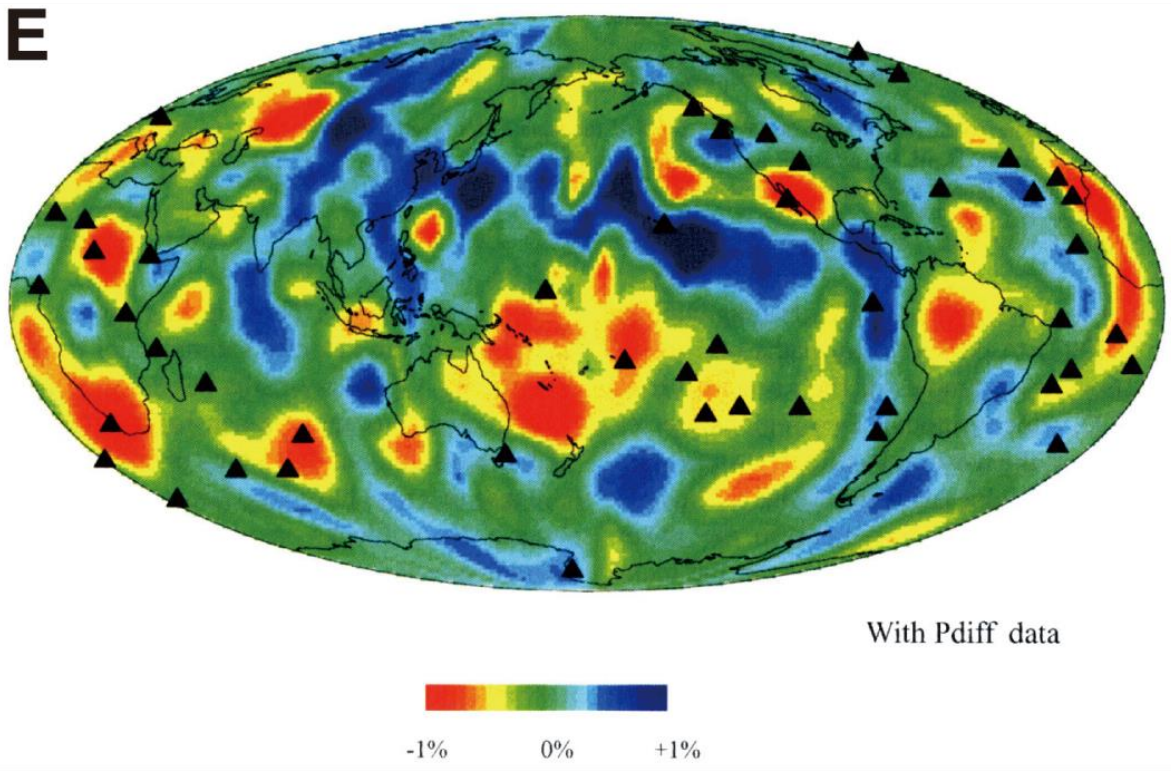
E
With Pdiff data
-1%
0%
+1%

Chapter 8 Origin and evolution of early Mars

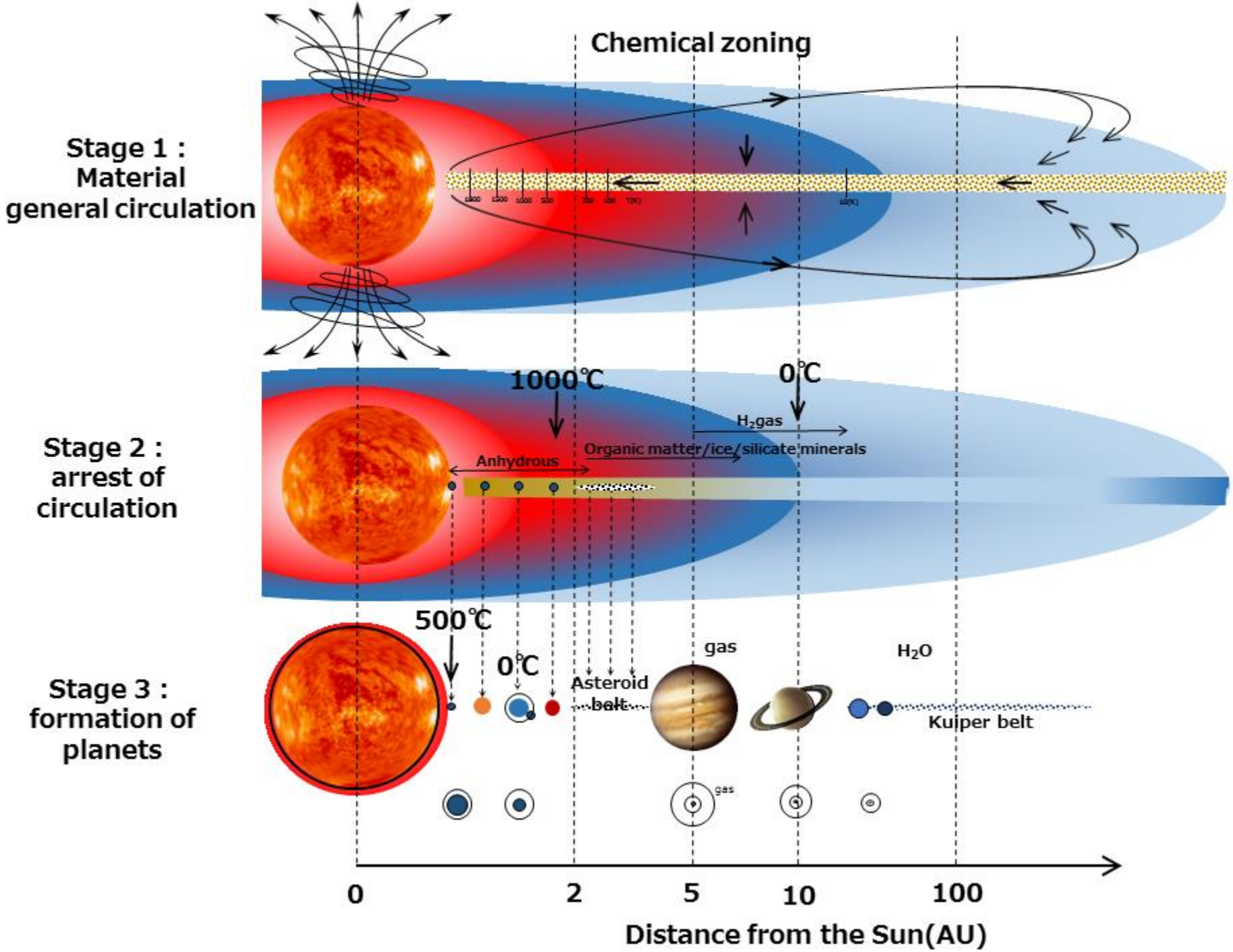
Chemical zoning
Stage 1 :
Material
general circulation
1000℃
0℃
H_2gas
Organic matter/ice/silicate minerals
Anhydrous
Stage 2 :
arrest of
circulation
500℃
0℃
gas
H_2O
Asteroid
belt
Kuiper belt
Stage 3 :
formation of
planets
0
2
5
10
100
Distance from the Sun(AU)

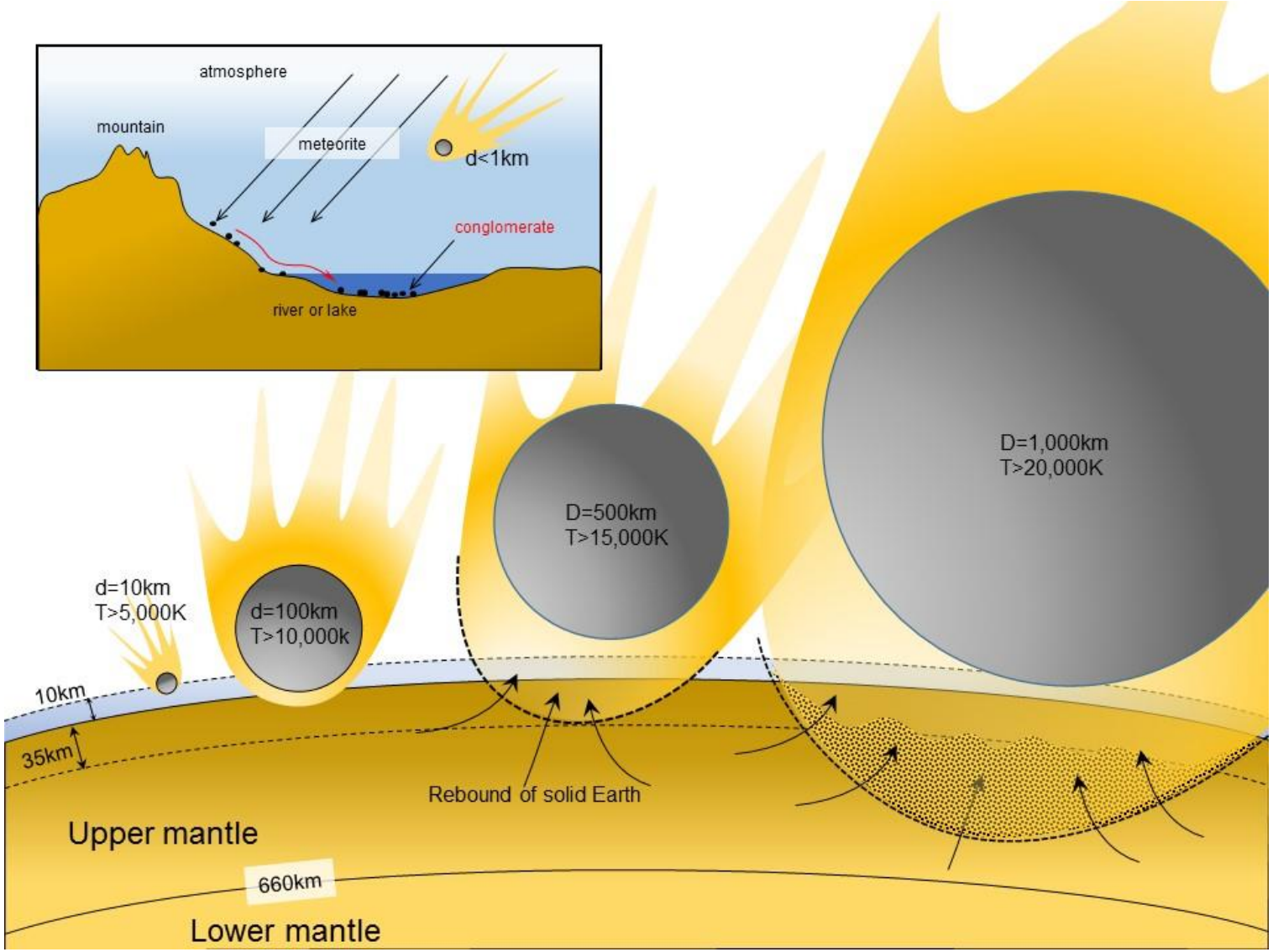
atmosphere
mountain
meteorite
d<1km
conglomerate
river or lake
D=1,000km
T>20,000K
D=500km
T>15,000K
d=10km
T>5,000K
d=100km
T>10,000k
10km
35km
Rebound of solid Earth
Upper mantle
660km
Lower mantle

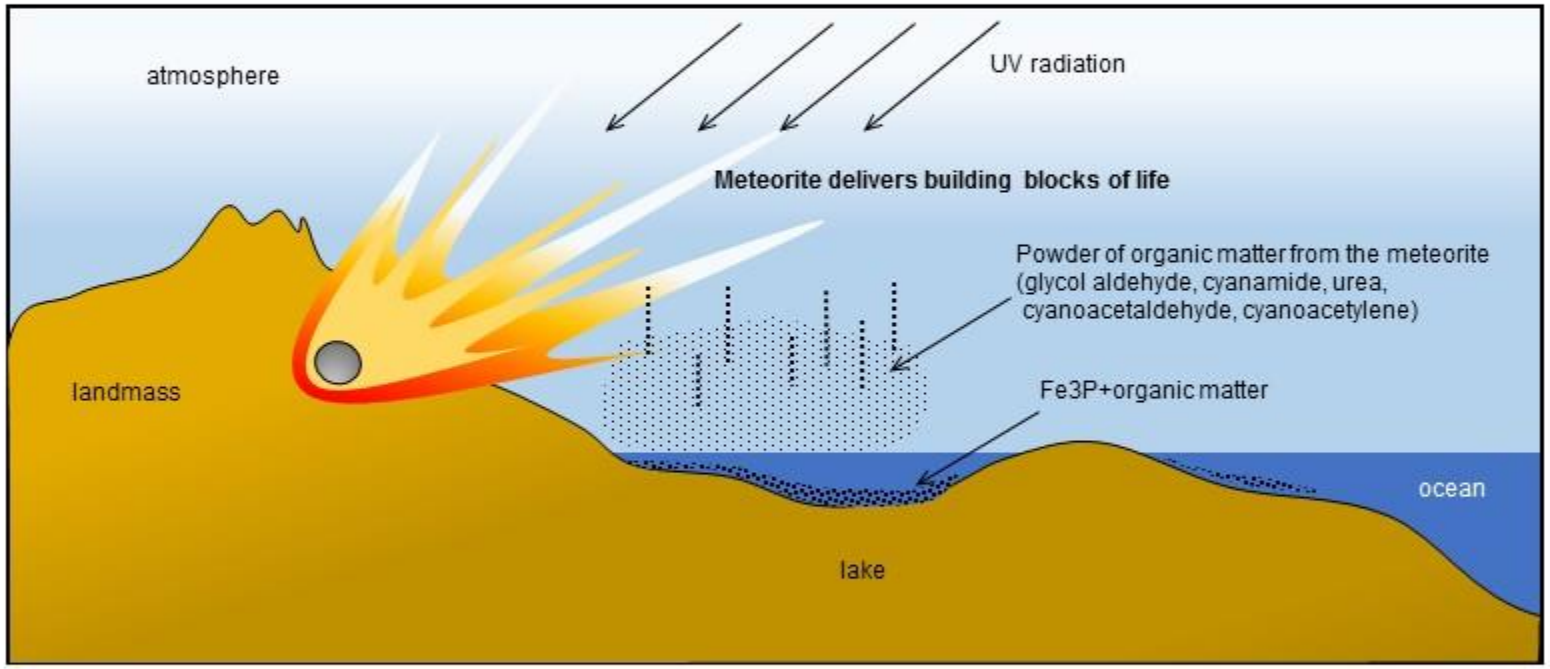
atmosphere
UV radiation
Meteorite delivers building blocks of life
Powder of organic matter from the meteorite
(glycol aldehyde, cyanamide, urea,
cyanoacetaldehyde, cyanoacetylene)
landmass
Fe3P+organic matter
ocean
lake

Oxygen isotope fractionation

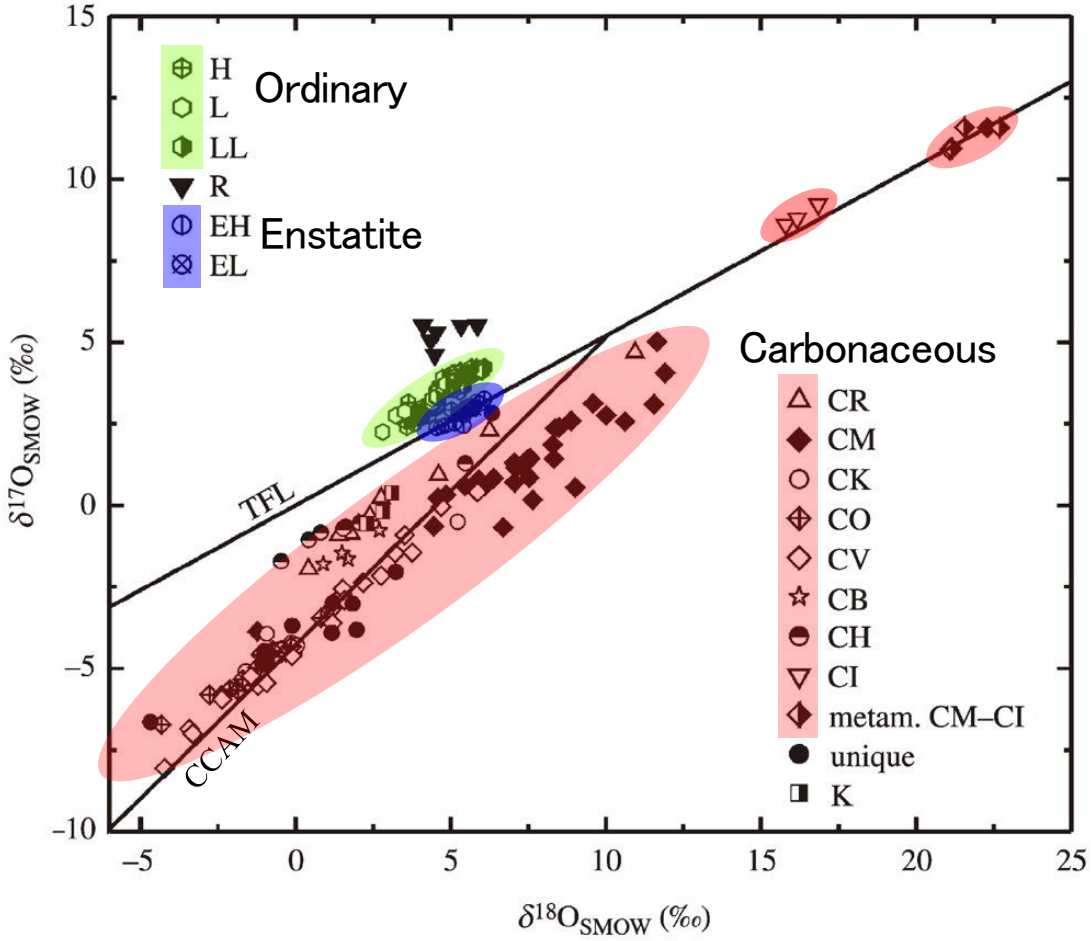

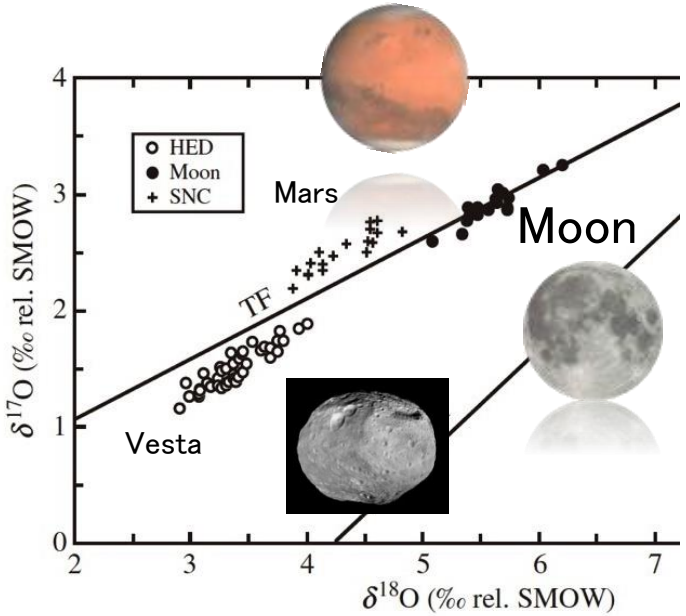

Chondrites

	Carbonaceous								Ordinary	Enstatite
zss →										
Group →	CI	CM	CO	CR	CB	CH	CV	CK	H L LL	EH EL
Petr. type →	1	1-2	3-4	1-2	3	3	3-4	3-6	3-6	3-6
Subgroup →					CB_a CB_b		CV_A CV_B CV_{red}			

Krot et al., in *Treatise on Geochemistry* **1.05**, 83 (2005)
Clayton, in *Treatise on Geochemistry* **1.06** 129 (2005)

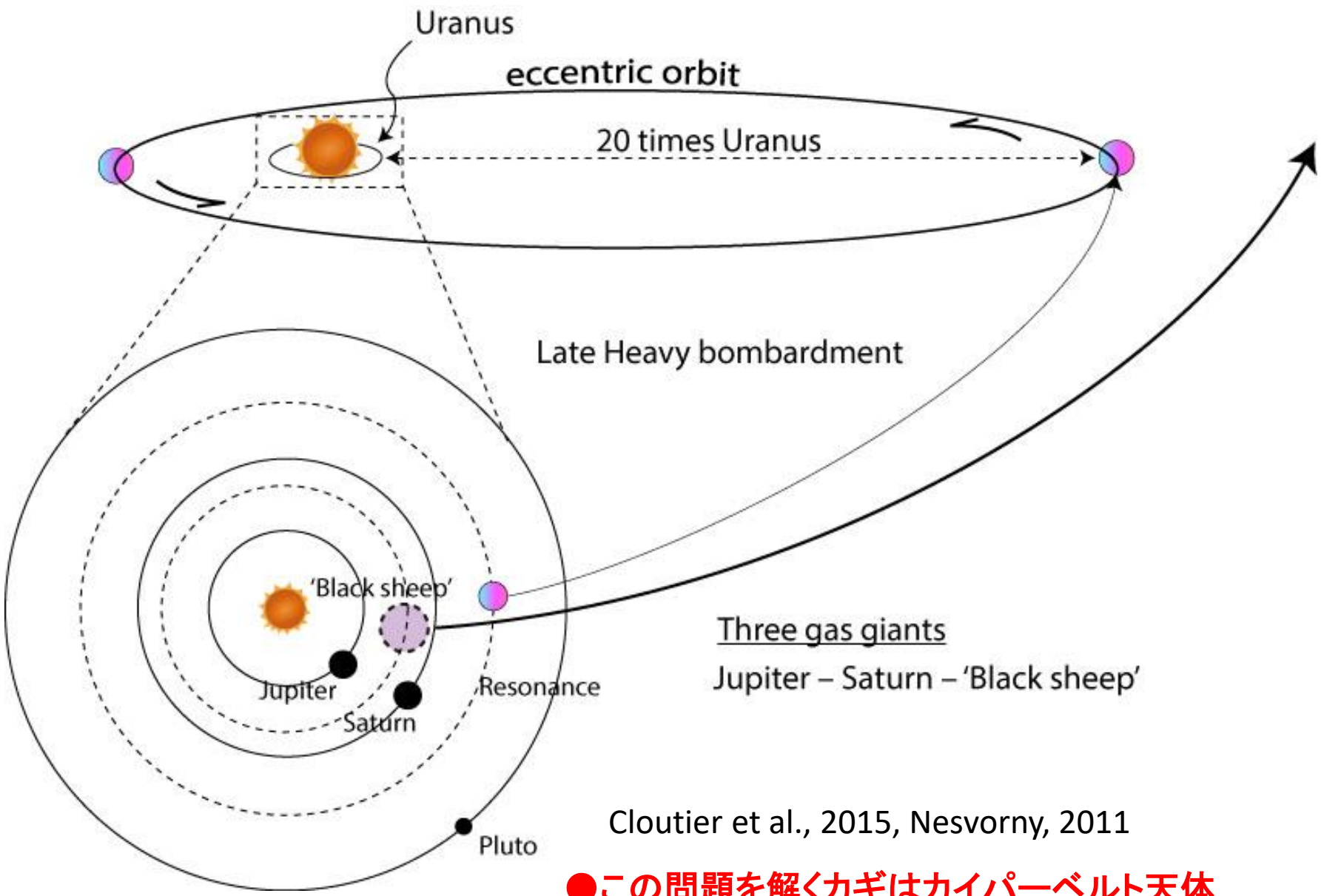

Three gas giants

Jupiter – Saturn – 'Black sheep'

Cloutier et al., 2015, Nesvorny, 2011

●この問題を解くカギはカイパーベルト天体

Escape speed of atmosphere

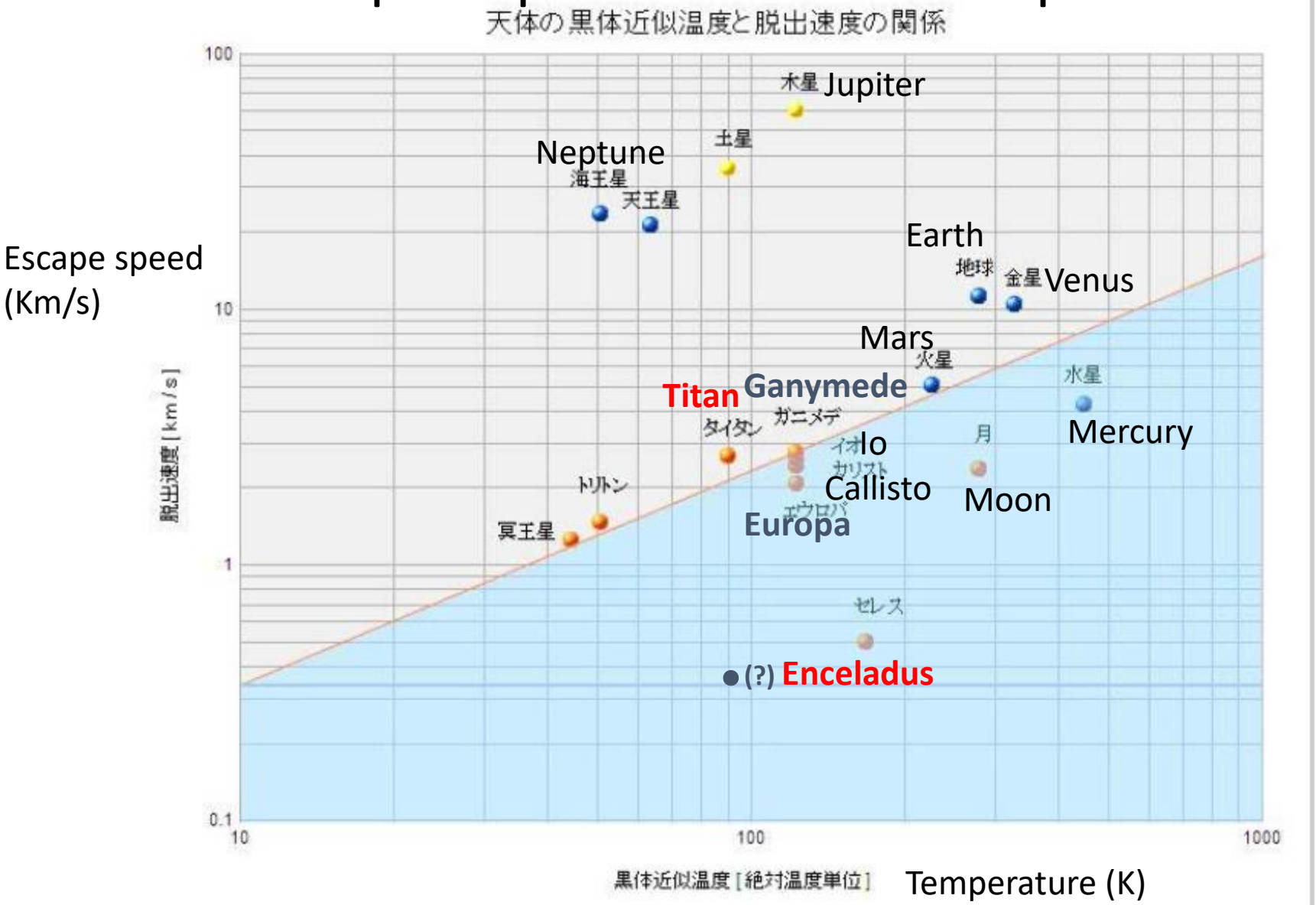

http://blogs.yahoo.co.jp/huriidorihi4sei/3005126.htmlより引用

(a) Slab pull force and ridge push force triggered by ABEL bombardment (4.37-4.20Ga)

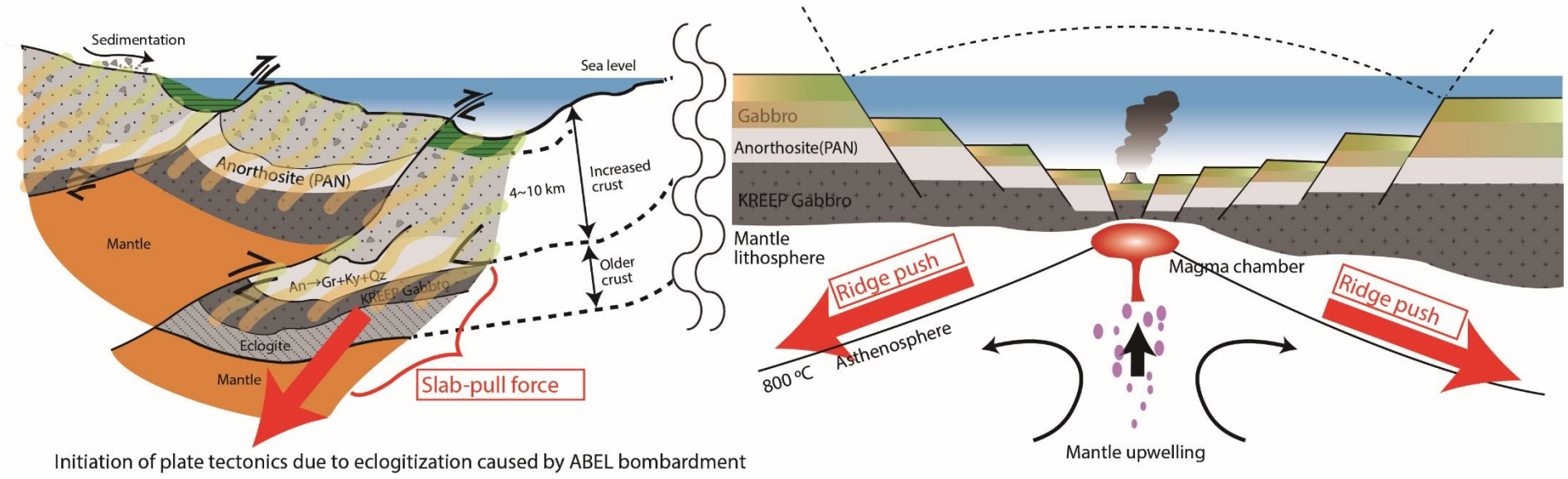

Initiation of plate tectonics due to eclogitization caused by ABEL bombardment

(b) Eclogitization (phase transition) initiated under the presence of fluid

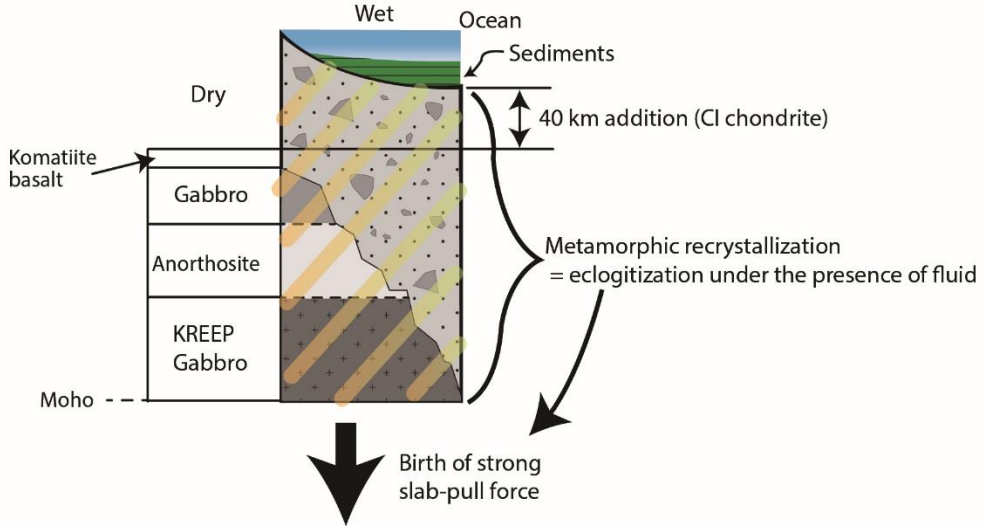

プレートの沈み込みによってCO2をマントルに捨てる

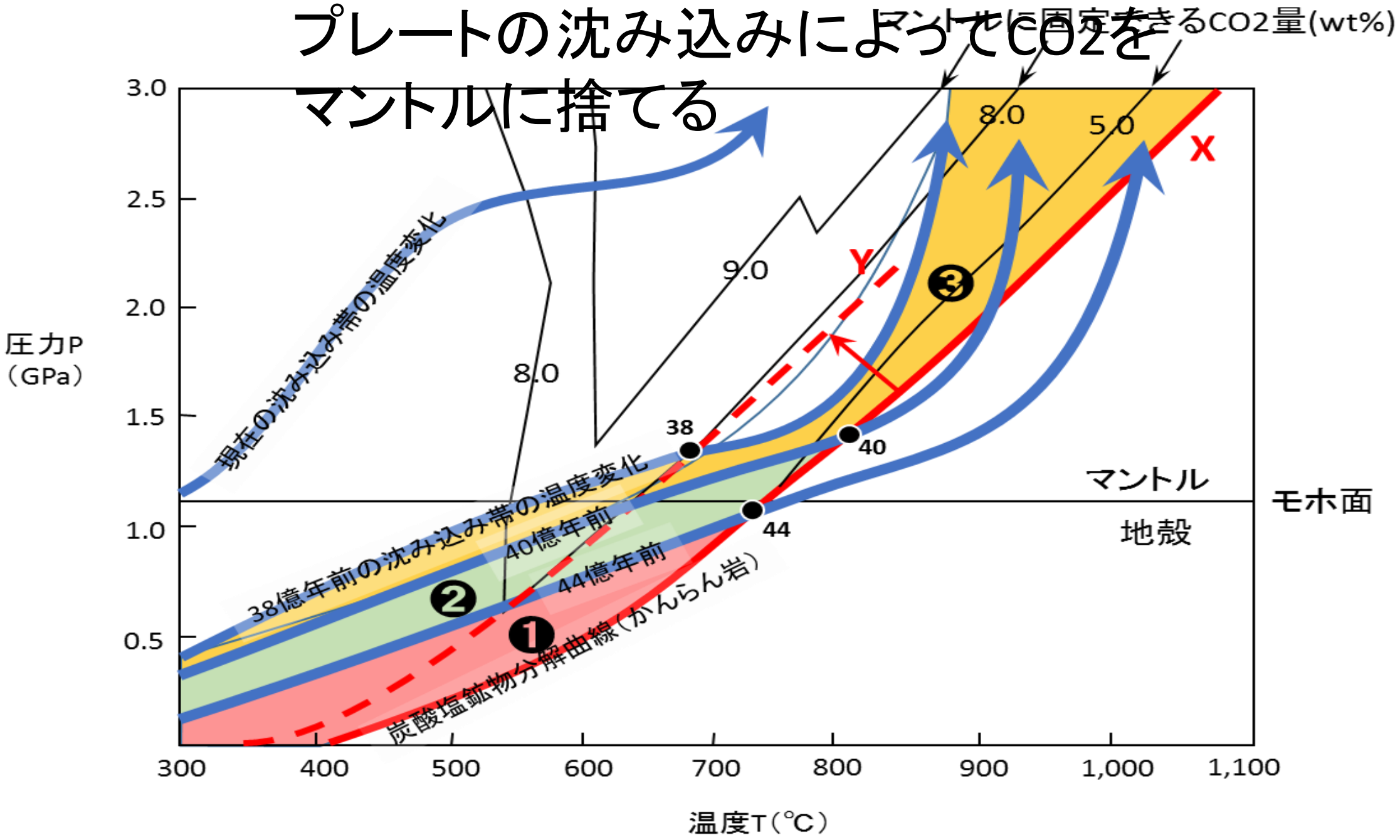

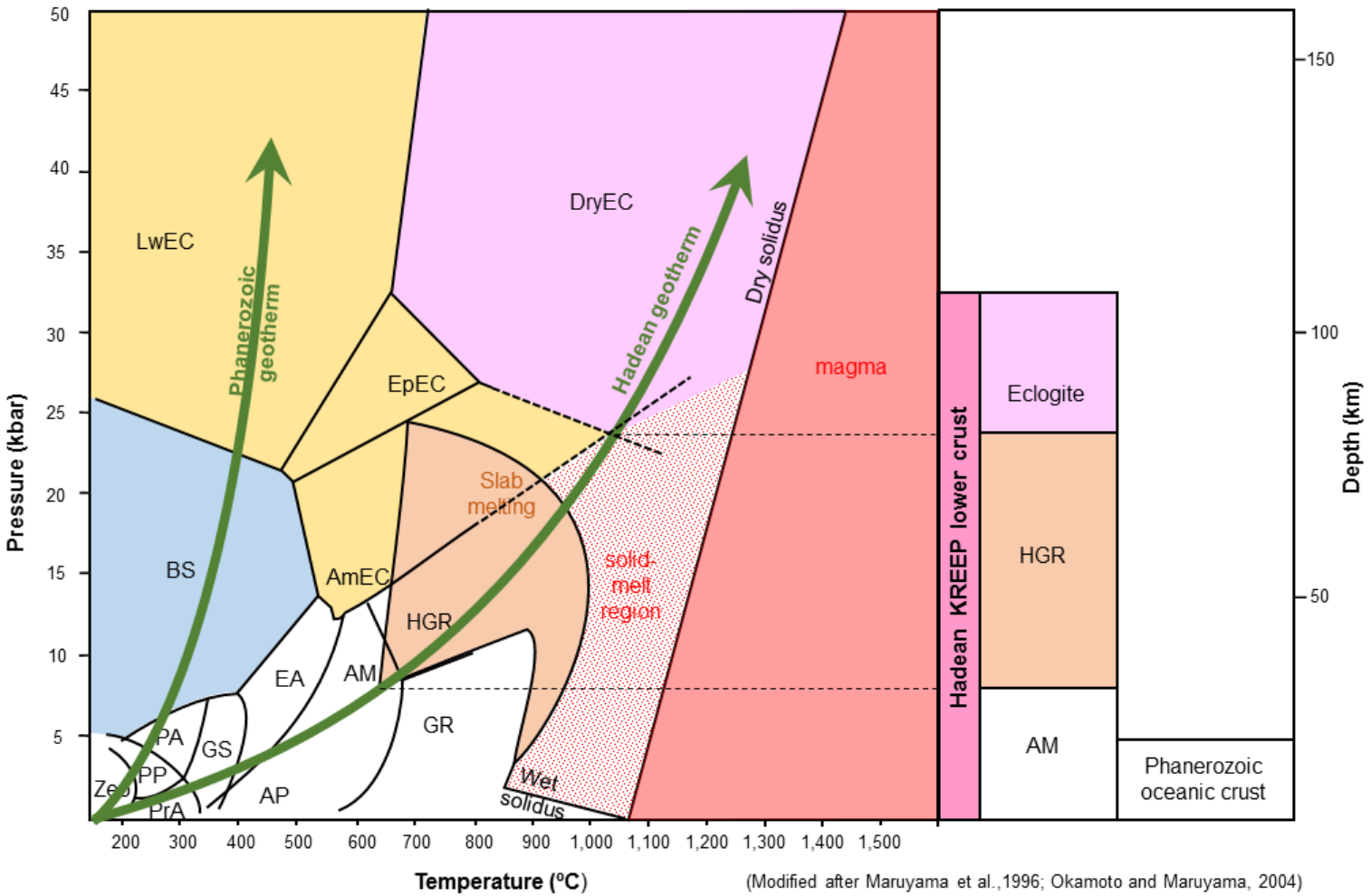

(Modified after Maruyama et al.,1996; Okamoto and Maruyama, 2004)

Sequential formation of planets through time

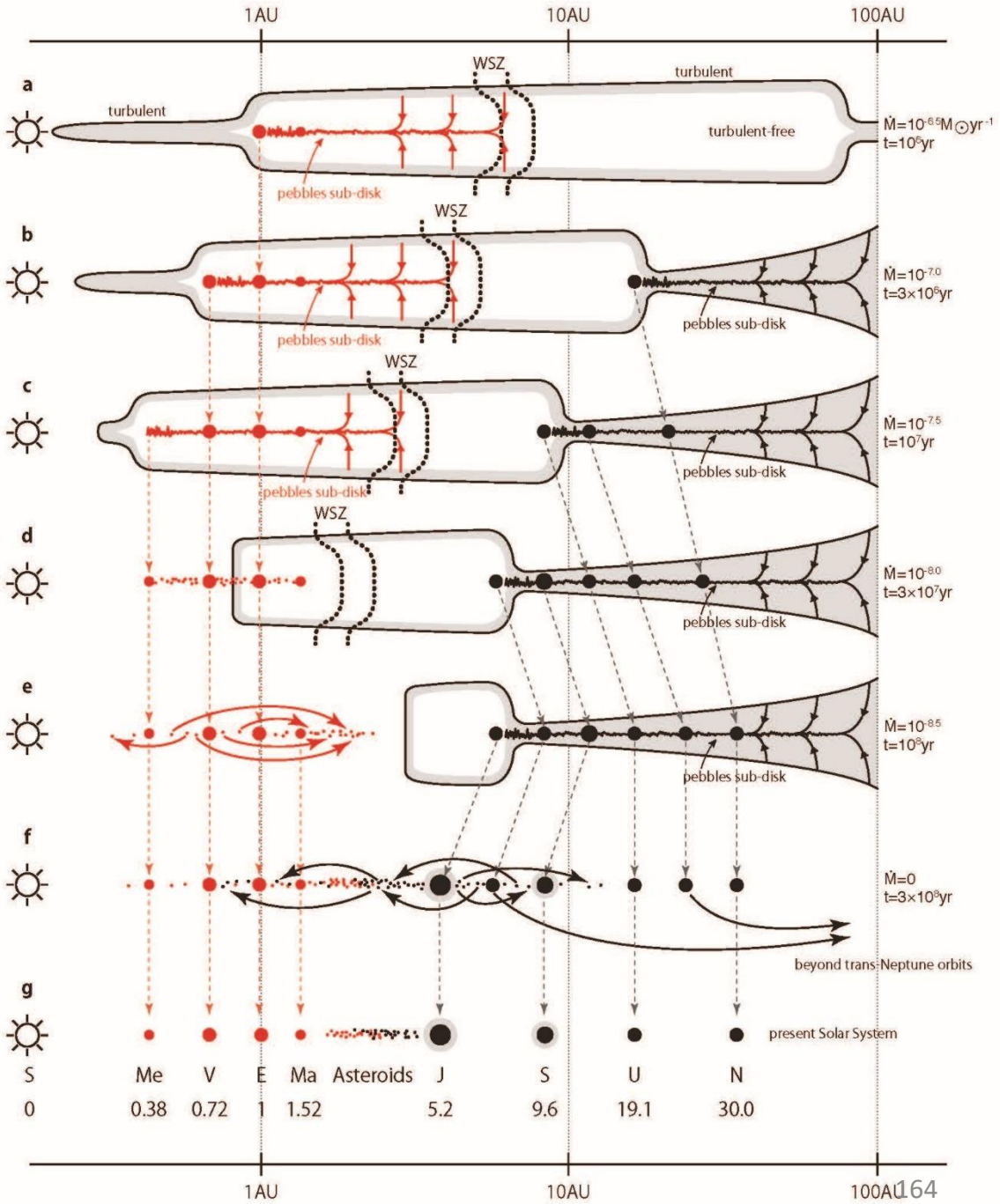

Diversified Eso-planets; how can we make them

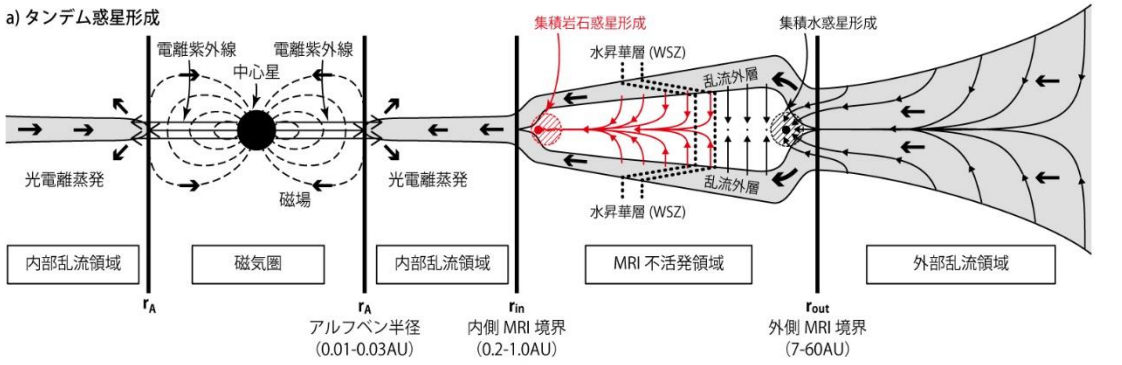

Our solar system

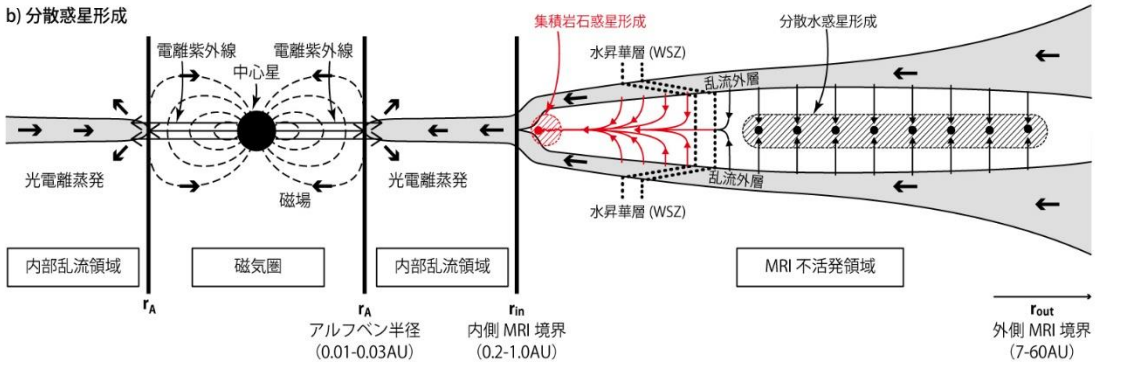

Under weak geomagnetism
Dispersed planets with high ecc
can be formed

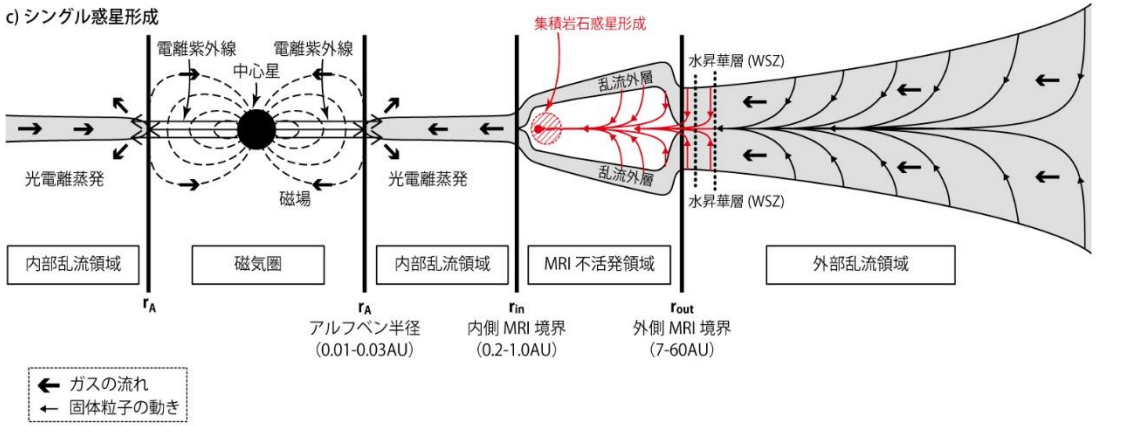

Hot Jupiters & Super Earths
under strong GCR

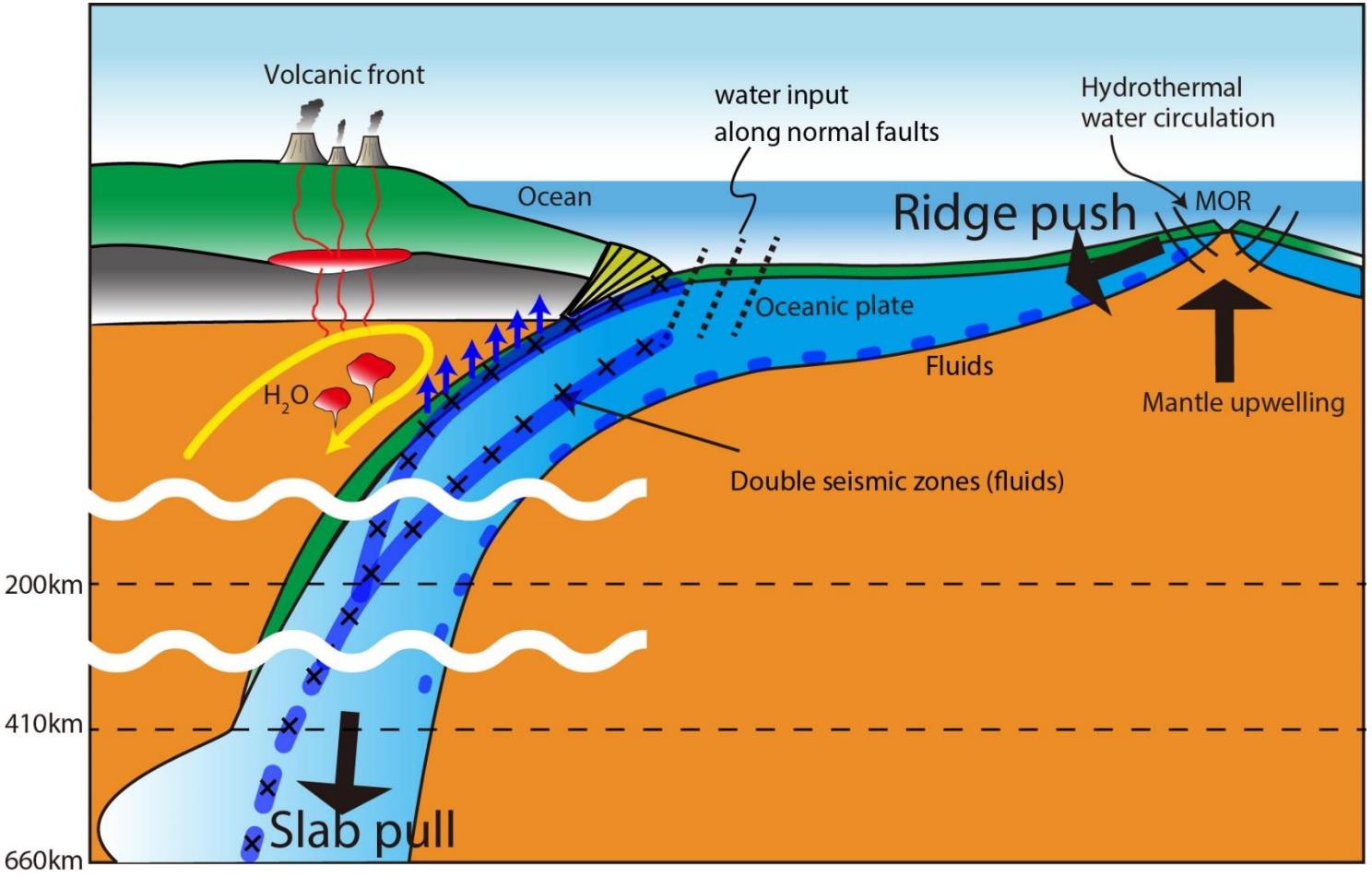
Volcanic front
water input
along normal faults
Hydrothermal
water circulation
Ocean
Ridge push
MOR
Oceanic plate
Fluids
H_2O
Mantle upwelling
Double seismic zones (fluids)
200km
410km
660km
Slab pull

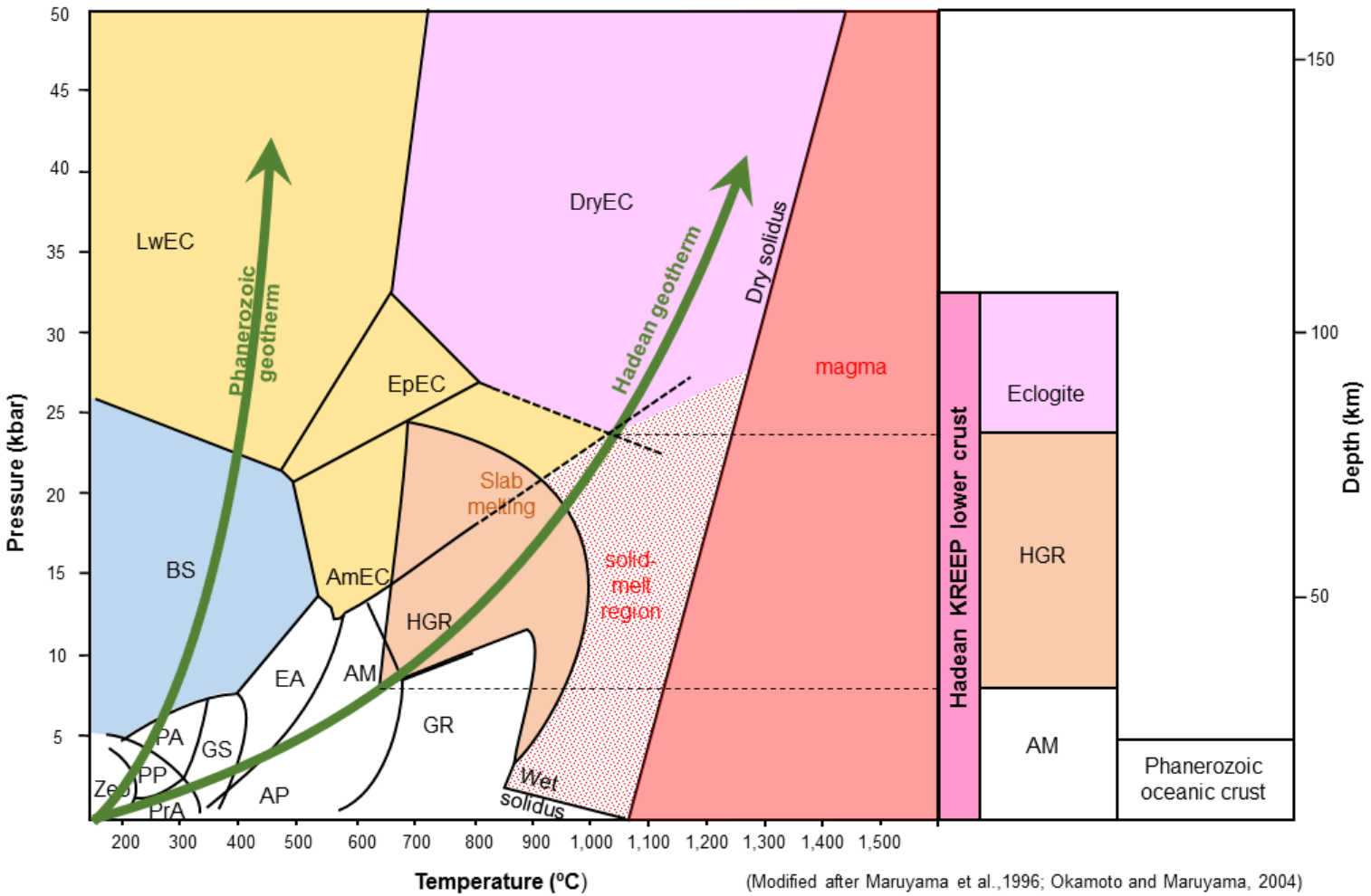

(Modified after Maruyama et al.,1996; Okamoto and Maruyama, 2004)

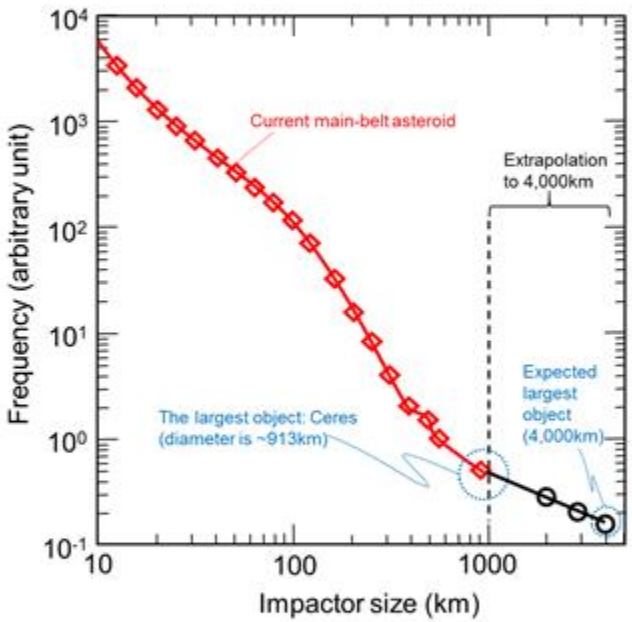

Modified after Marchi et al (2014)

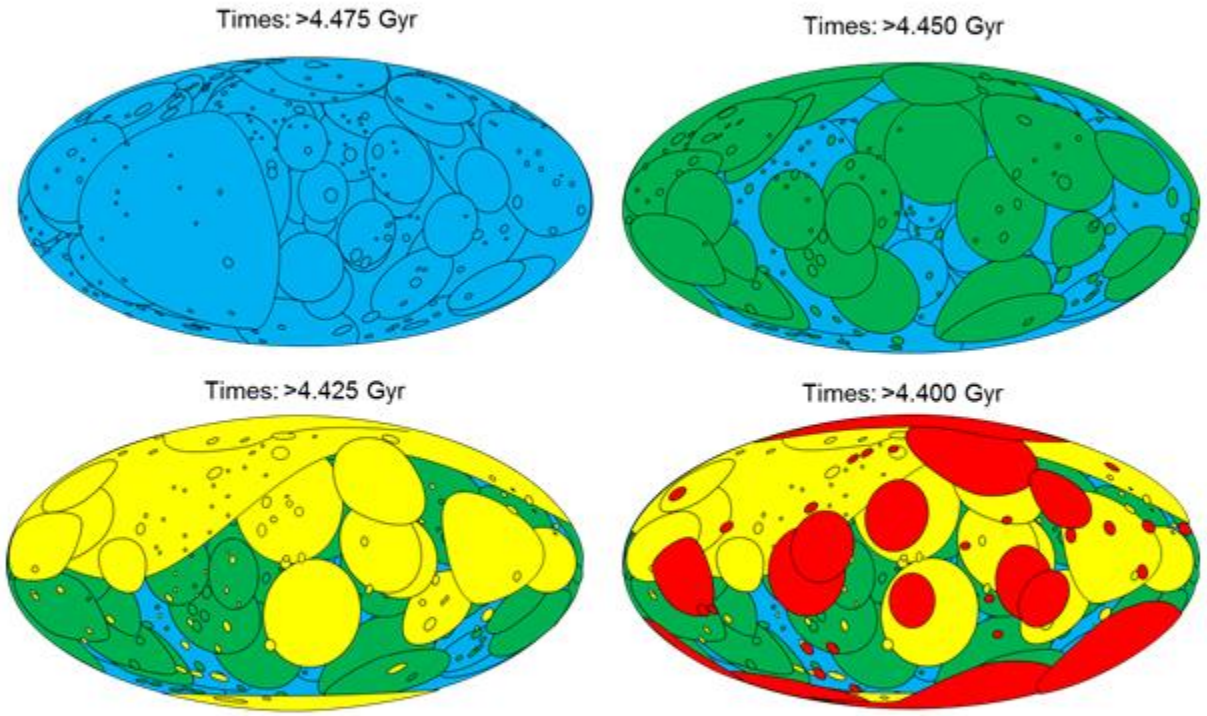

Marchi et al (2014)

CO_2 circulation

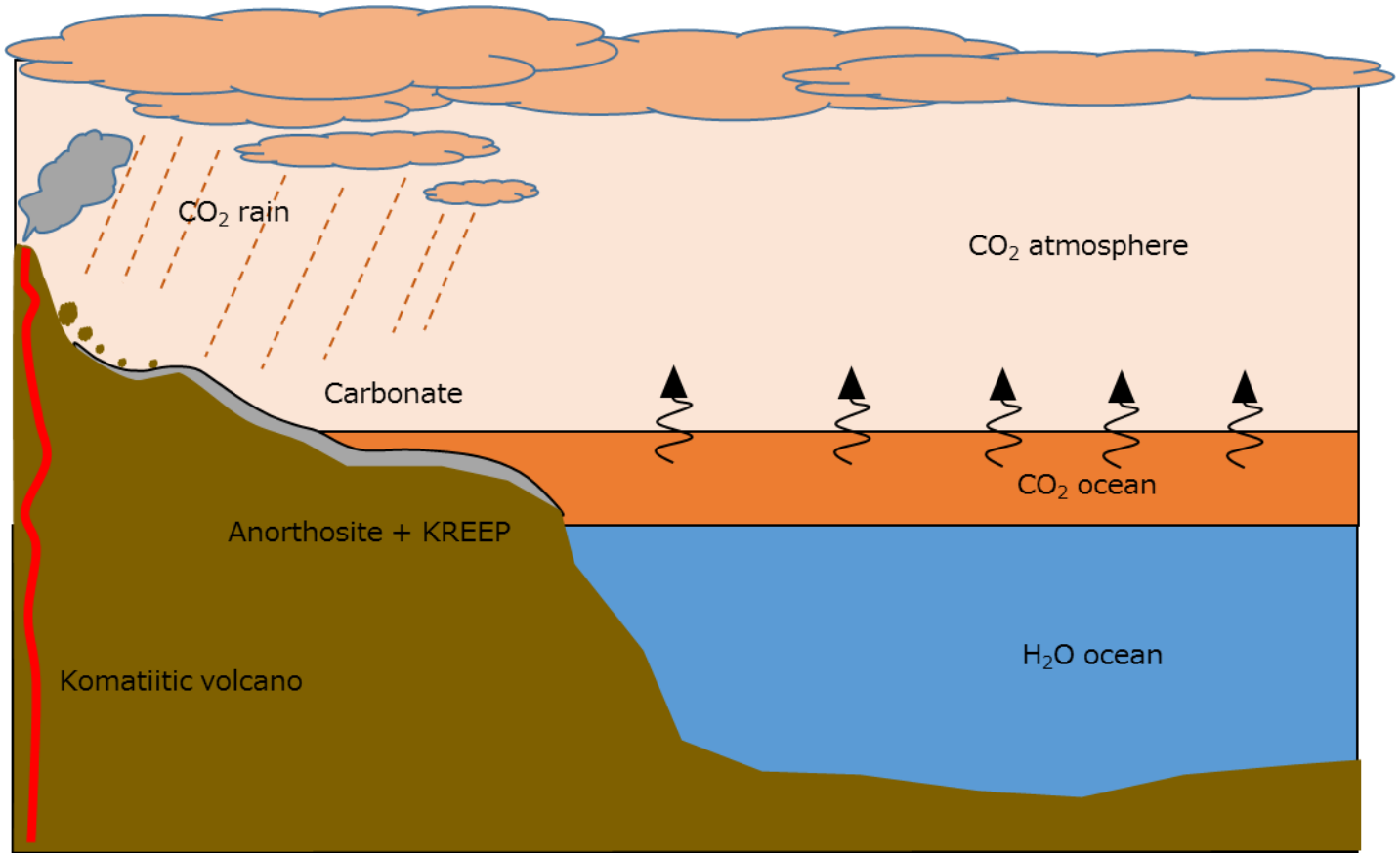

丸山、林、橋本、戎崎、2015

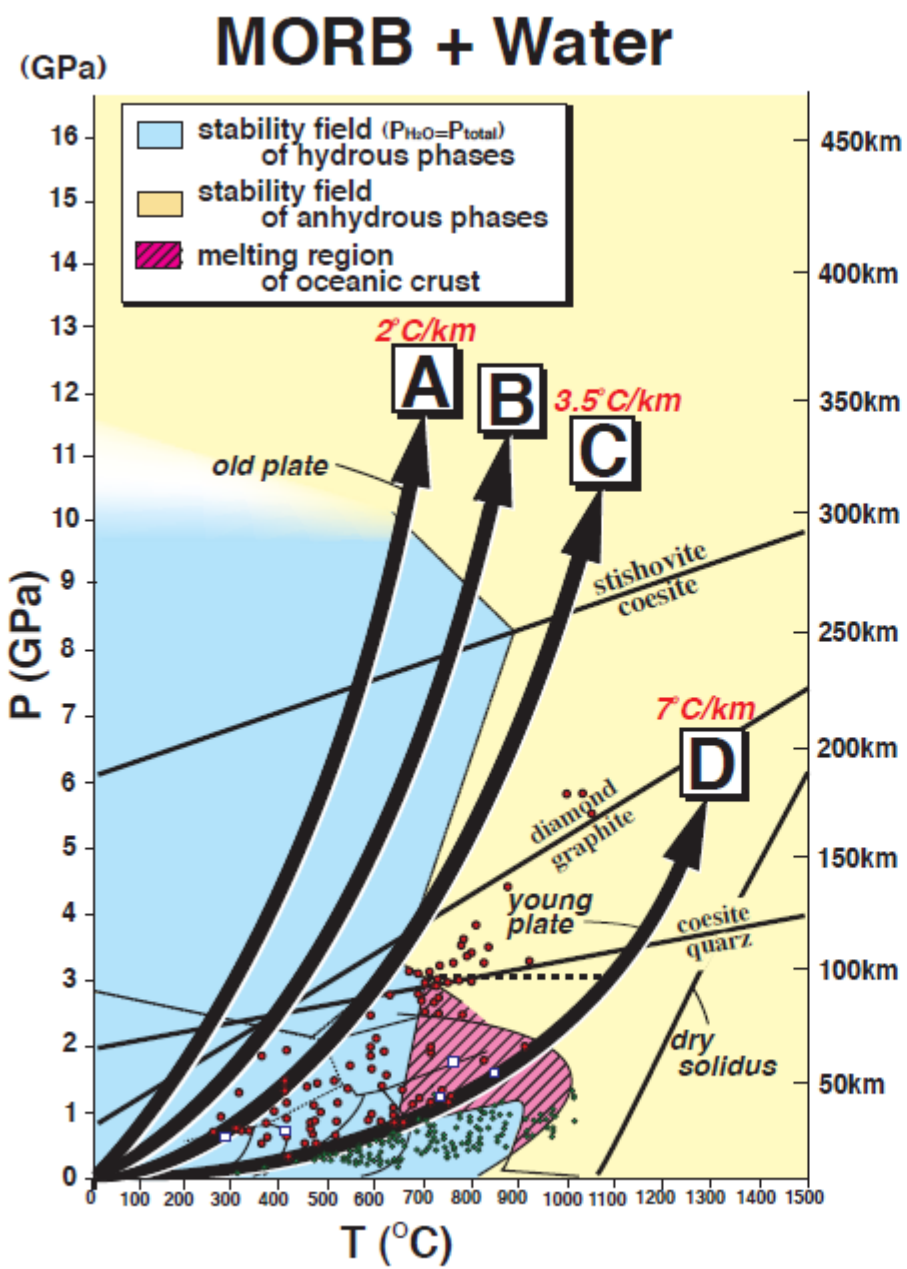

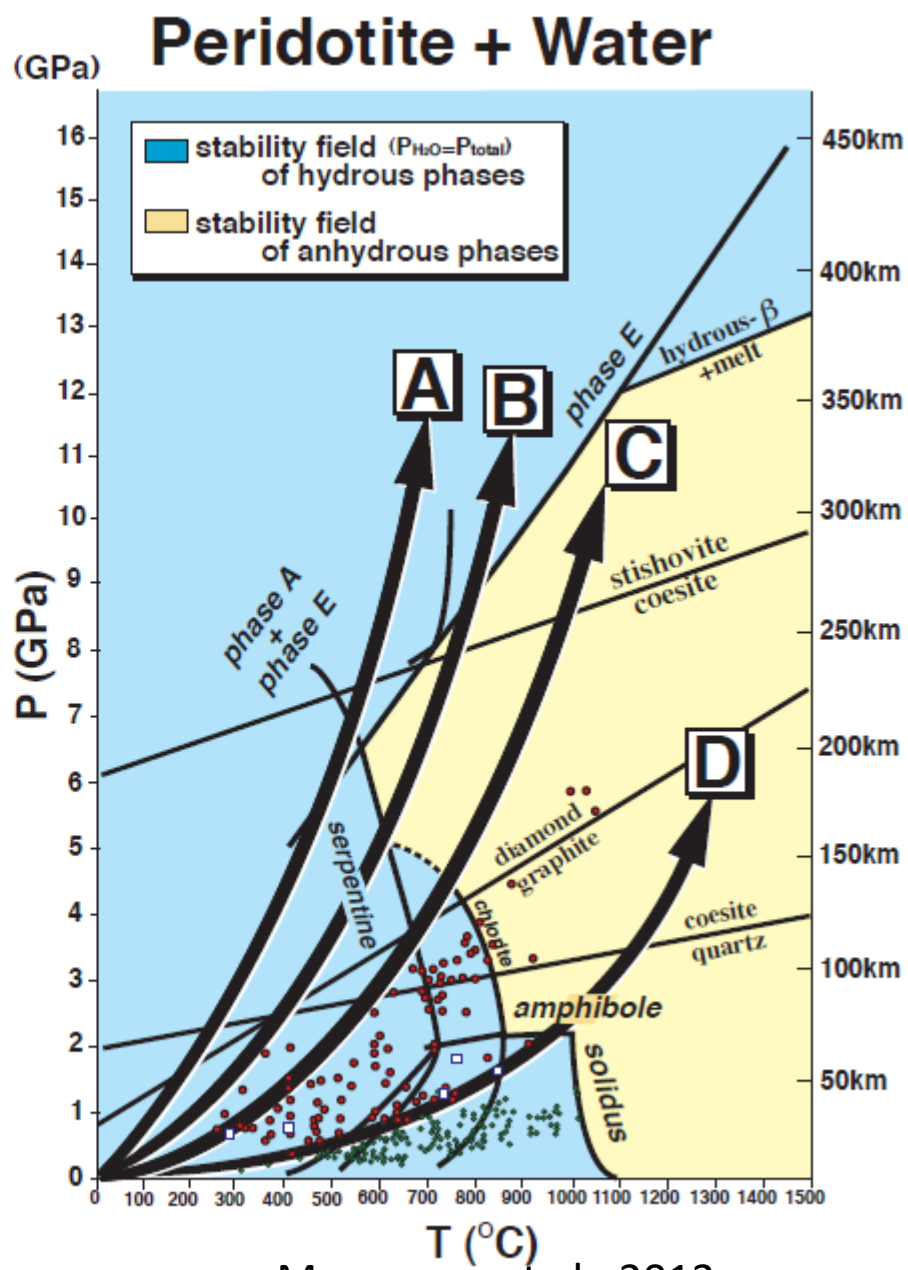

Maruyama et al., 2013

Mantle transition zone
huge water **tank=5 times**
as large as total ocean mass

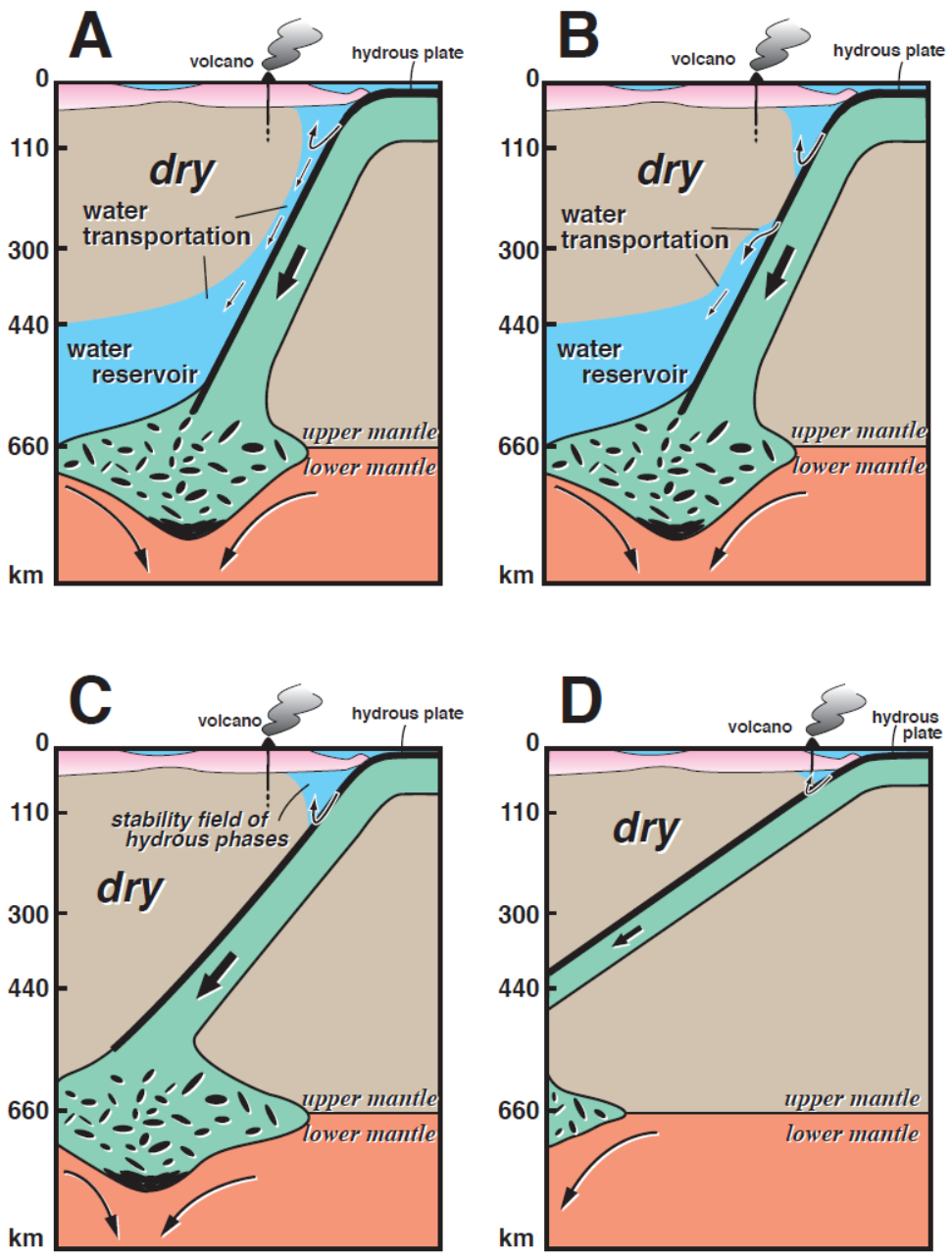

Maruyama & Okamoto (1998, 2001)

Huge water tank in MTZ (Inoue and others)

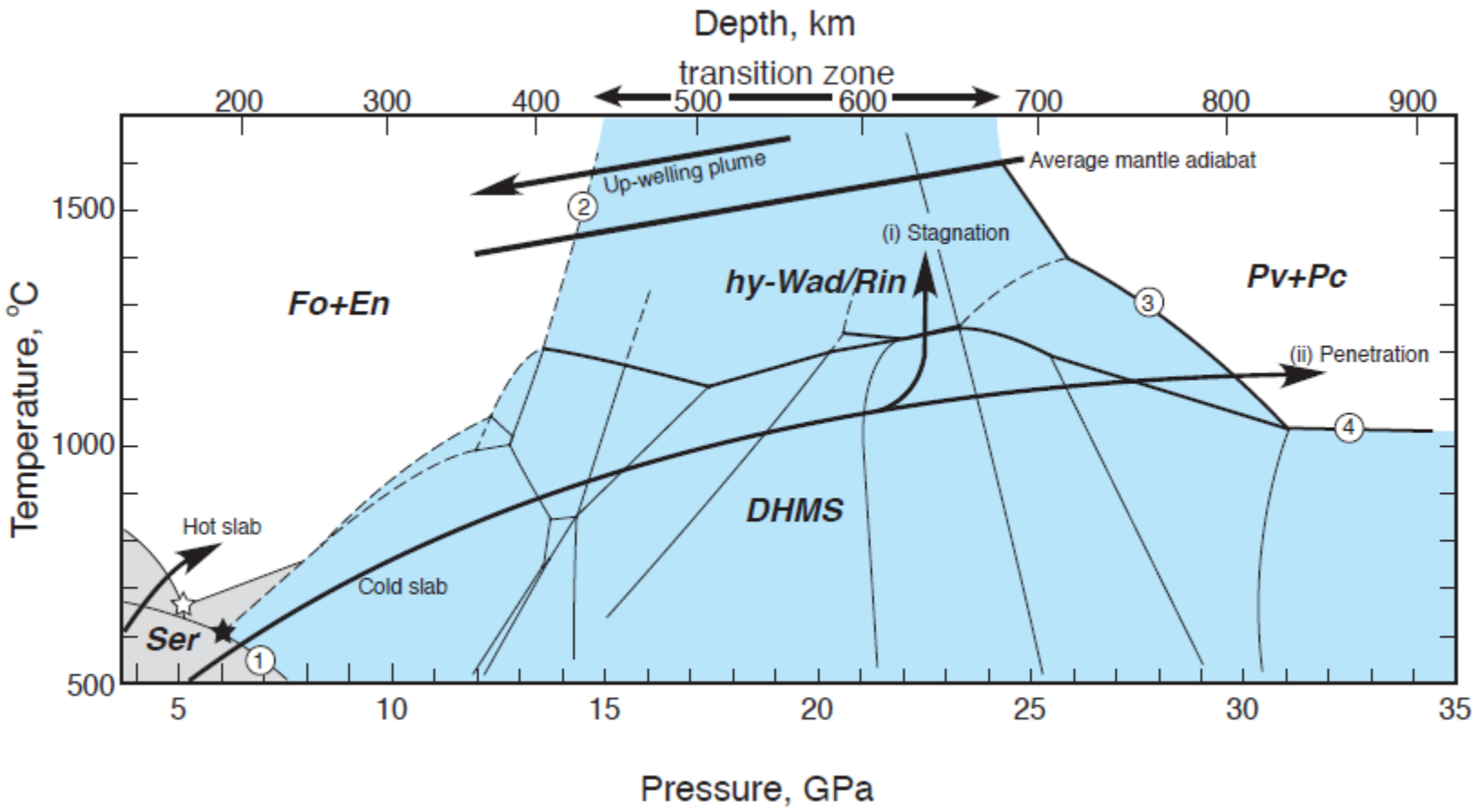

Komabayashi et al., 2008
Maruyama et al., 2013

Fate of water from MOR to deep subduction zone
Subduction zone geotherm = Top of descending slab

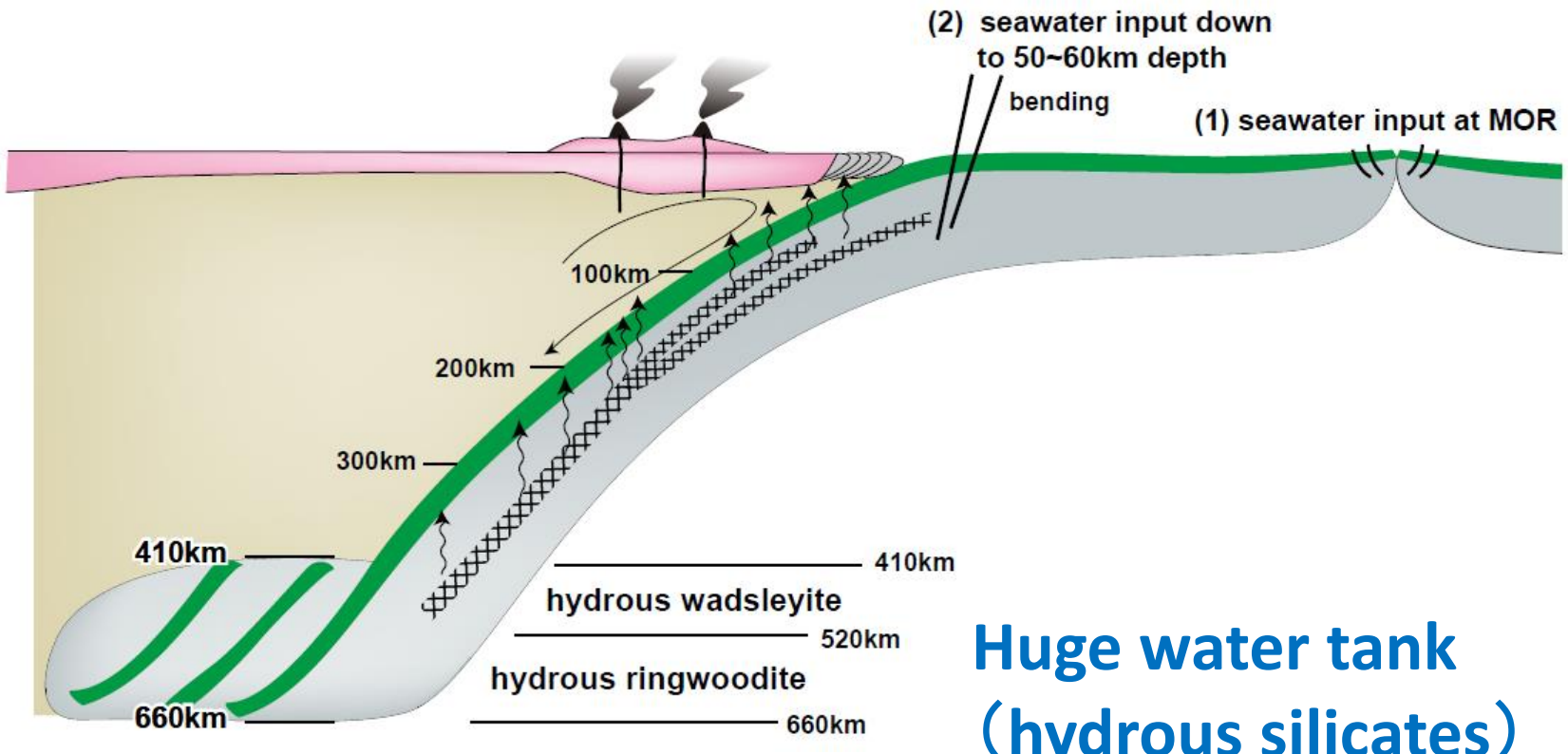

Huge water tank
（hydrous silicates）

Maruyama et al., 2013

小惑星帯の領域に質量の大きな欠損がある→木星が内側に移動して吸収した

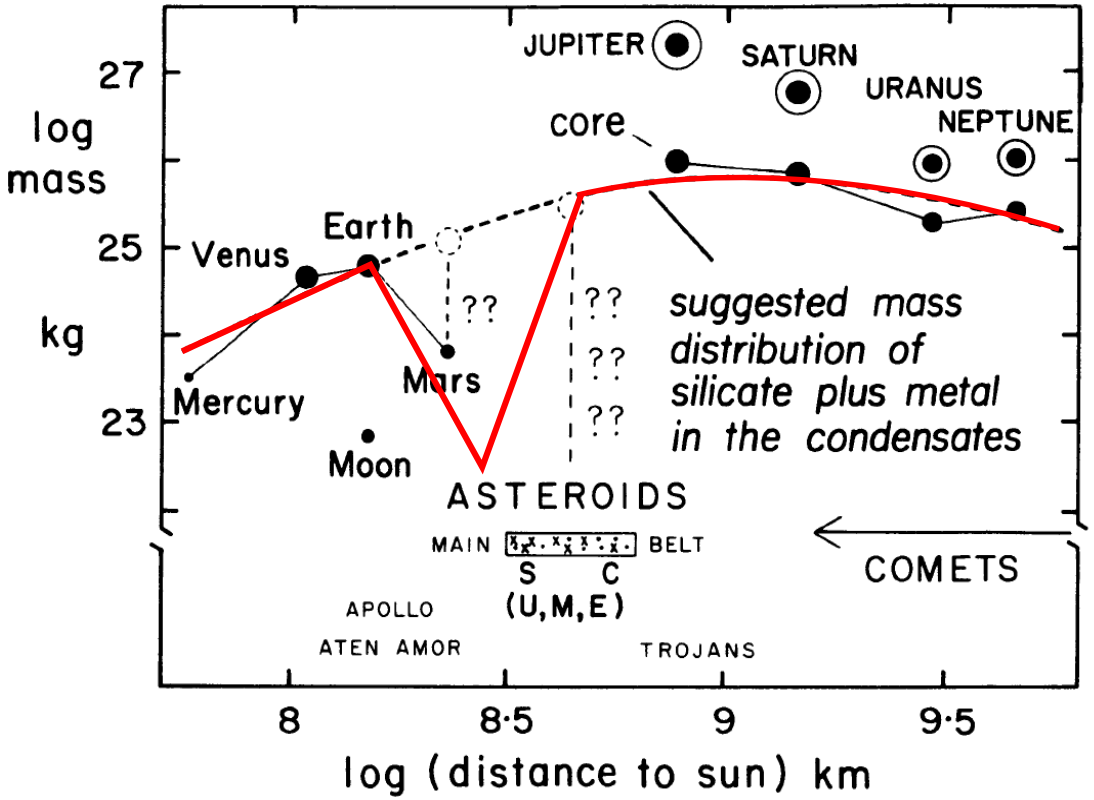

FIG. 6.—Mass-position diagram of solar system. The masses of the silicate-metal cores of the giant planets are taken from Hubbard and MacFarlane (1980), Gehrels (1976) and Slattery (1977). Note that the suggested mass distribution is shown in this way merely to give a pictorial comparison with the planets, and that the volume of each planetary zone must be taken into account (Weidenschilling 1978).

Smith (1982)

Chapter 7 Geotectonic history of Mars

Mars History; 7 major events

Chapter 9 Debate on Mars

Mass depletion between Outer and Inner Planets?

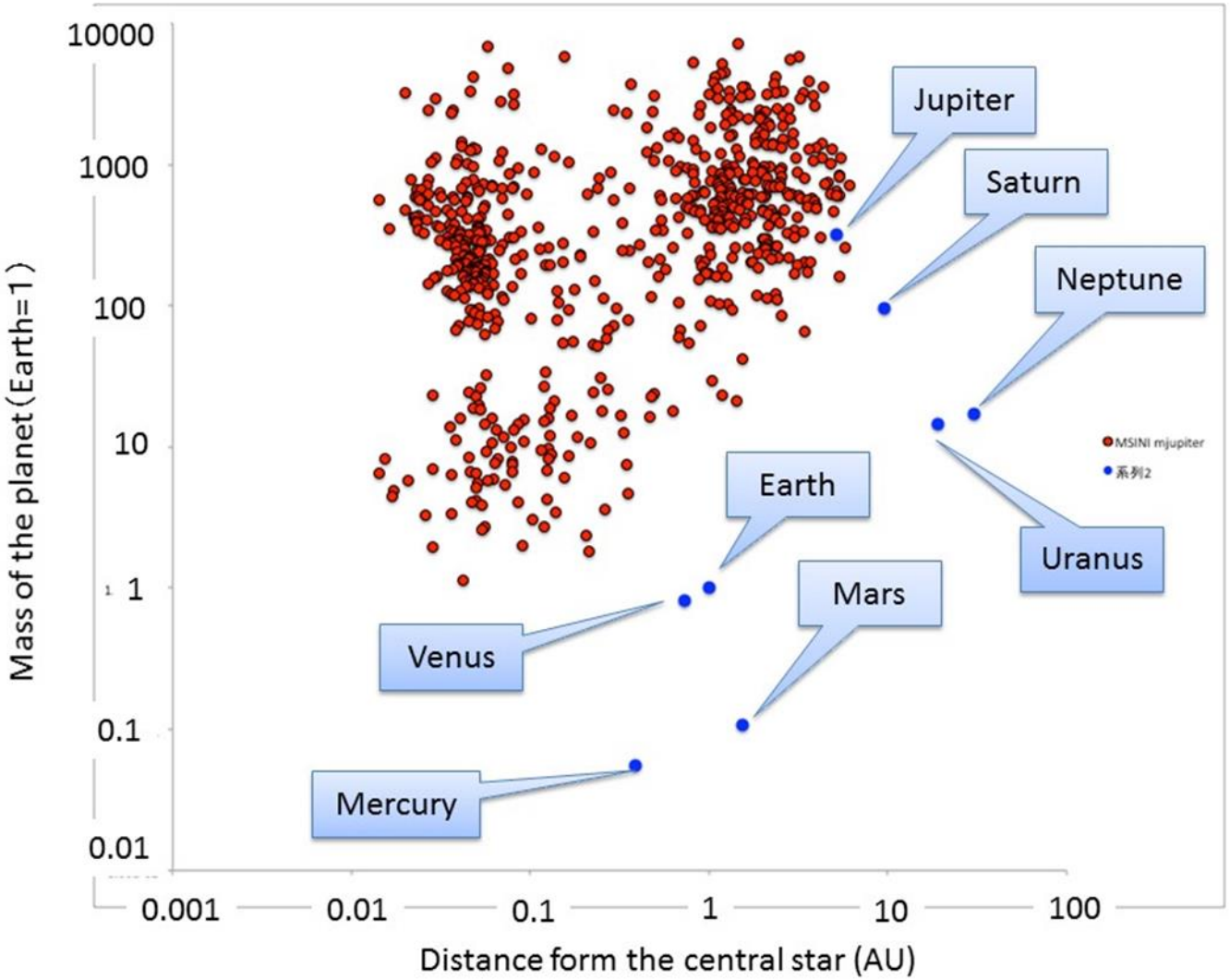

Write et al. 2011, PASP, 123, 412-422, Eso-planets＞6,000 (2016)

Hot Jupiter and Super-Earth

プレートテクトニクスの理論構造

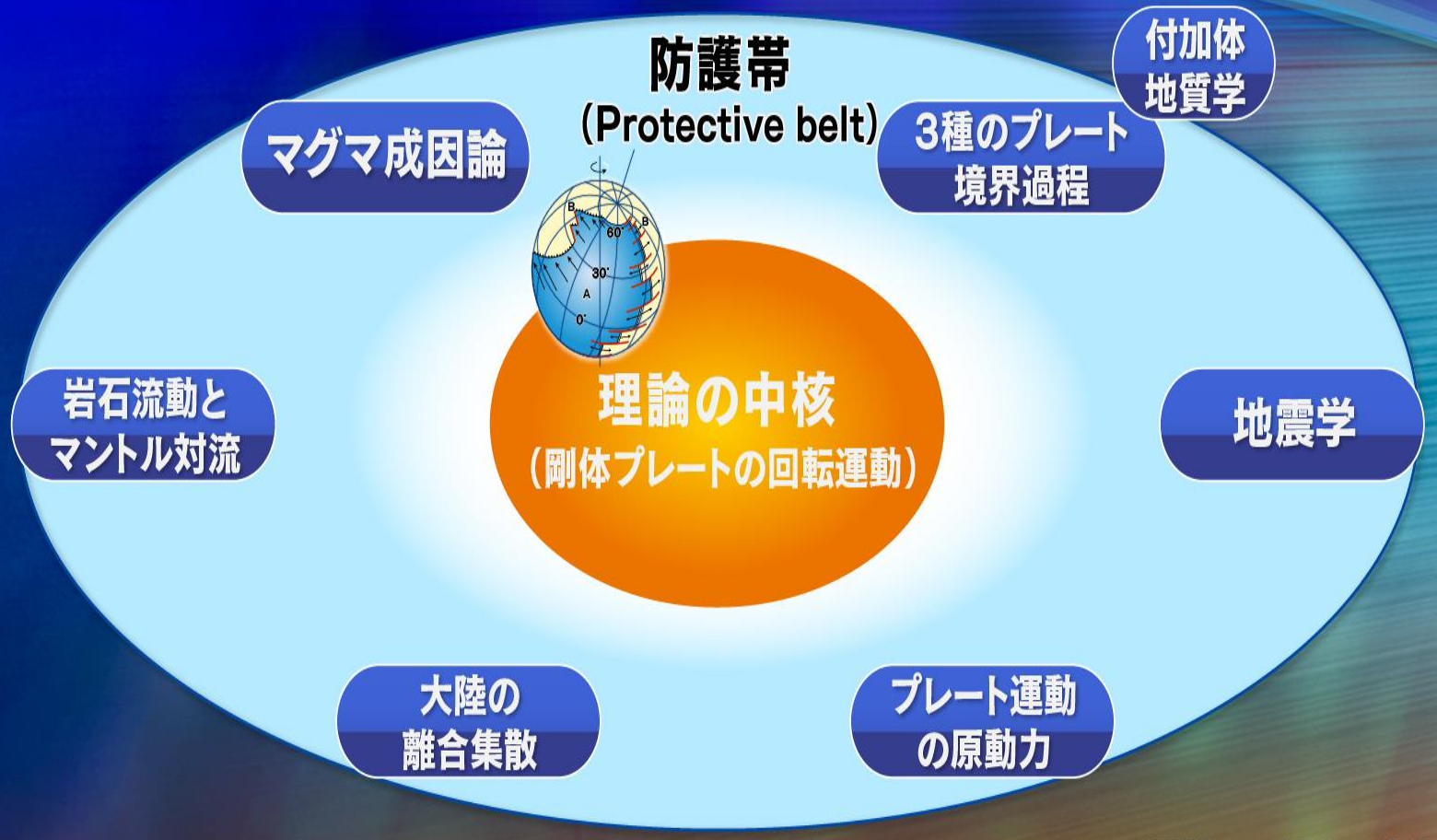

都城(1998)をもとに作成

Distribution of high-V anomaly of P-wave

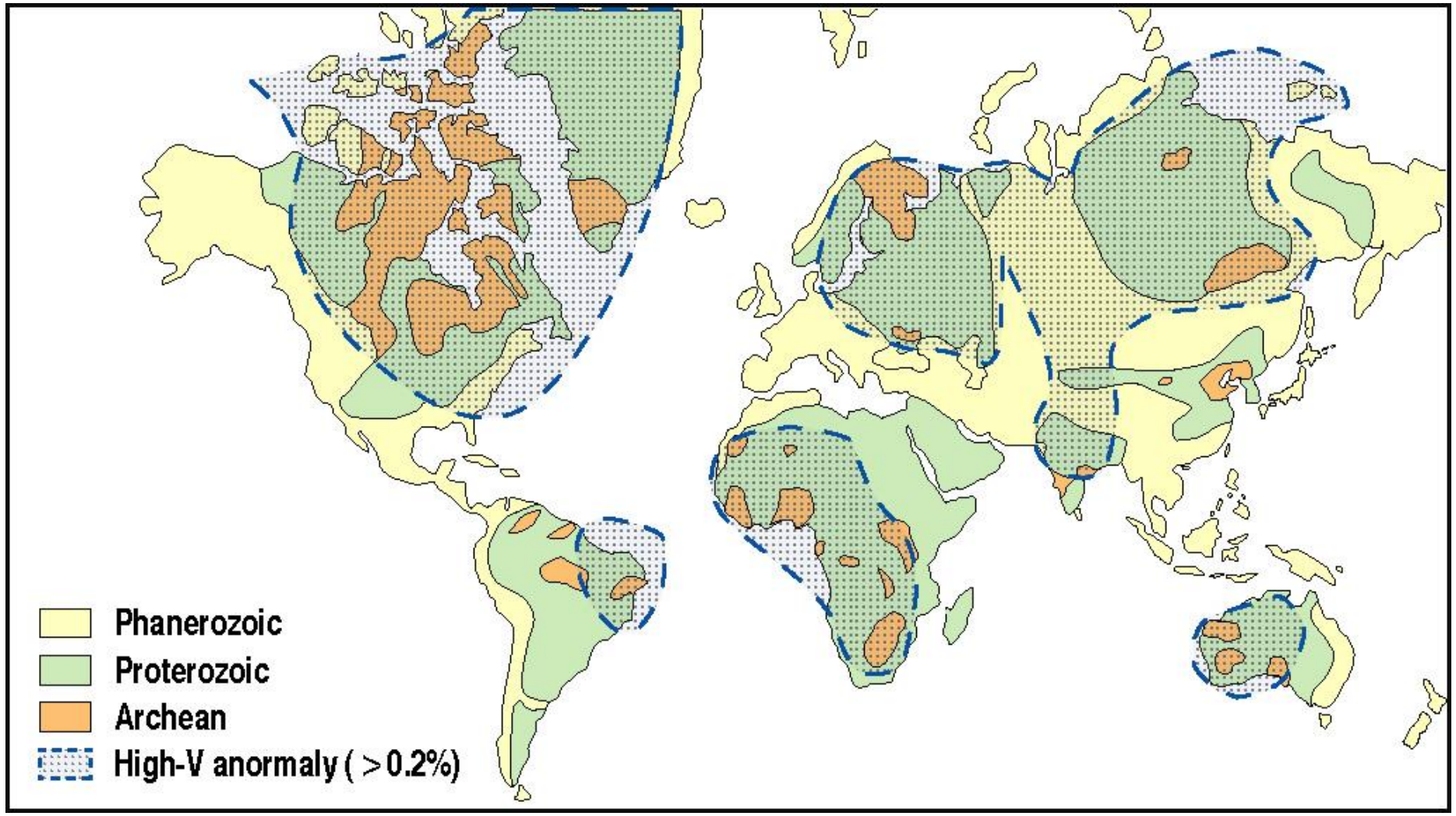

H2O

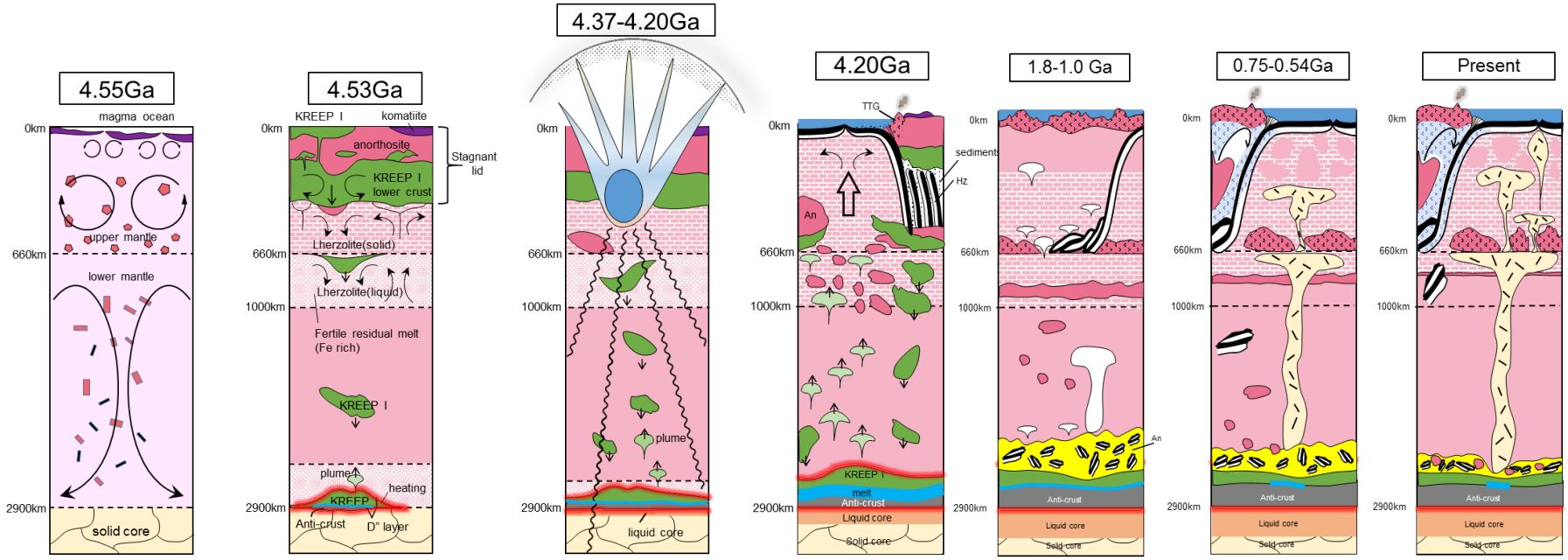
4.55Ga
magma ocean
0km
upper mantle
660km
lower mantle
2900km
solid core
4.53Ga
KREEP I
komatiite
0km
anorthosite
Stagnant lid
KREEP I
lower crust
Lherzolite(solid)
660km
Lherzolite(liquid)
1000km
Fertile residual melt
(Fe rich)
KREEP I
plume
heating
KREEP I
2900km
Anti-crust
D" layer
4.37-4.20Ga
0km
660km
1000km
plume
2900km
liquid core
4.20Ga
TTG
0km
sediment
Hz
An
660km
1000km
KREEP I
melt
Anti-crust
Liquid core
2900km
Solid core
1.8-1.0 Ga
0km
660km
1000km
An
Anti-crust
Liquid core
2900km
Solid core
0.75-0.54Ga
0km
660km
1000km
Anti-crust
Liquid core
2900km
Solid core
Present
0km
660km
1000km
Anti-crust
Liquid core
2900km
Solid core

Systematic compositional change within rocky planets
Planet density as a distance from the Sun (AU)

1st Step:
Bulk chemical composition of Solar Rocky Planets
（中心星からの距離の関数＝密度曲線）

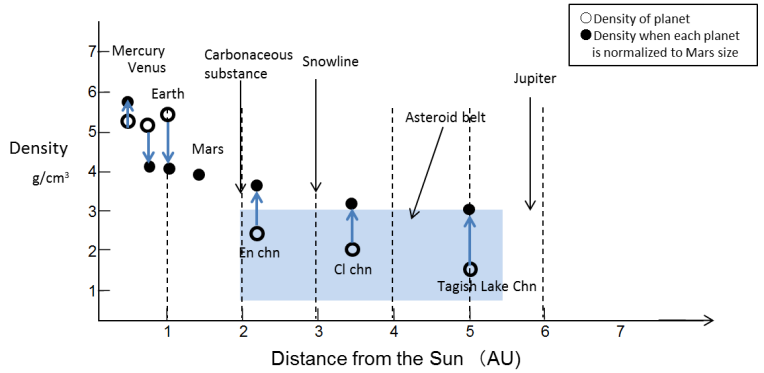

2nd Step:
Bulk chemical composition of Universal Rocky Planets determined as a function of Central Star (chemistry and size) and distance (from CS)（中心星の組成とサイズで密度曲線が変化）

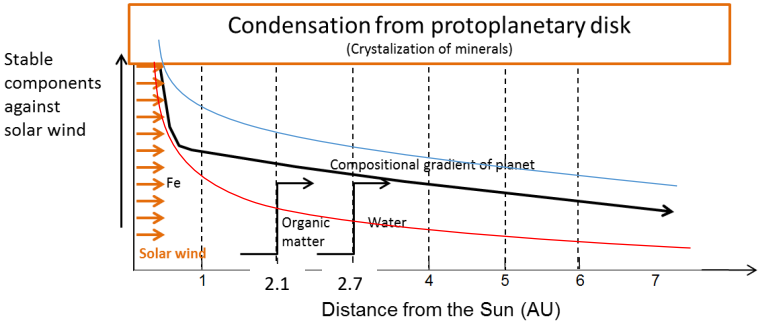

3rd Step:
The birth and evolution of Habitable Trinity Planet are determined by internal dynamics of solid planet
惑星内部の初期進化でHTPへ

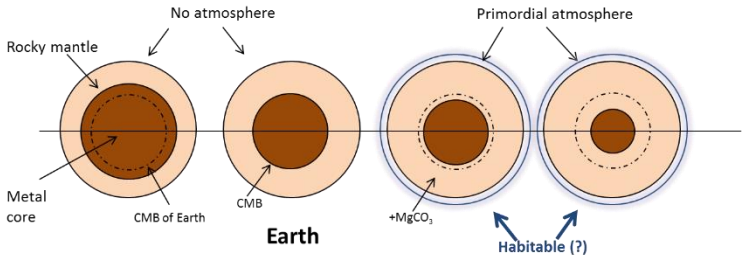

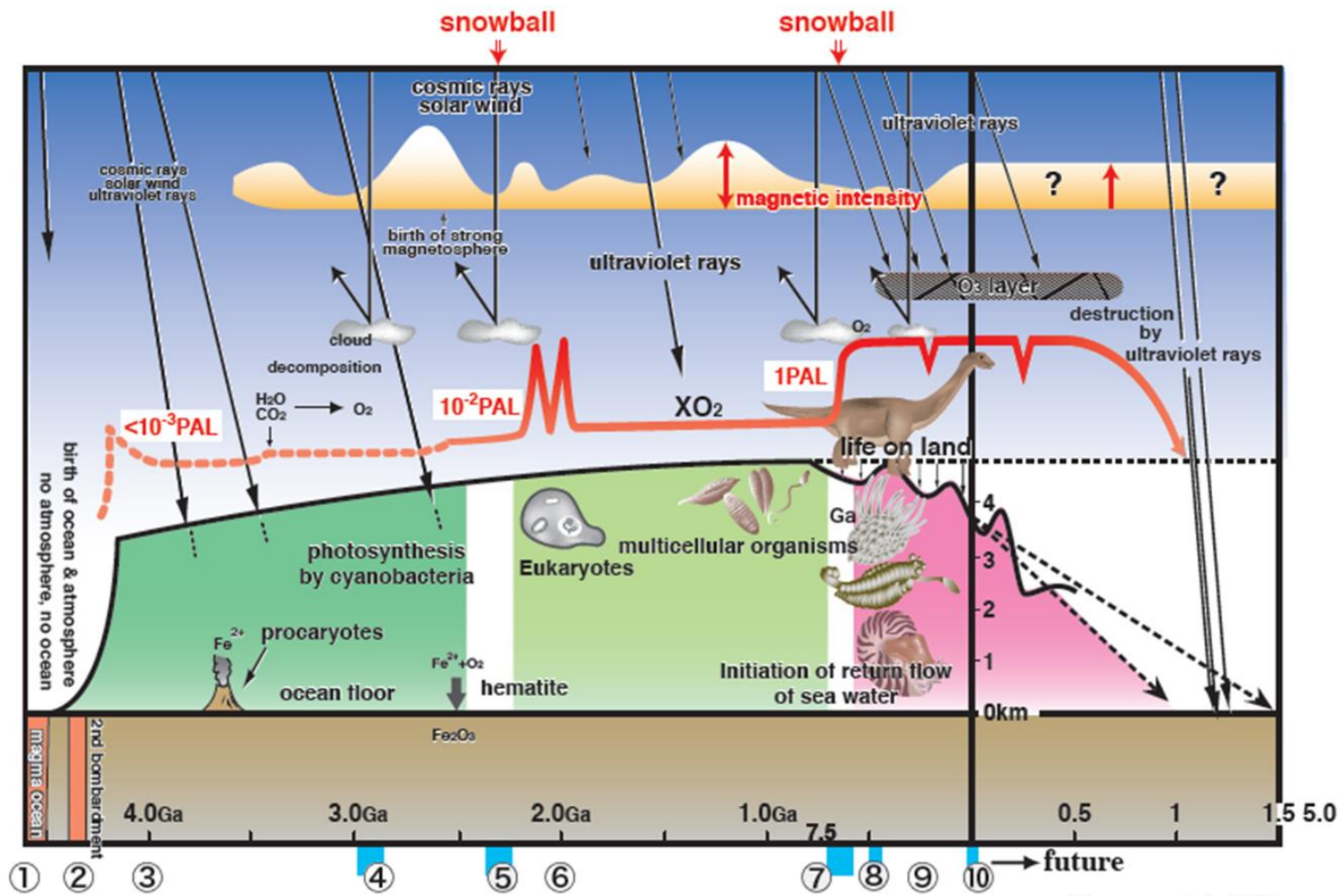

Maruyama et al., 2013

A way to establish Astrobiology

Planet	1st group (1)	1st group (2)	2nd group	3rd group	4th group (future)
Mercury	×	×	×	×	×
Venus	×	×	×	×	×
Earth	○	○	○	○	○
Moon	×	×	×	×	×
Mars	○	△	×	×	×
Satellites of Jupiter and Saturn	△	×	×	×	×
Europa	○	×	×	×	×
Ganymede	○	×	×	×	×
Titan	△	×	×	×	×
Uranus	○	×	×	×	×
Neptune	○	×	×	×	×

水の循環と海水の逆流

	冥王代	太古代	原生代末期	顕生代
表層の水の量	100	100	97	83
マントル内に取込まれた海水の量	0	0	3	17

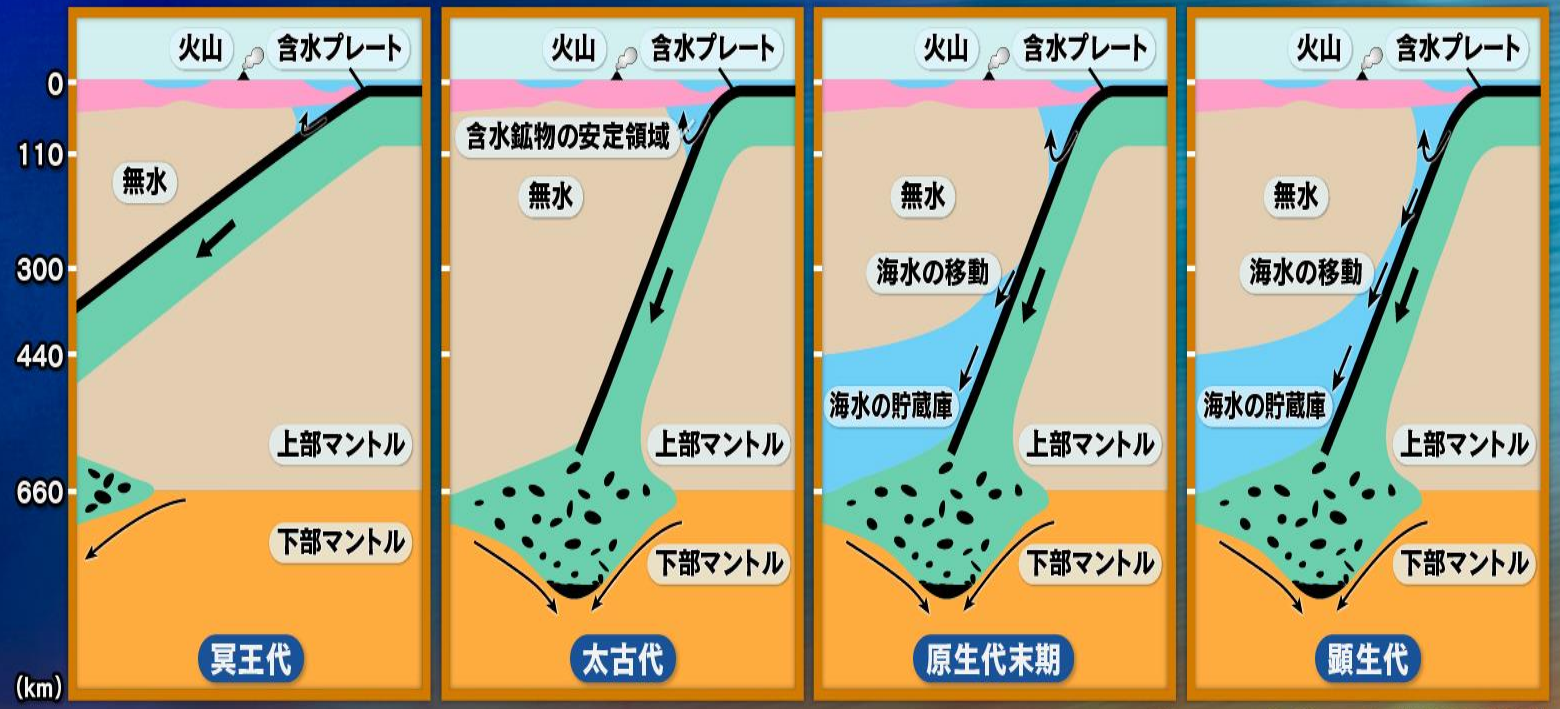

Maruyama & Okamoto (1998, 2001)

② プレートの厚さ、海洋地殻の厚さが分かる

太古代

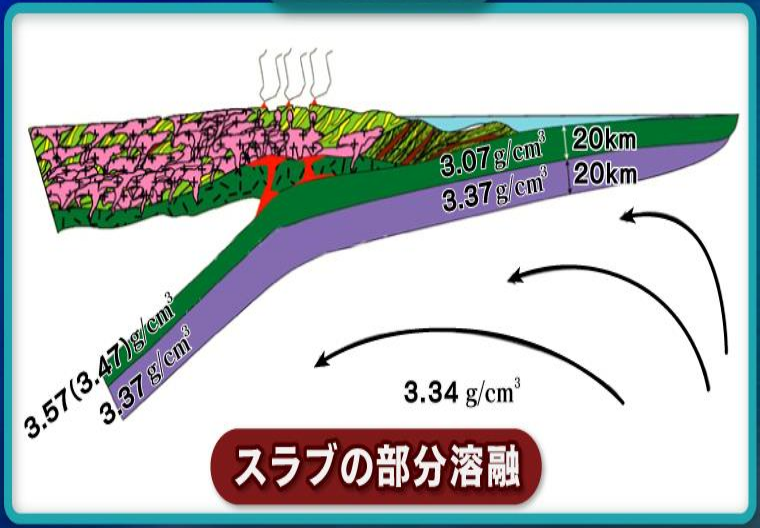

顕生代

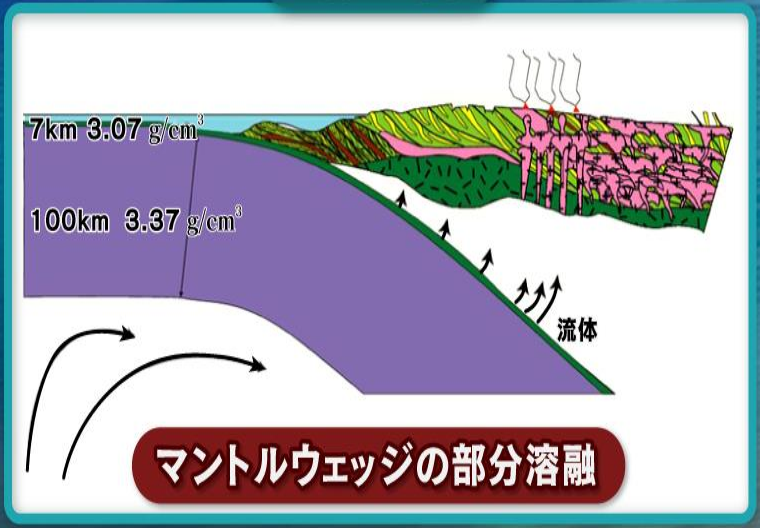

堆積岩ができた時代と量の変化

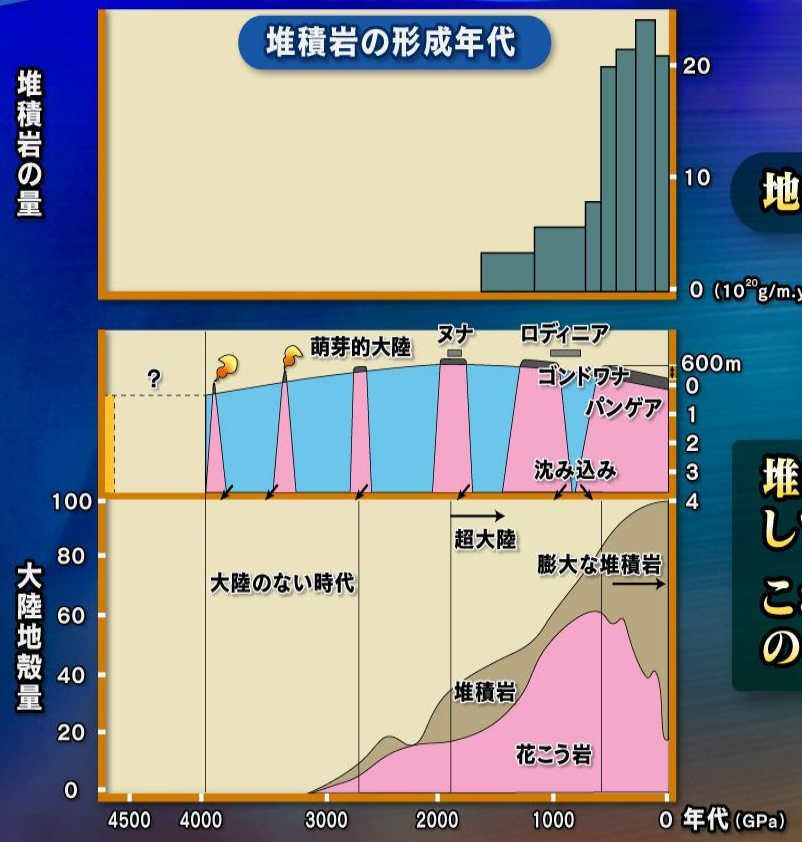

地球地質図から計算して求める

Ronov et al (1991)

堆積岩の形成年代は、時代に依存して大きく変化したことを示す。

これは酸素濃度の変化の歴史と正の対応関係を示す

Maruyama et al., 2013

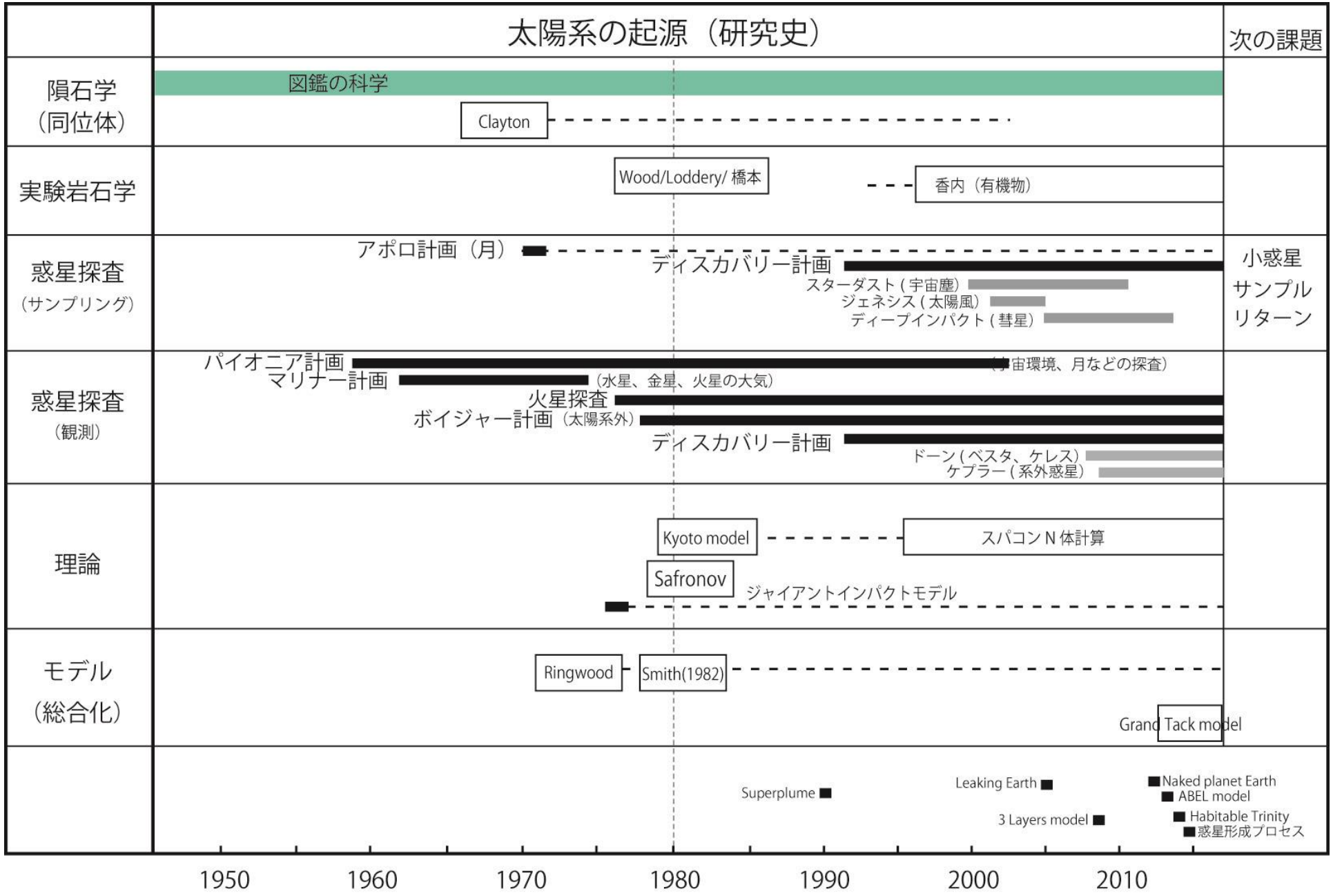
太陽系の起源（研究史）
次の課題
隕石学
（同位体）
図鑑の科学
Clayton
実験岩石学
Wood/Loddery/ 橋本
香内（有機物）
惑星探査
（サンプリング）
アポロ計画（月）
ディスカバリー計画
スターダスト（宇宙塵）
ジェネシス（太陽風）
ディープインパクト（彗星）
小惑星
サンプル
リターン
惑星探査
（観測）
パイオニア計画
（宇宙環境、月などの探査）
マリナー計画
（水星、金星、火星の大気）
火星探査
ボイジャー計画（太陽系外）
ディスカバリー計画
ドーン（ベスタ、ケレス）
ケプラー（系外惑星）
理論
Kyoto model
スパコン N 体計算
Safronov
ジャイアントインパクトモデル
モデル
（総合化）
Ringwood
Smith(1982)
Grand Tack model
Superplume
Leaking Earth
3 Layers model
Naked planet Earth
ABEL model
Habitable Trinity
惑星形成プロセス
1950
1960
1970
1980
1990
2000
2010

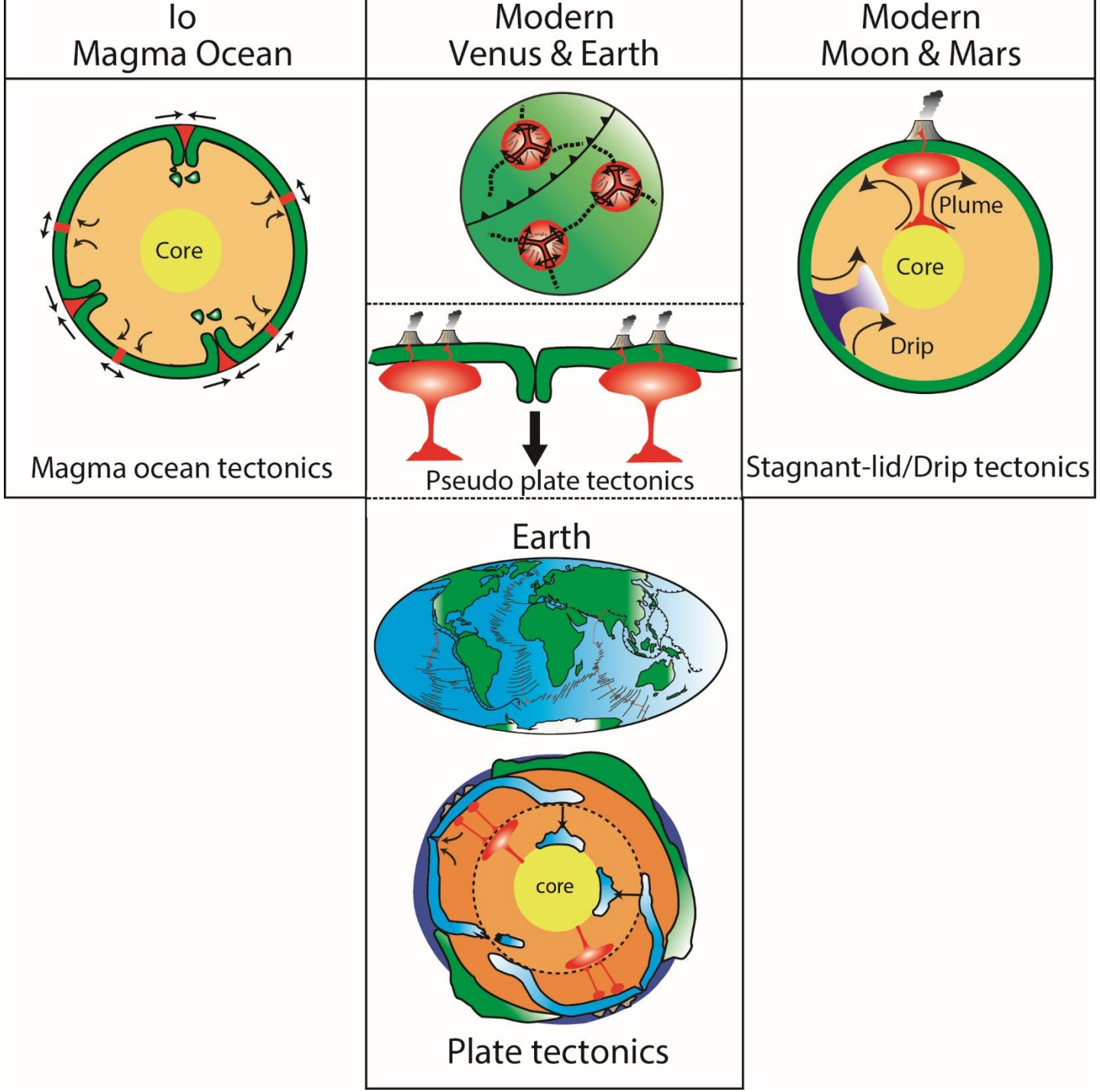
Io
Magma Ocean
Modern
Venus & Earth
Modern
Moon & Mars
Core
Magma ocean tectonics
Pseudo plate tectonics
Plume
Core
Drip
Stagnant-lid/Drip tectonics
Earth
core
Plate tectonics

Sparrow (2012) The Universe, Quercus Editions Ltd.

火星の歴史

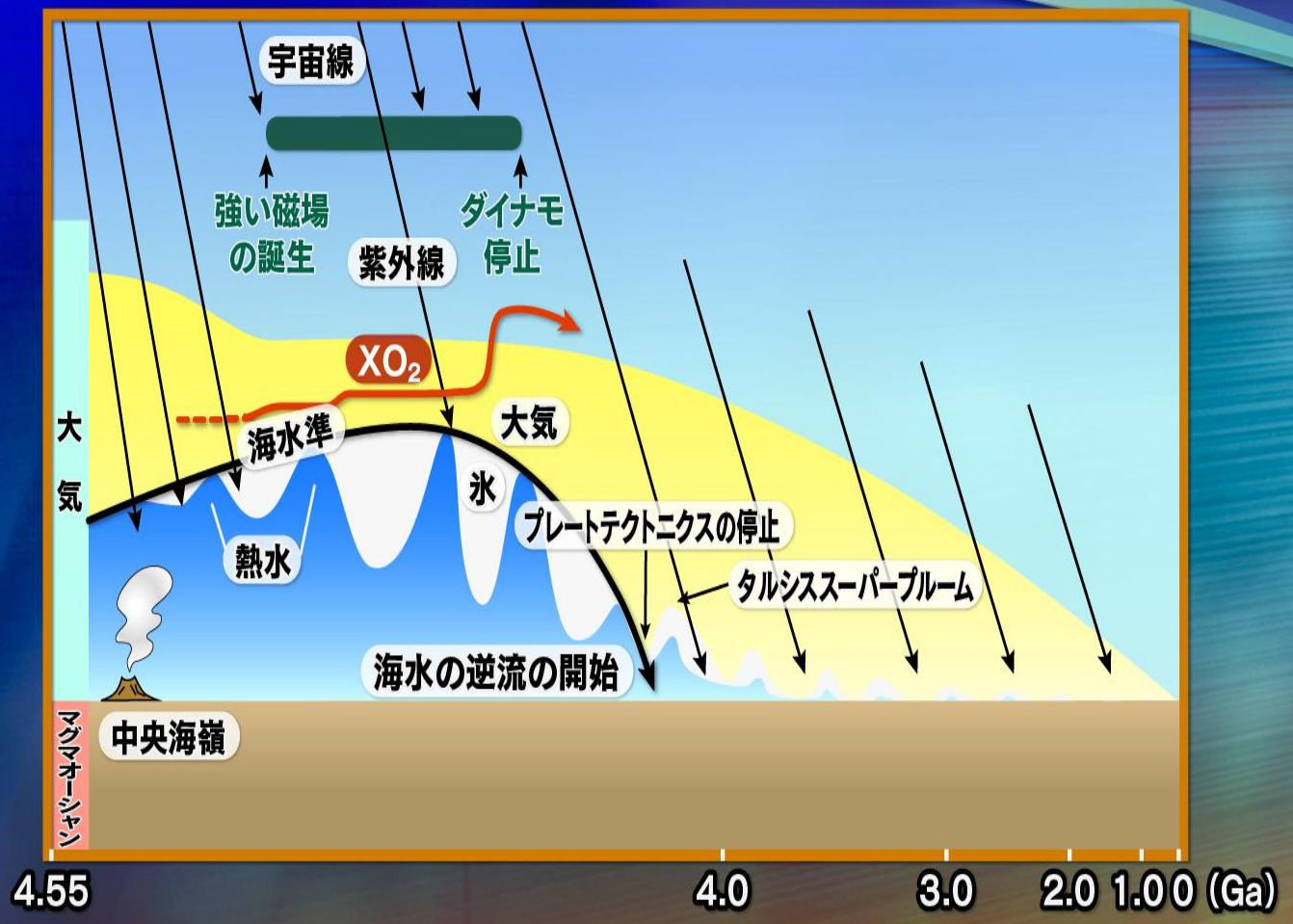
宇宙線
強い磁場の誕生
紫外線
ダイナモ停止
XO_2
大気
海水準
大気
氷
熱水
プレートテクトニクスの停止
タルシススーパープルーム
海水の逆流の開始
マグマオーシャン
中央海嶺
4.55
4.0
3.0
2.0
1.0
0 (Ga)

Paleogeography of the Earth since 4.567Ga

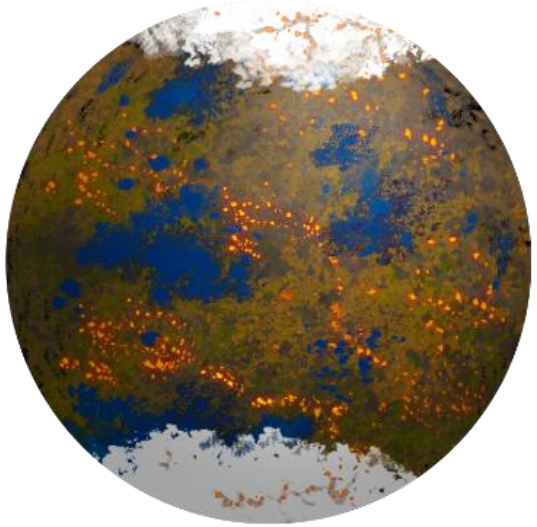

Fig: If another earth was created in asteroid belt

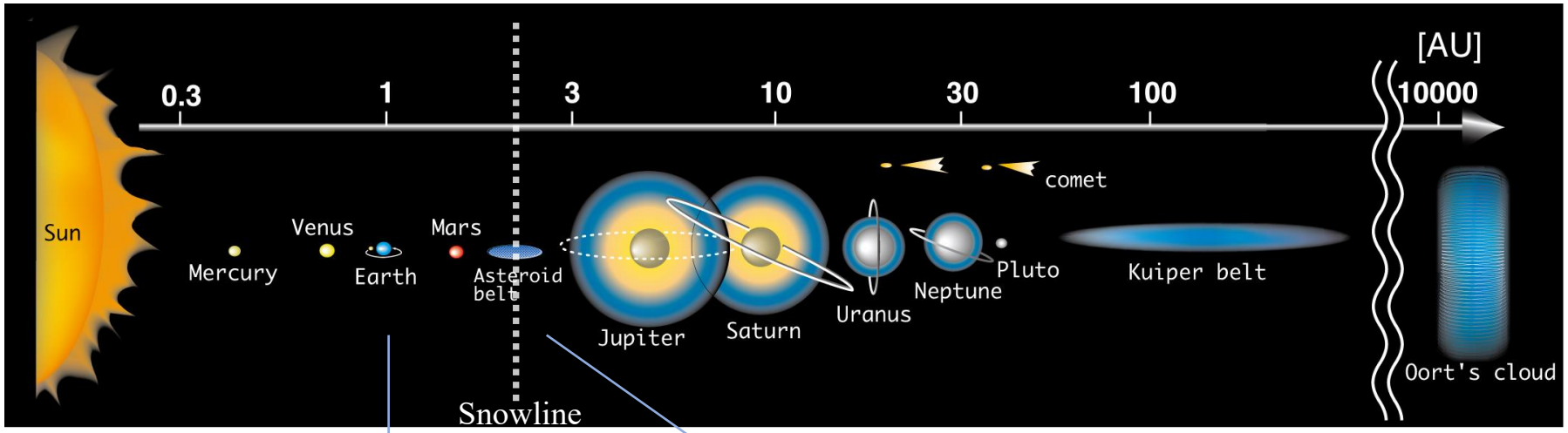

Maruyama et al., 2013

Earth

Dry and naked planet earth

Another Earth

Ocean: 400km thick

Made from $3H_2O$% chondrite

陸地がない→生命の誕生も進化もない

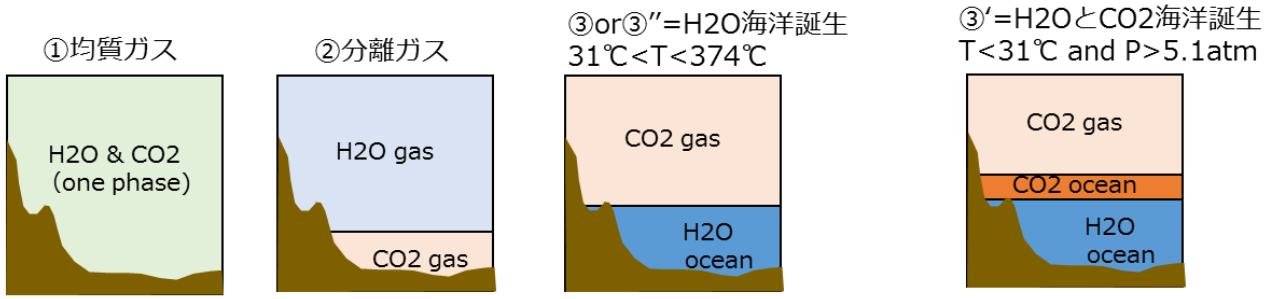

注意点：大気と岩石の反応はないものと仮定する

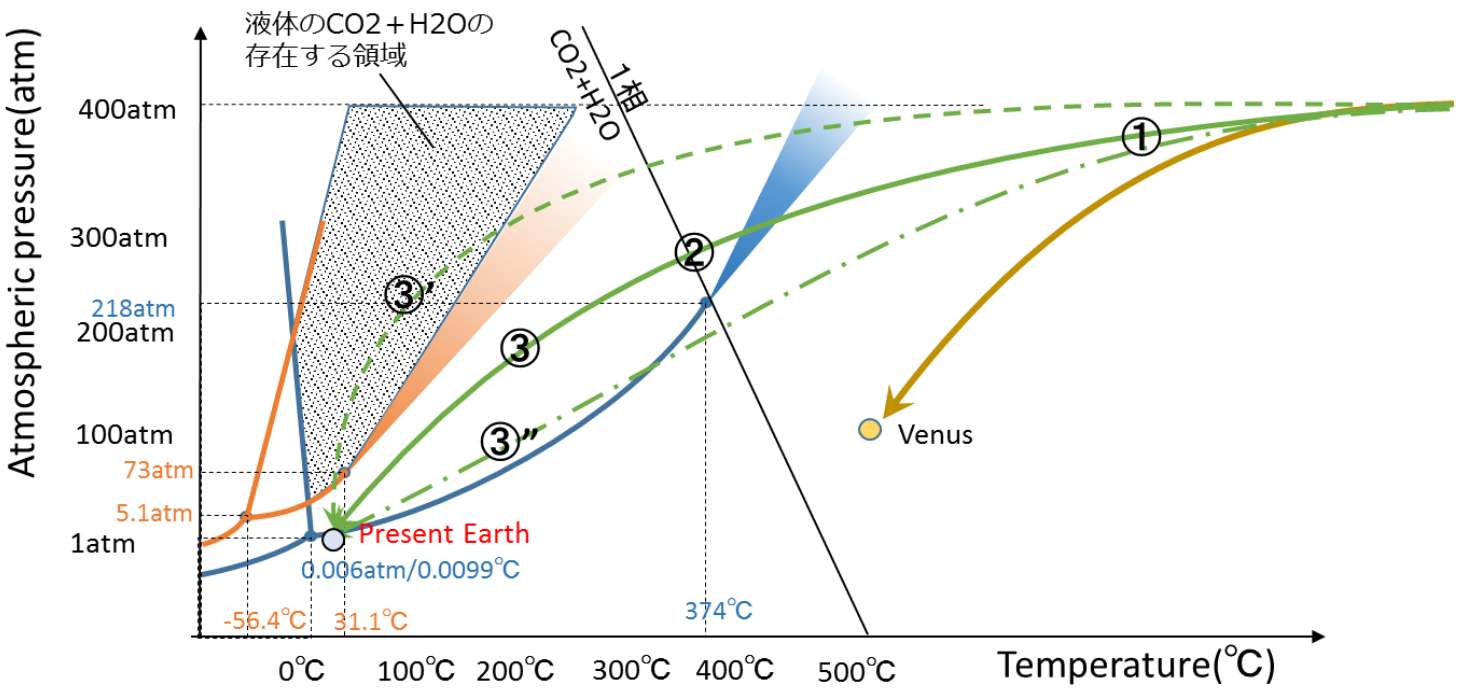

丸山、林、橋本、戎崎、2015

History of Venus and Earth

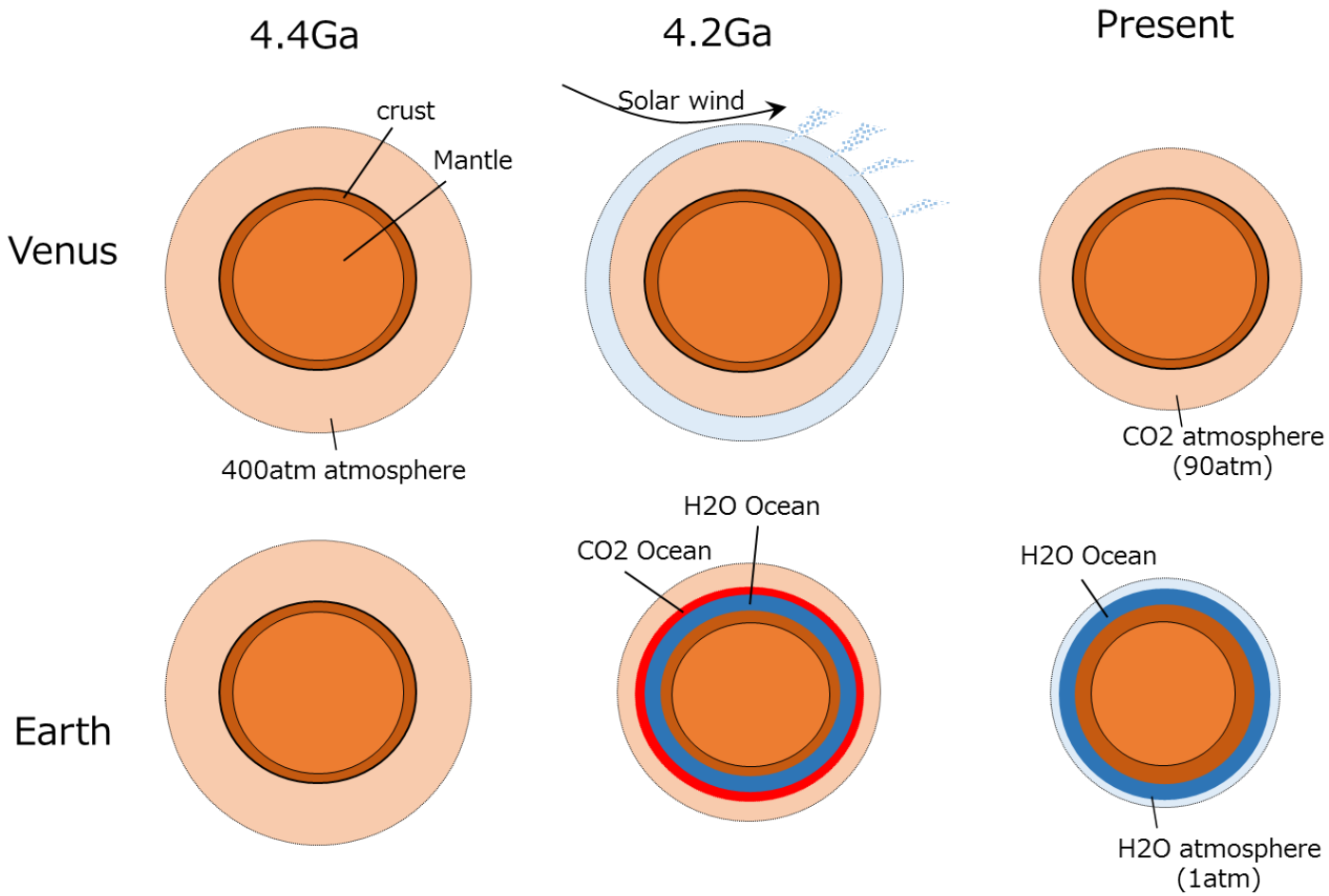

丸山、林、橋本、戎崎、2015

CO_2 circulation

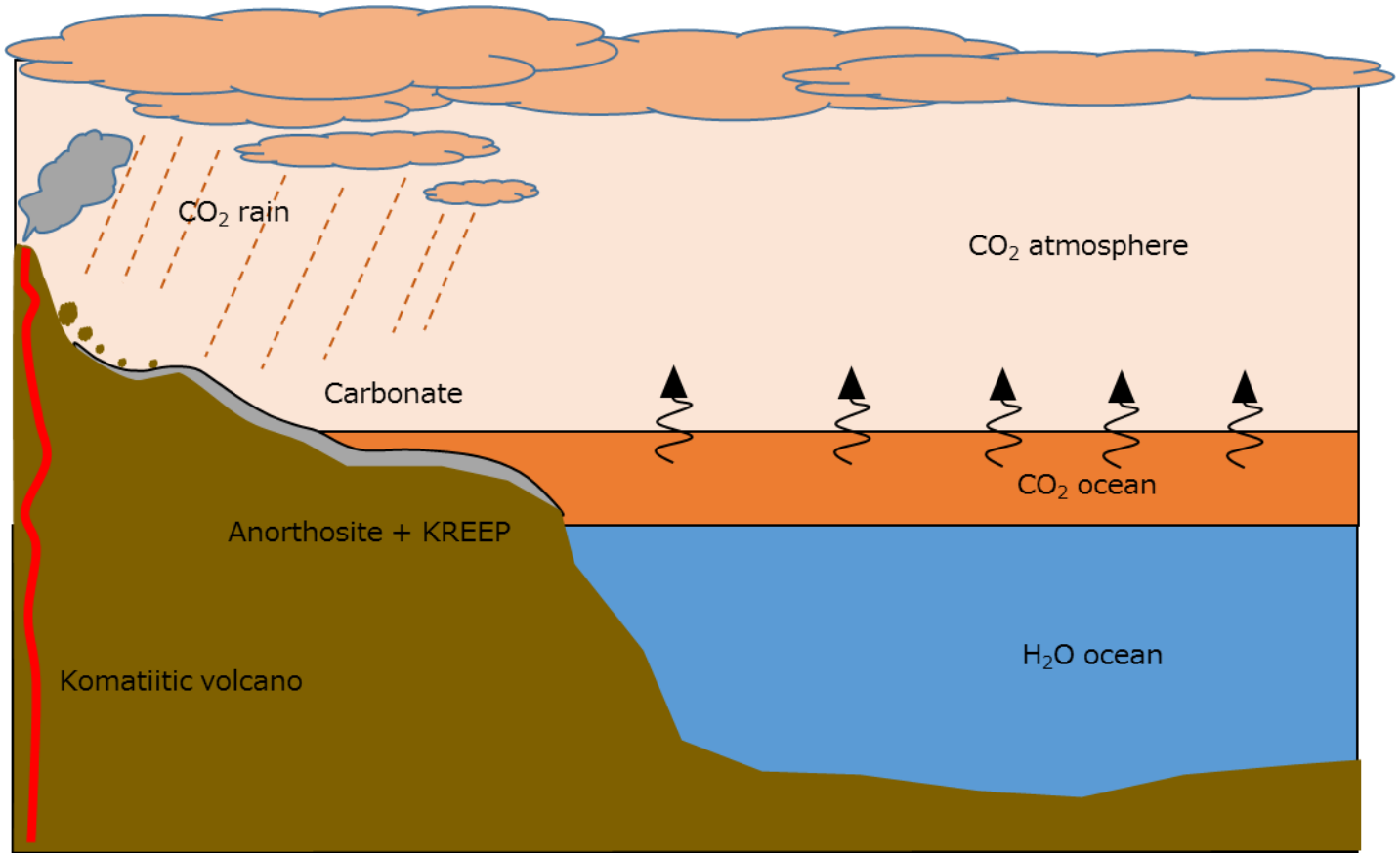

丸山、林、橋本、戎崎、2015

Towards the establishment of Astrobiology

→ Universal Formation Model of Habitable Trinity Planets

1st Step:
Bulk chemical composition of
Solar Rocky Planets
（中心星からの距離の関数＝
密度曲線）

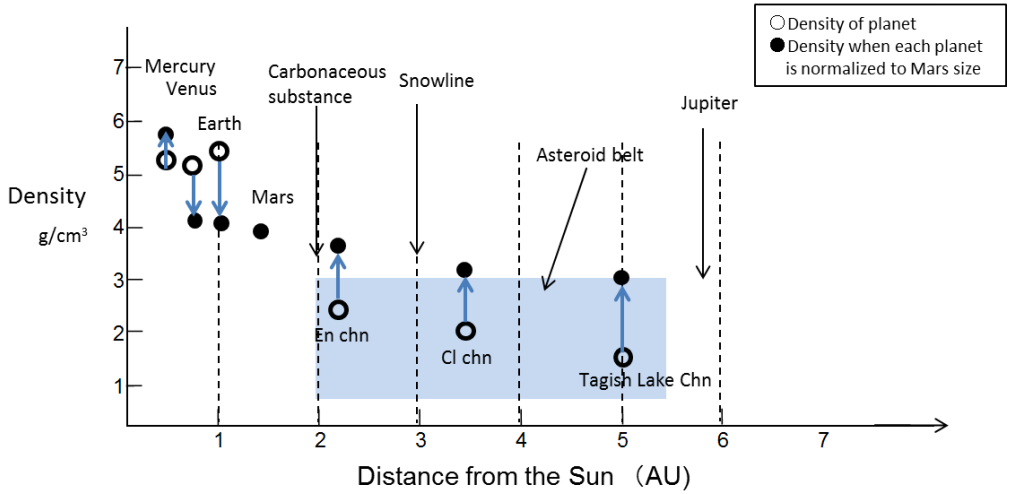

2nd Step:
Bulk chemical composition of
Universal Rocky Planets
determined as a function of
Central Star (chemistry and size)
and distance (from CS)（中心星の
組成とサイズで密度曲線が変化）

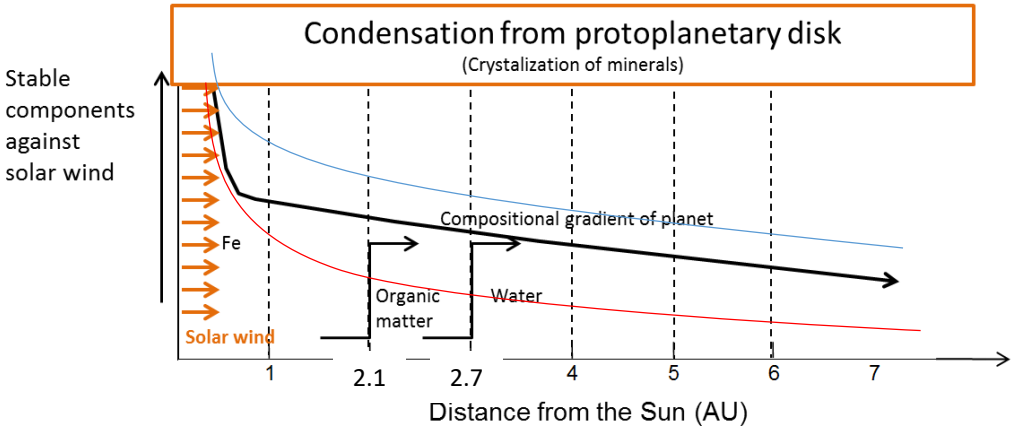

3rd Step:
The birth and evolution of
Habitable Trinity Planet
are determined by
internal dynamics of solid planet
惑星内部の初期進化でHTPへ

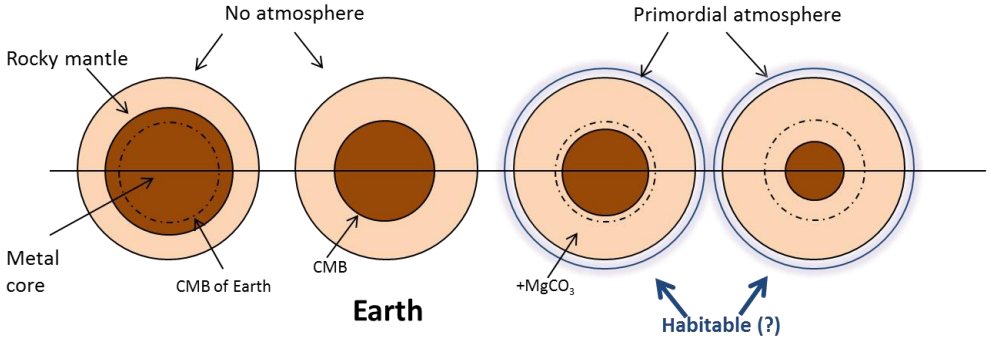

プレートテクトニクスの原理

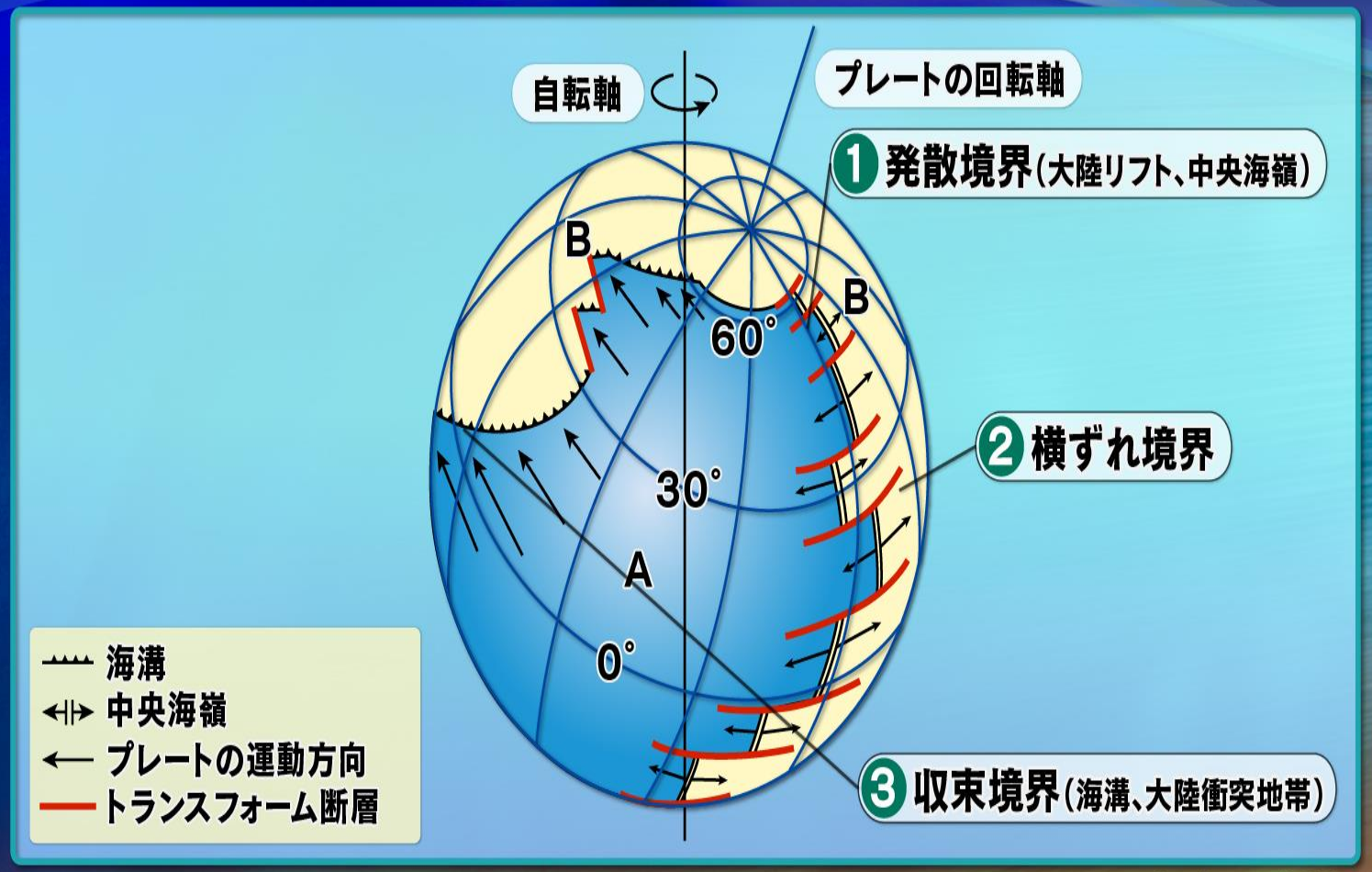

上田（1989）を修正

大陸分裂と表層環境変動の概要図

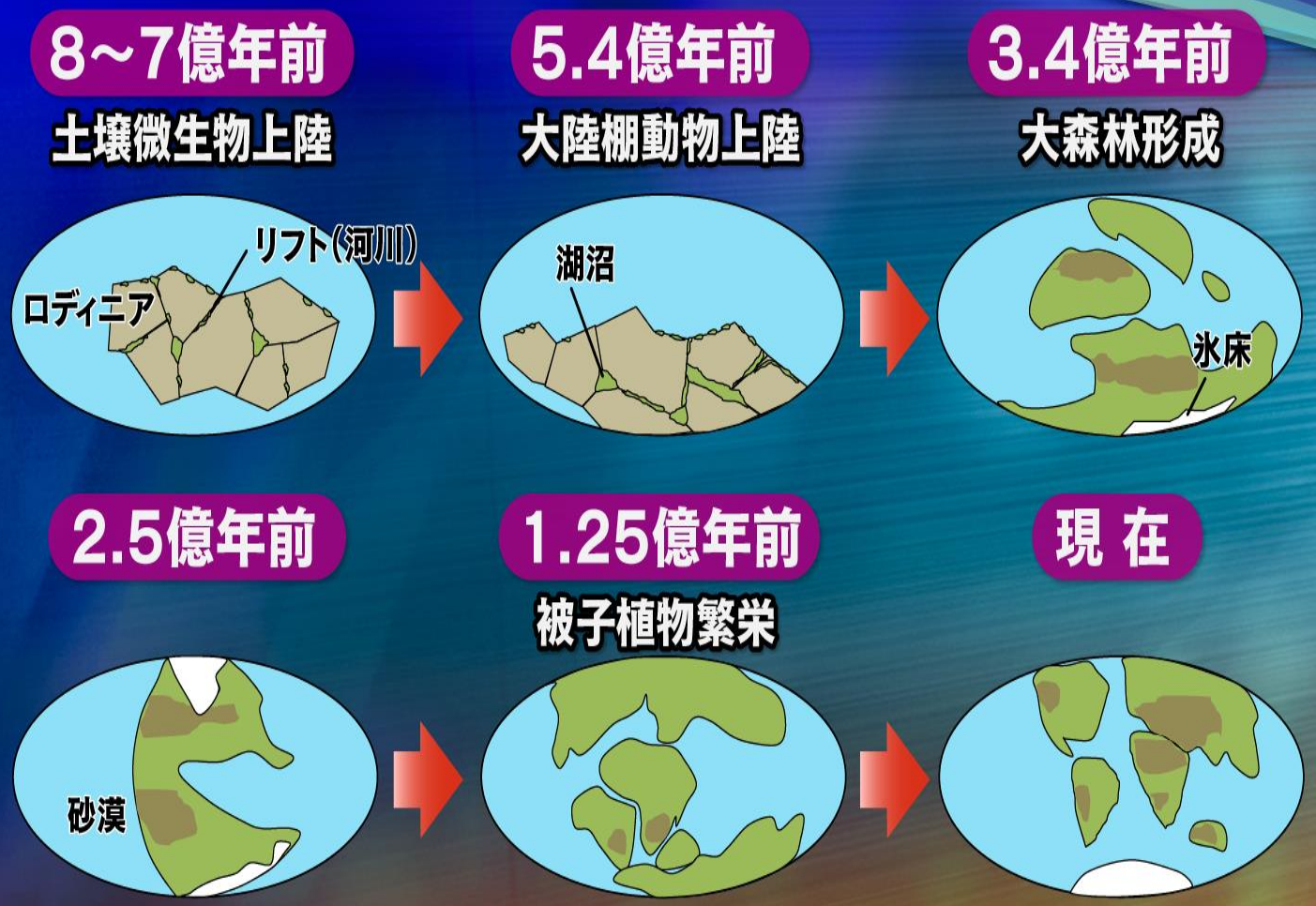

001 Ma

最近の寒冷化ピーク

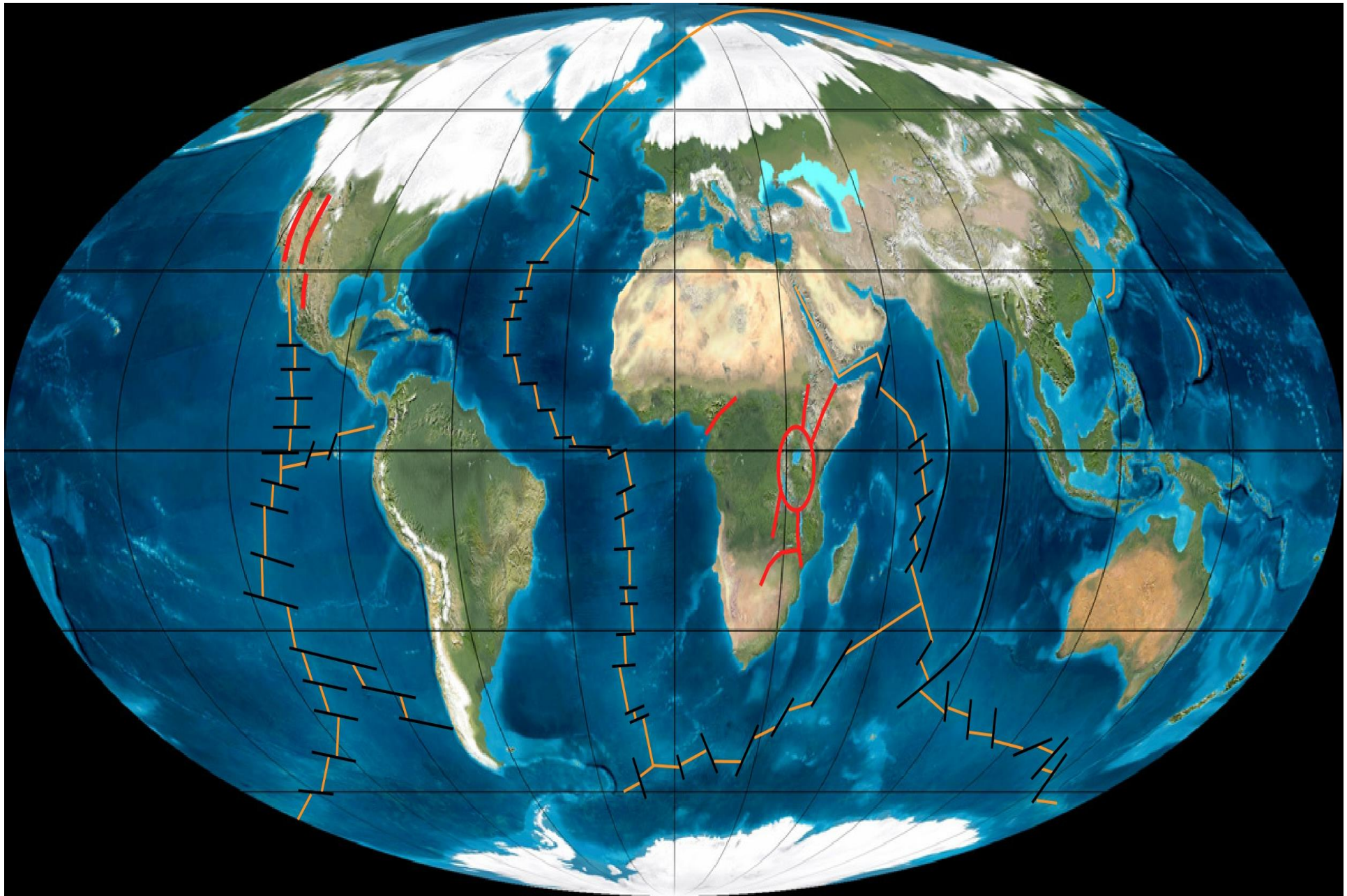

惑星サイズ-bimodal地殻形成-水の総量

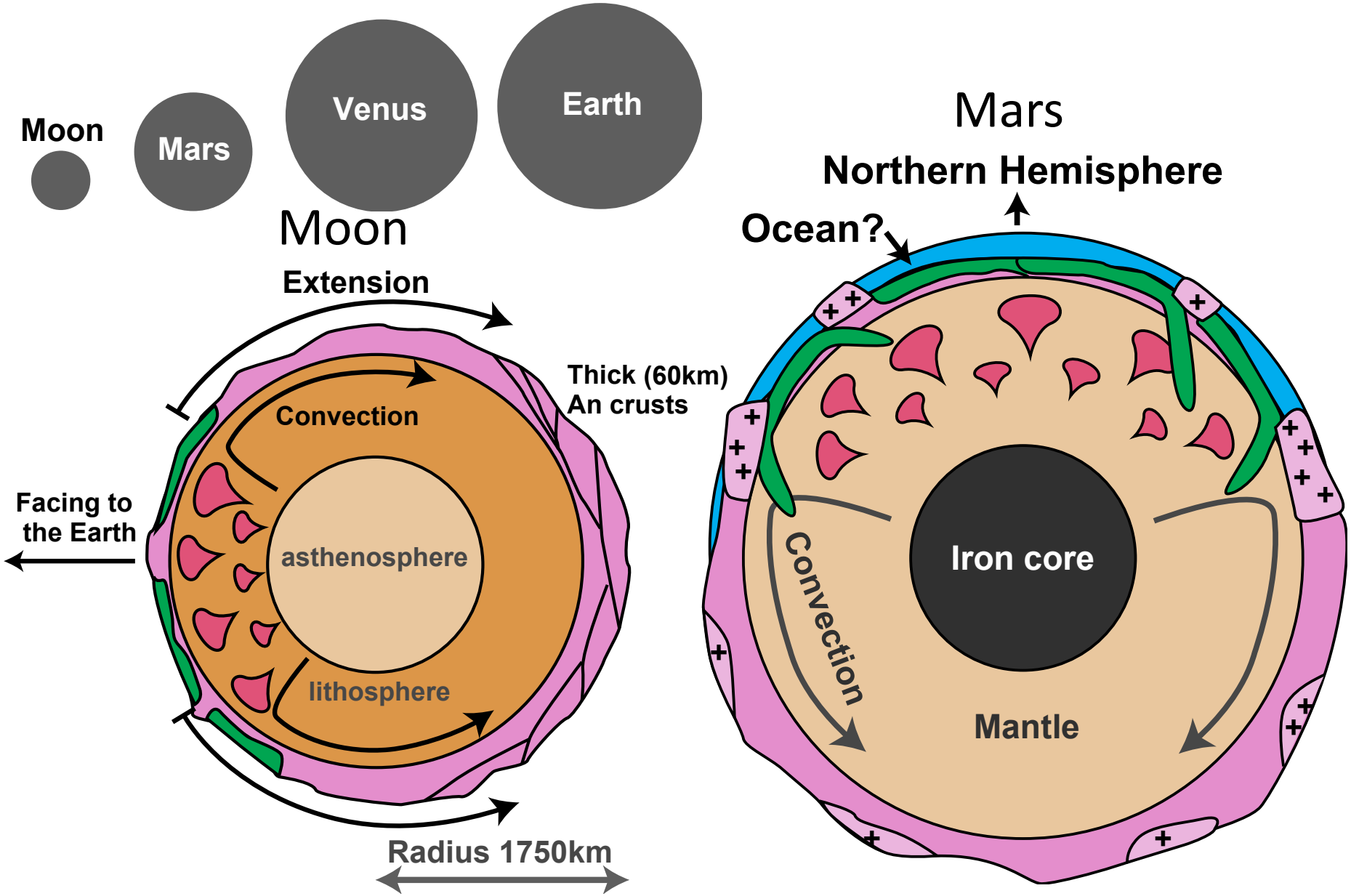

アノーソサイト岩体の浮上

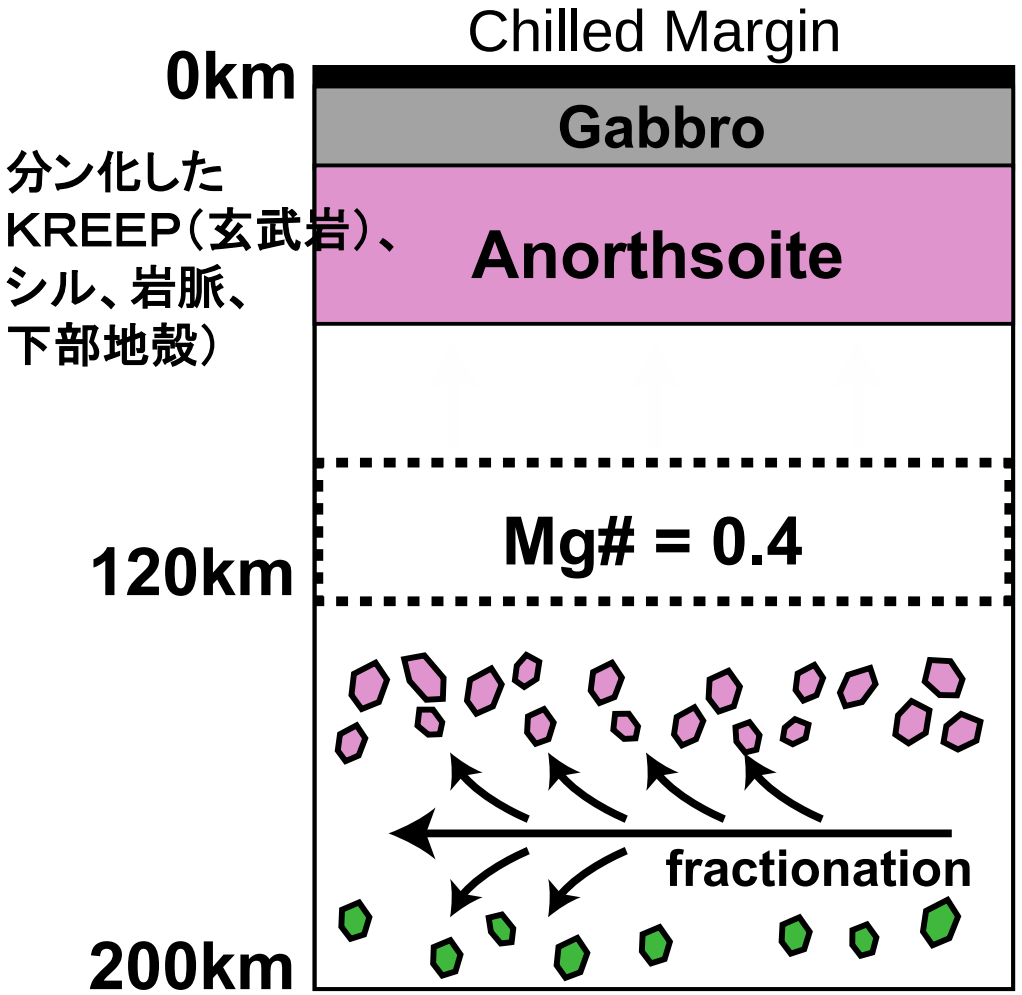

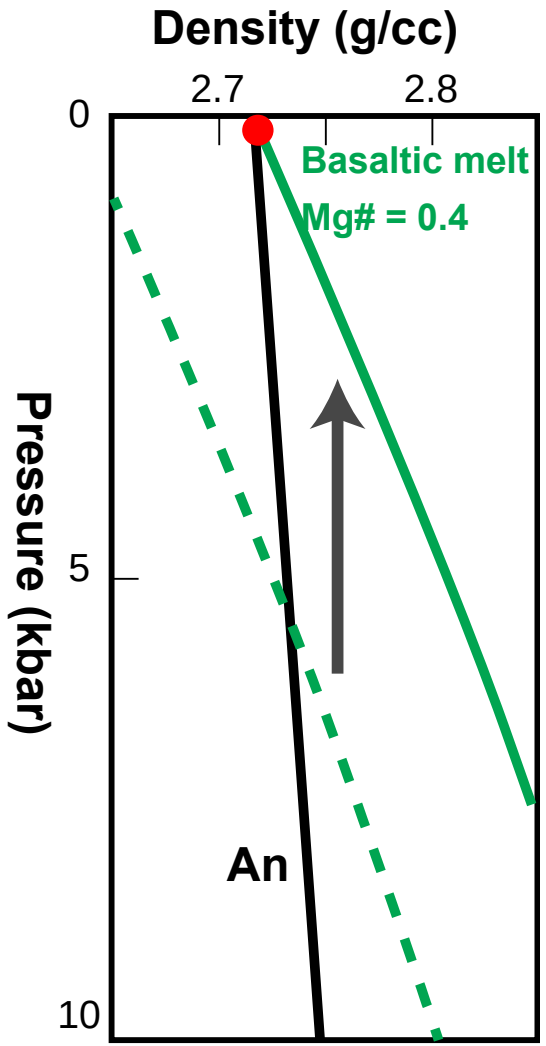

新井(修論)

メルトがFe-richになり、密度大きくなる。密度逆転層が上昇。
月の地質記録から検証する必要がある。

Tectonics

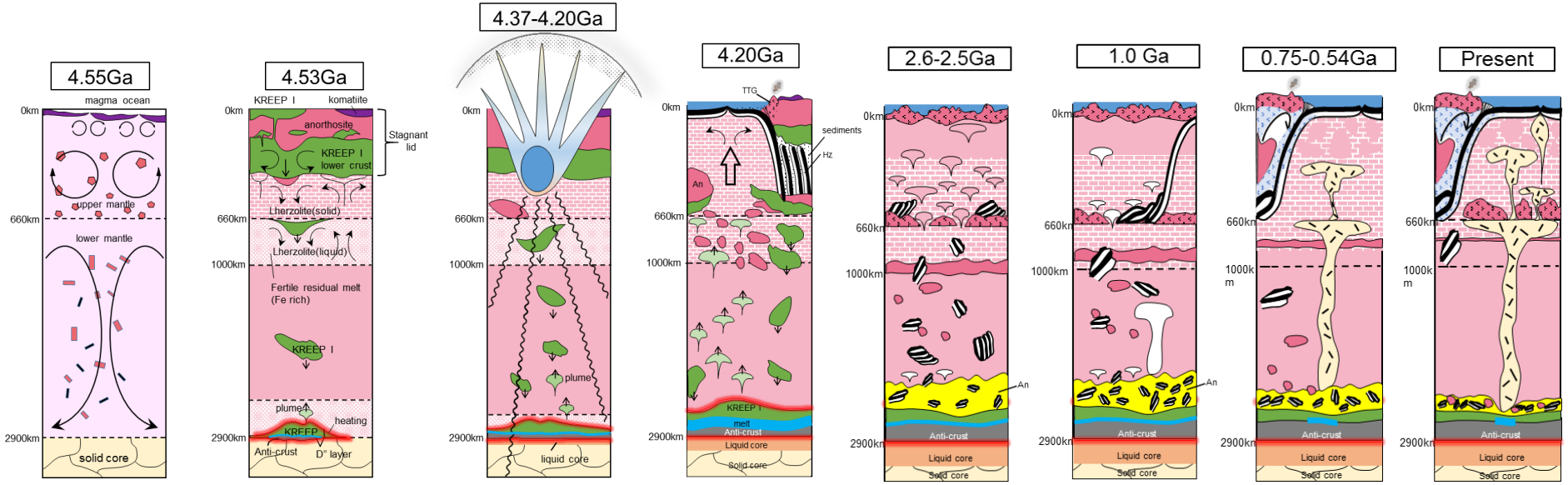

Magma ocean

Stagnant lid tectonics

ABEL Bombardment

Plate tectonics

Mantle overturn

Plate tectonics + superplume

Plate tectonics + superplume

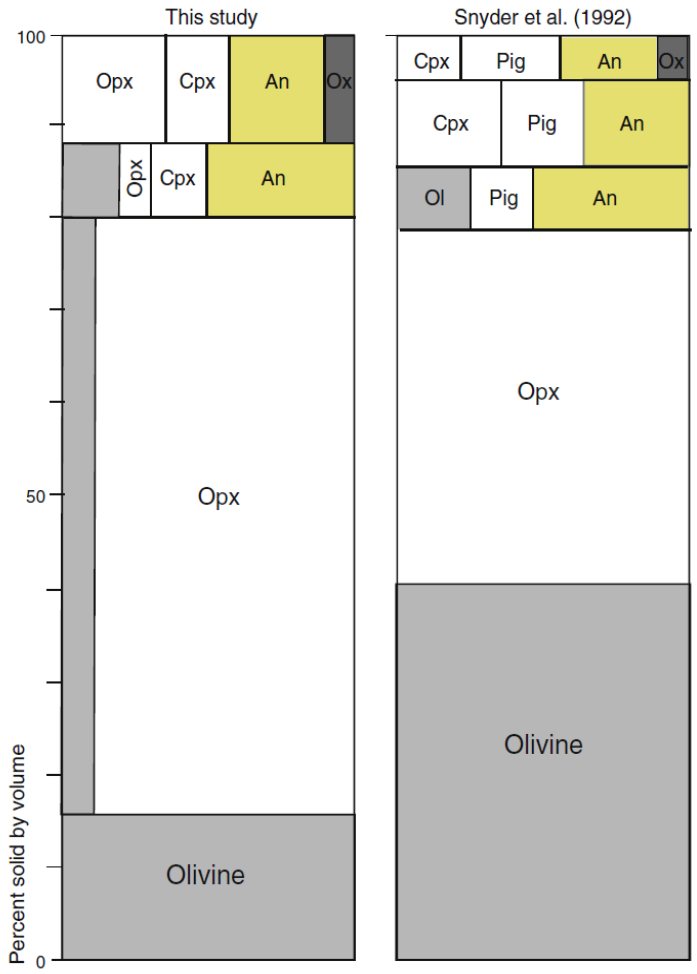

Fig. 2. Cumulate stratigraphy. Solidifying mantle mineral assemblages used in this paper (left) and by (Snyder et al., 1992) (right). Opx = orthopyroxene; Cpx = clinopyroxene; Pig = pigeonite; Ox = oxides, including ilmentite, as described in the text; An = anorthite feldspar (plagioclase). Width of mineral boxes indicates fraction in well-mixed phase assemblage. Note that when anorthite crystallizes it is assumed to float while other phases sink. This figure does not, therefore, represent the depth at which the minerals reside after solidification, just the ranges in solidification over which they are assumed to form. Models assumed different initial depths.

Elkins-Tanton (2011)

mantle

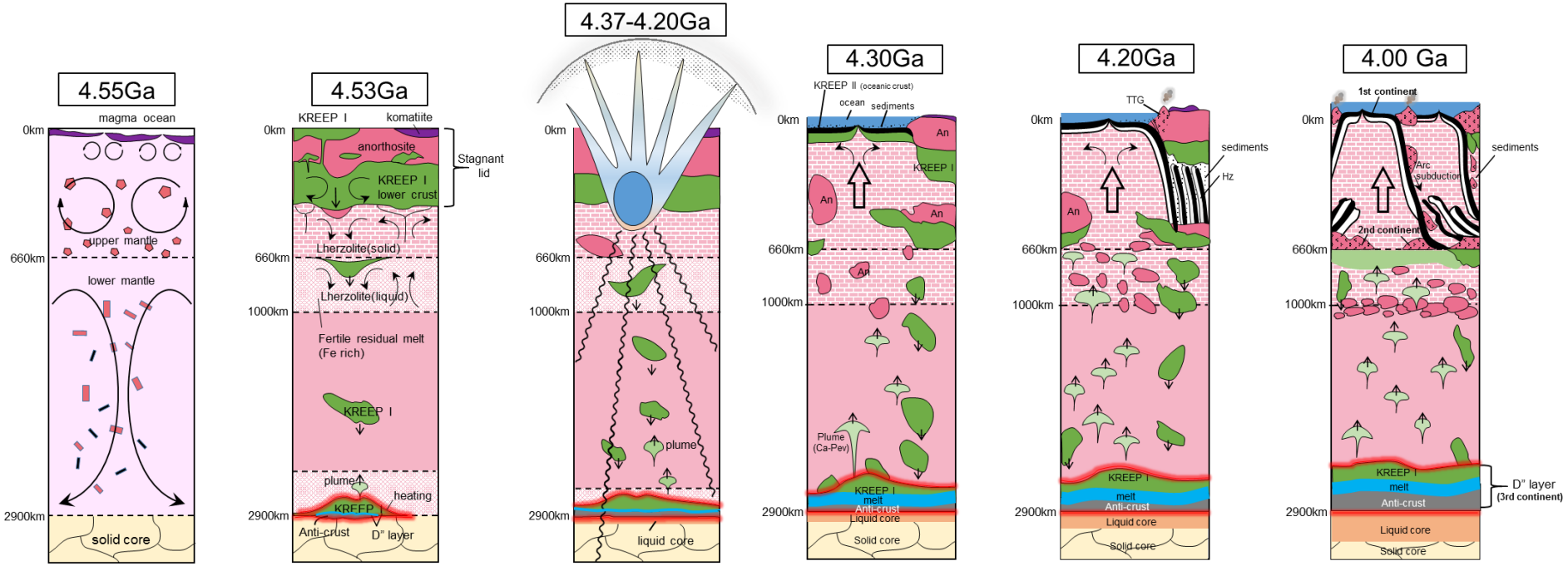
4.55Ga
magma ocean
0km
upper mantle
660km
lower mantle
2900km
solid core
4.53Ga
KREEP I
komatiite
0km
anorthosite
Stagnant lid
KREEP I lower crust
Lherzolite(solid)
660km
Lherzolite(liquid)
1000km
Fertile residual melt (Fe rich)
KREEP I
plume
heating
2900km
KREEP I
Anti-crust
D" layer
4.37-4.20Ga
0km
660km
1000km
plume
2900km
liquid core
4.30Ga
KREEP II (oceanic crust)
ocean
sediments
0km
An
KREEP I
660km
1000km
Plume (Ca-Pev)
KREEP I
melt
Anti-crust
Liquid core
2900km
Solid core
4.20Ga
TTG
0km
sediments
Hz
660km
1000km
KREEP I
melt
Anti-crust
Liquid core
2900km
Solid core
4.00 Ga
1st continent
0km
sediments
Arc subduction
2nd continent
660km
1000km
KREEP I
melt
Anti-crust
D" layer
(3rd continent)
Liquid core
2900km
Solid core

Tectonics

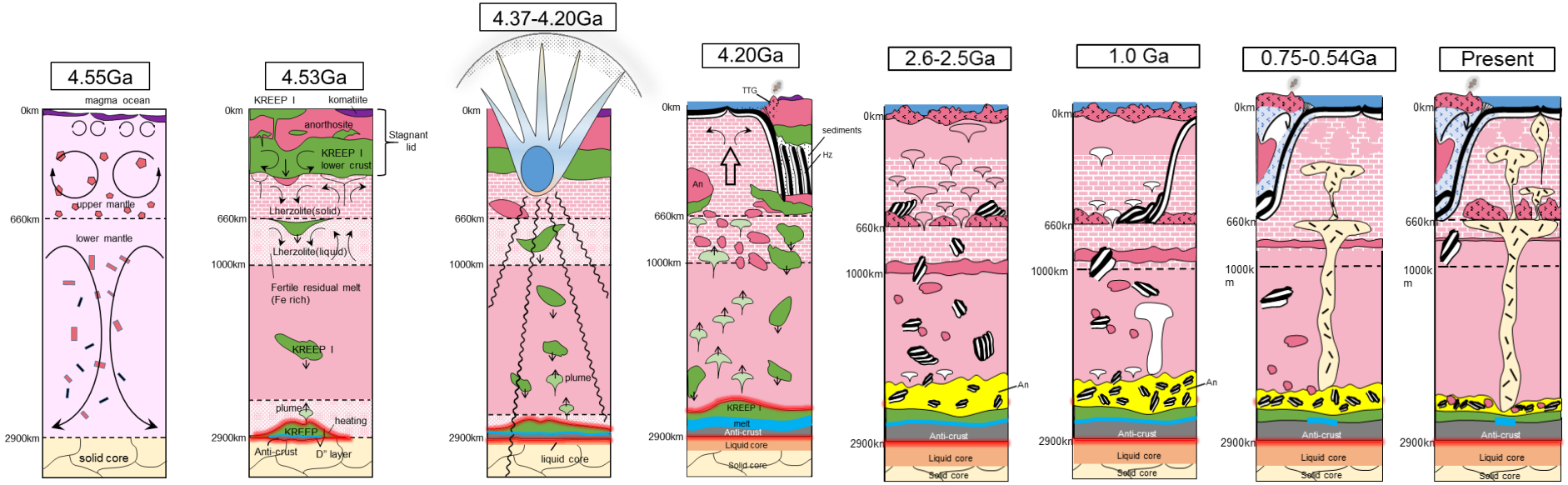

Magma ocean

Stagnant lid tectonics

ABEL Bombardment

Plate tectonics

Mantle overturn

Plate tectonics + superplume

Plate tectonics + superplume

3.8-3.7Ga

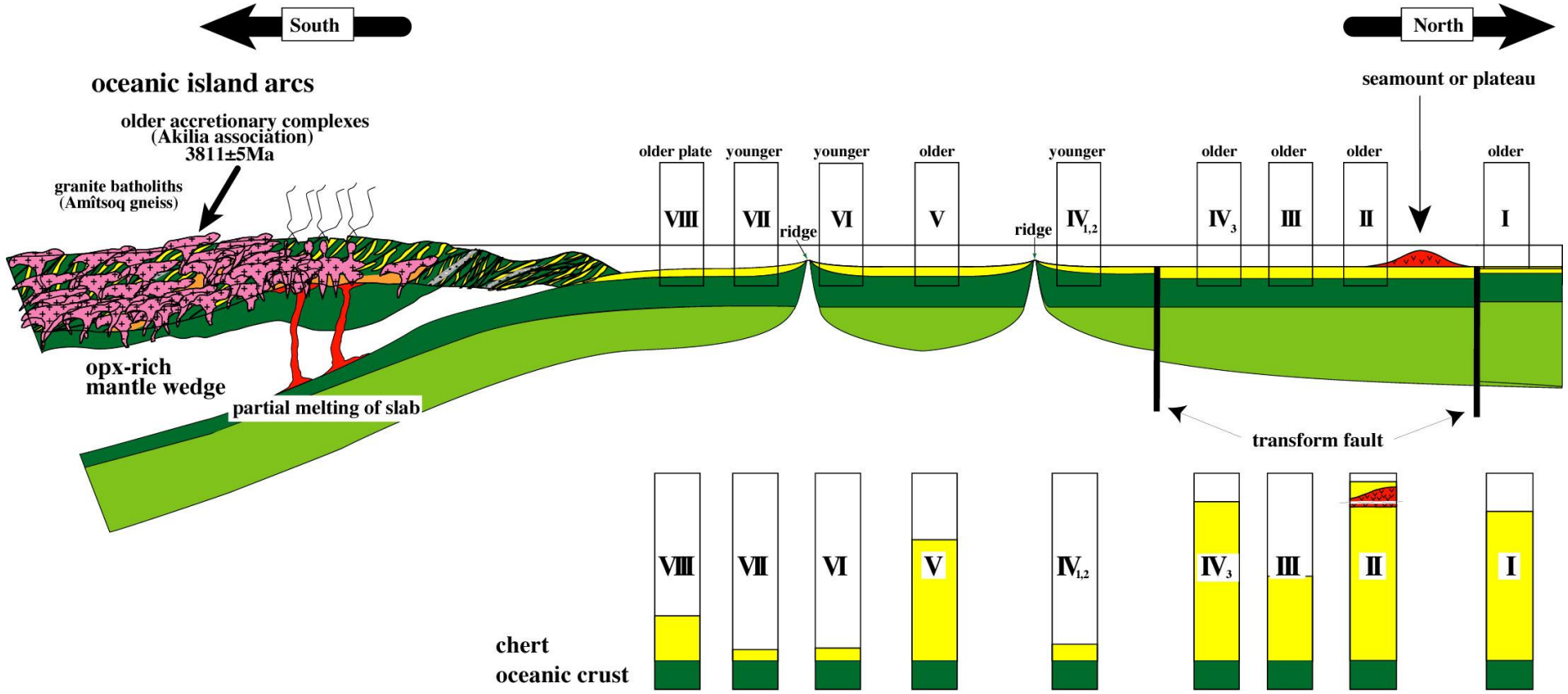
South
North
oceanic island arcs
older accretionary complexes
(Akilia association)
3811±5Ma
granite batholiths
(Amîtsoq gneiss)
opx-rich
mantle wedge
partial melting of slab
seamount or plateau
older plate
younger
younger
older
younger
older
older
older
older
VIII
VII
ridge
VI
V
ridge
IV1,2
IV3
III
II
I
transform fault
VIII
VII
VI
V
IV1,2
IV3
III
II
I
chert
oceanic crust

カンブリア紀の概観

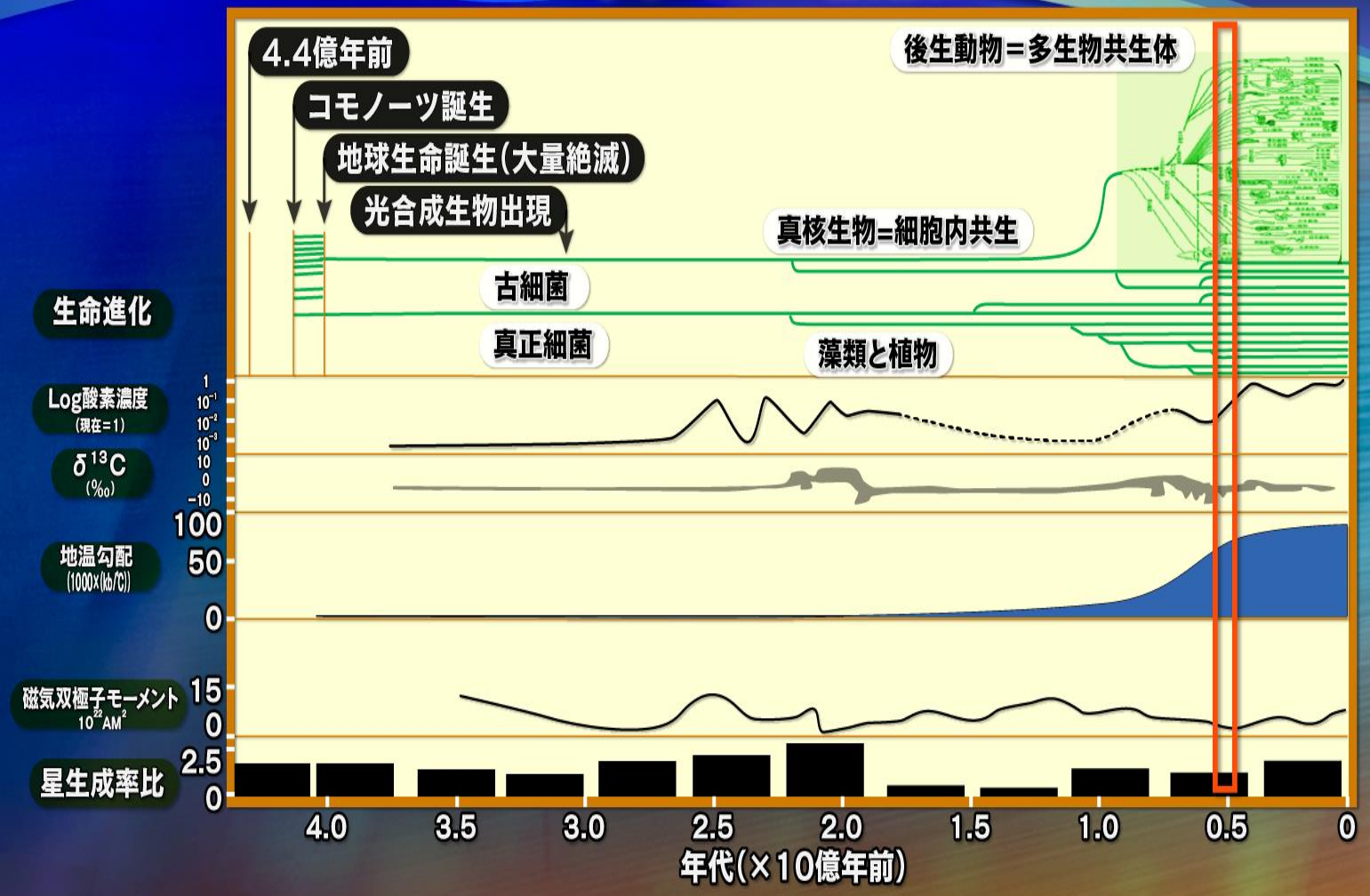
4.4億年前
コモノーツ誕生
地球生命誕生(大量絶滅)
光合成生物出現
後生動物=多生物共生体
真核生物=細胞内共生
古細菌
真正細菌
藻類と植物
生命進化
Log酸素濃度
(現在=1)
1
10^{-1}
10^{-2}
10^{-3}
$\delta^{13}C$
(‰)
10
0
-10
地温勾配
(1000×(kb/℃))
100
50
0
磁気双極子モーメント
$10^{22}AM^2$
15
0
星生成率比
2.5
0
4.0
3.5
3.0
2.5
2.0
1.5
1.0
0.5
0
年代(×10億年前)

原生代の大陸成長と配置

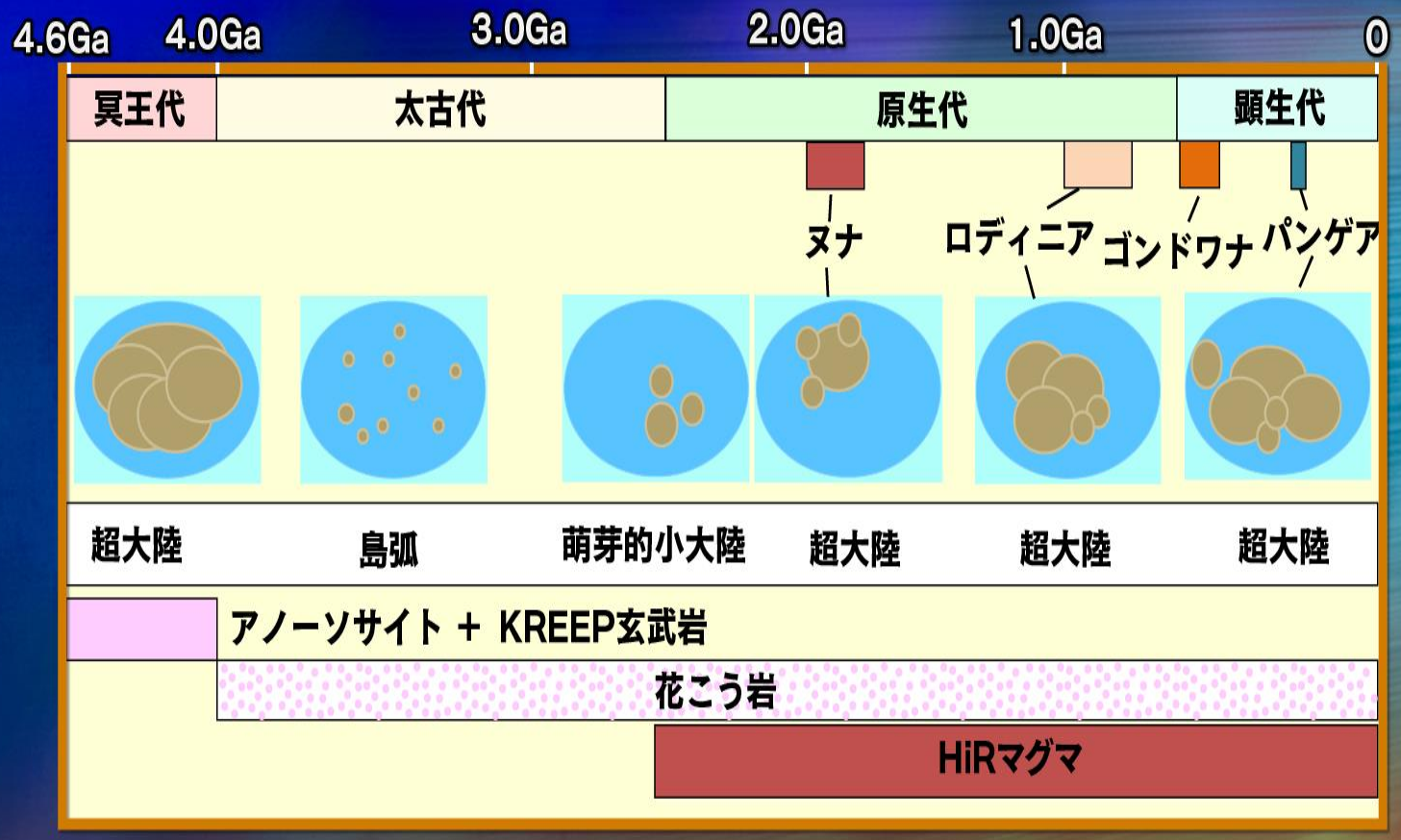

原核細胞と多細胞生物は、生物量で1兆倍の差がある
(log mm³)
O_2 < 0.1% PAL
PAL
O_2 > 100% PAL
原核生物
原生生物
動物(多細胞)
維管束植物
多細胞
100万倍
最大の単細胞生物
最大の原核生物
伊規須素子(2008)
内尾優子(2008)
生物体積
14
12
10
8
6
4
2
0
-2
-4
-6
-8
暁始生代
古始生代
中始生代
新始生代
古原生代
中原生代
新原生代
古生代
始 生 代
原 生 代
顕 生 代
-40
-30
-20
-10
0
億 年
Payne et al (2009)

炭酸塩岩のSr同位体比は過去の大陸の陸地面積を反映する

Shields and Veizer (2002)

① 太古代（35億年） 酸素濃度 < $\frac{1}{1,000}$ PAL

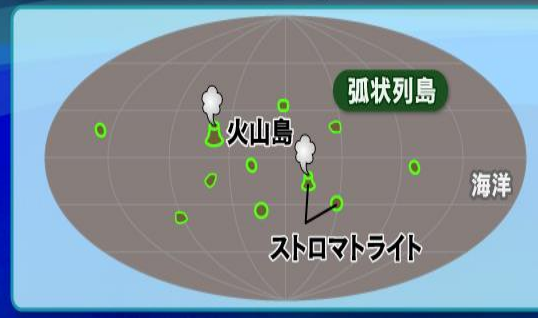

酸素ポンプ

小規模

② 原生代（21億年） 酸素濃度 < $\frac{1}{100}$ PAL

酸素ポンプ

中規模

③ 顕生代（5,4億年） 酸素濃度 < 1 PAL

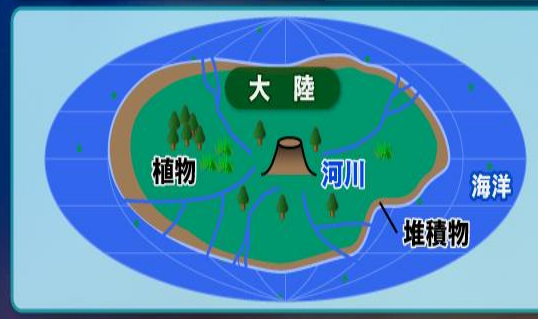

酸素ポンプ

巨大化

同期するのは何故か？

① 堆積岩の量　② 海水のSr同位体比
③ 海水の酸化度　④ 生物のサイズの変化

酸素ポンプの原理

太陽エネルギー

$$CO_2 + H_2O \rightleftarrows CH_2O + O_2$$

シアノバクテリア
（藻類、植物）

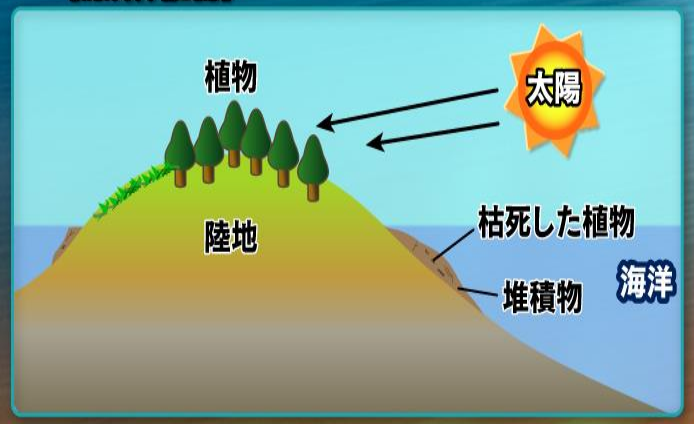

南中国プロジェクト

南中国の原生代末期の地層

- 浅海から深海まで様々な堆積場
- 豊富な化石
- 不整合(地層の欠如)が少ない
- 変質・変成作用を殆ど受けていない

6地域で21本の掘削試料

- 風化の影響が少ない
- 完全連続試料

多元素、多同位体分析

C, O, N, P, Ca, Fe, Mn, Sr, Mo, REE

↓

原生代末期の環境変動を読み解く

掘削試料を細かく分析精度を上げて測定

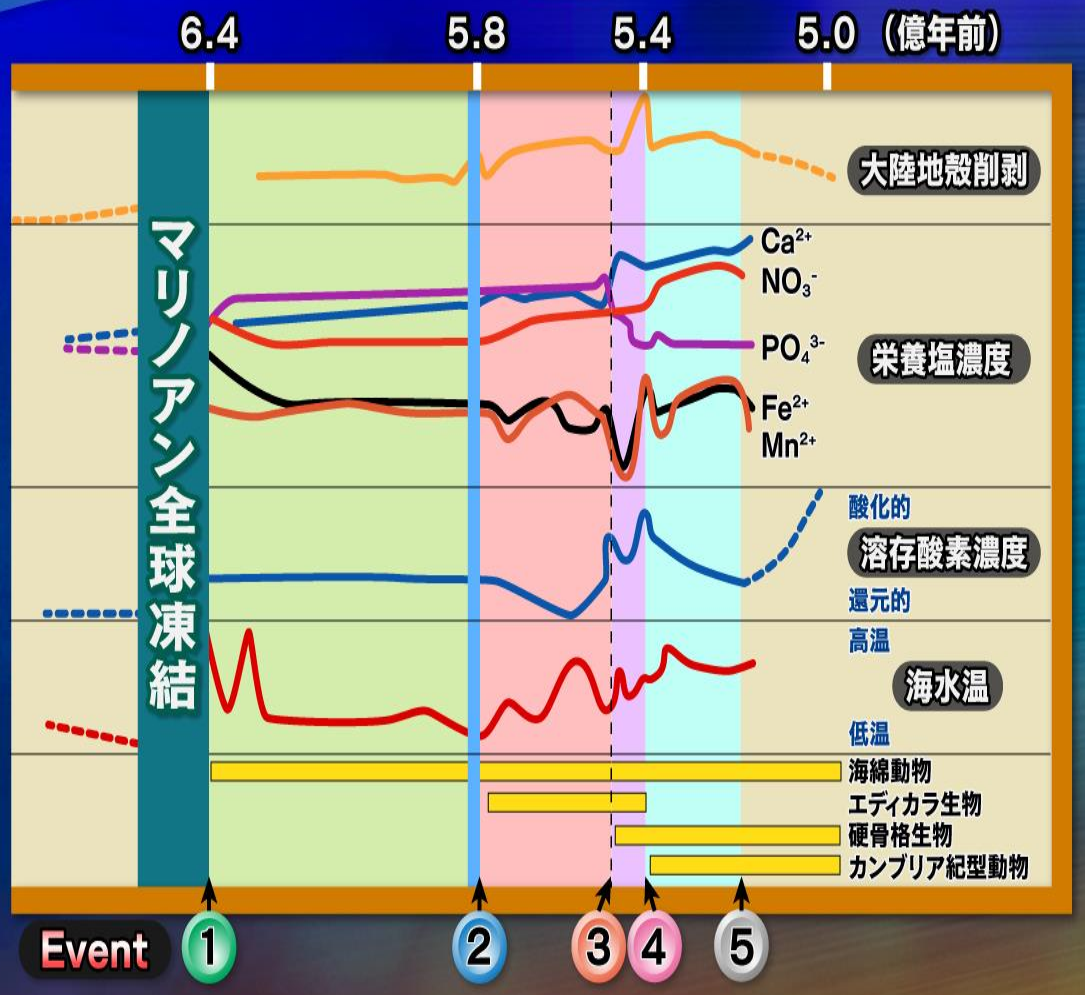

1 6.4億年前

海綿動物の出現
大陸削剥増、PO_4^{3-}増

2 5.8億年前

エディカラ動物の出現
大陸削剥増、NO_3^-増

3 5.5億年前

硬骨格生物の出現
酸素増、Ca^{2+}増
PO_4^{3-}減、Fe^{2+}減

4 5.4億年前

カンブリア紀型生物の出現
大陸削剥最大、NO_3^-増

5 5.2~5.0億年前

カンブリア紀の爆発的進化

澤木(2011)、石川他(2008)

原生代末期の環境変動

Event 0 マリノアン全球凍結(6.4億年前まで)

Event 1 海綿動物出現(6.4億年前)

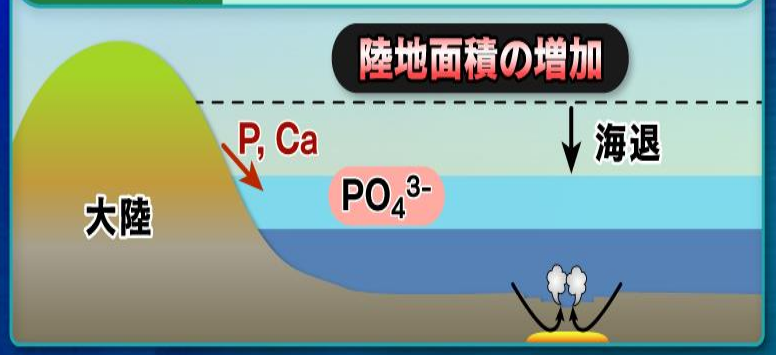

Event 2 エディアカラ生物出現(5.8億年前)

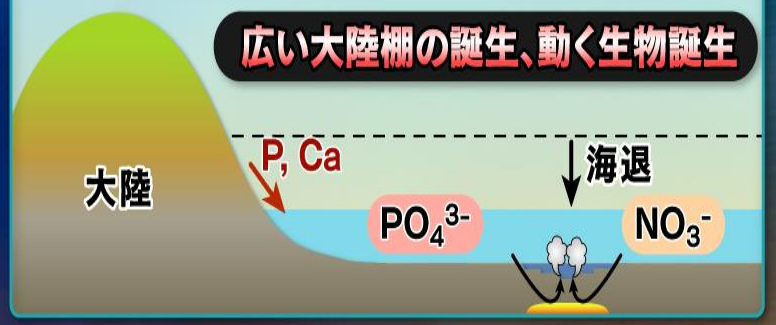

Event 3 硬骨格生物動物出現(5.5億年前)

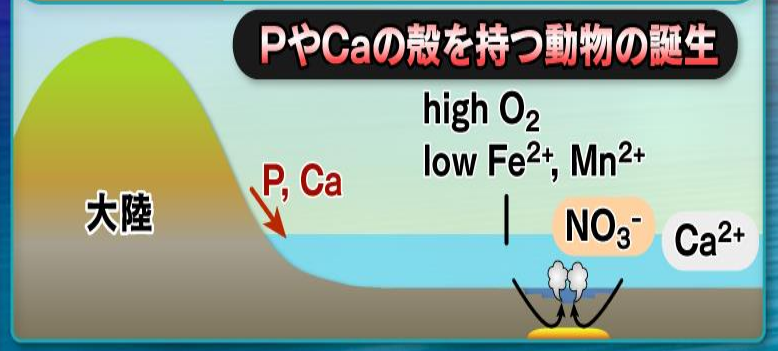

Event 4 カンブリア紀型生物出現(5.4億年前)

Event 5 カンブリア紀の爆発的生物進化
全ての動物門の出現、大型化(5.2~5.0億年前)

生命進化：2回の巨大化

Payne et al (2009)

The basic study for Astrobiology

Unraveling of the Earth history

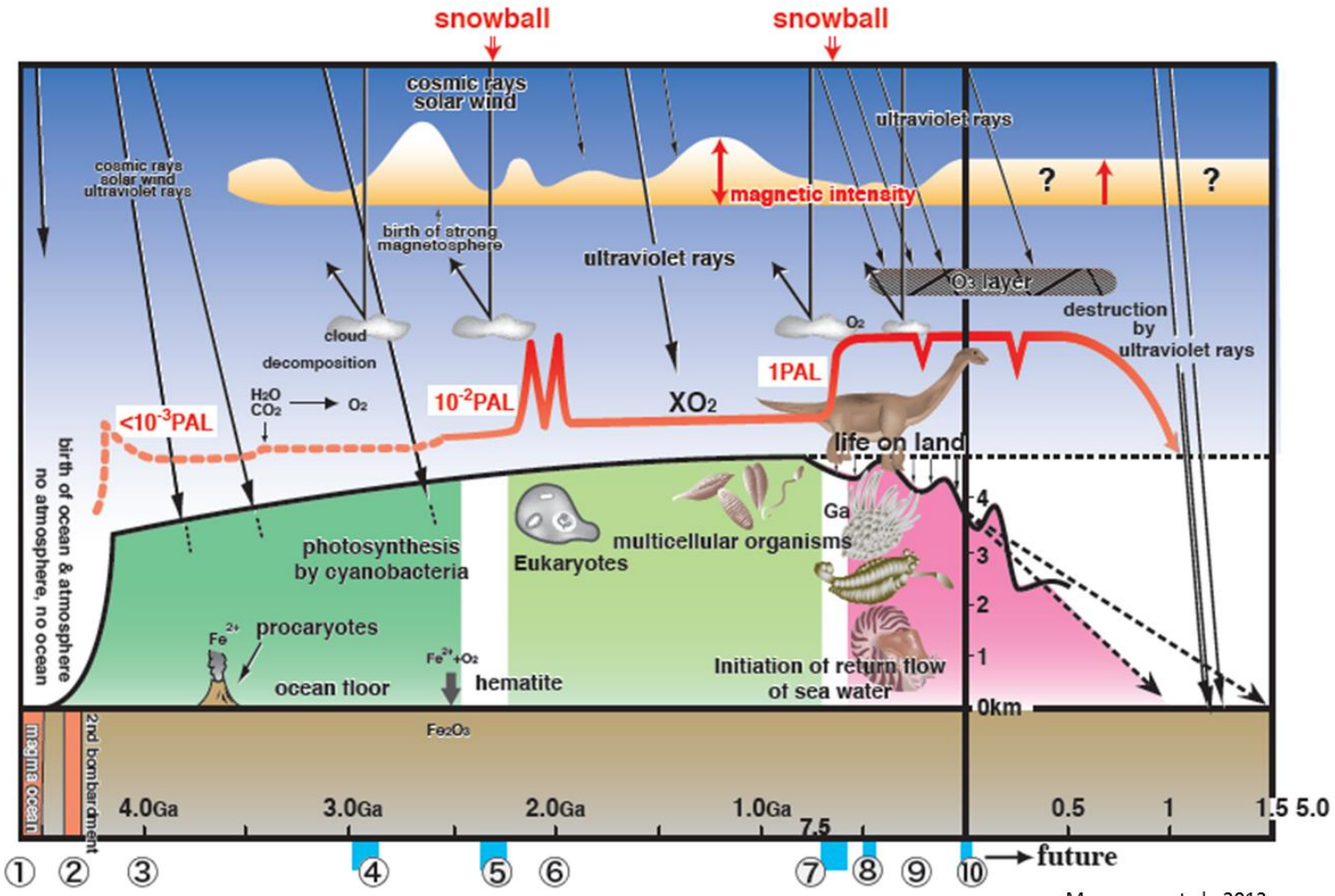

Maruyama et al., 2013

Secular variation of P-T conditions of regional metamorphic belts

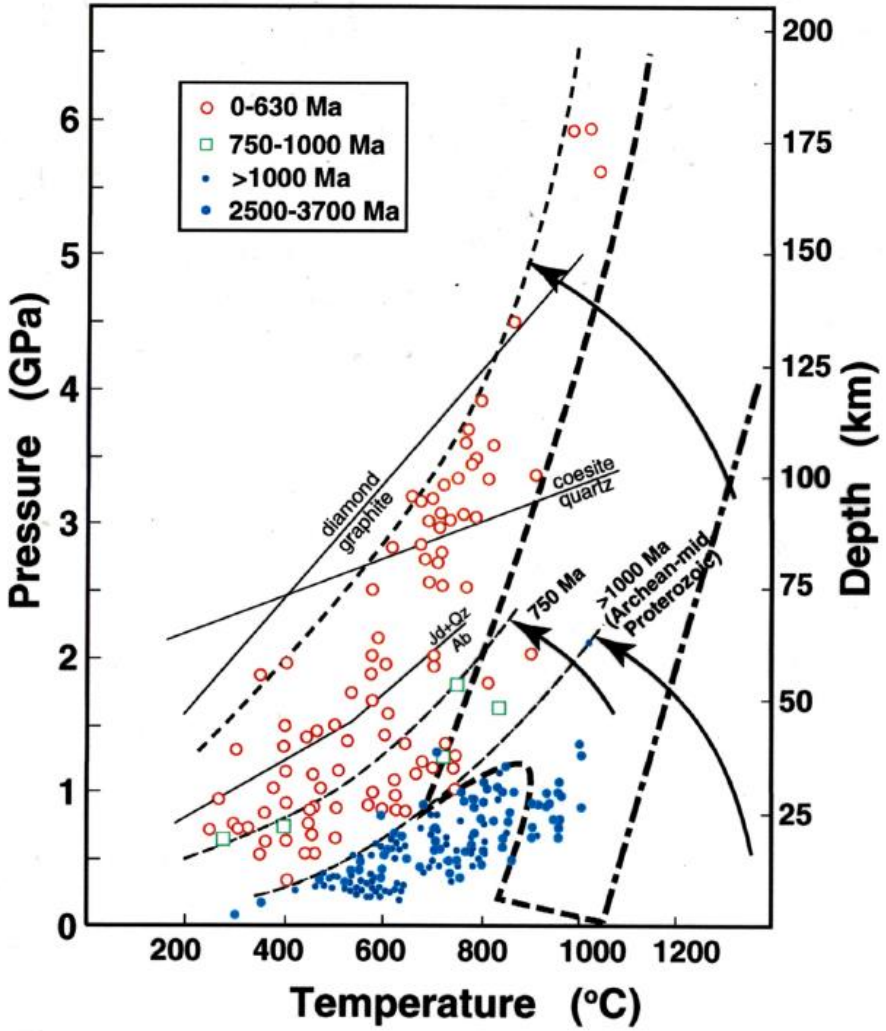

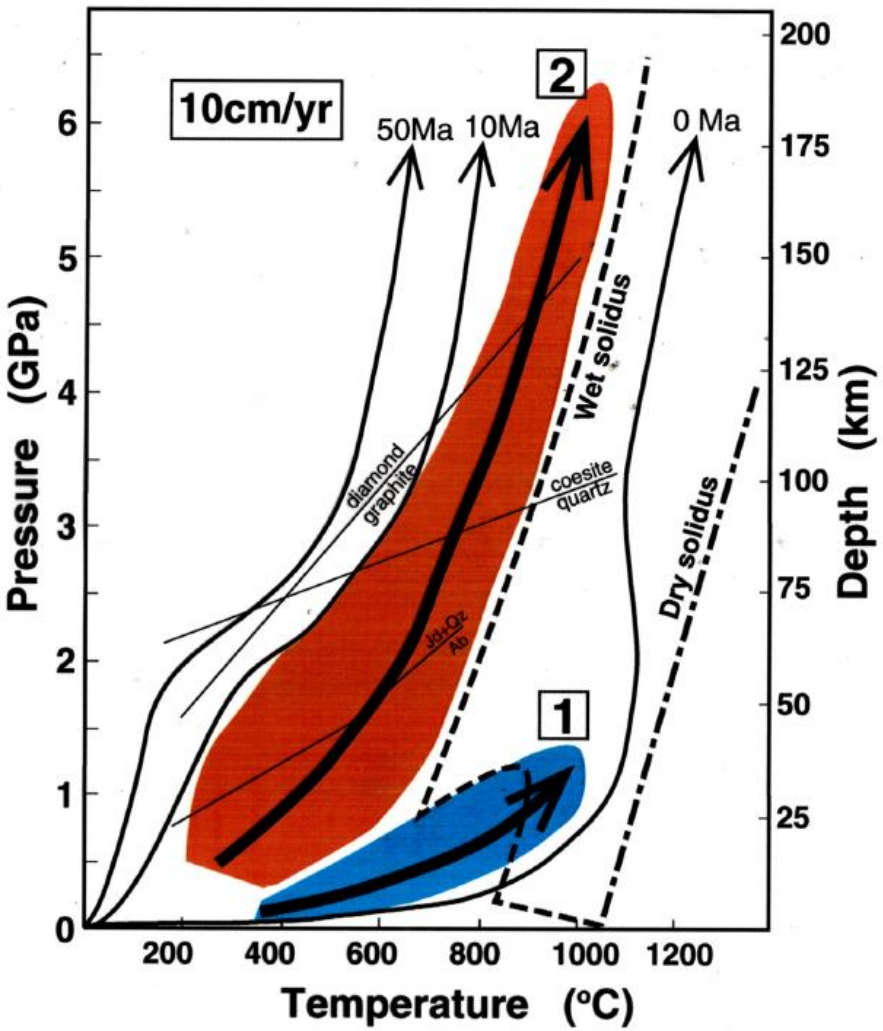

The subduction zone geothermal gradient has cooled gradually with time. UHP metamorphism has only occured after the Late Proterozoic.

Maruyama et al., 1996; Maruyama and Liou, 2005 Maruyama et al., 2013

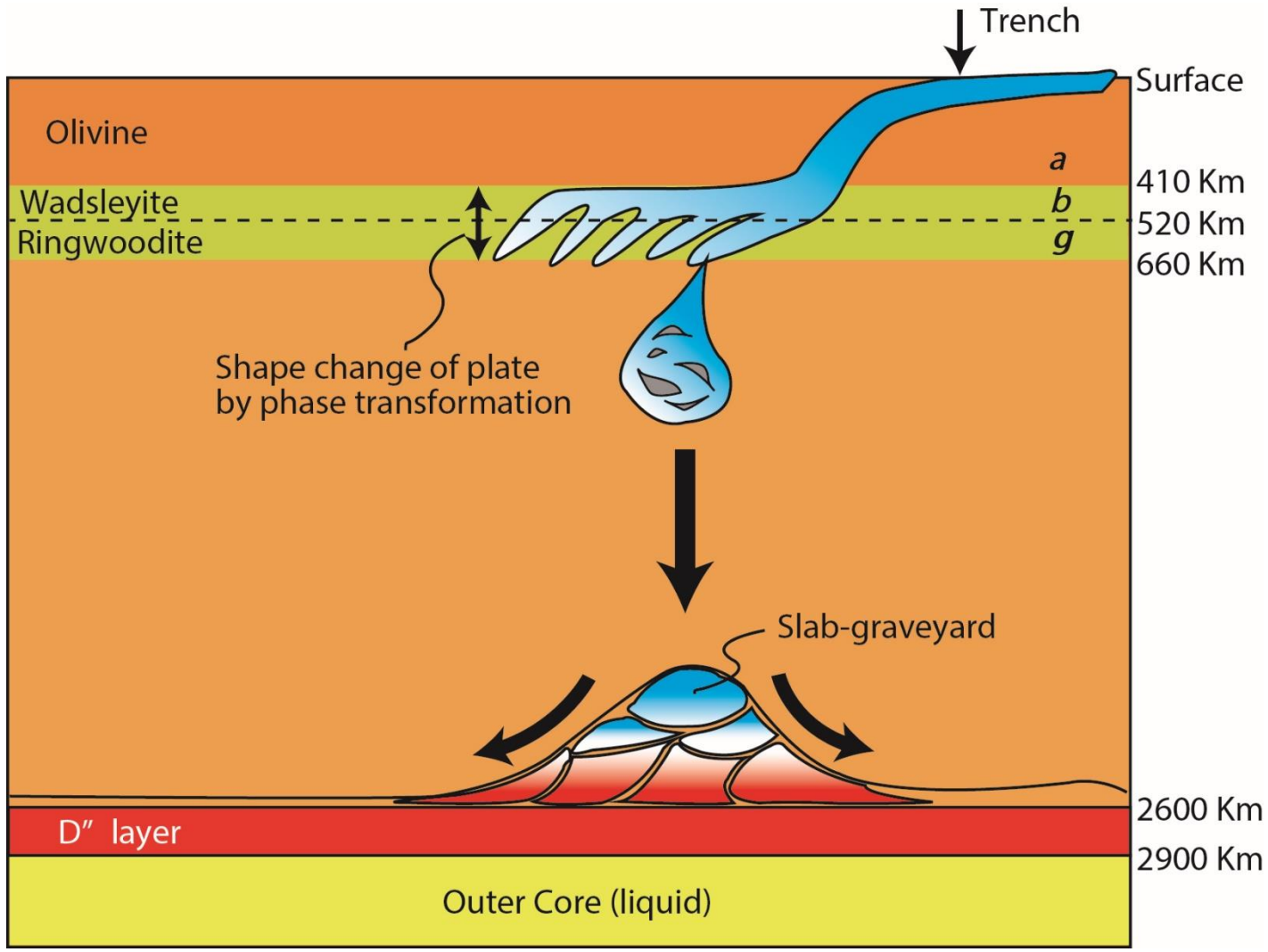
Trench
Surface
Olivine
a
410 Km
Wadsleyite
b
520 Km
Ringwoodite
g
660 Km
Shape change of plate
by phase transformation
Slab-graveyard
2600 Km
D″ layer
2900 Km
Outer Core (liquid)

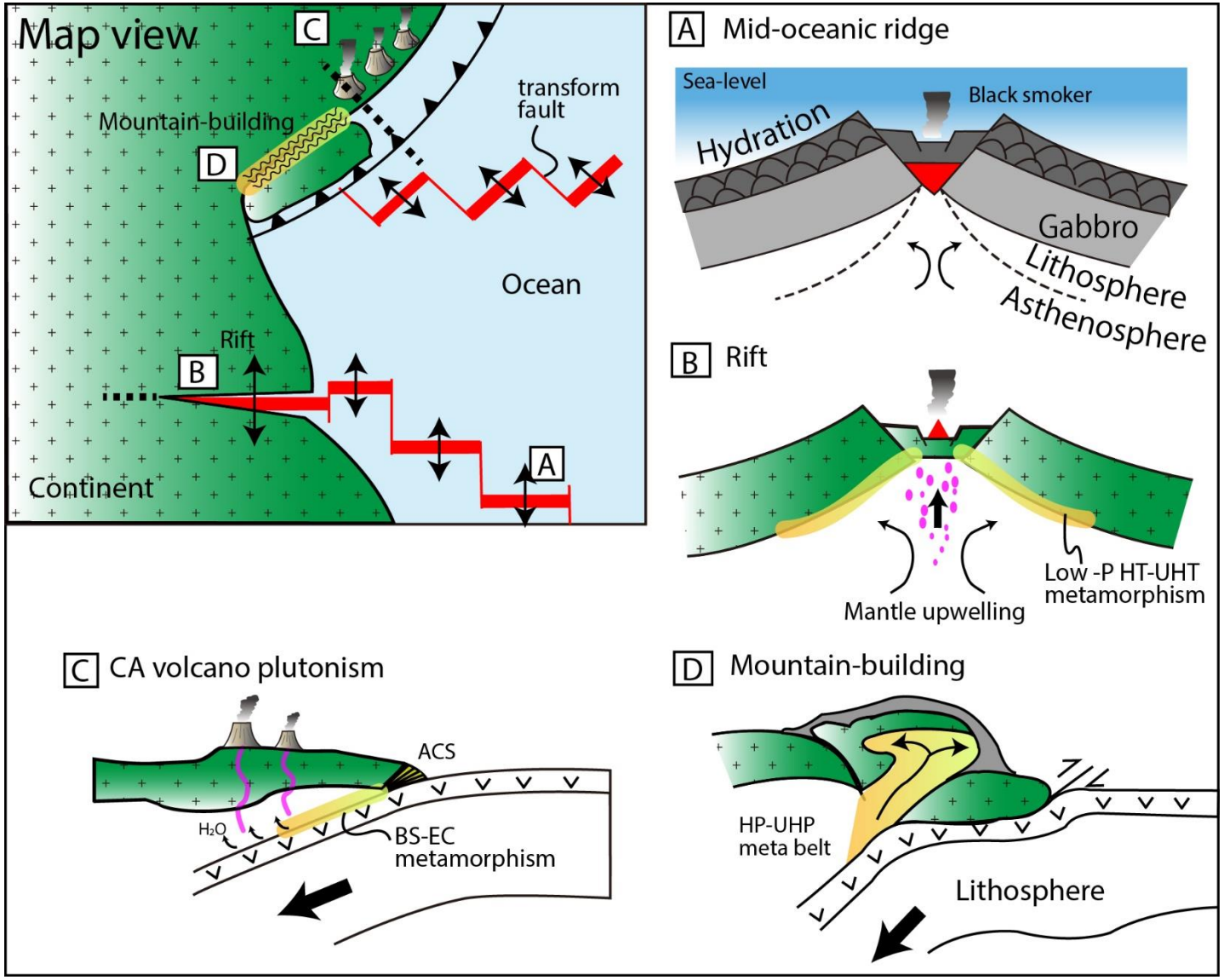
Map view
C
Mountain-building
D
transform fault
Ocean
Rift
B
A
Continent
A Mid-oceanic ridge
Sea-level
Black smoker
Hydration
Gabbro
Lithosphere
Asthenosphere
B Rift
Low -P HT-UHT metamorphism
Mantle upwelling
C CA volcano plutonism
ACS
H2O
BS-EC metamorphism
D Mountain-building
HP-UHP meta belt
Lithosphere

(a) Slab pull force and ridge push force triggered by ABEL bombardment (4.37-4.20Ga)

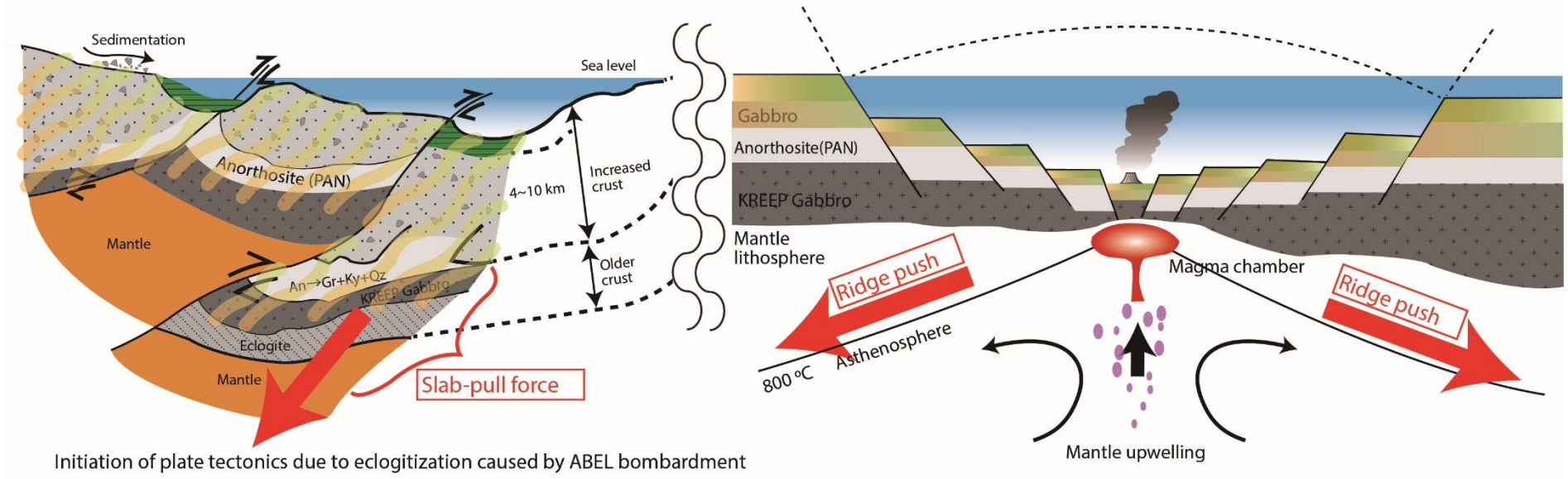

Initiation of plate tectonics due to eclogitization caused by ABEL bombardment

(b) Eclogitization (phase transition) initiated under the presence of fluid

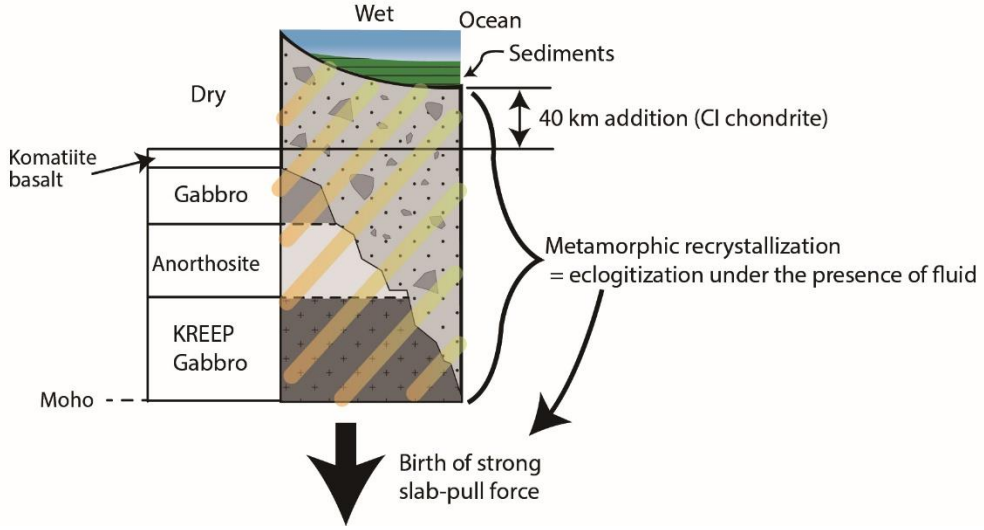

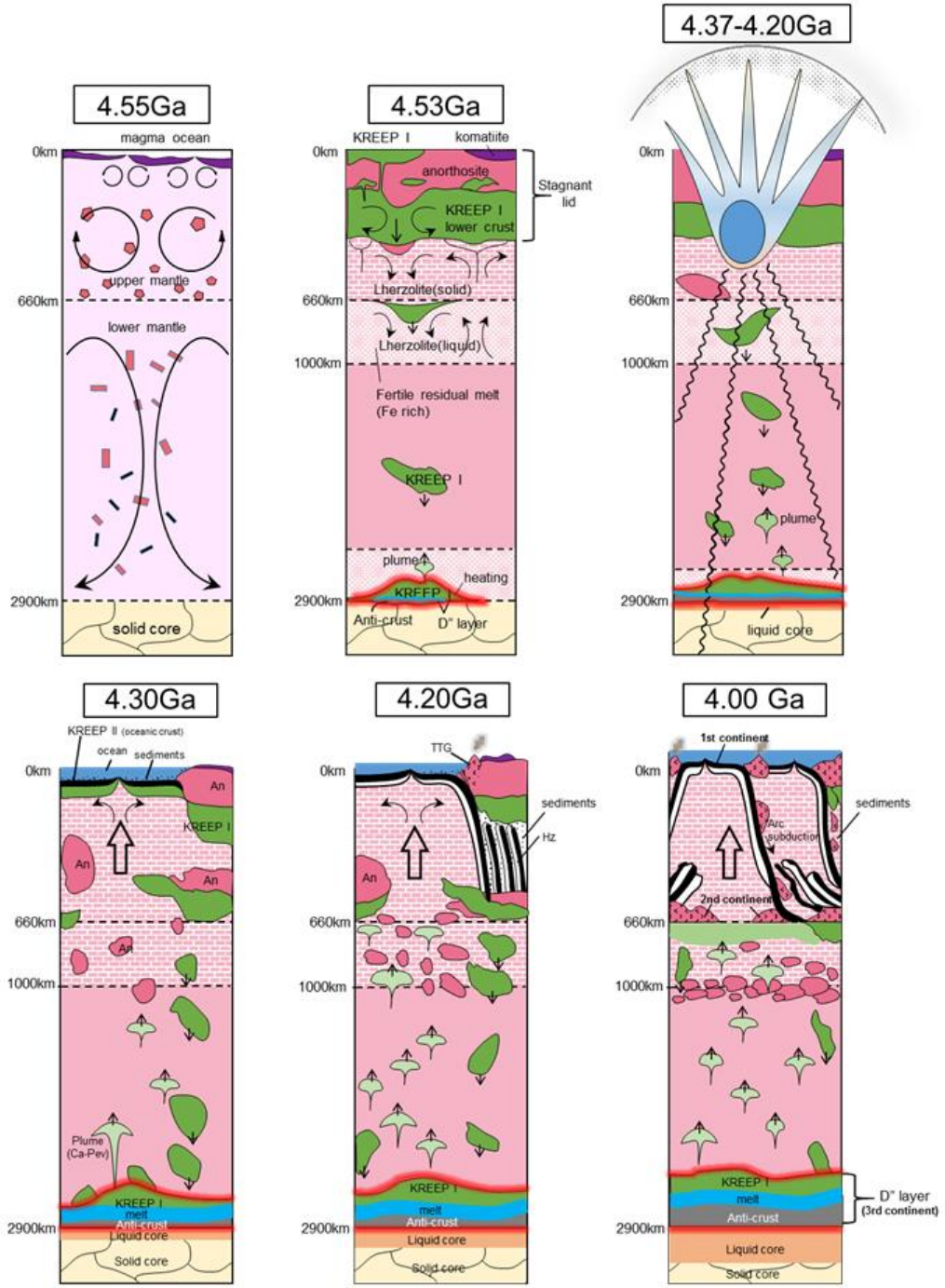
4.55Ga
magma ocean
0km
upper mantle
660km
lower mantle
2900km
solid core
4.53Ga
KREEP I
komatiite
0km
anorthosite
Stagnant lid
KREEP I lower crust
660km
Lherzolite(solid)
Lherzolite(liquid)
1000km
Fertile residual melt (Fe rich)
KREEP I
plume
heating
KREEP I
2900km
Anti-crust
D" layer
4.37-4.20Ga
0km
660km
1000km
plume
2900km
liquid core
4.30Ga
KREEP II (oceanic crust)
ocean
sediments
0km
An
KREEP I
An
An
660km
An
1000km
Plume (Ca-Pev)
KREEP I
melt
Anti-crust
2900km
Liquid core
Solid core
4.20Ga
TTG
0km
sediments
Hz
An
660km
1000km
KREEP I
melt
Anti-crust
2900km
Liquid core
Solid core
4.00 Ga
1st continent
0km
sediments
Arc subduction
2nd continent
660km
1000km
KREEP I
melt
Anti-crust
D" layer
(3rd continent)
2900km
Liquid core
Solid core

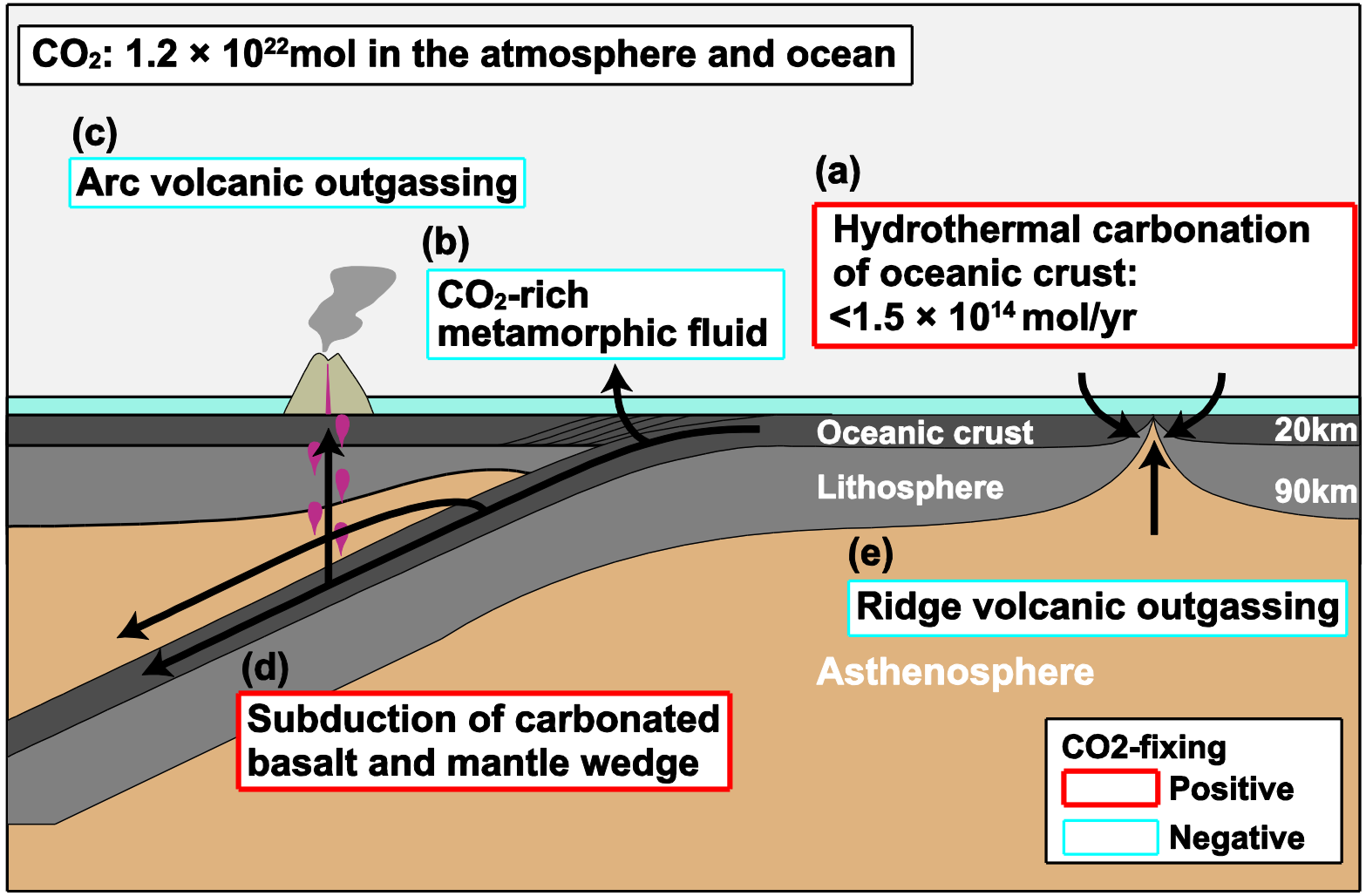
CO_2: 1.2 × 10^{22}mol in the atmosphere and ocean
(c)
Arc volcanic outgassing
(b)
CO_2-rich metamorphic fluid
(a)
Hydrothermal carbonation of oceanic crust: <1.5 × 10^{14} mol/yr
Oceanic crust
20km
Lithosphere
90km
(e)
Ridge volcanic outgassing
Asthenosphere
(d)
Subduction of carbonated basalt and mantle wedge
CO2-fixing
Positive
Negative

Paleogeography of the Earth since 4.567Ga

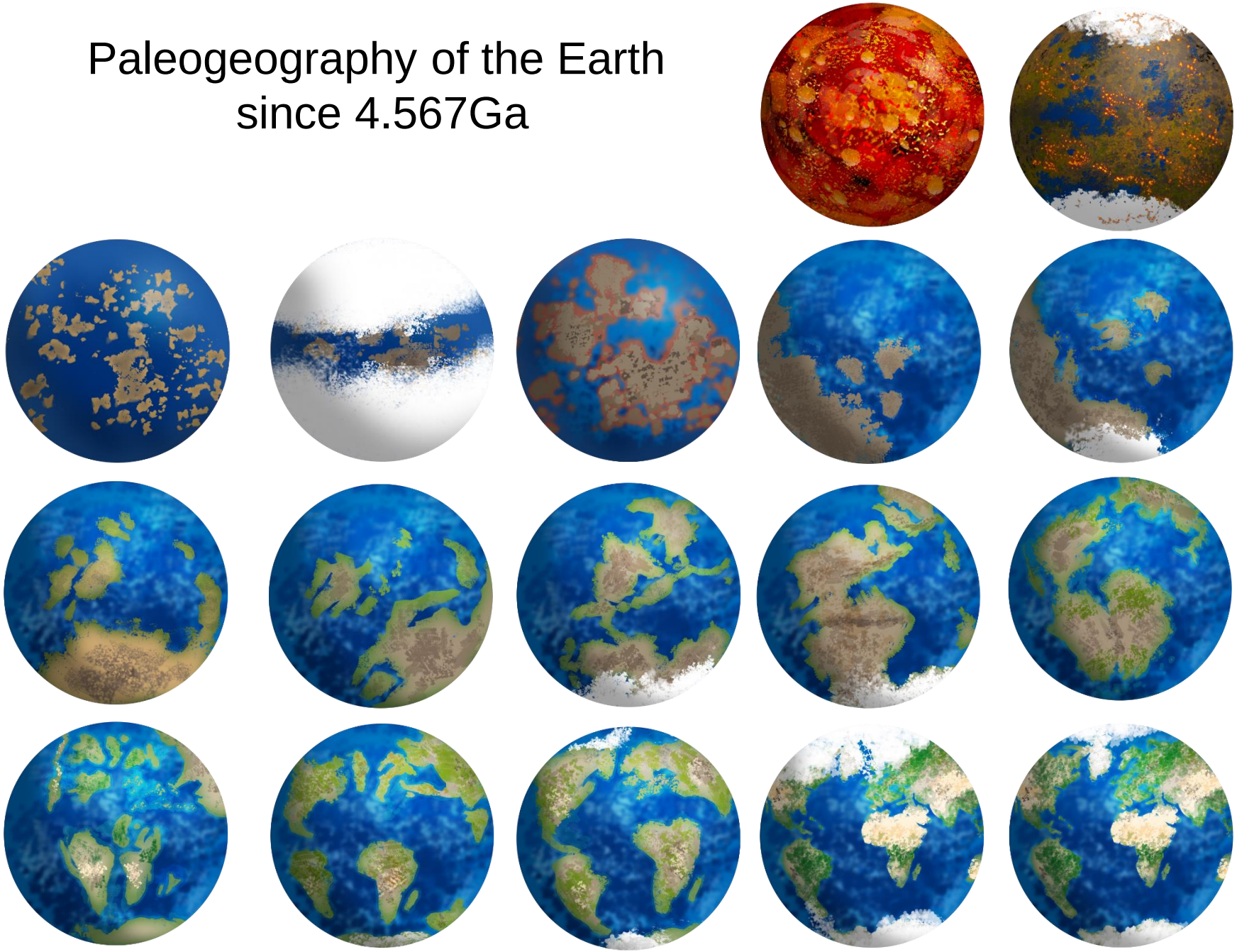

生命と地球の歴史

ー宇宙生命学の体系化ー

丸山茂徳（ELSI,東工大）

原生代の大陸成長と配置

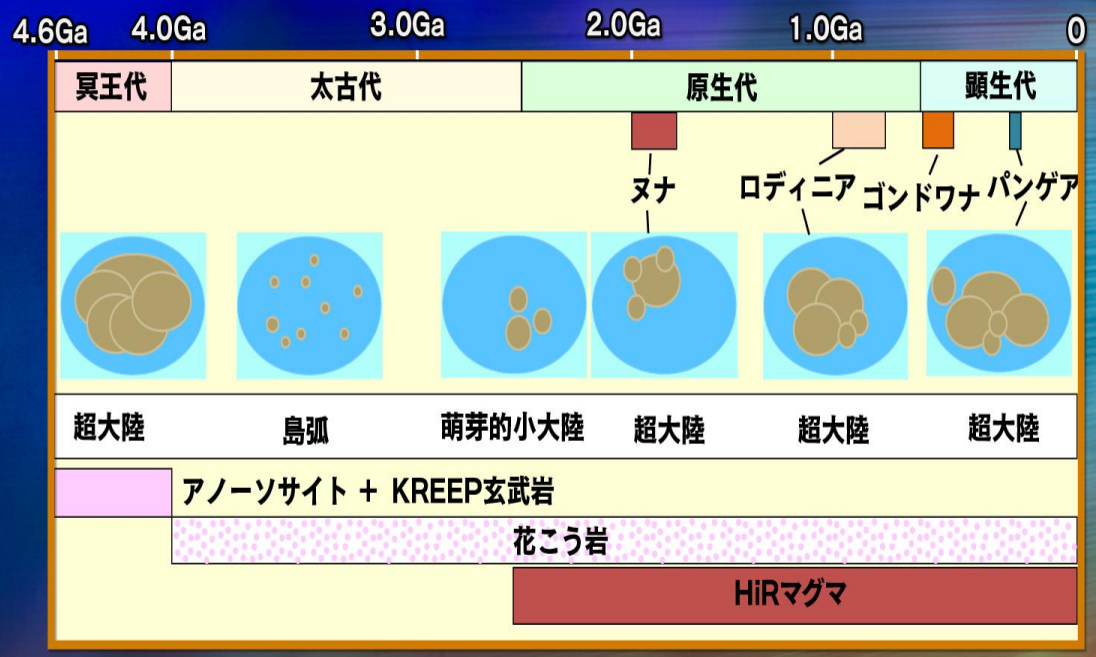

小惑星帯内部の小惑星のタイプ（化学組成）と太陽からの距離の関係

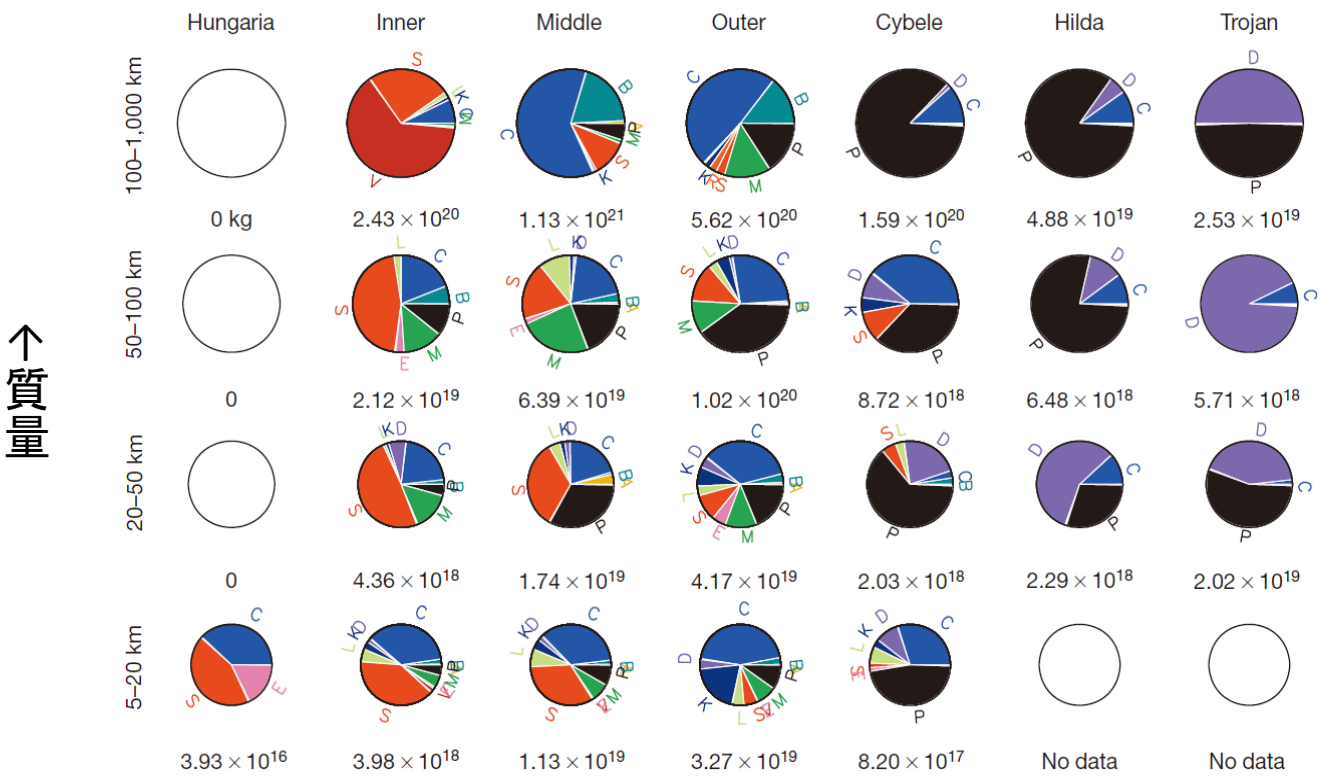

Figure 4 | The compositional mass distribution as a function of size throughout the main belt out to the Trojans. The mass is calculated for each individual object with a diameter of 50 km and greater, using its albedo to determine size and the average density[39] for that asteroid's taxonomic class. For the smaller sizes we determine the fractional contribution of each class at each size and semi-major axis, and then apply that fraction to the distribution of all known asteroids from the Minor Planet Center (http://minorplanetcenter.org/) including a correction for discovery incompleteness at the smallest sizes in the middle and outer belt[19]. Asteroid mass is grouped according to objects within four size ranges, with diameters of 100–1,000 km, 50–100 km, 20–50 km and 5–20 km. Seven zones are defined as in Fig. 1: Hungaria, inner belt, middle belt, outer belt, Cybele, Hilda and Trojan. The total mass of each zone at each size is labelled and the pie charts mark the fractional mass contribution of each unique spectral class of asteroid. The total mass of Hildas and Trojans are underestimated because of discovery incompleteness. The relative contribution of each class changes with both size and distance.

DeMeo and Carry (2014)

小惑星の地質学＋観測が鍵

Chemical zoning in asteroid belt

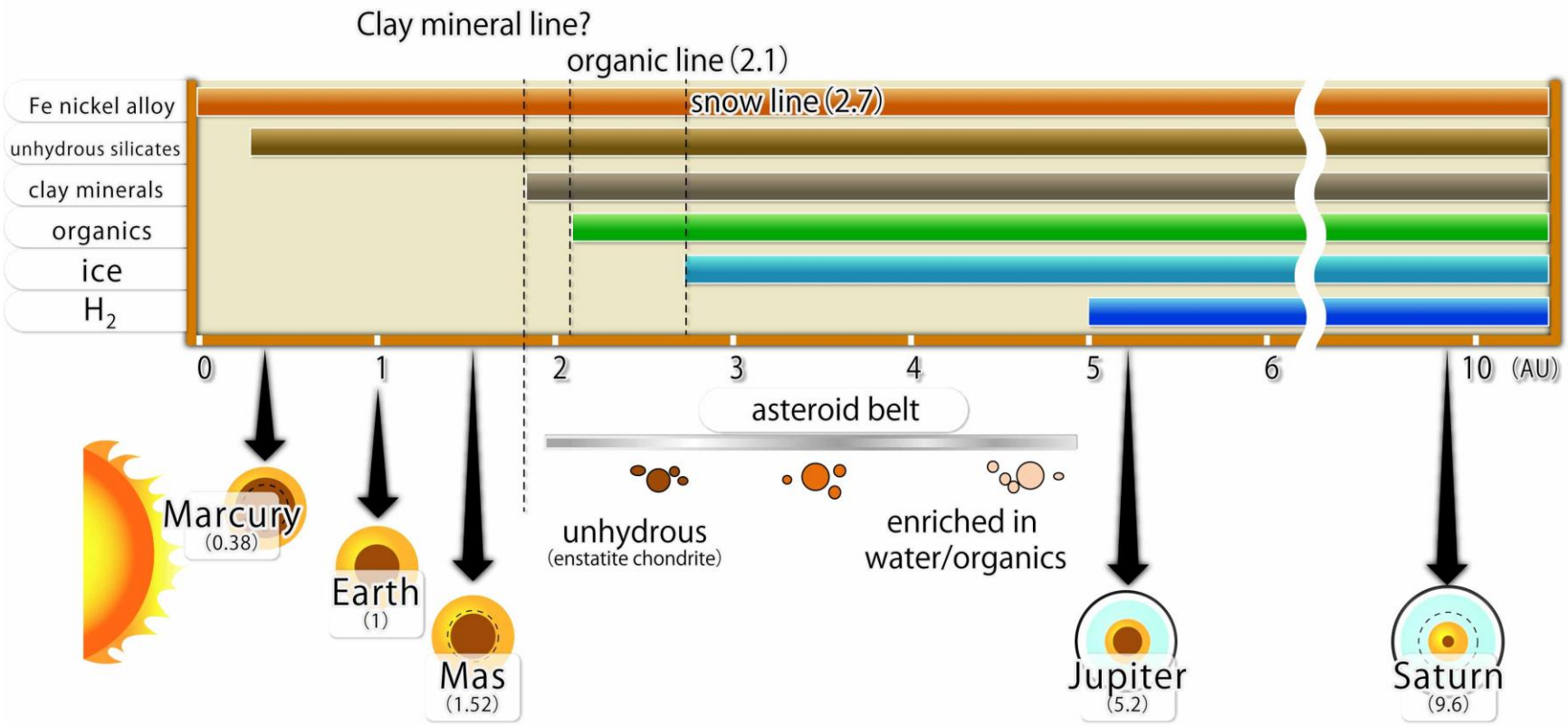

Maruyama and Ebisuzaki, 2016

Accretionary process of Earth

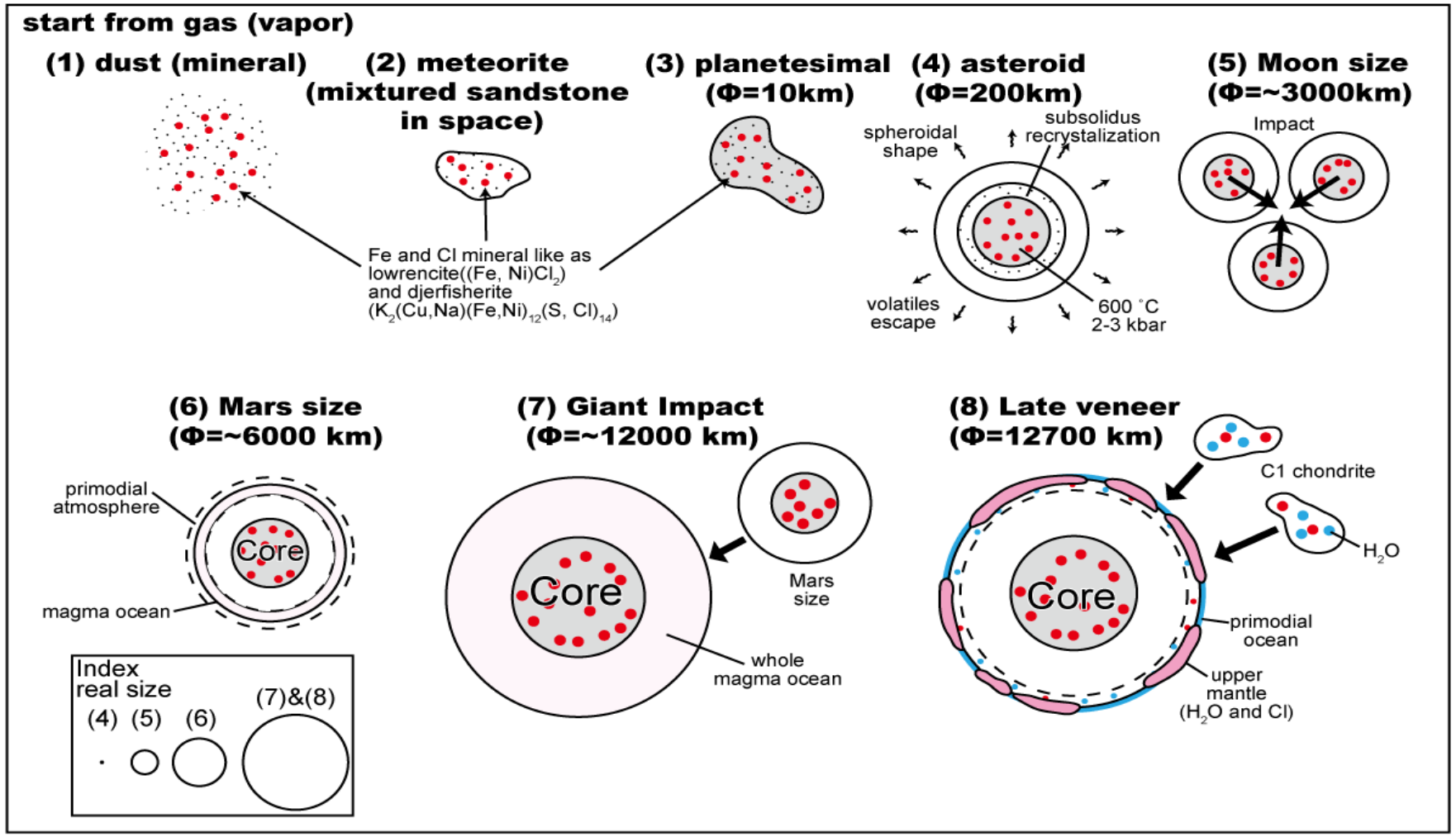

Formation of meteorite parent body

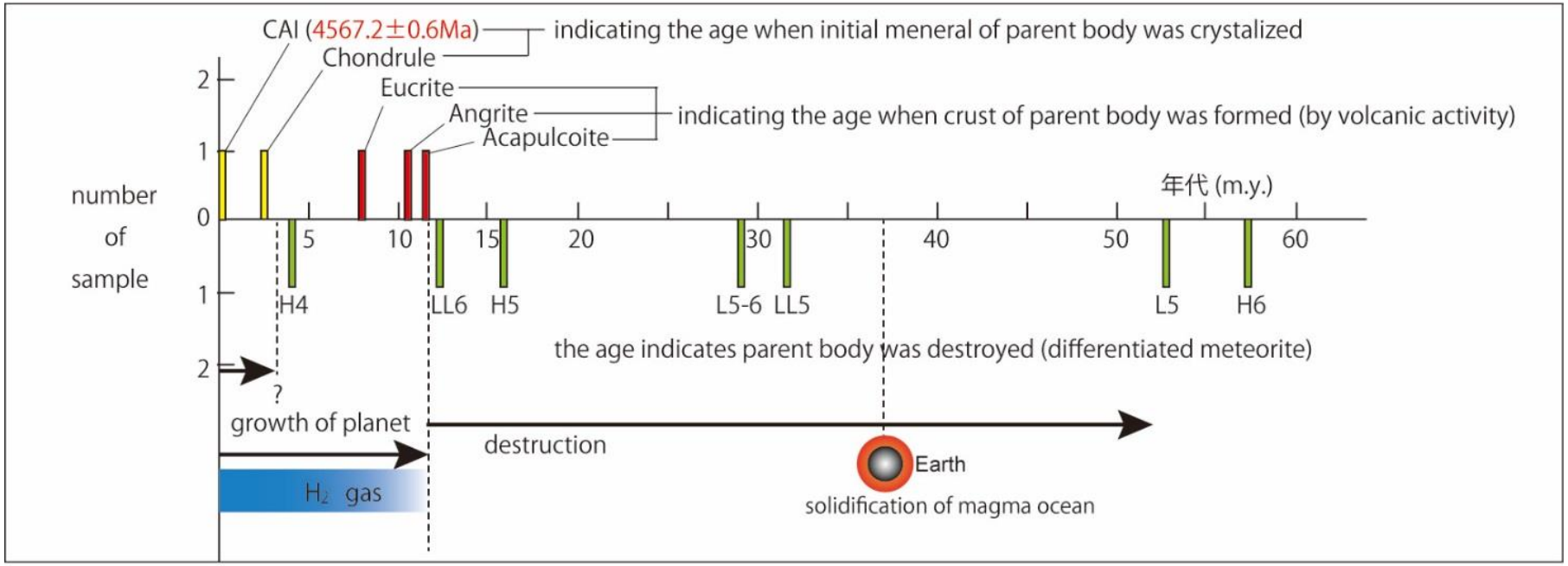

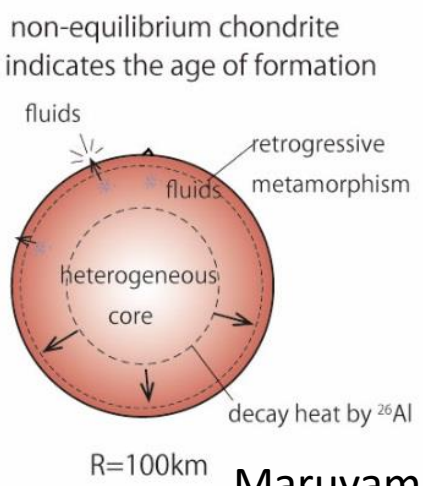

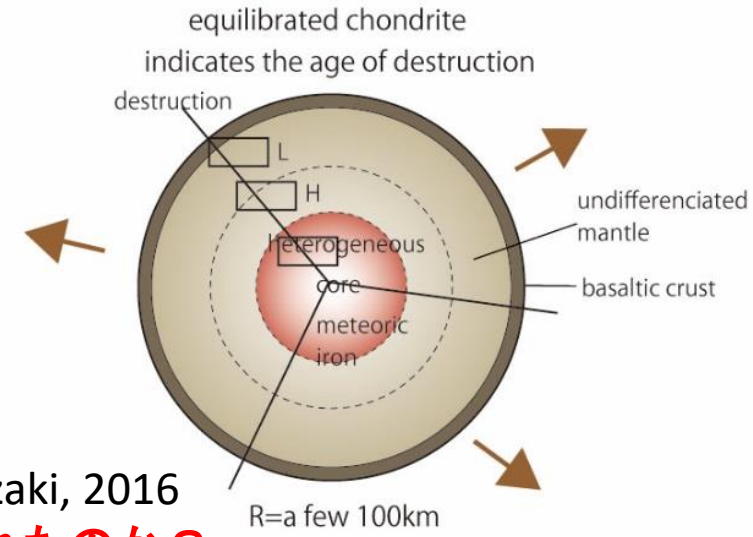

Maruyama and Ebisuzaki, 2016

水素ガスはいつ晴れたのか？

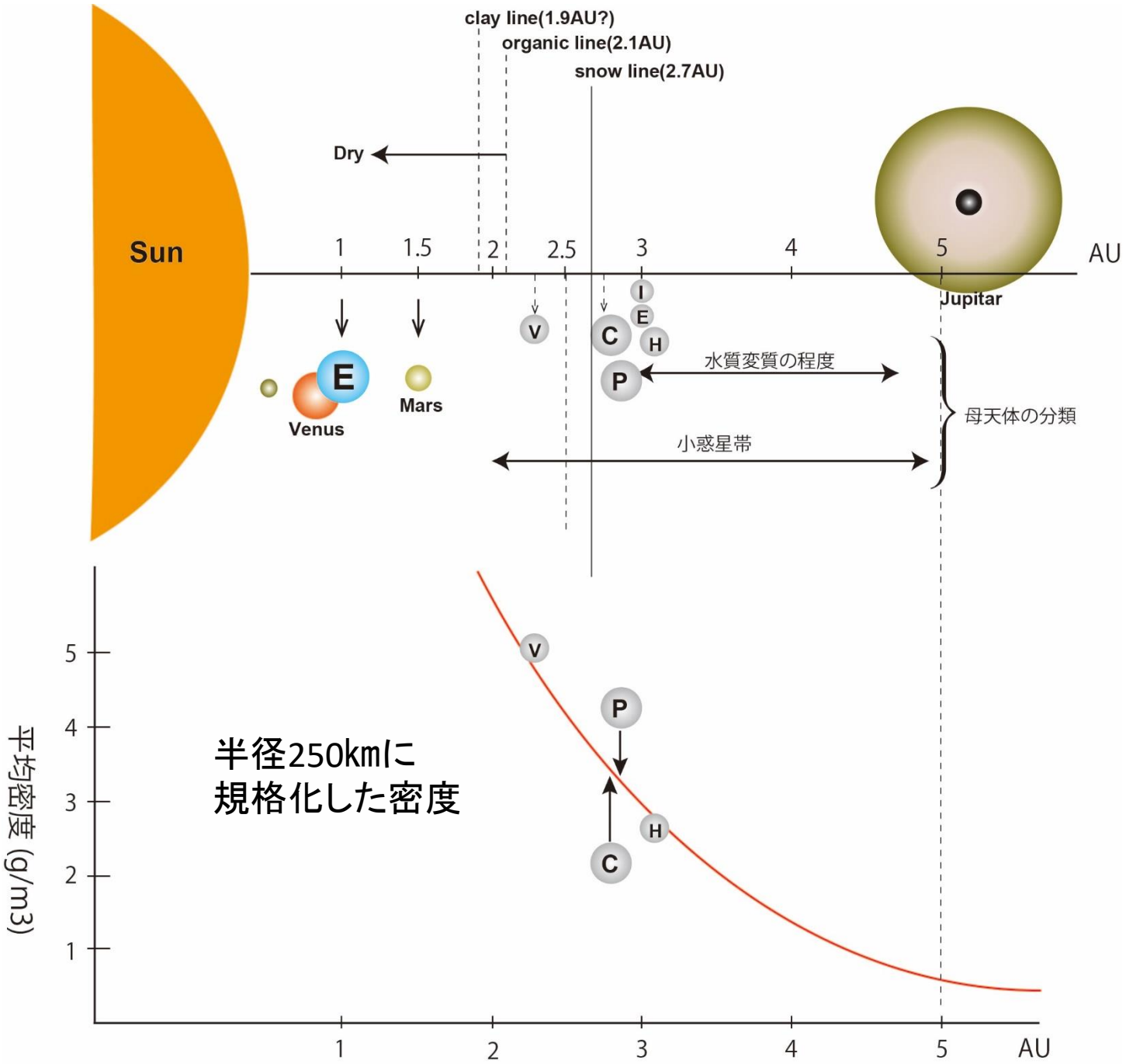
clay line(1.9AU?)
organic line(2.1AU)
snow line(2.7AU)
Dry
Sun
1
1.5
2
2.5
3
4
5
AU
Jupitar
Venus
Mars
E
V
C
I
E
H
P
水質変質の程度
母天体の分類
小惑星帯
平均密度 (g/m3)
5
4
3
2
1
半径250kmに
規格化した密度

Accretinary process of Earth

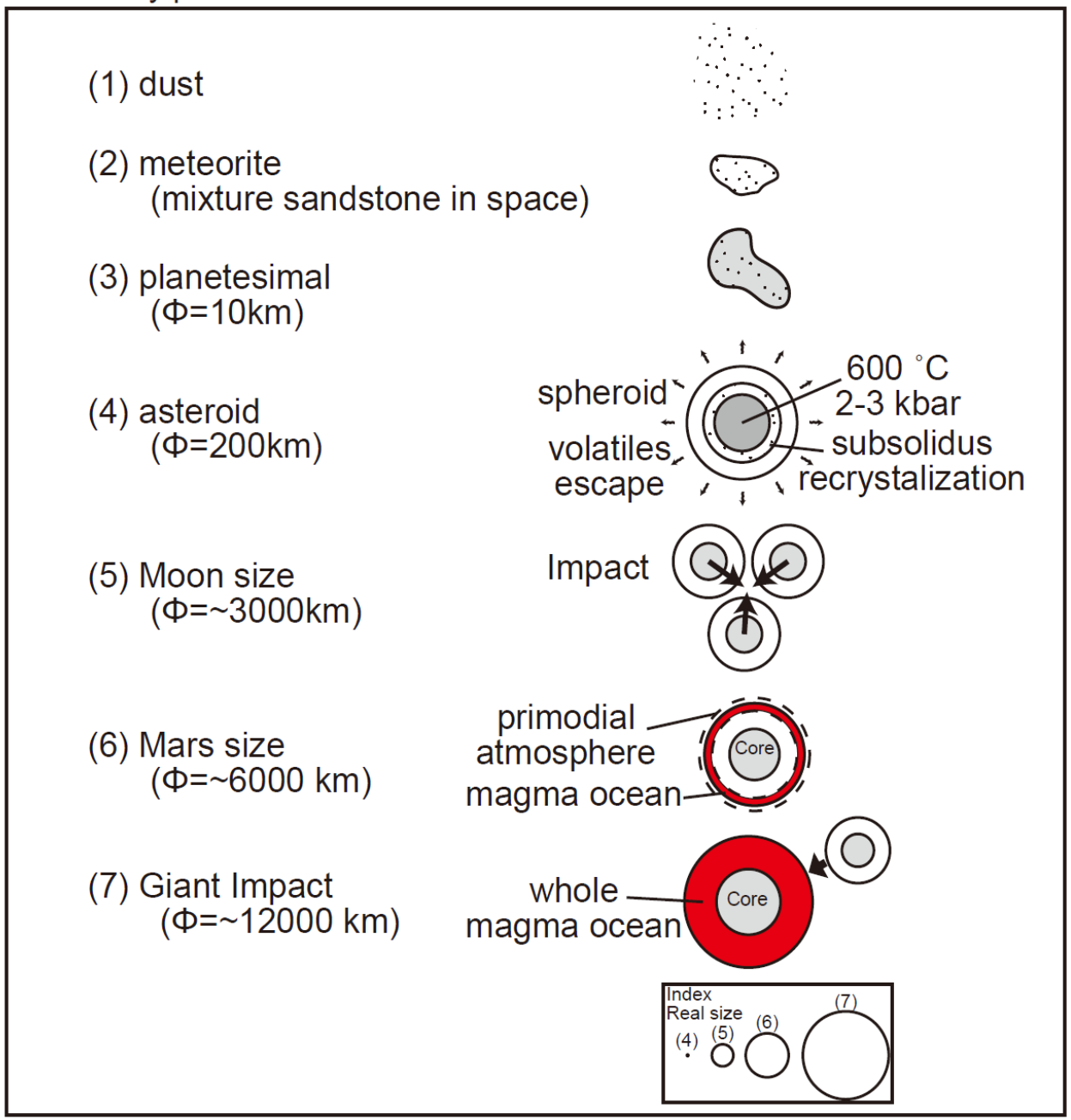

001 Ma

最近の寒冷化ピーク

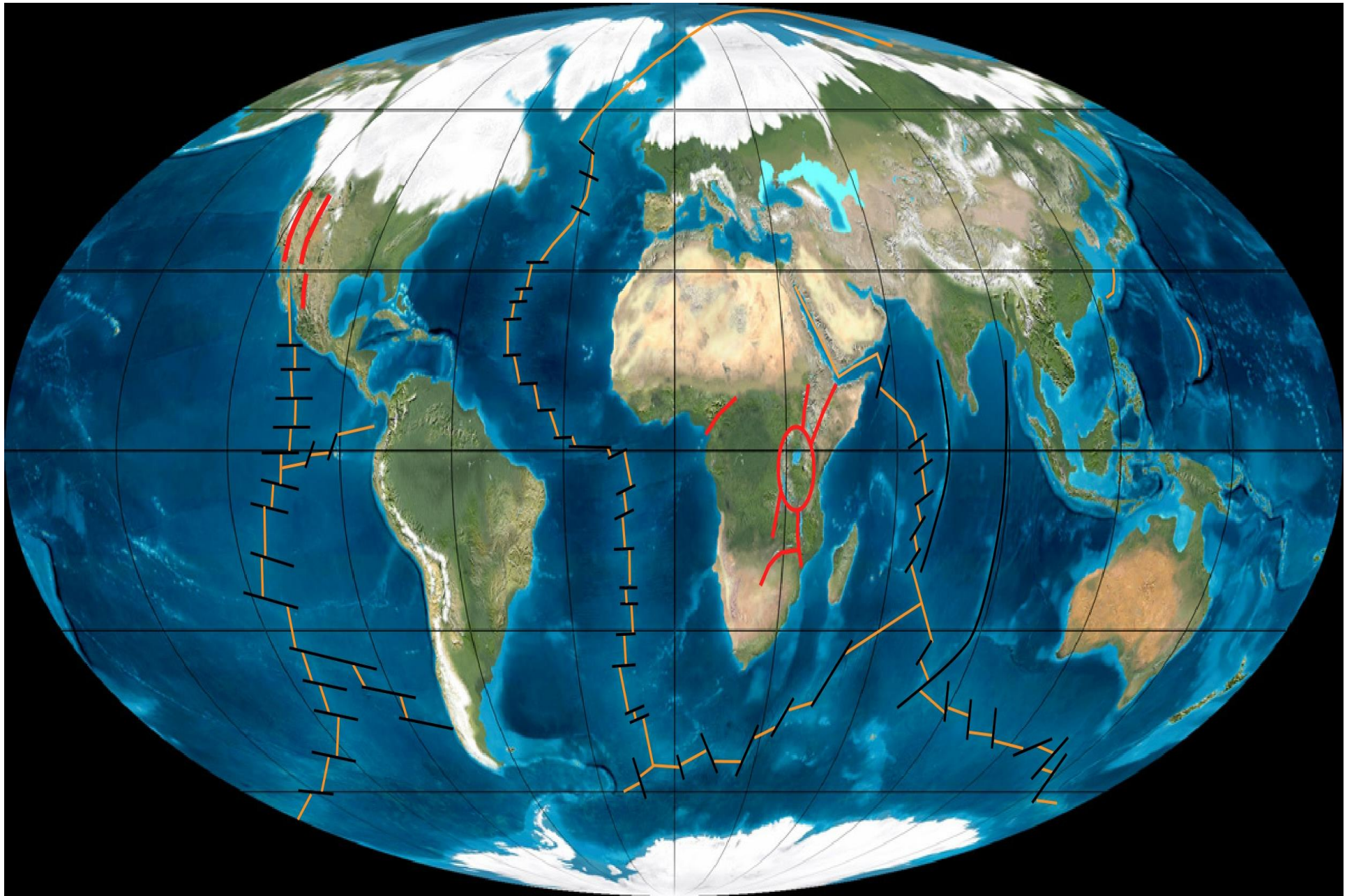

Volatile and Organic Compositions of Sedimentary Rocks in Yellowknife Bay, Gale Crater, Mars

D. W. Ming,[1*] P. D. Archer Jr.,[2] D. P. Glavin,[3] J. L. Eigenbrode,[3] H. B. Franz,[3,4] B. Sutter,[2] A. E. Brunner,[3,5] J. C. Stern,[3] C. Freissinet,[3,6] A. C. McAdam,[3] P. R. Mahaffy,[3] M. Cabane,[7] P. Coll,[8] J. L. Campbell,[9] S. K. Atreya,[10] P. B. Niles,[1] J. F. Bell III,[11] D. L. Bish,[12] W. B. Brinckerhoff,[3] A. Buch,[13] P. G. Conrad,[3] D. J. Des Marais,[14] B. L. Ehlmann,[15,16] A. G. Fairén,[17] K. Farley,[15] G. J. Flesch,[16] P. Francois,[8] R. Gellert,[9] J. A. Grant,[18] J. P. Grotzinger,[15] S. Gupta,[19] K. E. Herkenhoff,[20] J. A. Hurowitz,[21] L. A. Leshin,[22] K. W. Lewis,[23] S. M. McLennan,[21] K. E. Miller,[24] J. Moersch,[25] R. V. Morris,[1] R. Navarro-González,[26] A. A. Pavlov,[3] G. M. Perrett,[9] I. Pradler,[9] S. W. Squyres,[17] R. E. Summons,[24] A. Steele,[27] E. M. Stolper,[15] D. Y. Sumner,[28] C. Szopa,[8] S. Teinturier,[8] M. G. Trainer,[3] A. H. Treiman,[29] D. T. Vaniman,[30] A. R. Vasavada,[16] C. R. Webster,[16] J. J. Wray,[31] R. A. Yingst,[30] MSL Science Team†

H_2O, CO_2, SO_2, O_2, H_2, H_2S, HCl, chlorinated hydrocarbons, NO, and other trace gases were evolved during pyrolysis of two mudstone samples acquired by the Curiosity rover at Yellowknife Bay within Gale crater, Mars. H_2O/OH-bearing phases included 2:1 phyllosilicate(s), bassanite, akaganeite, and amorphous materials. Thermal decomposition of carbonates and combustion of organic materials are candidate sources for the CO_2. Concurrent evolution of O_2 and chlorinated hydrocarbons suggests the presence of oxychlorine phase(s). Sulfides are likely sources for sulfur-bearing species. Higher abundances of chlorinated hydrocarbons in the mudstone compared with Rocknest windblown materials previously analyzed by Curiosity suggest that indigenous martian or meteoritic organic carbon sources may be preserved in the mudstone; however, the carbon source for the chlorinated hydrocarbons is not definitively of martian origin.

Table 1. Evolved gas abundances released during SAM pyrolysis runs of samples (<150 μm fraction) obtained from the John Klein and Cumberland drill holes. Rocknest aeolian material evolved gas abundances are provided for comparison with the Sheepbed mudstone materials.

	John Klein				Cumberland			CB- 5	Rocknest† Average of four runs
	JK-1	JK-2	JK-3*	JK- 4	CB-1	CB-2	CB-3		
					Molar abundances (μmol)				
H_2O	57.4 ± 32.7‡	54.2 ± 30.8	59.9 ± 33.7	44.7 ± 25.0	42.7 ± 28.8	54.0 ± 29.5	62.4 ± 31.5	45.0 ± 25.4	55.1 ± 35.3
CO_2	7.0 ± 1.9	8.1 ± 1.7	6.6 ± 1.6	5.7 ± 1.3	2.0 ± 0.5	2.5 ± 0.7	3.1 ± 0.6	3.1 ± 0.7	9.9 ± 1.2
SO_2	1.6 ± 0.6	1.4 ± 0.1	2.9 ± 0.1	2.0 ± 0.0	0.4 ± 0.02	1.3 ± 0.2	1.2 ± 0.2	1.4 ± 0.2	12.2 ± 0.9
O_2	0.6 ± 0.1	0.8 ± 0.1	2.1 ± 0.3	0.9 ± 0.1	2.6 ± 0.3	8.4 ± 1.0	9.9 ± 1.2	11.2 ± 1.4	3.9 ± 0.2
H_2	9.3 ± 1.8	5.1 ± 1.0	4.9 ± 0.9	5.3 ± 1.0	6.9 ± 1.3	11.6 ± 2.2	4.3 ± 0.8	4.1 ± 0.8	Not measured directly
					High-temperature H_2O (%)§				
	21 ± 8	21 ± 8	26 ± 9	34 ± 11	26 ± 26	31 ± 8	19 ± 1	31 ± 11	
					Molar abundances (nmol)				
HCl	58.5 ± 26.1	72.4 ± 32.2	536.1 ± 238.7	155.1 ± 69.1	44.1 ± 19.6	179.9 ± 80.1	267.7 ± 119.2	584.9 ± 260.5	36.5 ± 10.4
H_2S	79.0 ± 35.2	57.0 ± 25.4	95.2 ± 42.4	36.1 ± 16.1	18.7 ± 8.3	67.4 ± 30.0	38.9 ± 17.3	34.4 ± 15.3	61.0 ± 13.9
NO	190 ± 38	188 ± 38	162 ± 32	129 ± 26	190 ± 38	331 ± 66	389 ± 78	374 ± 75	175 ± 40
					Sample weight (%)				
H_2O	2.3 ± 1.6	2.2 ± 1.5	2.4 ± 1.5	1.8 ± 1.2	1.7 ± 1.3	2.2 ± 1.5	2.5 ± 1.6	1.8 ± 1.2	2.0 ± 1.3
CO_2	0.7 ± 0.3	0.8 ± 0.4	0.6 ± 0.2	0.6 ± 0.3	0.2 ± 0.09	0.2 ± 0.1	0.3 ± 0.1	0.3 ± 0.1	0.9 ± 0.1
SO_3 equiv.	0.3 ± 0.1	0.2 ± 0.1	0.5 ± 0.12	0.4 ± 0.1	0.1 ± 0.0	0.2 ± 0.1	0.2 ± 0.09	0.2 ± 0.10	2.0 ± 0.2
Cl_2O_7 equiv.	0.07 ± 0.03	0.09 ± 0.04	0.24 ± 0.06	0.10 ± 0.04	0.3 ± 0.1	1.0 ± 0.4	1.2 ± 0.5	1.3 ± 0.5	0.4 ± 0.1

*Three sample portions (~135 ± 31 mg) of John Klein drill material were delivered to SAM for the JK-3 experimental run. The numbers in this column have been normalized to one sample portion (45 mg). †Average of four SAM runs of the Rocknest aeolian material (*10*). ‡ Errors reported for molar abundances of CO_2, SO_2, and O_2 are the 2σ standard deviation from the mean of calculations done with different *m/z* values for the same species. H_2O error bars are based on the uncertainty in prelaunch water abundance calibration. Errors for other species include the uncertainty in differences in ionization efficiency between masses with a calibrated mol/counts value and uncalibrated values (*10*). Weight % values were calculated with an estimated sample mass of 45 ± 18 mg (2σ), with errors propagated including the uncertainty in molar abundance (*10*). §High-temperature H_2O is the percentage of the H_2O released between 450° and 835°C, which is the temperature region for dehydroxylation of a 2:1 phyllosilicate, compared to the total H_2O released. Errors are the 2σ standard deviation from the mean.

Ming et al 2014

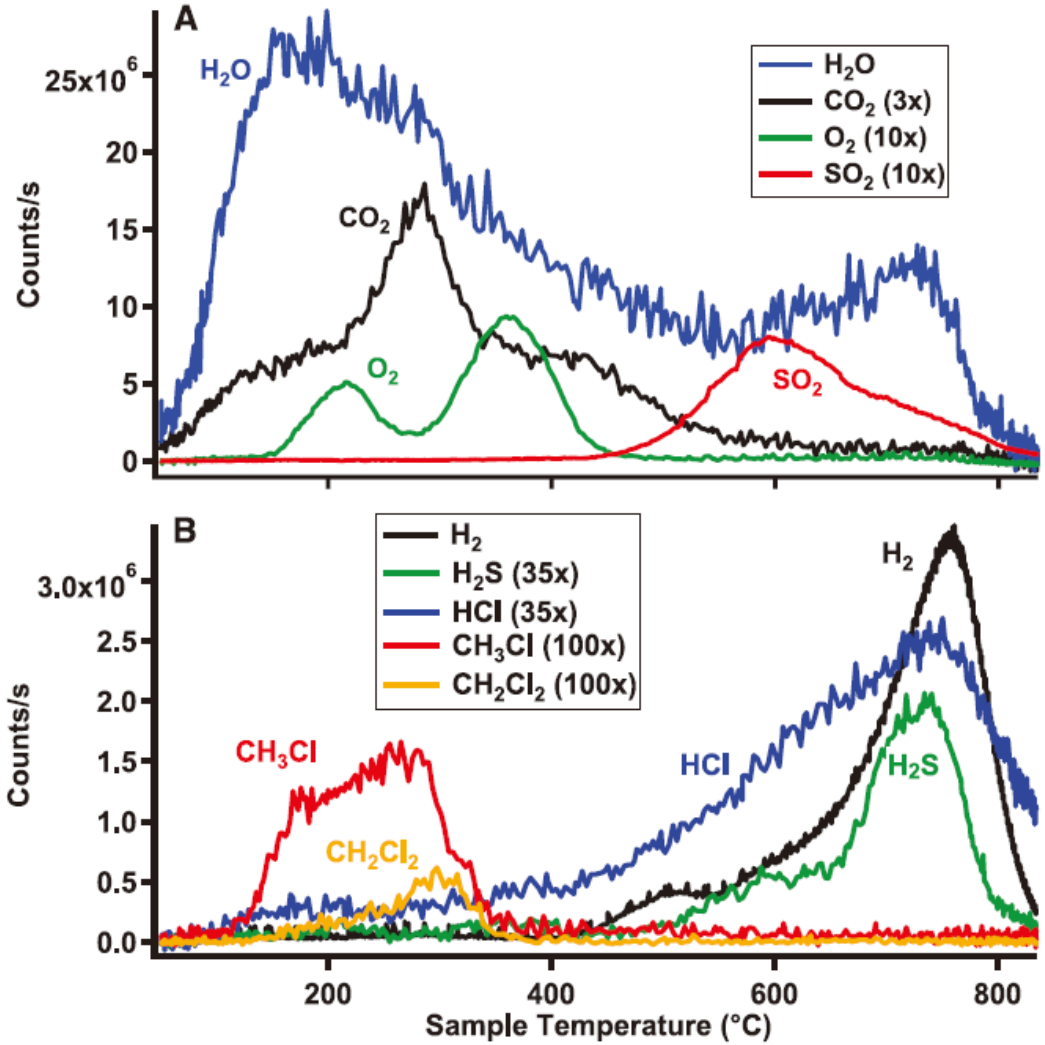

Fig. 1. Evolved gas analysis for a continuous ramp SAM pyrolysis of drill material (<150 μm) from the Sheepbed mudstone JK-4 sample. (**A**) Most-abundant evolved gases [CO_2 has been scaled up 3 times; SO_2 and O_2 have been scaled up 10 times]. (**B**) Evolved gas traces for H_2, H_2S, HCl, CH_3Cl, and CH_2Cl_2 [H_2S and HCl traces have been scaled up 35 times; CH_3Cl and CH_2Cl_2 have been scaled up 100 times]. Isotopologs were used to estimate species that saturated the QMS detector (m/z = 12 for CO_2 and m/z = 20 for H_2O).

Ming et al 2014

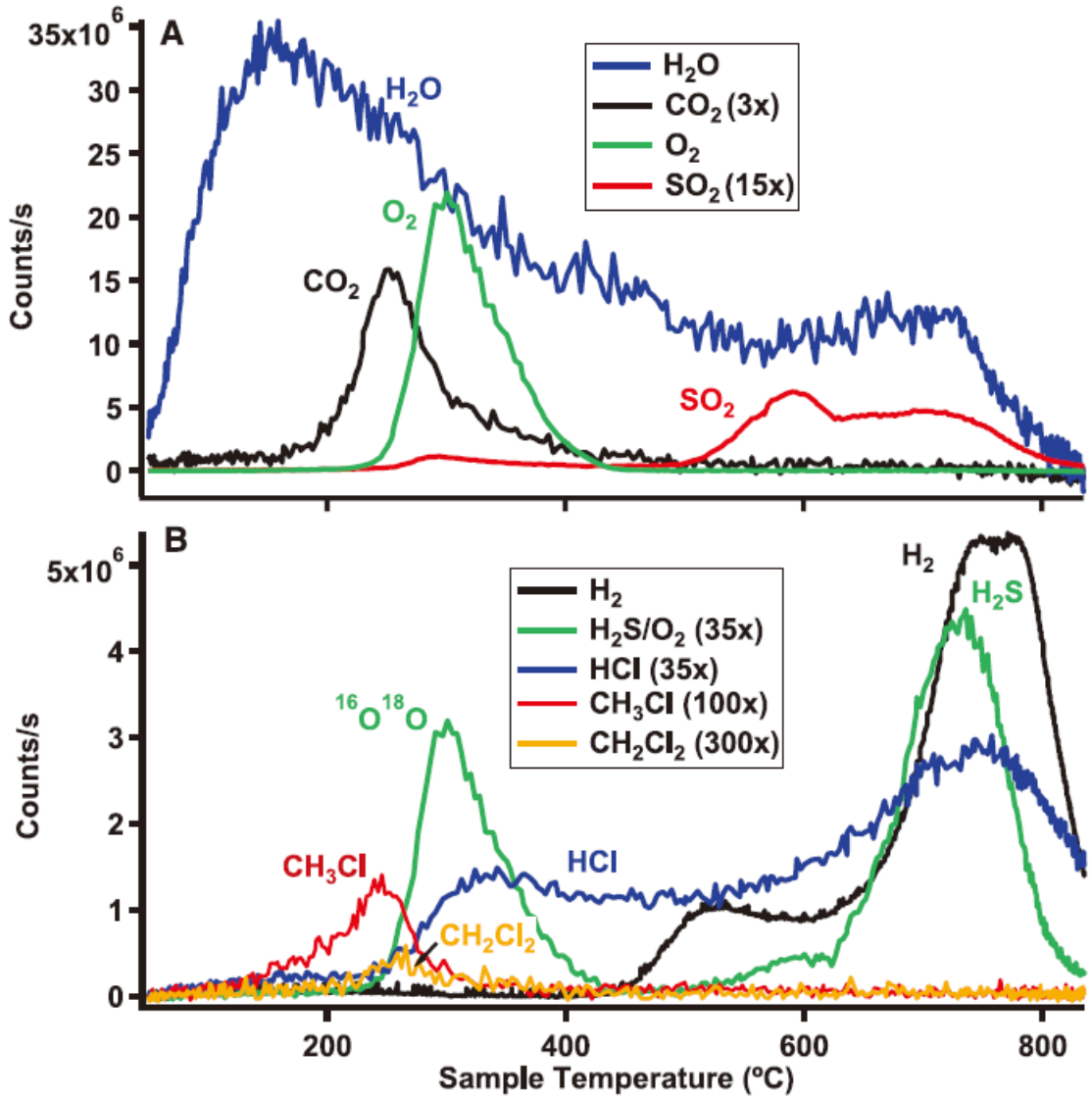

Fig. 2. Evolved gas analysis for a continuous ramp SAM pyrolysis of drill material (<150 μm) from the Sheepbed mudstone CB-2 sample. (**A**) Most-abundant evolved gases [CO_2 and SO_2 counts have been scaled up 3 and 15 times, respectively]. (**B**) Evolved gas traces for H_2, H_2S, HCl, CH_3Cl, and CH_2Cl_2 [H_2S and HCl traces have been scaled up 35 times; CH_3Cl and CH_2Cl_2 have been scaled up 100 and 300 times, respectively]. Isotopologs were used to estimate species that saturated the QMS detector (m/z = 12 for CO_2 and m/z = 20 for H_2O).

Ming et al 2014

Fig. 3. Major evolved gases from the JK and CB samples compared with EGA of analog minerals under SAM-like oven operating conditions (*14*). (**A**) Evolved H_2O for nontronite, montmorillonite, and saponite compared with JK and CB evolved H_2O. (**B**) Evolved O_2, SO_2, HCl, and H_2S for CB-2 compared with pyrrhotite mixed with a Ca-perchlorate run under SAM-like operating conditions in laboratory experiments (HCl evolution coincides with O_2 release for CB-2 and laboratory pyrrhotite/perchlorate experiments). (**C**) Evolved O_2 for several perchlorate salts compared with JK and CB evolved O_2.

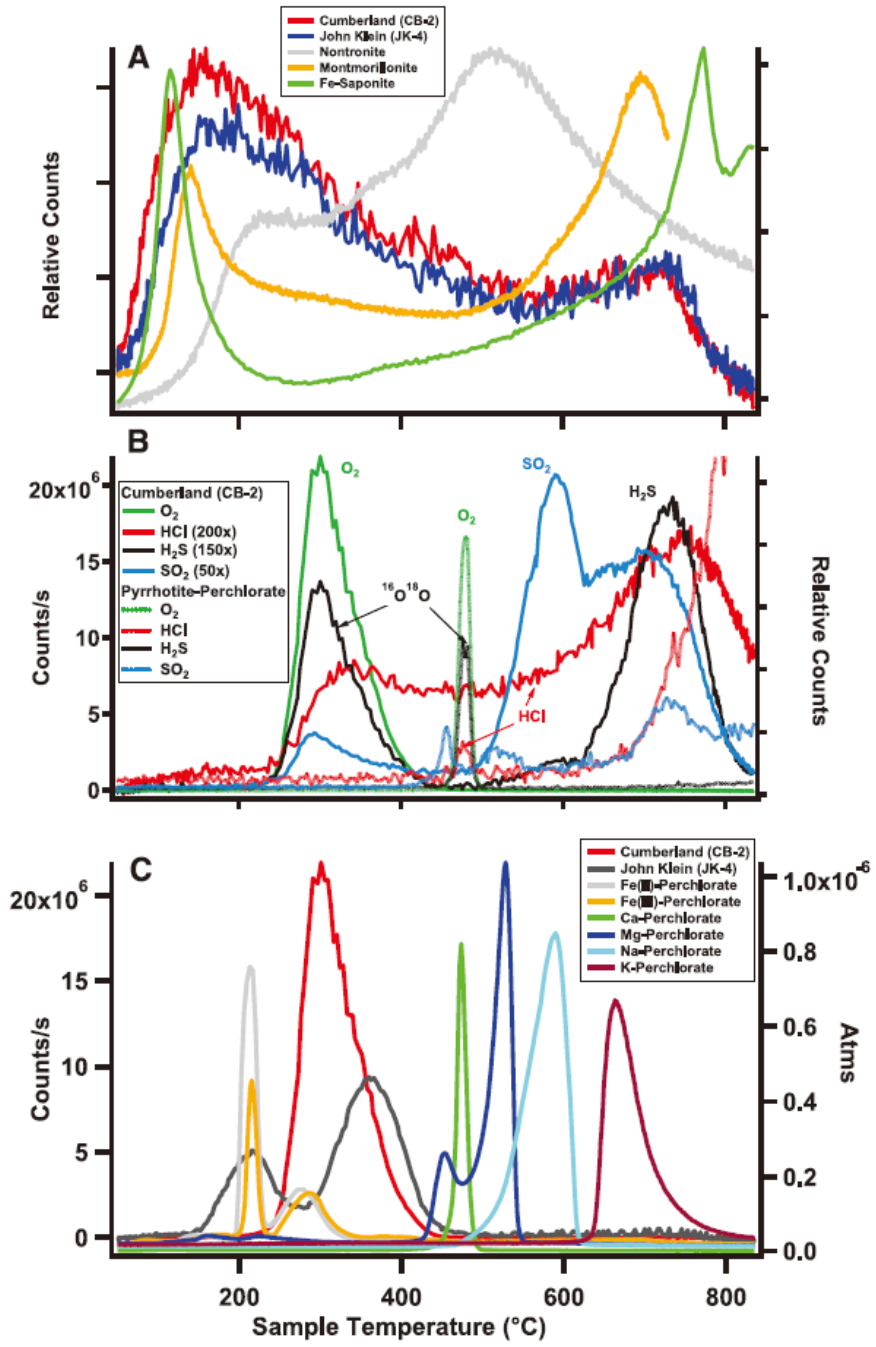

Ming et al 2014